Synthesis of Porphyrin-Chromophore Conjugates

A thesis submitted in partial fulfillment of the requirement to the degree of

Doctor of Philosophy

by

Rajesh Kisan Raut

Department of Chemistry and Biomolecular Sciences

Macquarie University

September 2014

Preface

The work described herein was carried out in the Department of Chemistry and Biomolecular Sciences at Macquarie University between September 2010-August 2014 under the supervision of Assoc. Prof. Andrew Try. The theoretical studies described in Chapter Seven were carried out in the Department of Dyestuff Technology, at the Institute of Chemical Technology, Mumbai, India under the guidance of Prof. N. Sekar, between July 2012-August 2012. Unless otherwise stated, the results are those of the author.

Sections of this Thesis were / will be presented in the following journals and conferences:

Publication

- Rajesh K. Raut, Rahul Telore, N. Sekar, Thomas A. Somerville, Danny K. Y. Wong and Andrew C. Try. Synthesis and theoretical nonlinear optical properties of pyridyl containing 1,3-diketone boron complexes and their quaternary salts. *Submitted to Tetrahedron*.

Conference

- Paper presented at National Symposium on Functional Applications of Colorants Mumbai, India, Oct 2011. Title: Absorption and fluorescence emission studies of benzyloxy substituted 1,3-diketones and their boron complexes.
- Paper presented at New Zealand Institute of Chemistry conference, Hamilton, New Zealand. Nov-Dec 2011. Title: Synthesis, characterization and photo-physical properties of several new 1,3-diketones and their boron complexes.
- Paper presented at IUPAC International Conference on Organic Synthesis, Melbourne, Australia. July 2012. Title: Synthesis and photo-physical studies of pyridyl-functionalized boron 1,3-diketonates with Zn-porphyrins.

- Paper presented at Light Harvesting Processes, Banz Monastery, Germany. Apr 2013. Title: Synthesis, characterization and photo-physical properties of porphyrins conjugated to boranil chromophores.

Acknowledgements

A journey is easier when you travel together. Interdependence is certainly more valuable than independence. This thesis is the result of four years of my life whereby I have been accompanied and supported by many people. It is a pleasant aspect that I have now the opportunity to express my gratitude for all of them.

First and foremost, I wish to thank my supervisor Assoc. Prof. Andrew C. Try. His excellent advice, constant encouragement, reassurance and extensive knowledge made him stand separate from others. His caring nature, calm attitude and patience with me throughout, helped me to complete this thesis. He stood by me during a very difficult time of my life. Thank you. During the last four years I have really enjoyed his company; he was more of a friend. I will always remember our discussions about cricket.

I would like to thank Dr. Christopher McRae for training me in the use of the elemental analysis apparatus and the Differential Scanning Colorimeter, and also Dr. Danny Wong for his help with Cyclic Voltammetry.

I would like to express my sincere gratitude to all other CBMS faculty and the support staff, especially Maria Hyland, Michelle Kang, Catherine Wong, Anthony Gurlica and Jenny Minard for their continuous assistance. Thanks also to the laboratory technical staff, Keith, Tony, Mark, Hong and Thulasy for their training on various instruments and the provision of "emergency" chemicals on short notice.

I enjoyed the company and time-to-time discussions on the projects with past and present members of the Try group; especially Mohammad Hashemi, Michael Howden and Nima Sayyadi. I would like to also thank Thanh Le, Rashid Javaid, Imam Ansari, Masoud Rostami, Murali Paranjothy, Eloise and Aziza.

I would like to extend my thanks to Alpesh, Wendy, Michael, Soumit, Girish, Harry, Ryan, Ketan, Umesh, Jashan, Thomas, Chandrika, Bhumika, Jane, Francesca, Heather, Jacob, Karthik and his wife for many discussions on my project and the enjoyable social moments that we shared.

To the academics back in India who shaped my career and life, particularly Prof. N. Sekar and all the chemistry staff of VES, thank you.

My parents provided love, care and emotional support during not only this period, but my entire life. I wish my Father was here with me and my family today. I hope he is watching us and that he is happy for us. I would like to thank my brother, who took family responsibility during the most difficult time of our lives. I would like to extend my thanks to all my family members; Mummy, Anuradha, Dattu bau, Vahini, Balu Mama-Mami, Anil Mama-Mami and the two little devils, Jay and Akshay. I would like to thank my in-laws for their understanding and constant support. Thank you so much Mummy, Baba, Manisha, Megha, Mayuresh, Sachin and my little sweetheart Sonakshi.

Above all, I am grateful to have my wife Manjaree (Jerry) with me during this period. This thesis wouldn't have been possible without her constant support, encouragement and love, together with her great patience.

I am grateful to have friends like Amit, Shyam, Shweta, Deepak, Pramod, Deepa, Nitesh, Sheshnath, Rahul, Ramdev, Sugam, Nandan, Amol, Anand and Vishal for their constant encouragement.

I would like to extend my thanks to my best friend Deepa for all our social activities and discussions during coffee breaks and at lunchtimes.

I am grateful to know the extraordinary Mistry family; Nosh, Deepali and their kids, Elisha and Ahan (god bless his soul), and thank you for encouraging me to do more in life.

I would like to express my gratitude to this Land and its people; Australia and every soul that has I touched me during my stay, that has provided me with a comfortable atmosphere, as if it was my second home, and also the encouragement and enrichment with culture that I have experienced. Alex and Paul, the first few people I met in this country, I am really thankful to have them as friends and the best housemates. I am grateful to Dr. Christopher Choong at Royal North Shore Hospital and Dr. Peter Royale at the Macquarie University Clinic.

Finally, I am grateful to the Lord Ganesha for all his blessings.

Declaration

I certify that the work in this thesis entitled "Synthesis of Porphyrin-Chromophore Conjugates" has not previously been submitted for a degree, nor has it been submitted as part of requirements for a degree to any other university or institution other than Macquarie University. I also certify that the thesis is an original piece of research and it has been written by me. Any help and assistance that I have received in my research work and the preparation of the thesis itself have been appropriately acknowledged. In addition, I certify that all information sources and literature used are indicated in the thesis.

Rajesh Kisan Raut

(SN: 42027888)

29/08/2014

This Thesis is dedicated to the memory of my Father

Abstract

Several porphyrin-chromophore conjugate systems have been synthesized for future energy / electron transfer studies. This thesis discusses the systematic approach used in the synthesis of three chromophores (boranils, α-cyanostilbenes and 1,3-diketone boron complexes) linked to porphyrins *via* either covalent bonds or supramolecular interactions. The UV-visible absorption and fluorescence emission spectra, together with the relative quantum yields of the conjugates were examined in order to establish any structure-property relationships that may exist.

Three different porphyrin frameworks were prepared for use in the syntheses of covalently linked porphyrin-chromophore conjugates. The first of these was a porphyrin ring mono-functionalised on one of the *meso*-aryl rings. The second framework had a functionalised phenyl ring connected to an imidazole ring that was fused to the porphyrin at adjacent β-pyrrolic carbons. The third framework was functionalised on a quinoxaline ring that was fused to the porphyrin at adjacent β-pyrrolic carbons.

Porphyrin-boranil conjugates were synthesized by condensation of amine-functionalised porphyrins with salicylaldehyde or 2-hydroxynaphthaldehyde to afford the corresponding 2-hydroxyaryl imines (also known as anils), followed by reaction with boron trifluoride to afford the boron complexes.

Aldehyde-functionalised porphyrins were condensed with the reactive methylene group present in 4-nitrophenylacetonitrile, 4-bromophenylacetonitrile and benzyl cyanide to afford α-cyanostilbene-porphyrin conjugates.

Two series of 1,3-diketone boron complexes were synthesized for future studies involving a supramolecular approach to porphyrin-chromophore conjugate assembly. One series contains a 4-hydroxyphenyl unit (for coordination to tin(IV) porphyrins) and the second series contains a 4-pyridyl unit (for coordination to zinc(II) porphyrins). A titration experiment (monitored with UV-

visible spectroscopy) was conducted with one of the 4-pyridyl appended 1,3-diketone boron complexes and a zinc(II) porphyrin. The results indicated that a complex was formed.

The 4-pyridyl appended 1,3-diketone boron complexes were converted to their *N*-methylpyridinium salts, and a computational study was also conducted to calculate their non-linear optical properties.

List of Abbreviations and Symbols

μ	micro
α	dipole moment
β	hyperpolarizability
λ	wavelength
ε	molar extinction coefficient
ϕ	quantum yield
η	refractive index
Δλ	Stokes shift
Å	angstrom
app.	apparent
b.p.	boiling point
br	broad
B3LYP	Becke3-Lee-Yang-Paar
°C	degrees Celsius
d	doublet
dd	doublet of doublets
DCE	1,2-dichloroethane
DCM	dichloromethane
$CDCl_3$	chloroform-*d*
$CHCl_3$	chloroform
DFT	density functional theory
DMF	*N*,*N*-dimethylformamide
DMSO	dimethylsulfoxide
DMSO d_6	dimethylsulfoxide-d_6
DSSC	dye sensitized solar cell
FTIR	Fourier transform infrared spectroscopy
EtOH	ethanol
eV	electron volt
g	gram

h	hour
Hz	hertz
IR	infrared
J	coupling constant
K	binding constant
$LiAlH_4$	lithium aluminium hydride
m	multiplet
Me	methyl
mg	milligram
min	minute
mmol	millimole
m.p.	melting point
$NaBH_4$	sodium borohydride
NMR	nuclear magnetic resonance
OAc	acetate
Ph	phenyl
ppm	parts per million
p-TSA	*p*-toluenesulfonic acid
q	quartet
r.t.	room temperature
s	singlet
sh	shoulder
t	triplet
t-Bu	*tertiary*-butyl
TDDFT	time dependent density functional theory
TEA	triethylamine
TLC	thin layer chromatography
THF	tetrahydrofuran
UV	ultra-violet

Table of Contents

Chapter One

Introduction

1.1 Background

Solar energy is the ultimate, renewable source of energy, is environmentally friendly, and a potential alternative to conventional energy sources. Natural photosynthesis converts 95% of absorbed light to electrical-charge through chemical processes.[1] The green pigment chlorophyll (Figure 1.1) plays a crucial role in natural photosynthesis as a photosensitizer, in combination with numerous other pigments.

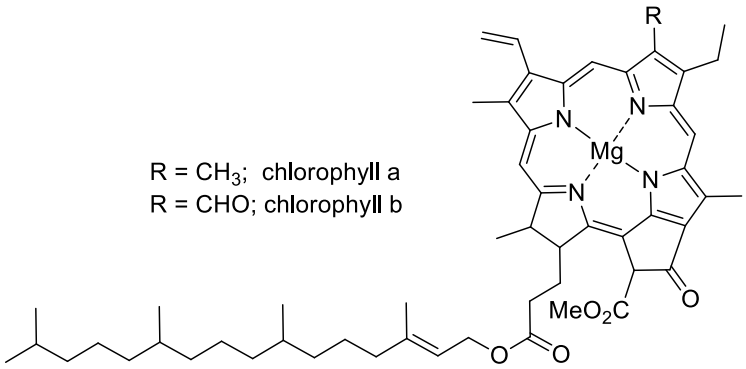

Figure 1.1: The structure of chlorophyll a and b.

One of the key features behind the efficiency of the photosynthetic reaction centre (PRC) is the manner in which light energy is harvested and electrons/energy are transferred from one chromophore to another (leading to the formation of charge-separated species). In natural systems (the result of millions of years of evolution), the chromophores are held at defined geometries with respect to one another by virtue of protein scaffolds.[2,3]

As noted above, plants and bacteria capture light using chlorophyll (Figure 1.1) as a critical component. Chlorophylls (which are chlorins) belong to the porphyrin class of compounds (Figure 1.2), but in the case of chlorins, one of the β-β pyrrole bonds has been reduced. This has led to the use of porphyrins, being relatively easy to prepare in the laboratory (see Section 1.2.1), being used for light harvesting studies for many years. Along with structural similarities with chlorophyll, porphyrins possess a high molar extinction coefficient at the Soret band (400-450 nm) and moderate absorption at the Q bands (550-600 nm).

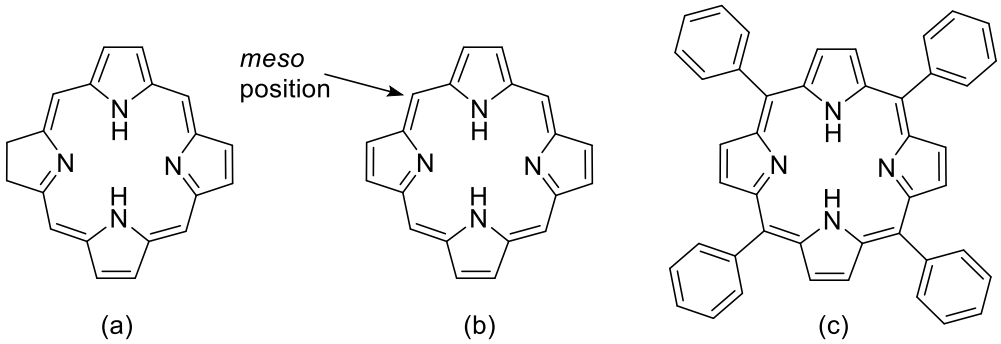

Figure 1.2: The structure of (a) chlorin,the core unit of chlorins, (b) porphyrin, the core unit of porphyrins and (c) 5,10,15,20-tetraphenylporphyrin, an example of a tetra-aryl porphyrin.

Porphyrins with extended conjugated π-systems have been reported to exhibit favourable charge-transfer kinetics[4] and metallo-porphyrins undergo facile redox reactions.[5] Porphyrins undergo minimal structural changes during electron transfer reactions[6] and the photo-physical properties of porphyrins can be tailored by changing metal ion chelation and/or peripheral substitution. Accordingly, numerous investigations have been made in order to understand the structure-photophysical relationships of porphyrin derivatives in combination with a variety of secondary chromophores, connected to porphyrins through different chemistry, and at different points, have been studied in order to better understand the photo-induced electron and/or energy transfer processes in synthetic light-harvesting arrays. Some of the more commonly studied porphyrin-chromophore combinations are briefly highlighted in Section 1.2.2 – 1.2.6.

1.2 Porphyrins in Light Harvesting Mimetics

1.2.1 Porphyrin Synthesis

The most readily accessible synthetic porphyrins are those symmetric compounds bearing aryl substituents at the *meso* positions (tetra-aryl porphyrins (Figure 1.2(c)). Such compounds were first available *via* the Rothemund condensation reaction (equimolar mixture of pyrrole and aryl aldehydes in a mixture of pyridine and methanol, heated at 115 °C in a sealed tube),[7,8] that was subsequently improved upon by Alder and Longo (equimolar mixture of pyrrole and aryl

aldehydes in propanoic acid).[9,10] In many cases the crude porphyrin precipitates from the reaction mixture, which is a major advantage as part of the isolation and purification procedure. In the Alder-Longo method, oxygen serves as the oxidising agent, transforming the initially formed porphyrinogen-type compounds (Figure 1.3) into the desired porphyrins, however the product is typically contaminated with some chlorin product.[11] Among the disadvantages of the Alder-Longo method are its limitations to aldehydes bearing substituents capable of surviving refluxing propanoic acid, and its poor yields in the case of sterically hindered aryl aldehydes (eg, 2,6-substituted benzaldehydes).

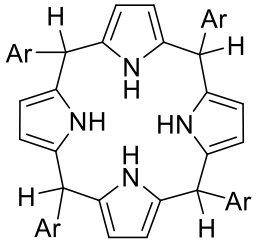

Figure 1.3: The generic structure of a porphyrinogen.

The Lindsey method (equimolar mixture of pyrrole and aryl aldehydes in dichloromethane or chloroform, room temperature, TFA or BF_3-etherate as a catalyst, DDQ or *p*-chloranil as oxidant) has the mildest reaction conditions and the broadest scope of aldehydes.[12,13] A drawback of this method is the need to evaporate large volumes of solvent if the reaction is done on moderate to large scales (0.01 – 0.1 M) and the use of chromatography to obtain the purified product.

For certain applications, compounds in which not all *meso* aryl units are the same may be desired. In such cases a stepwise approach is sometimes suitable. For example, access to *trans*-A_2B_2 porphyrins is made possible through initial formation of 5-substituted dipyrromethanes (*via* acid-catalysed condensation of an aldehyde with an excess of pyrrole), followed by condensation of the dipyrromethane with a second aldehyde (Figure 1.4). However, scrambling

of the preformed dipyrromethane units (*via* cleavage of the *meso*-carbon-β-pyrrolic bonds and recombination with other reaction components) is known to occur, to varying degrees.[14]

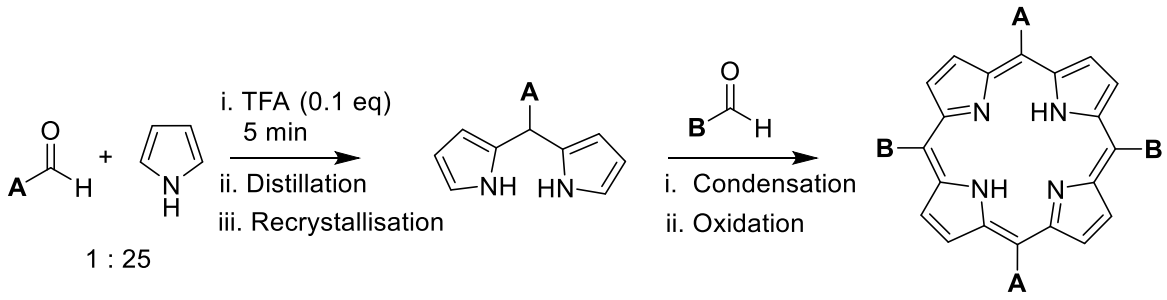

Figure 1.4: A route to *trans*-A_2B_2 porphyrins.

For other applications, it may be desirable to access a porphyrin in which three, or possibly all four *meso* aryl units are different from one another. In this case, a more convoluted synthesis is necessary, and is illustrated with the synthesis of the important building blocks shown in Figure 1.5.[15] The key steps here are the syntheses of the mono- and di-acyl functionalized dipyrromethanes and their reduction to mono- and di-carbinols.

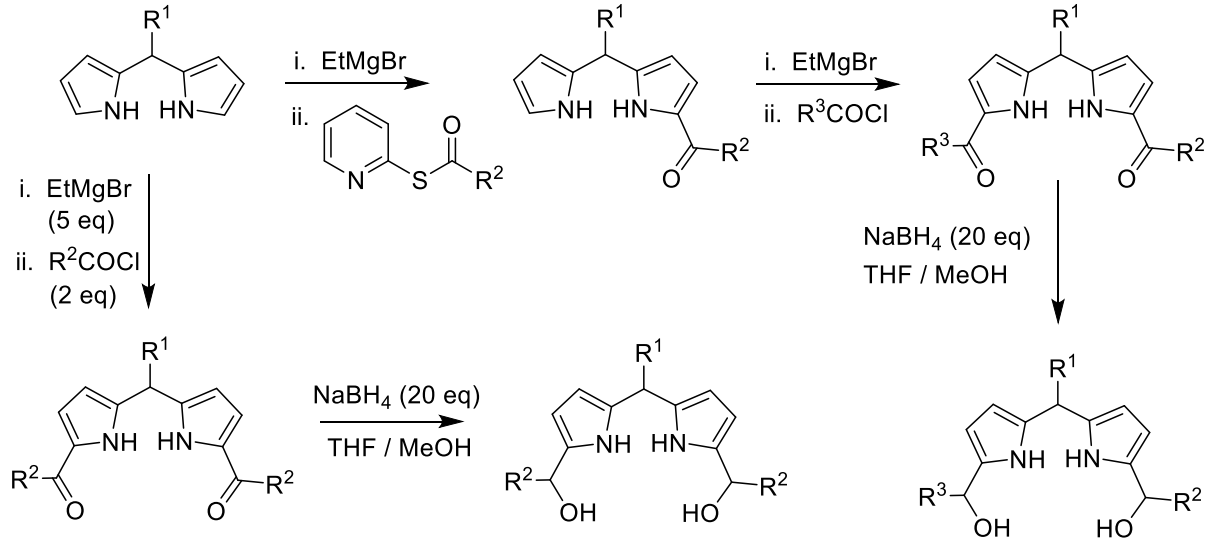

Figure 1.5: Preparation of acyl and carbinol functionalized dipyrromethanes.

The carbinol building blocks can be combined in numerous ways with other building blocks to afford porphyrins of the type illustrated in Figure 1.6.

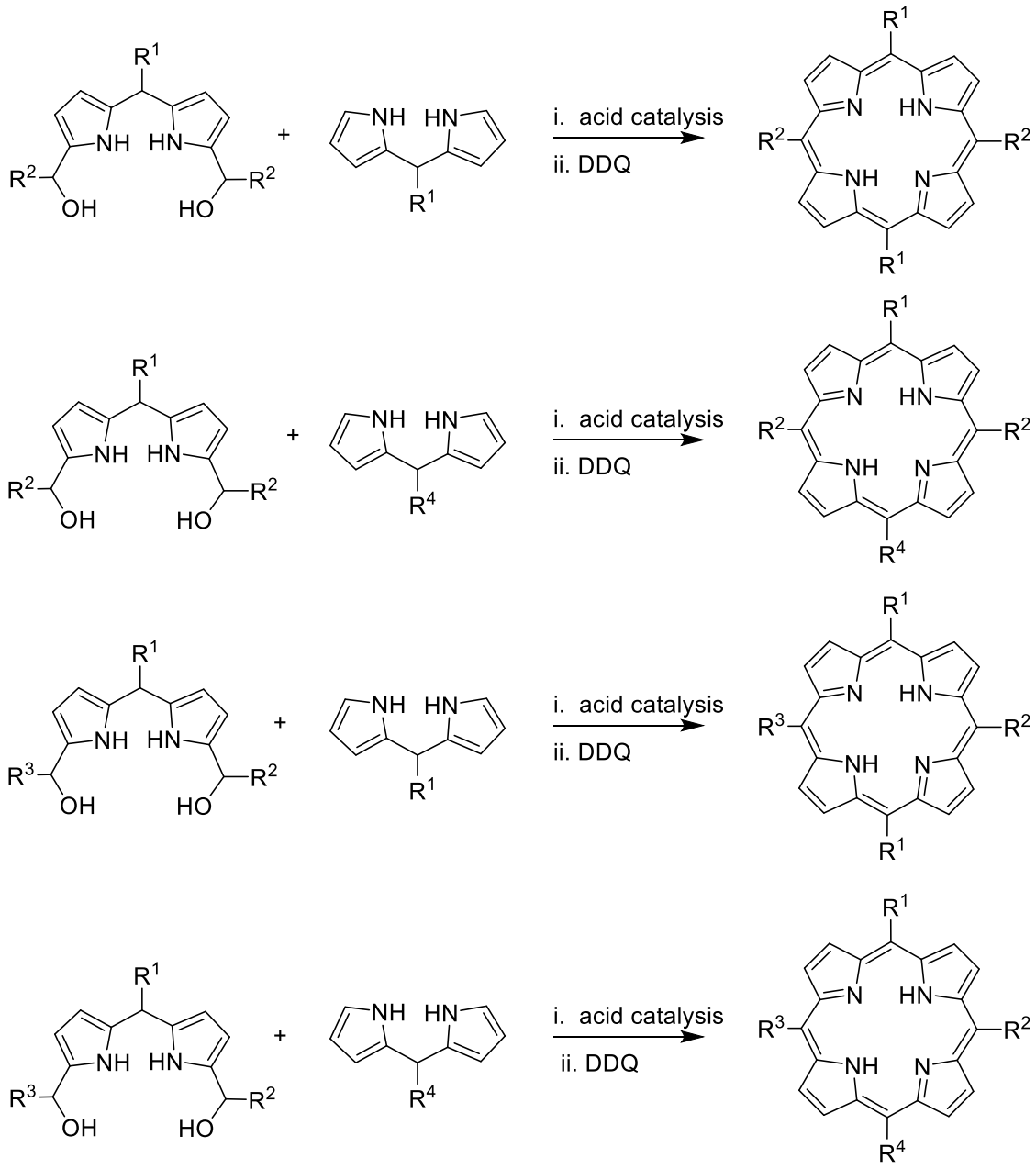

Figure 1.6: Stepwise preparation of non-symmetric porphyrins.

Where only two different aryl units are required, another approach is simply to use the Lindsey method with different ratios of the two different aryl aldehydes, depending upon the targeted porphyrin of interest, and then to chromatograph the statistical distribution of six possible porphyrin products.[13] This is exemplified schematically in Figure 1.7.

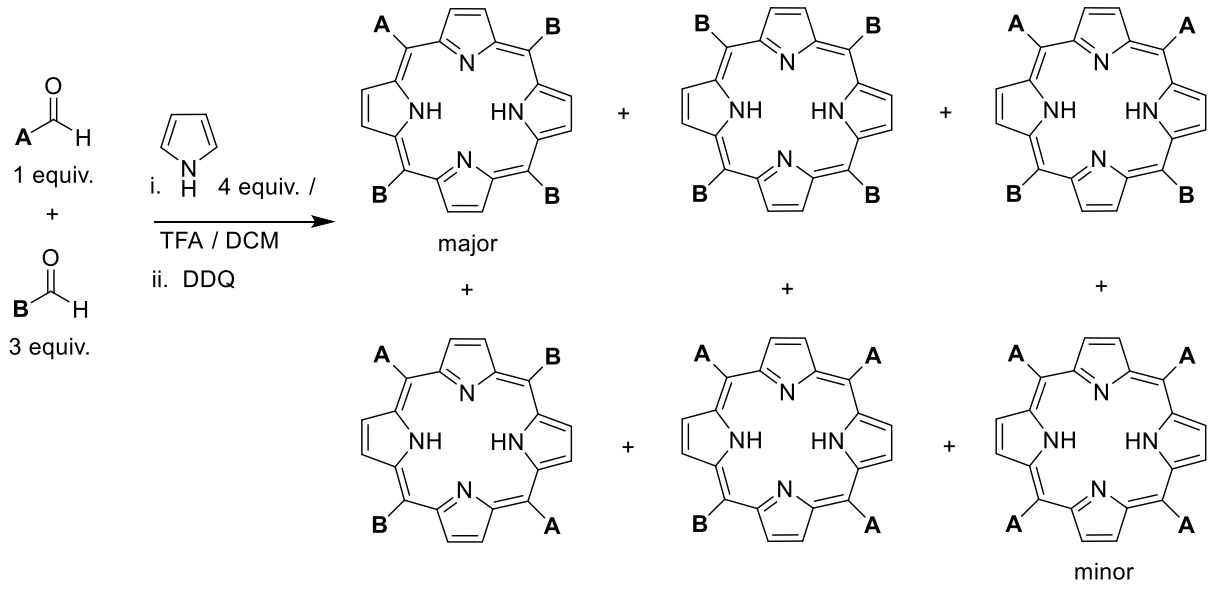

Figure 1.7: A one-pot mixed-aldehyde condensation approach non-symmetric porphyrins. In this example, a monoA-trisB (AB_3) aryl porphyrin was the target.

Building blocks prepared in one of the above methods were used in the construction of the porphyrin systems highlighted below.

1.2.2 Porphyrin-BODIPY Conjugates

The electron and energy transfer between BODIPY dyes and porphyrins have been widely studied. Khan *et al*. extensively reviewed the conjugation of BODIPY with porphyrins.[16] Examples include BODIPYs conjugated covalently to porphyrins *via* a range of linkages through the *para*-position of a *meso*-phenyl ring on the porphyrin and the *para*-position of the *meso*-aryl ring of the BODIPY chromophore; the nature of the linkages include an acetylene bridge,[17] an ether bridge,[18] an amide bridge,[19] a cyanuric bridge,[20] a triazole bridge,[21] as well as many others (Figure 1.8). As a variation, the BODIPY unit has also been connected at an α-pyrrolic linkage, as shown in the final structure of Figure 1.8.[22]

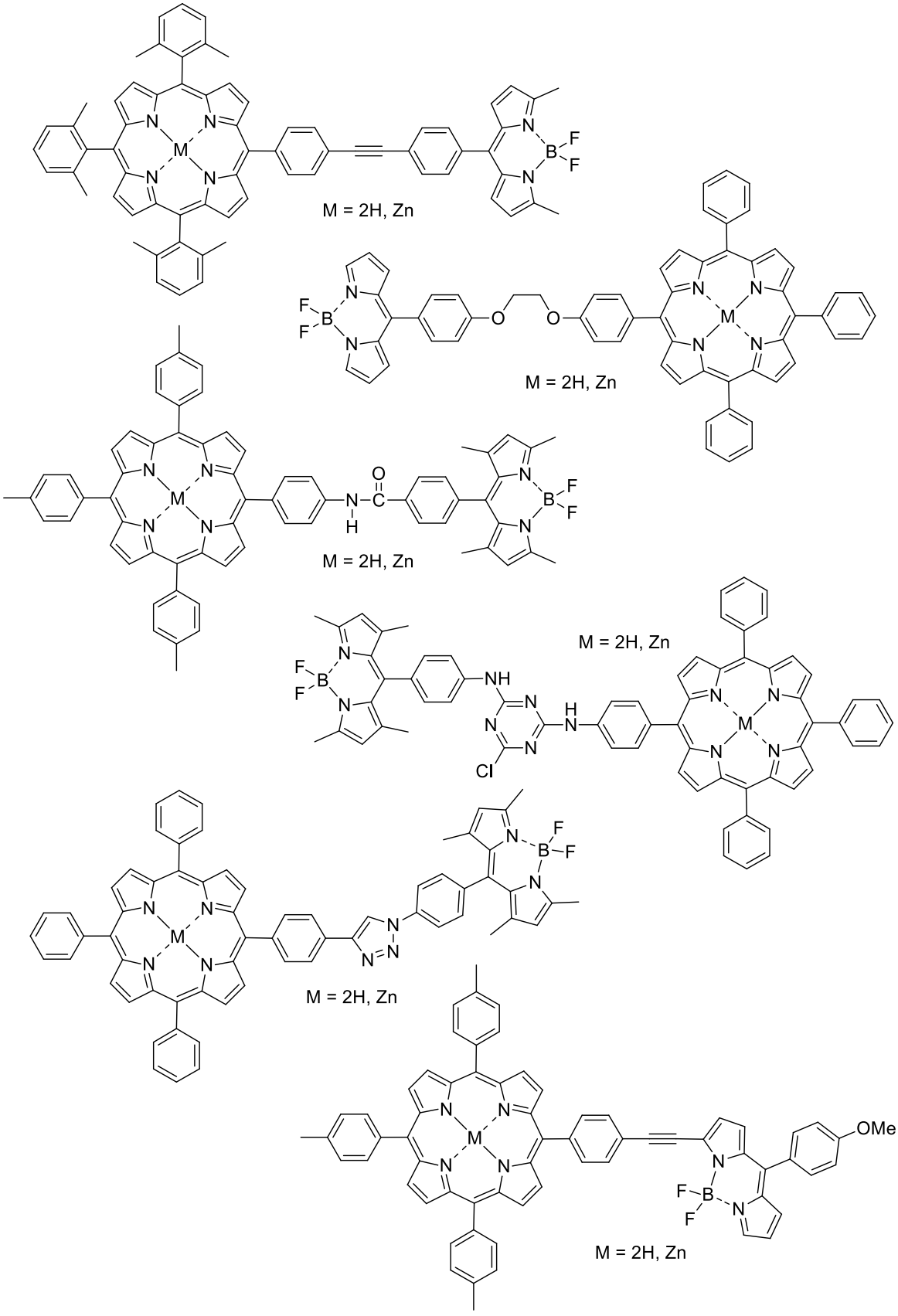

Figure 1.8: A selection of BODIPY-porphyrin conjugates that have been studied. See the associated text for references.

Non-covalent assemblies have also been reported (Figure 1.9), with examples including complexes formed between pyridine-functionalised BODIPYs and a zinc(II) porphyrin (Figure 1.9 (a),[23] as well as tin(IV) porphyrins and either phenolate or carboxylate-functionalised BODIPYs, Figure 1.9 (b) and (c), respectively.[24]

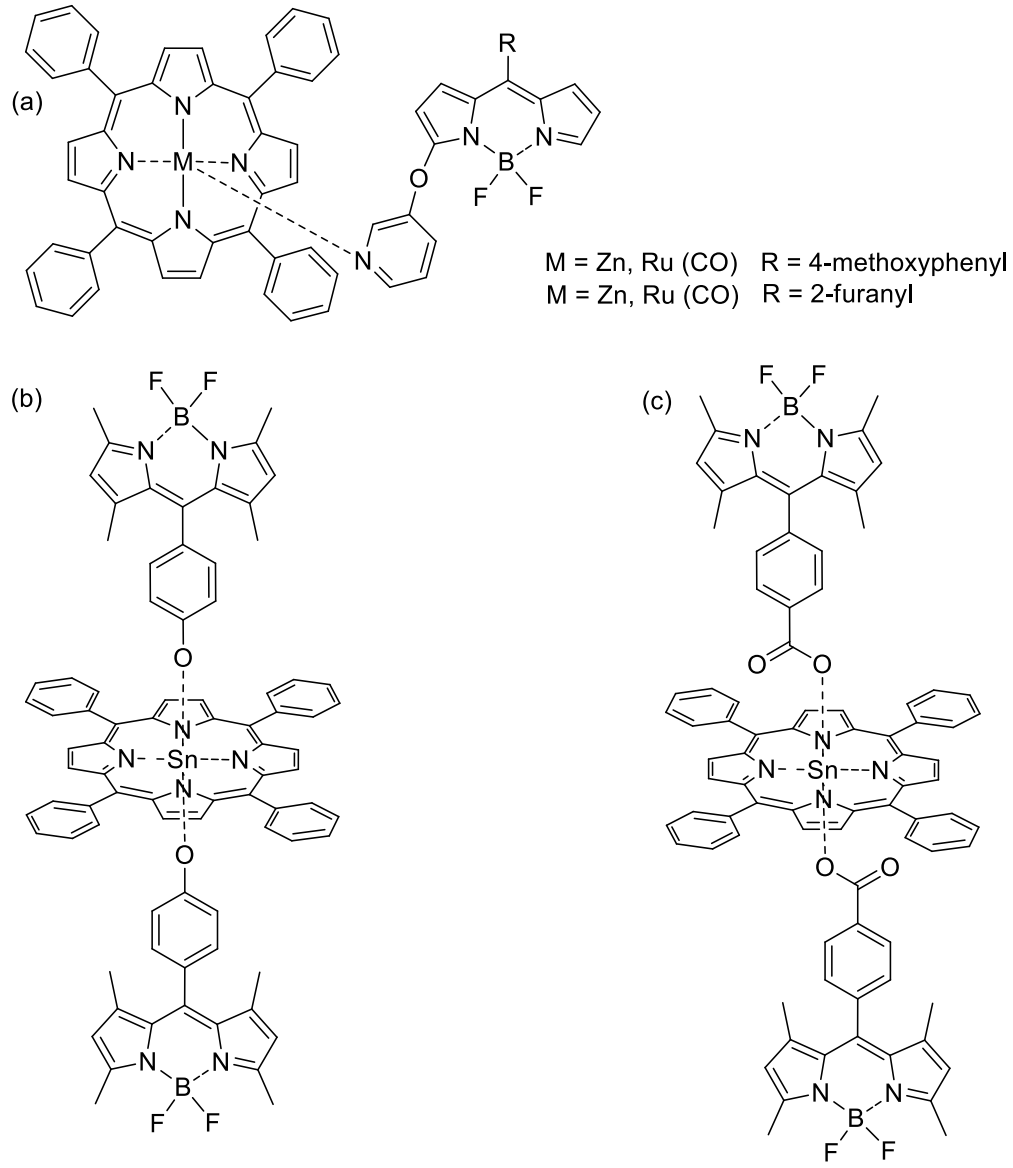

Figure 1.9: Some examples of supramolecular assemblies involving BODIPY and porphyrin units. See the associated text for references.

Porphyrins have also been prepared with two or more BODIPYs, for example see Figure 1.10(a)[21] as well as BODIPYs with two porphyrins (Figure 1.10(b)).[25]

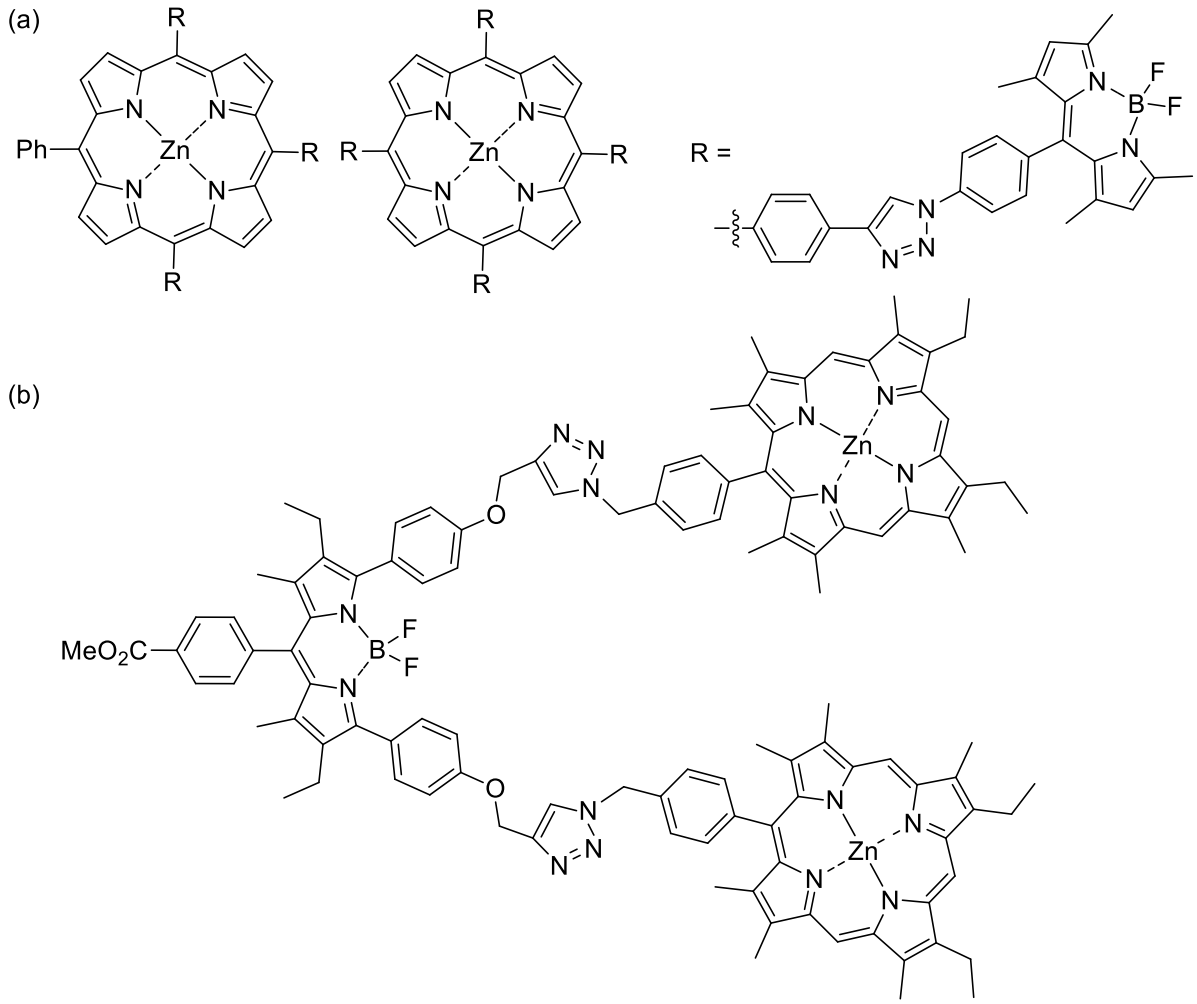

Figure 1.10: (a) Examples of a porphyrin with multiple BODIPY units attached and (b) a BODIPY linked to two porphyrin units.

Photo-physical studies have also been carried out on various triads containing fullerene,[18,26] squaraine units,[27] azaBODIPY[28] along with BODIPYs and porphyrins to enhance the understanding of photo-physical properties.

1.2.3 Porphyrin-Carotenoid Conjugates

Carotenoids are pivotal for survival in photosynthetic processes in plants as well as photosynthetic organisms. Carotenoids serve as both a photo-sensitizer, which transfers excitation energy to chlorophyll, and also to protect the photosynthetic system from photo-oxidation reactions.[29] With both of these functions in mind, carotenoids conjugated to

porphyrins have been studied in artificial light harvesting systems. Gust *et al.*[30] synthesized series of photosensitizers (Figure 1.11) mimicking natural carotenoid protection and antenna functions. In the following year, Osuka *et al.*[29] studied electron transfer in porphyrin-carotenoid dyads and carotenoid-porphyrin-pyromellitimide triads (Figure 1.12) along with variety of spacers ("SP" in Figure 1.12). Olguin *et al.*[31] reported a carotenoid-porphyrin-fullerene triad (Figure 1.13), which does not lower the charge transfer rate, as reported previously for extended π-conjugated systems.

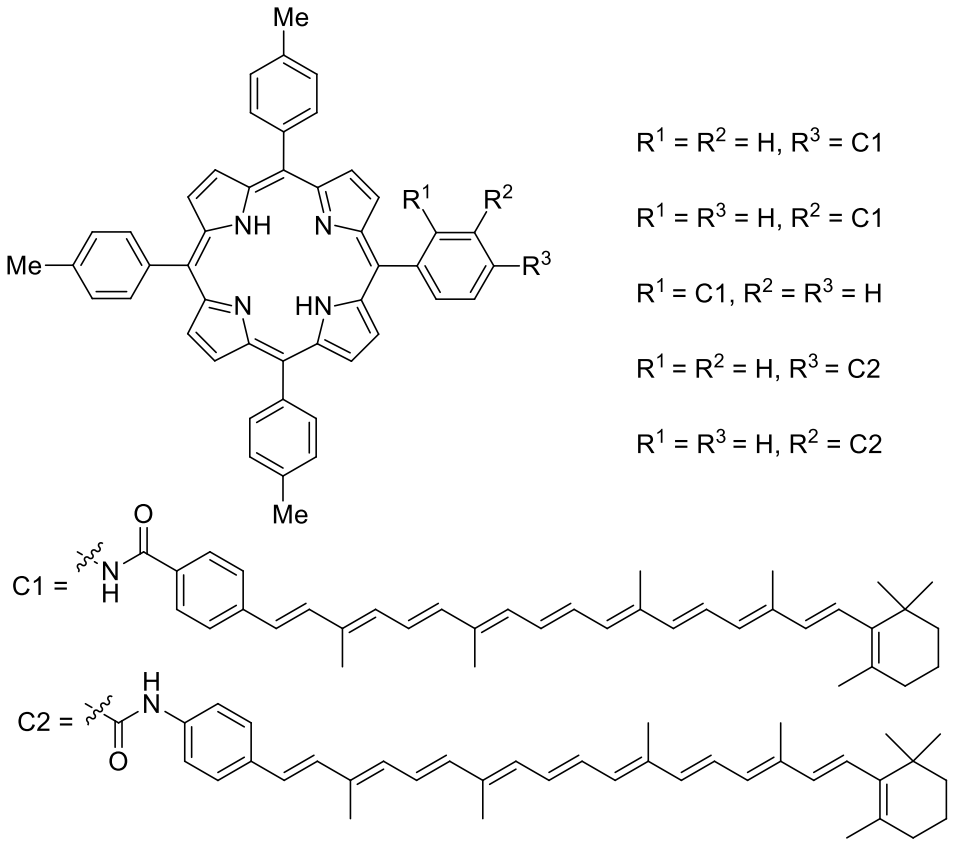

Figure 1.11: Carotenoid-porphyrin conjugates of Gust *et al.*[30]

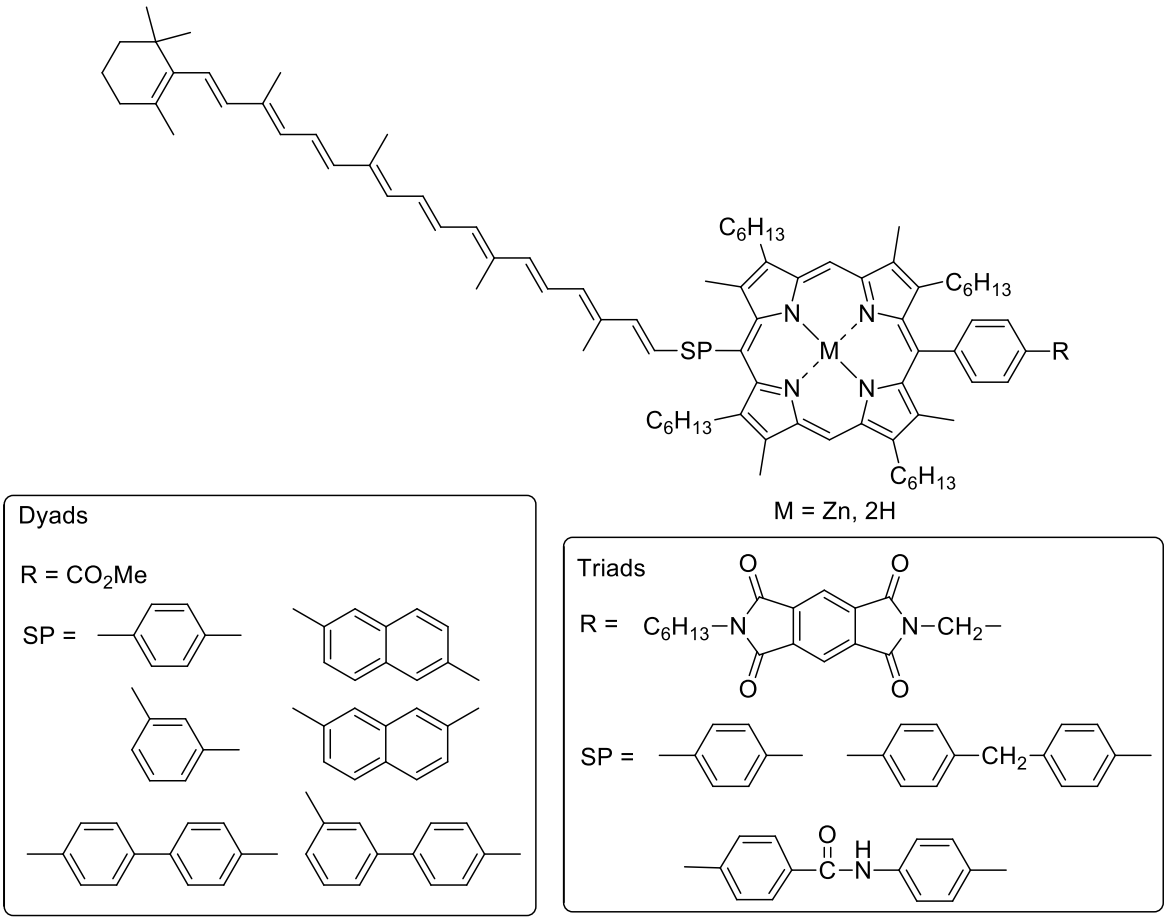

Figure 1.12: Dyad and triad systems of Osuka *et al*.[29]

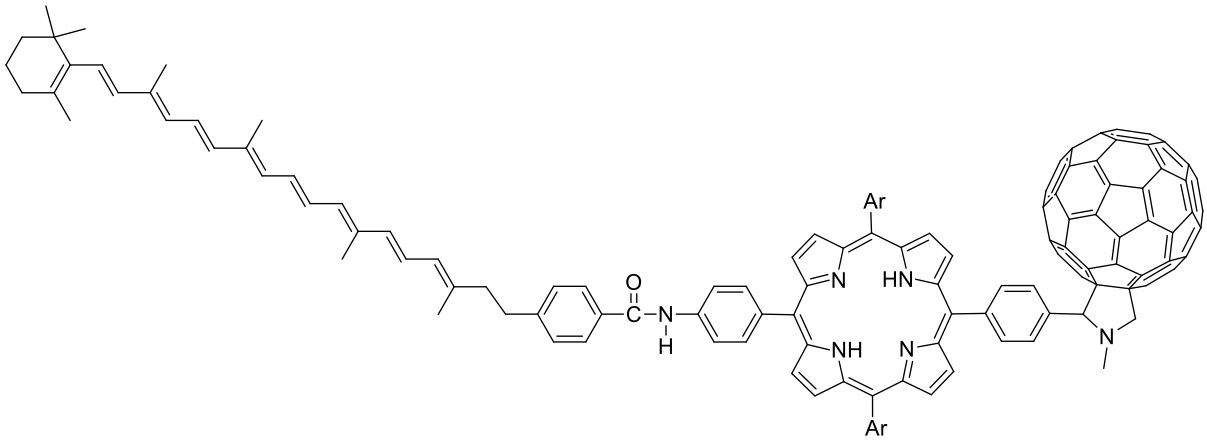

Figure 1.13: The carotenoid-porphyrin-fullerene triad of Olguin *et al*.[31]

1.2.4 Porphyrin-Fullerene Conjugates

Since their discovery, fullerenes have been known to participate in electron transfer reactions.[32] Fullerene contains an extensively conjugated three-dimensional π–system and possesses three

degenerate, low lying lowest unoccupied molecular orbitals (LUMOs) that allow it to accept up to six electrons.[6] In fact, fullerene is reported as an electron acceptor with a first electrode potential similar to quinone derivatives, the naturally occurring electron acceptor in photosynthetic systems.[33] Fullerenes have been reported in DSSC applications as an electron acceptor in donor-π-acceptor systems due to their photo-physical, electrochemical and chemical properties.[6,33,34] Figure 1.14 illustrates a dyad in which the fullerene is linked *via* a *meso*-phenyl unit, with different orientations with respect to the porphyrin ring.[6]

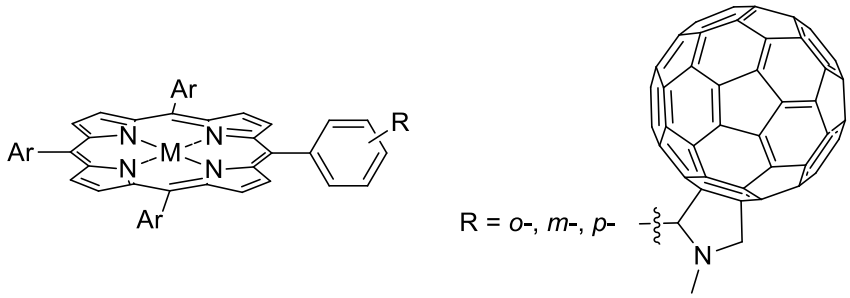

Figure 1.14: Porphyrin-fullerene dyads of Imahori *et al*.[6]

Shinkai and coworkers extensively reviewed the synthesis and properties of porphyrin-fullerene conjugates,[35] with some of the different conjugates shown in Figure 1.15.

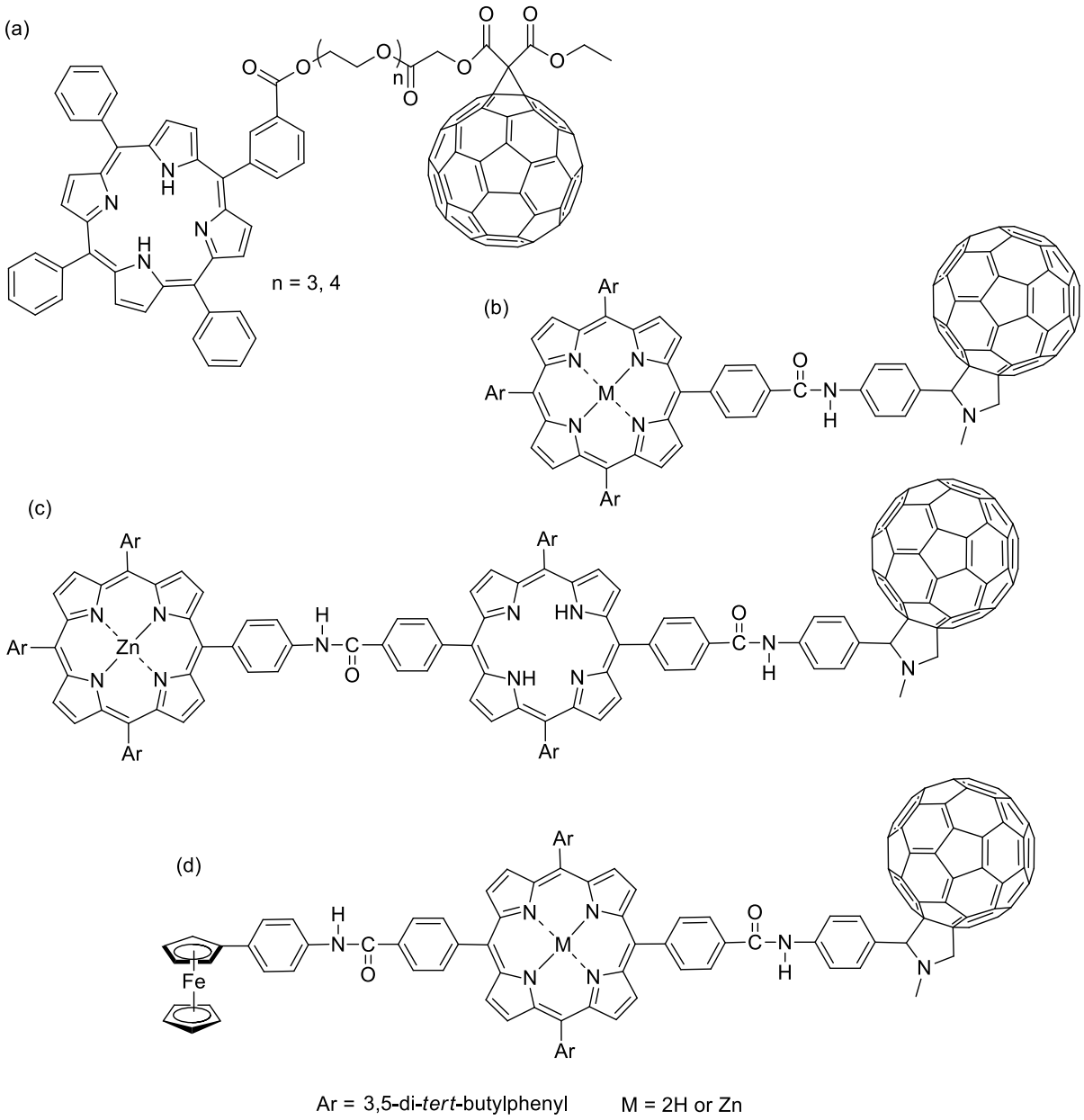

Figure 1.15: (a) The flexibly linked dyads of Schuster *et al.*,[33] and (b), (c) and (d) the rigid systems of Imahori *et al.*[36]

1.2.5 Miscellaneous Porphyrin Conjugates

Lindsey and co-workers found that excited state energy transfer from a perylene moiety to a free-base porphyrin is extremely fast in the structure depicted in Figure 1.16(a). The authors also studied various porphyrin-phthalocyanine dyads and found that they could achieve strong absorption in the blue and red region of the visible spectrum (Figure 1.16(b)).[37] A linear array

(Figure 1.16(c)) was also prepared and it was found to exhibit superior light harvesting properties, and that perylene and phthalocyanine components are useful as energy input and output units for porphyrin-based systems.[38]

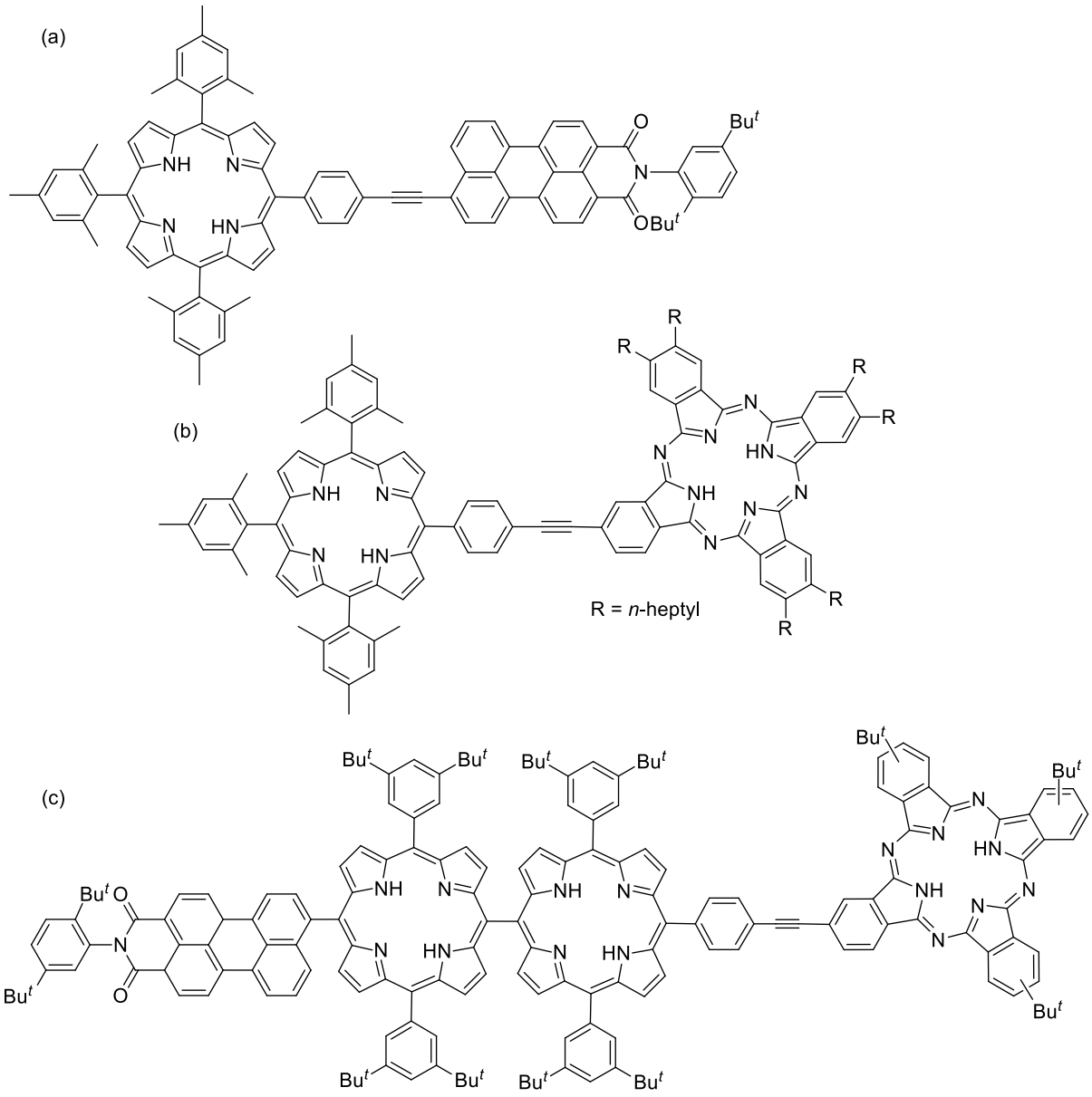

Figure 1.16: Several porphyrin conjugates studied by the Lindsey group.[37,38]

Toa *et al*.[39] reported efficient photo-induced energy and photo-induced electron transfer from porphyrin to anthraquinone resulting in a charge separated state with a long lifetime for the relatively flexibly linked porphyrin-anthraquinone dyad shown in Figure 1.17.

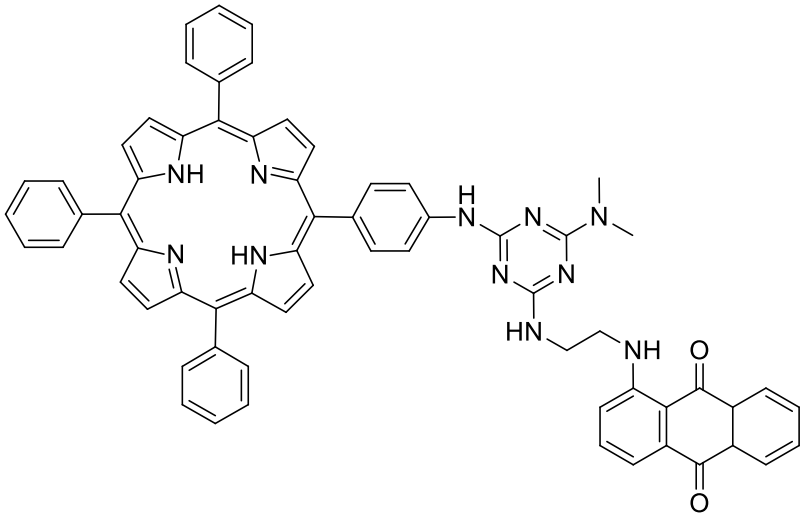

Figure 1.17: A porphyrin-anthraquinone dyad system.[39]

1.2.6 Oligomeric Porphyrin Arrays

In order to better understand the processes involved in natural systems, there is interest in the syntheses of oligomeric porphyrin arrays. To establish electronic communication between porphyrins, the geometry (orientation), the nature of linkages and the distance between the porphyrin units are all parameters that have been varied.[40] Considerable work has been carried out in this area and it has been extensively reviewed.[40,41,42] However, as it is not directly relevant to the work conducted in this thesis, it will not be discussed in any further detail.

1.3 Other Chromophores of Interest in the Present Work

1.3.1 Boron Complexes

Boron complexes have various applications, such as laser dyes,[43] chemosensors,[44] biolabelling[45,46] and sensitizers for solar cells.[44,47] BODIPY derivatives have emerged as widely used extrinsic fluorophores as a result of their desirable photo-physical properties, such as a high molar extinction coefficient in the range of 500-600 nm, fluorescence emission in the region 500-650 nm and with a quantum yield of close to one.[48]

However, BODIPY derivatives tend to exhibit a small Stokes shift and can be industrially challenging to prepare.[49] In addition, BODIPY molecules are weakly photostable when

excited[50,51] and prone to photo-bleach by up to 20-40%.[52] In search of enhanced photo-physical properties, researchers have designed and studied a wide range of related boron complexes. Some examples (there are many more) of the core units of these alternate compounds, together with BODIPY, are shown in Figure 1.18.

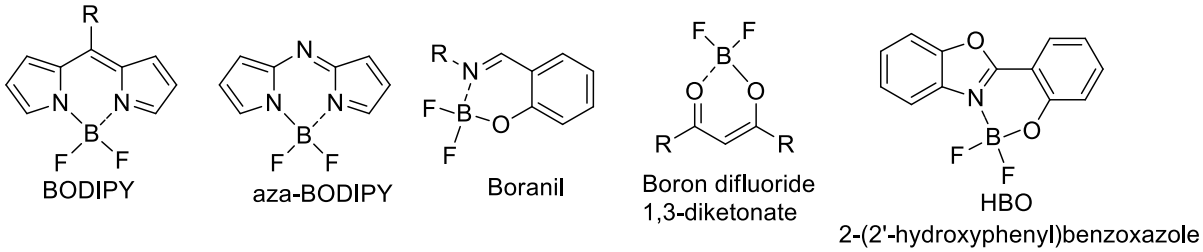

Figure 1.18: Schematic representation of boron complexes of some simple ligand frameworks (unfunctionalised on the aryl units); R = aryl ring.

Porphyrin-BODIPY conjugates were discussed in Section 1.2.2. In this Thesis, both boranils and boron difluoride 1,3-diketonates were used. These chromophores can be accessed *via* the retrosynthetic strategies shown in Figure 1.19.

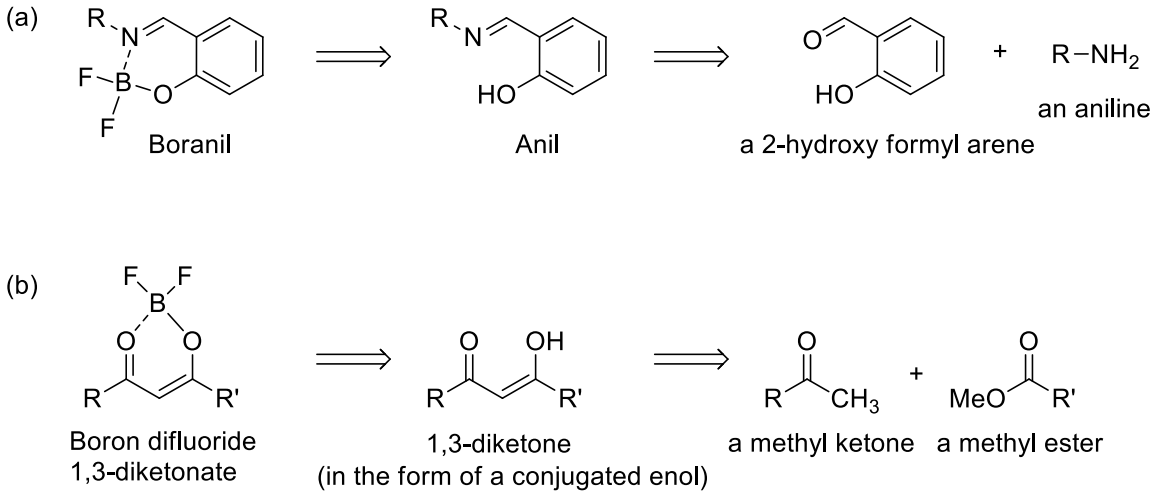

Figure 1.19: Retrosynthetic analysis of (a) boranils and (b) boron difluoride 1,3-diketonates.

1.3.2 α-Cyanostilbene

The role of the α-cyanostilbene (Figure 1.20) unit in organic optoelectronic materials was recently reviewed[53] and a 4-nitro α-cyanostilbene-C60 dyad has shown potential as an acceptor for use in high-performance polymer solar cells.[54]

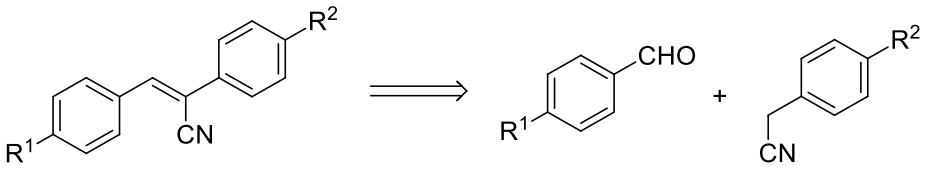

Figure 1.20: Structure of the α-cyanostilbene unit, and its component building blocks.

This family of molecules typically absorbs at around 500 nm and fluorescence emission can be tuned out to 600 nm.[53]

1.4 Aims of this Project

The main objective of the work described in this thesis was to prepare several families of porphyrin-chromophore conjugates, where the conjugates were either boranils, α-cyanostilbenes or boron 1,3-diketonates. A preliminary examination of photo-physical structure-property relationships between related molecules was also conducted using UV-visible absorption and fluorescence emission spectroscopy, basically looking for any evidence of interactions between the chromophores.

Three different porphyrin frameworks were chosen, as illustrated in Figure 1.21.

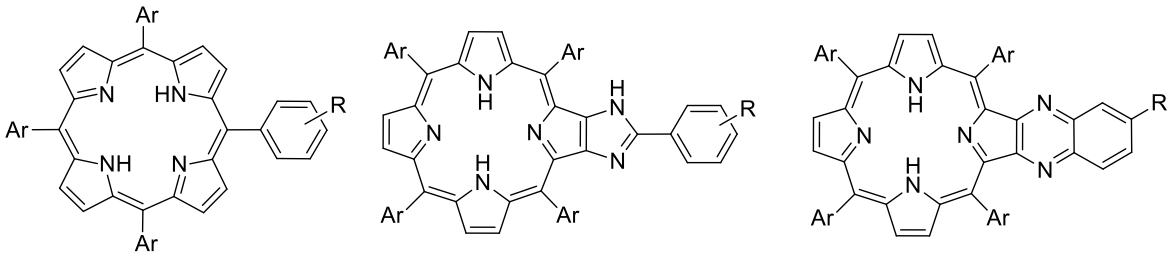

(a) Ar = 3,5-di-*tert*-butylphenyl (b) (c)

R = boranil chromomphore (*via* an amino group, introduced initially as a nitro group) or
α-cyanostilbene chromophore (*via* a formyl group, introduced initially as an ester group) or
boron difluoride 1,3-diketonate (*via* a methyl ester group)

Figure 1.21: The three porphyrin frameworks that were targeted for conjugation to boranil, α-cyanostilbene and boron difluoride 1,3-diketonate chromophores.

Framework (a) allows a comparison between different spatial arrangements of the secondary chromophore with respect to the porphyrin macrocycle. It is known that the placement of an electron-donating or electron-withdrawing group at a β-pyrrolic position causes greater electronic effects than a similar placements at the *meso*-position, as a result of perturbation of the molecular orbital energies, and in turn plays a role in tuning the photo-physical properties.[71] This was the rationale in the choice of frameworks (b) and (c), that both contain fused heterocyclic moieties at the β-pyrrolic positions. Framework (b) also allows for some spatial variation in terms of secondary chromophore placement, with the secondary chromophore located more remotely from the macrocyclic ring than for framework (a). Between these three classes of framework, it was hoped that some systematic trends would be observed with respect to the photo-physical properties of the compounds.

In this regard, the specific aims of the work described in this Thesis were to:

(i) Prepare amino-functionalised porphyrin frameworks of the type illustrated in Figure 1.21, where R = NH_2.

(ii) Use the amino building blocks from (i) to synthesise boranil-porphyrin conjugates, with linkages through the *meso*-phenyl ring, a phenyl-appended imidazole-fused porphyrin and a quinoxaline-fused porphyrin.

(iii) Prepare formyl-functionalised porphyrin frameworks of the type illustrated in Figure 1.21, where R = CHO.

(iv) Use the formyl-functionalised building blocks from (iii) to synthesise α-cyanostilbene-porphyrin conjugates, with linkages through the *meso*-phenyl ring, a phenyl-appended imidazole-fused porphyrin and a quinoxaline-fused porphyrin.

(v) Prepare ester-functionalised porphyrin frameworks of the type illustrated in Figure 1.21, where R = CO_2Me.

(vi) Use the ester-functionalised building blocks from (v) to synthesise boron difluoride 1,3-diketonate-porphyrin conjugates, with linkages through the *meso*-phenyl ring, a phenyl-appended imidazole-fused porphyrin and a quinoxaline-fused porphyrin.

(vii) Conduct preliminary photo-physical studies on the systems prepared in (ii), (iv) and (vi) by examining their UV-visible absorption and fluorescence emission spectra.

(viii) Prepare two different families of boron difluoride 1,3-diketonates capable of forming complexes with metalloporphyrins; one series bearing a phenolate unit for coordination to tin(IV) porphyrins, and the other series bearing a 4-pyridyl unit for coordination to zinc(II) porphyrins.

1.5 References

1. Lee, C. Y.; Farha, O. K.; Hong, B. J.; Sarjeant, A. A.; Nguyen, S. T.; Hupp, J. T. *J. Am. Chem. Soc.* **2011**, *133* (40), 15858-15861.
2. Deisenhofer, J.; Michel, H. *Bioscience Reports* **1989,** *9*, 383-419.
3. Kraub, N.; Schubert, W.-D.; Klukas, O.; Fromme, P.; Witt, H. T.; Saenger, W. *Nature Struct. Biol.* **1996,** *3*, 965-973.
4. Eu, S.; Hayashi, S.; Umeyama, T.; Matano, Y.; Araki, Y.; Imahori, H. *J. Phy. Chem., C* **2008**, *112*, 4396-4405.

5. Liao, M. S.; Scheiner, S. *J. Chem. Phy.* **2002**, *117*, 205-219.

6. Tkachenko, N. V.; Lemmetyinen, H.; Sonoda, J.; Ohkubo, K.; Sato, T.; Imahori, H.; Fukuzumi, S. *J. Phys. Chem. A* **2003**, *107*, 8834-8844.

7. Rothemund, P. *J. Am. Chem. Soc.* **1935**, *57*, 2010-2011.

8. Rothemund, P. *J. Am. Chem. Soc.* **1936**, *58*, 625-627.

9. Adler, A. D.; Longo, F. R.; Shergalis, W. *J. Am. Chem. Soc.* **1964**, *86*, 3145-3149.

10. Adler, A. D.; Longo, F. R.; Finarelli, J. D.; Goldmacher, J.; Assour, J.; Korsakoff, L. *J. Org. Chem.* **1967**, *32*, 476.

11. In: The Porphyrin Handbook: Synthesis and Organic Chemistry, **2000**, Vol. 1, 80-81. Ed. Karl M. Kadish, Kevin M. Smith, Roger Guilard. Academic Press, UK.

12. Lindsey, J. S.; Hsu, I. C.; Schreiman, I. C. *Tetrahedron Lett.* **1986**, *27*, 4969-4970.

13. Lindsey, J. S.; Schreiman, I. C.; Hsu, H. C.; Kearney, P. C. *J. Org. Chem.* **1987**, *52*, 827-836.

14. Littler, B. J.; Ciringh, Y.; Lindsey, J. S. *J. Org. Chem.* **1999**, *64*, 2864-2872.

15. Rao, P. D; Dhanalekshmi, S.; Littler, B. J.; Lindsey, J. S. *J. Org. Chem.*, **2000**, *65*, 7323-7344.

16. Khan, T. K.; Broring, M.; Mathur, S.; Ravikanth, M. *Coord. Chem. Rev.* **2013**, *257* (15-16), 2348-2387.

17. Li, F.; Yang, S. I.; Ciringh, Y.; Seth, J.; Martin, C. H.; Singh, D. L.; Kim, D.; Birge, R. R.; Bocian, D. F.; Holten, D.; Lindsey, J. S. *J. Am. Chem. Soc.* **1998**, *120* (39), 10001-10017.

18. D'Souza, F.; Smith, P. M.; Zandler, M. E.; McCarty, A. L.; Itou, M.; Araki, Y.; Ito, O. *J. Am. Chem. Soc.* **2004**, *126* (25), 7898-7907.

19. Maligaspe, E.; Kumpulainen, T.; Subbaiyan, N. K.; Zandler, M. E.; Lemmetyinen, H.; Tkachenko, N. V.; D'Souza, F. *Phys. Chem. Chem. Phys.* **2010**, *12* (27), 7434-7444.

20. Lazarides, T.; Charalambidis, G.; Vuillamy, A.; Reglier, M.; Klontzas, E.; Froudakis, G.; Kuhri, S.; Guldi, D. M.; Coutsolelos, A. G. *Inorg. Chem.* **2011**, *50* (18), 8926-8936.

21. Leonardi, M. J.; Topka, M. R.; Dinolfo, P. H. *Inorg. Chem.* **2012**, *51* (24), 13114-13122.

22. Khan, T. K.; Ravikanth, M. *Tetrahedron* **2011**, *67* (32), 5816-5824.

23. Khan, T. K.; Ravikanth, M. *Tetrahedron* **2012**, *68* (3), 830-840.

24. Lazarides, T.; Kuhri, S.; Charalambidis, G.; Panda, M. K.; Guldi, D. M.; Coutsolelos, A. G. *Inorg. Chem.* **2012**, *51* (7), 4193-4204.

25. Eggenspiller, A.; Takai, A.; El-Khouly, M. E.; Ohkubo, K.; Gros, C. P.; Bernhard, C.; Goze, C.; Denat, F.; Barbe, J.-M.; Fukuzumi, S. *J. Phy. Chem. A* **2012**, *116* (15), 3889-3898.

26. Woggon, W.-D. *Acc. Chem. Res.* **2005**, *38* (2), 127-136.

27. Warnan, J.; Buchet, F.; Pellegrin, Y.; Blart, E.; Odobel, F. *Org. Lett.* **2011**, *13* (15), 3944-3947.

28. Bandi, V.; Ohkubo, K.; Fukuzumi, S.; D'Souza, F. *Chem. Commun.* **2013**, *49* (28), 2867-2869.

29. Osuka, A.; Yamada, H.; Maruyama, K.; Mataga, N.; Asahi, T.; Ohkouchi, M.; Okada, T.; Yamzaki, I.; Y., N. *J. Am. Chem. Soc.* **1993**, *115*, 9439-9452.

30. Gust, D.; Moore, T. A.; Moore, A. L.; Devadoss, C.; Liddell, P. A.; Hermant, R.; Nieman, R. A.; Demanche, L. J.; DeGraziano, J. M.; Gouni, I. *J. Am. Chem. Soc.* **1992**, *114* (10), 3590-3603.

31. Olguin, M.; Basurto, L.; Zope, R. R.; Baruah, T. *J. Chem. Phy.* **2014**, *140* (20), 204309.

32. Kroto, H. W.; Heath, J. R.; O'Brien, S. C.; Curl, R. F.; Smalley, R. E. *Nature* **1985**, *318*, 162-163.

33. Schuster, D. I.; MacMahon, S.; Guldi, D. M.; Echegoyen, L.; Braslavsky, S. E. *Tetrahedron* **2006**, *62* (9), 1928-1936.

34. Guldi, D. M. *Chem. Soc. Rev.* **2002**, *31*, 22-36.

35. Konishi, T.; Ikeda, A.; Shinkai, S. *Tetrahedron* **2005**, *61* (21), 4881-4899.

36. Imahori, H.; Tamaki, K.; Guldi, D. M.; Luo, C.; Fujitsuka, M.; Ito, O.; Sakata, Y.; Fukuzumi, S. *J. Am. Chem. Soc.* **2001**, *123* (11), 2607-2617.

37. Yang, S. K.; Li, J.; Cho, S. H.; Kim, D.; Bocian, D. F.; Holten, D.; Lindsey, J. S. *J. Mat. Chem.* **2000**, *10* (2), 283-296.

38. Miller, M. A.; Lammi, R. K.; Prathapan, S.; Holten, D.; Lindsey, J. S. *J. Org. Chem.* **2000**, *65* (20), 6634-6649.

39. Toa, M.; Liu, L.; Liu, D.; Zhou, X. *Dyes Pigm.* **2010**, *85*, 21-26.

40. Vicente, M. G. H.; Jaquinod, L.; Smith, K. M. *Chem. Commun.* **1999**, 1771-1782.

41. Kim, D.; Cho, H. S.; Osuka, A.; Aratani, N. *J. Photochem. Photobio., C* **2002**, *3*, 25-52.

42. Imahori, H. *J. Phys. Chem., B* **2004**, *108*, 6130-6143.

43. Shah, M.; Thangaraj, K.; Soong, M.-L.; Wolford, L. T.; Boyer, J. H.; Politzer, I. R.; Pavlopoulos, T. G. *Heteroat. Chem.* **1990**, *1* (5), 389-399.

44. Suzuki, S.; Kozaki, M.; Nozaki, K.; Okada, K. *J. Photochem. Photobiol., C* **2011**, *12* (4), 269-292.

45. Monsma, F. J.; Barton, A. C.; Chol Kang, H.; Brassard, D. L.; Haugland, R. P.; Sibley, D. R. *J. Neurochem.* **1989**, *52* (5), 1641-1644.

46. Kobayashi, H.; Ogawa, M.; Alford, R.; Choyke, P. L.; Urano, Y. *Chem. Rev.* **2009**, *110* (5), 2620-2640.

47. Lammi, R. K.; Ambroise, A.; Balasubramanian, T.; Wagner, R. W.; Bocian, D. F.; Holten, D.; Lindsey, J. S. *J. Am. Chem. Soc.* **2000**, *122* (31), 7579-7591.

48. Ziessel, R.; Ulrich, G.; Harriman, A. *New J. Chem.* **2007**, *31* (4), 496-501.

49. Chibani, S.; Charaf-Eddin, A.; Le Guennic, B.; Jacquemin, D. *J. Chem. Theory Comput.* **2013**, *9* (7), 3127-3135.

50. Loudet, A.; Burgess, K. *Chem. Rev.* **2007**, *107* (11), 4891-4932.

51. Yogo, T.; Urano, Y.; Ishitsuka, Y.; Maniwa, F.; Nagano, T. *J. Am. Chem. Soc.* **2005**, *127* (35), 12162-12163.

52. Komatsu, T.; Oushiki, D.; Takeda, A.; Miyamura, M.; Ueno, T.; Terai, T.; Hanaoka, K.; Urano, Y.; Mineno, T.; Nagano, T. *Chem. Commun.* **2011**, *47* (36), 10055-10057.

53. Zhu, L.; Zhao, Y. *J. Mater. Chem. C* **2013**, *1* (6), 1059-1065.

54. Balanay, M. P.; Kim, K. H.; Lee, S. H.; Kim, D. H. *J. Photochem. Photobio., A* **2012**, *248*, 63-72.

Chapter Two

Porphyrin Building Blocks

2.1 Background

This Chapter discusses the syntheses of key porphyrin intermediates for use in the preparation of porphyrin-boranil (Chapter Three, requiring the presence of an amino group), porphyrin-α-cyanostilbene (Chapter Four, requiring the presence of a formyl group) and porphyrin-boron difluoride 1,3-diketonate (Chapter Five, requiring the presence of an ester group) conjugates.

All porphyrins in this work were prepared with 3,5-di-*tert*-butylbenzaladehyde as either three or all four of the aryl units, as the presence of the *tert*-butyl groups imparts greatly enhanced solubility on the resultant porphyrins, in comparison with simple phenyl units.

The three secondary chromophores were to be linked to the porphyrin chromophore in three different ways, through a *meso* aryl ring (with attachment at the *p*-, *m*- and *o*-positions), through a phenyl-appended imidazole ring fused to the porphyrin at the β-pyrrolic position, and through a quinoxaline ring fused to the porphyrin at the β-pyrrolic position, as discussed in Section 1.4 and illustrated in Figure 1.21.

2.2 Synthesis of *meso*-Aryl Functionalised Porphyrins

Meso-aryl functionalised porphyrins were made using a mixed aldehyde approach (as discussed in Section 1.2.1, Figure 1.7), in which a nitro or ester functionalised benzaldehyde was combined with 3,5-di-*tert*-butylbenzaldehyde **1** (prepared as outlined in Scheme 2.1) in a 1:3 ratio, followed by the introduction of pyrrole, as shown in Schemes 2.2 and 2.3, respectively. Using this statistical approach, the desired mono-functionalised porphyrins could be obtained, after chromatography, in yields of 15-22%. In all cases the first porphyrin eluted from the column was 5,10,15,20-tetrakis(3,5-di-*tert*-butylphenyl)porphyrin **2**. Bis-functionalised porphyrins (two isomers, adjacent and opposing *meso*-phenyl rings bearing nitro/ester functionalisation), tris- and tetrakis-functionalised porphyrins were also produced in these reactions but no attempt was made to separate these compounds from one another as they were not used in this work.

Compound **1** was prepared following a literature procedure (Scheme 2.1).[1] Bromination of 3,5-di-*tert*-butyltoluene with *N*-bromosuccinimide and catalytic amount of benzoyl peroxide afforded the 3,5-di-*tert*-benzyl bromide which was then oxidized to **1** in a Sommelet reaction, in an overall yield of 50%.

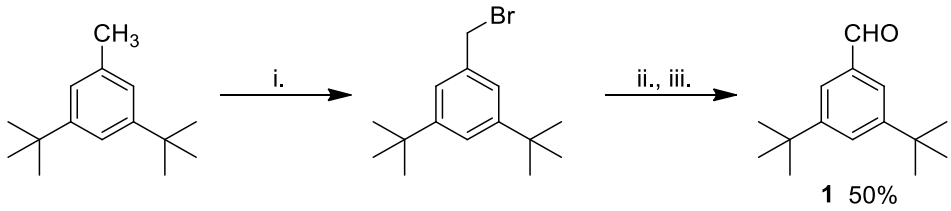

Scheme 2.1: i. NBS, C_6H_6, benzoyl peroxide, reflux; ii. hexamine, EtOH, H_2O, heat; iii. 10 M HCl, reflux.

Meso-functionalised nitroporphyrins **3-5** (*p*-, *m*-, and *o*-isomers) were synthesized by reacting the substituted nitrobenzaldehyde (*p*-, *m*-, and *o*-isomers), one equivalent, with three equivalents of **1**, and four equivalents of pyrrole in chloroform with a catalytic amount of boron trifluoride diethyl etherate, followed by addition of *p*-chloranil as a final oxidation step. In each case, the desired mono-functionalised porphyrins (**3-5** and **12-14**) were isolated from the statistical mixture of porphyrins (see Section 1.2.1, Figure 1.7) as the second band eluted from a chromatography column, after the initial elution of the least polar tetrakis(3,5-di-*tert*-butylphenyl)porphyrin **2**. Reduction of **3-5** was achieved by reaction with tin(II) chloride and concentrated hydrochloric acid in dichloromethane in the dark and under an argon atmosphere, affording **6-8** in moderate to good yields (Scheme 2.2).

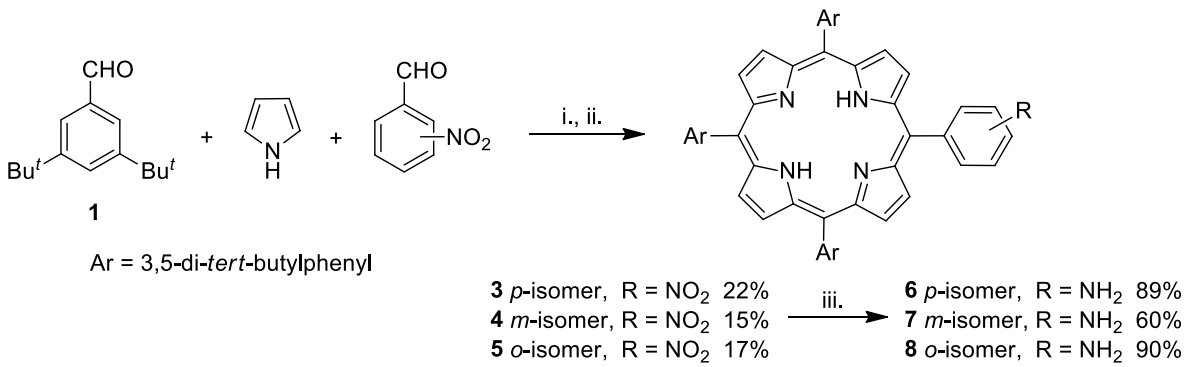

Scheme 2.2: i. BF_3OEt_2, $CHCl_3$, r.t.; ii. *p*-chloranil, reflux; iii. $SnCl_2$, conc. HCl, CH_2Cl_2.

These nitro- and amino-*meso*-phenyl functionalised porphyrins were originally reported in the synthesis of zinc(II) porphyrin C_{60} dyads 1.18.[2] The ester-functionalised benzaldehydes required for the synthesis of ester-functionalised *meso*-phenyl porphyrins were prepared from the corresponding benzoic acids. Methyl 4-formylbenzoate **9** and methyl 3-formylbenzoate **10** were synthesized by esterification of 4-formyl benzoic acid and 3-formyl benzoic acid, in 81% and 83% yields, respectively, as previously reported,[3] using methanol as a solvent and a reagent and sulfuric acid as a catalyst. Methyl 2-formylbenzoate **11** was synthesized in 88% yield by refluxing 2-formylbenzoic acid, methyl iodide and potassium carbonate in *N*,*N*-dimethylformamide according to the literature procedure.[3]

The *meso*-ester functionalised porphyrins **12-14** (*p*-, *m*-, and *o*-isomers) were synthesized in an analogous fashion to their nitro-functionalised relatives (Scheme 2.3).

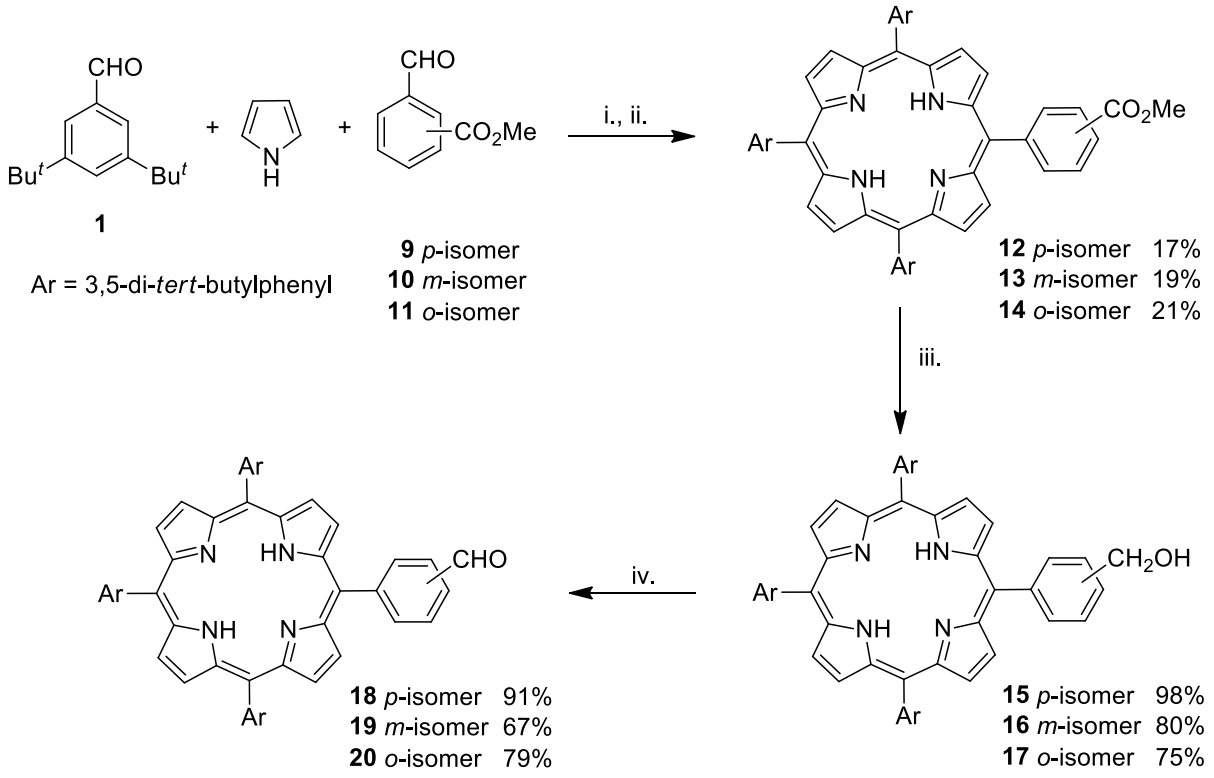

Scheme 2.3: i. BF_3OEt_2, $CHCl_3$, r.t.; ii. *p*-chloranil, reflux; iii. $LiAlH_4$, THF; iv. MnO_2, CH_2Cl_2.

The ester porphyrins **12-14** were reduced to porphyrin alcohols **15-17** in good to excellent yields, using lithium aluminium hydride in dry tetrahydrofuran. Aldehyde porphyrins **18-20** were synthesized by oxidation of **15-17** using manganese dioxide in dichloromethane. All reactions were monitored *via* TLC analysis and the structures of the desired products were confirmed with the aid of ^{1}H and ^{13}C NMR spectroscopy, as well as IR analysis. ^{1}H NMR spectroscopy shows the effect of the porphyrin ring-current on functional groups substituted at the *ortho*-position. Shielding of the methyl ester proton was observed, as the chemical shift of the methyl group moved from 4.15 ppm (*p*-isomer, **12**) or 3.99 (*m*-isomer, **13**) to 2.80 ppm for the *o*-isomer **14**. Similar, though less dramatic, trends were observed for CH_2 protons of the alcohol derivatives (5.05 ppm for the *p*-isomer **15** to 4.40 ppm for the *o*-isomer **17**) and the aldehyde proton (10.38 for the *p*-isomer **18** to 9.55 ppm for the *o*-isomer **20**). The largest chemical shift difference ($\Delta\ \delta$ = 1.35 ppm) for the methyl ester protons (as opposed to the methylene alcohol or aldehyde protons) can be rationalized based on the fact that the methyl ester protons are projected the furthest over the porphyrin ring.

Compound **15** has been used previously in the synthesis of porphyrin dimers incorporating a phenanthroline-ruthenium complex.[4] Compound **18** has been used in the construction of multiporphyrin arrays.[5] Compounds **19** and **20** have been used previously in the preparation of porphyrin-C_{60} dyads, where the formyl group was used in the construction of an *N*-methylpyrrolidine ring that is fused to the C_{60} unit.[6]

2.3 Synthesis of 2,3-dioxo-5,10,15,20-tetrakis(3,5-di-*tert*-butylphenyl)porphyrin

Crossley's porphyrin dione, 2,3-dioxo-5,10,15,20-tetrakis(3,5-di-*tert*-butylphenyl)porphyrin **21**,[7] was a key building block for the synthesis of functionalised fused imidazole (Section 2.4) and quinoxaline-porphyrins (Section 2.5) bearing amino (*via* nitro) or formyl (*via* ester and alcohol) functionality.

The synthesis of **21** involves six steps, using a previously reported method,[7] as shown in Scheme 2.4.

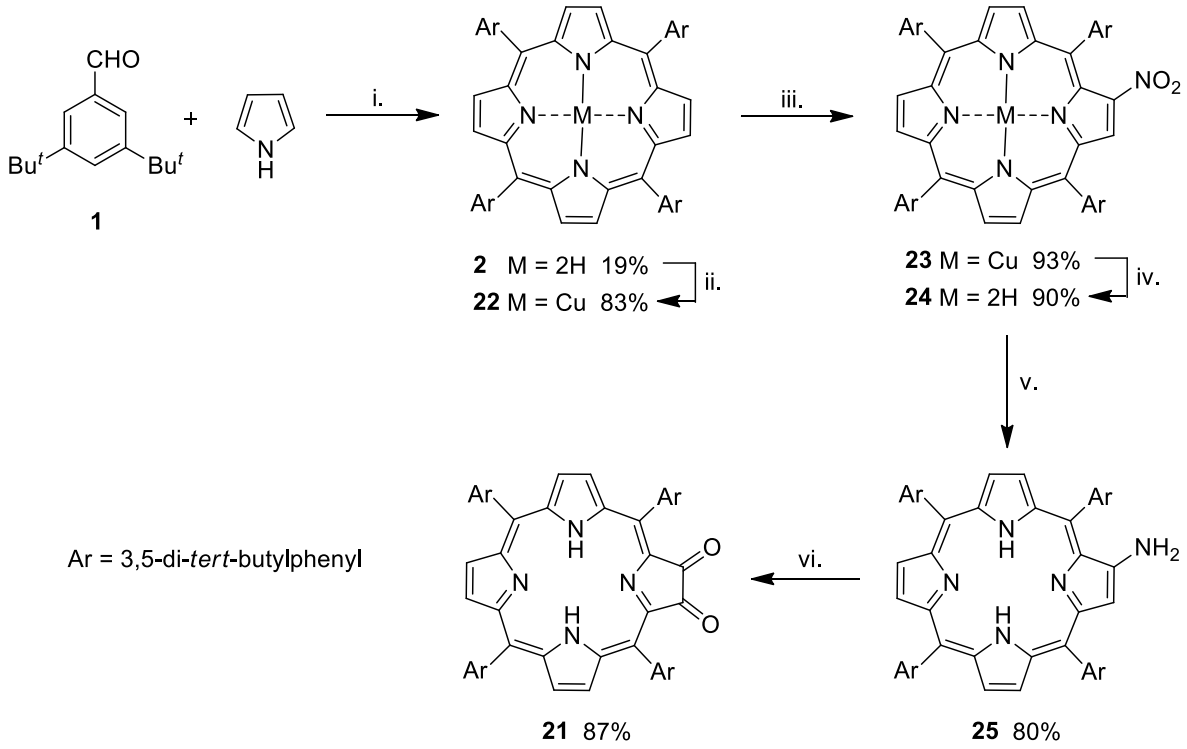

Scheme 2.4: i. Propanoic acid, reflux; ii. $Cu(OAc)_2$, CH_2Cl_2, reflux; iii. 0.5 % (w/v) NO_2 in hexane, CH_2Cl_2; iv. conc. H_2SO_4, CH_2Cl_2; v. $SnCl_2$, conc. HCl, CH_2Cl_2; vi. hν, CH_2Cl_2.

Porphyrin **2** was synthesized by refluxing 3,5-di-*tert*-butylbenzaldehyde **1** and pyrrole in propanoic acid for 1 h. Crude **2** was used without purification for synthesis of copper(II) porphyrin **22** in 83% yield after chromatography. Copper(II) 2-nitro-porphyrin **23** was obtained in 93% yield *via* nitration of **22** with nitrogen oxide in hexane. Demetallation of **23** using concentrated sulfuric acid in dichloromethane afforded **24** in 90% yield after purification. Reduction of **24** was achieved by reaction with tin(II) chloride and concentrated hydrochloric acid in dichloromethane to afford 2-aminoporphyrin **25** in 80% yield. Photo-oxidation of **25** in dichloromethane afforded porphyrin dione **21** in 87% yield after purification.

2.4 Synthesis of Imidazole-fused Porphyrins

Scheme 2.5 and Scheme 2.6 illustrate the synthetic pathways for the preparation of amino-functionalised phenyl imidazoles (*via* the nitro compounds) and formyl-functionalised phenyl imidazoles (*via* the ester and alcohol precursors).

Nitrophenyl imidazole porphyrins **26-28** were synthesized by refluxing **21** with substituted nitrobenzaldehyde (*p*-, *m*-, and *o*-isomers) with ammonium acetate in a mixture of chloroform and glacial acetic acid (Scheme 2.5). Imidazole-fused porphyrins were first reported by Crossley,[8] although all of the analogues prepared for the current work are reported for the first time.

The amino-functionalised imidazole-porphyrins **29-31** were obtained from the nitro compounds **26-28** *via* reduction with tin(II) chloride in a mixture of concentrated hydrochloric acid and dichloromethane.

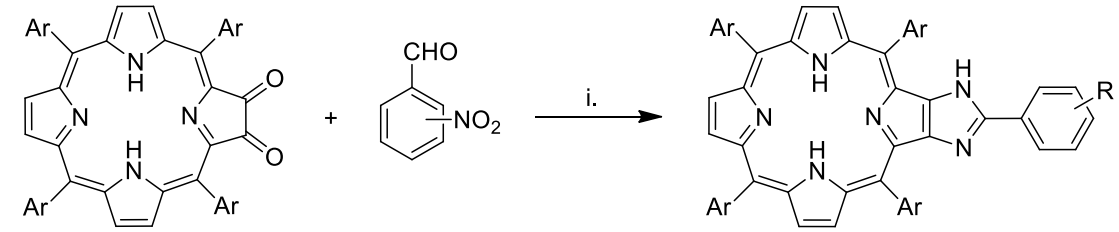

Scheme 2.5: i. NH_4OAc, $CHCl_3$/AcOH (1:1), reflux; ii. $SnCl_2$, conc. HCl, CH_2Cl_2.

The ester-functionalised phenyl imidazole porphyrins **32-34** were synthesized in an analogous fashion to the nitro derivatives, by refluxing **21** with an appropriately substituted formyl methyl benzoate **9-11** (*p*-, *m*-, and *o*-isomers) and ammonium acetate in a mixture of chloroform and glacial acetic acid (Scheme 2.6). The reduction of **32-34** was carried out with lithium aluminium hydride in tetrahydrofuran, to afford the alcohol-functionalised porphyrins **35-36**. The reduction of **34** was unsuccessful, with no trace of **37** from TLC analysis, nor from ^1H

NMR analysis of the reaction mixture after work-up. This was despite the use of various equivalents of either lithium aluminium hydride or sodium borohydride with reaction times of up to several days. The lack of reaction of **34** may be the result of an interaction of the ester group with the imidazole NH. There is evidence of such an interaction in the ^{1}H NMR spectrum, as the imidazole NH proton is visible in the spectrum of **34**, at δ 11.52 ppm, (but not in any of the other ester-, alcohol- or aldehyde-functionalised compounds in this series). Interestingly, the imidazole NH proton is also visible in the spectrum of **28** (the *o*-nitro isomer), at δ 9.48 ppm, (but not in the spectra of the *m*- or *p*-nitro isomers). Oxidation of **35** and **36** to the corresponding aldehydes **38** and **39** proceeded in good yields.

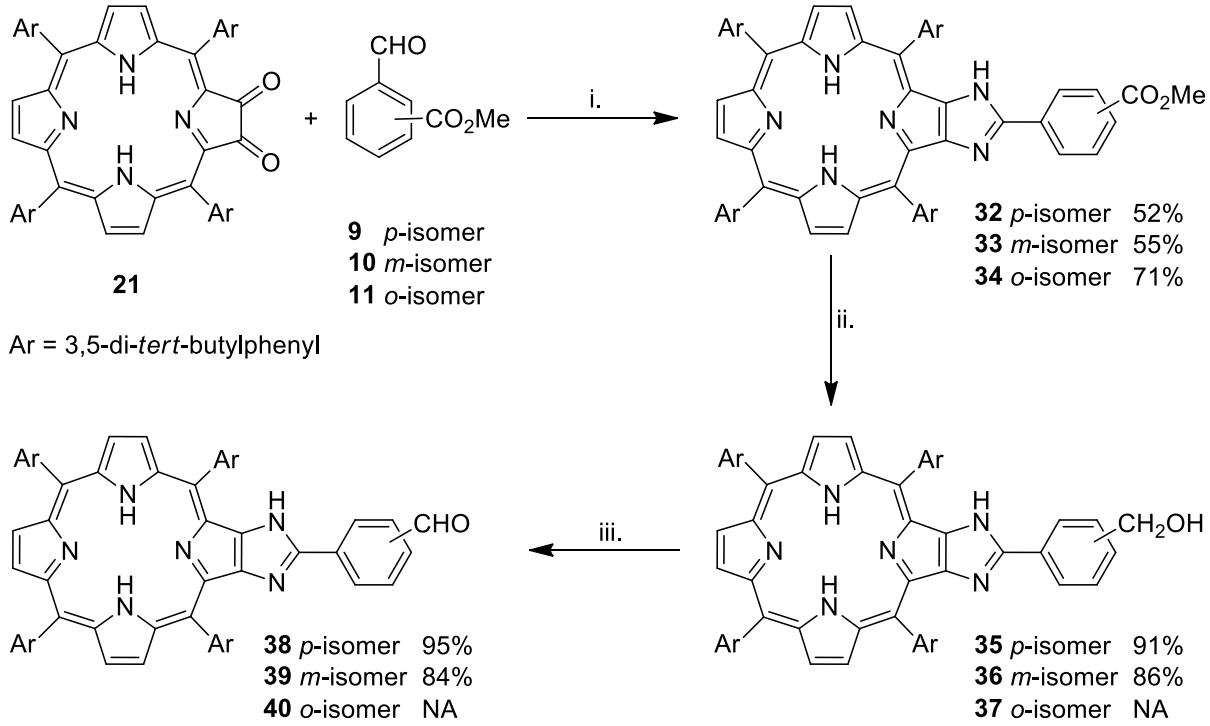

Scheme 2.6: i. NH_4OAc, $CHCl_3$/AcOH (1:1), reflux; ii. $LiAlH_4$, THF; iii. MnO_2, CH_2Cl_2.

The ^{1}H (and ^{13}C) NMR spectra of all imidazole-fused porphyrins prepared in this Chapter, and their derivatives made in Chapters Three and Four, lacked the features of the anticipated symmetry if the imidazole is considered to exist in rapid tautomeric equilibrium on the ^{1}H NMR

timescale, and if there is free rotation about the bond connecting the phenyl and imidazole rings, as illustrated in Figure 2.1.

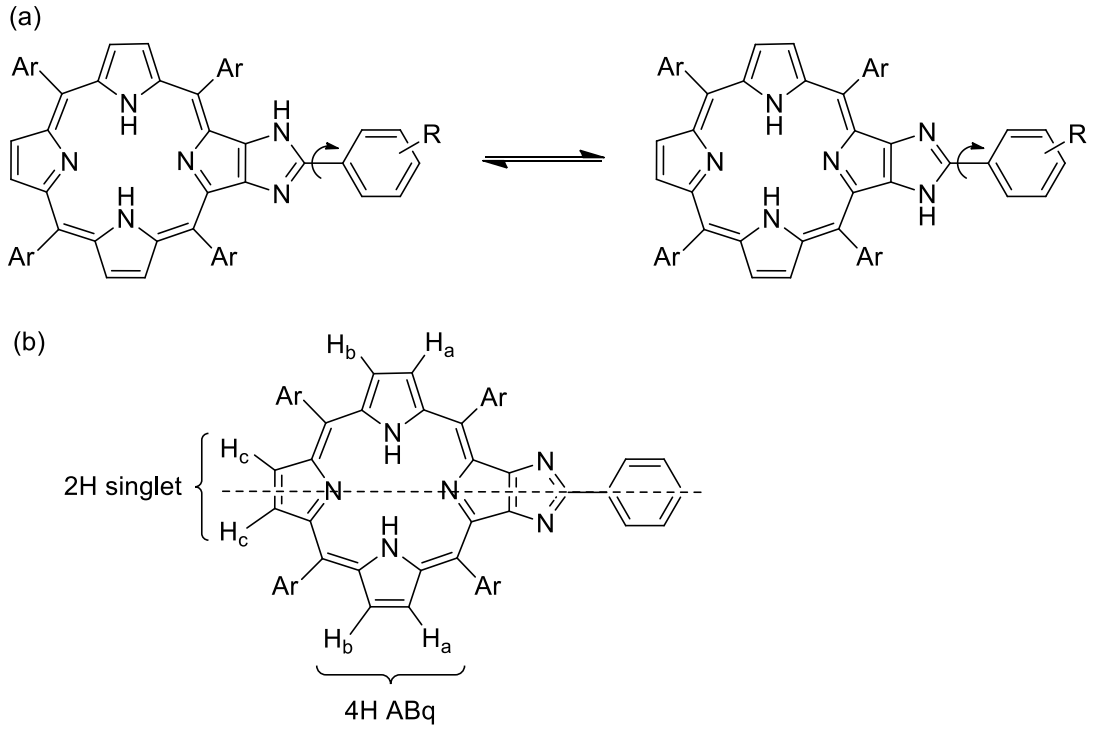

Figure 2.1: (a) Two equivalent tautomers of phenyl-substituted imidazole-fused porphyrins. If there is free-rotation about the bond connecting the phenyl and imidazole rings, the presence of a substitutent on the phenyl ring at the *o*-, *m*- or *p*-positions should not alter the symmetry of the porphyrin unit. (b) The expected plane of symmetry dissecting the porphyrin macrocycle, assuming rapid proton exchange on the imidazole nitrogens on the ^{1}H NMR timescale; the three expected β-pyrrolic environments are highlighted. The imidazole NH proton is omitted to show symmetry.

The reality of the proton environments is quite different from the expectations, as exemplified for the β-pyrrolic environments of **26**, **27** and **28** (*p*-, *m*- and *o*-NO_2 substituted systems) in Figure 2.2 and compounds **32**, **33**, **38** and **39** (*p*- and *m*-methyl ester substituted, and *p*- and *m*-formyl substituted systems) in Figure 2.3.

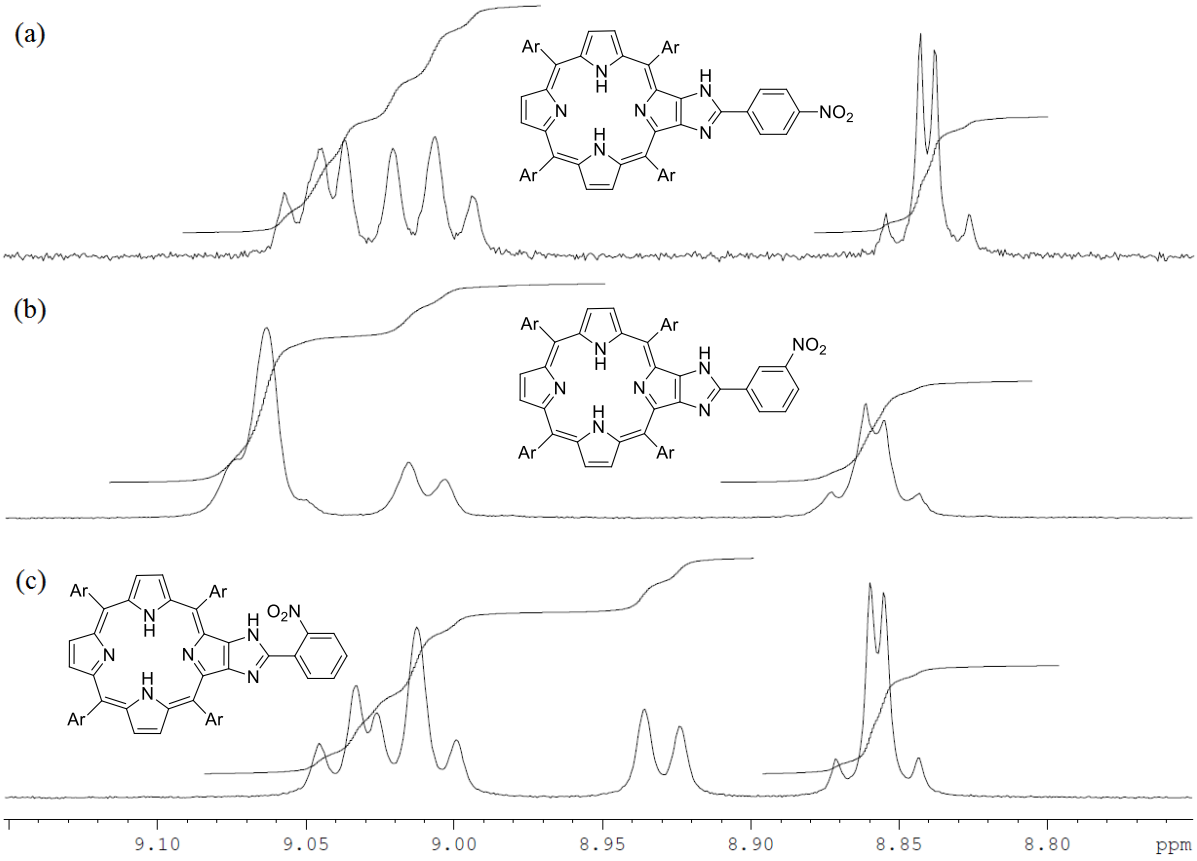

Figure 2.2: A section of the 400 MHz ^{1}H NMR spectra in $CDCl_3$ at 298 K showing the β-pyrrolic protons of (a) **26** (*p*-nitrophenyl imidazole porphyrin), (b) **27** (*m*-nitrophenyl imidazole porphyrin) and (c) **28** (*o*-nitrophenyl imidazole porphyrin).

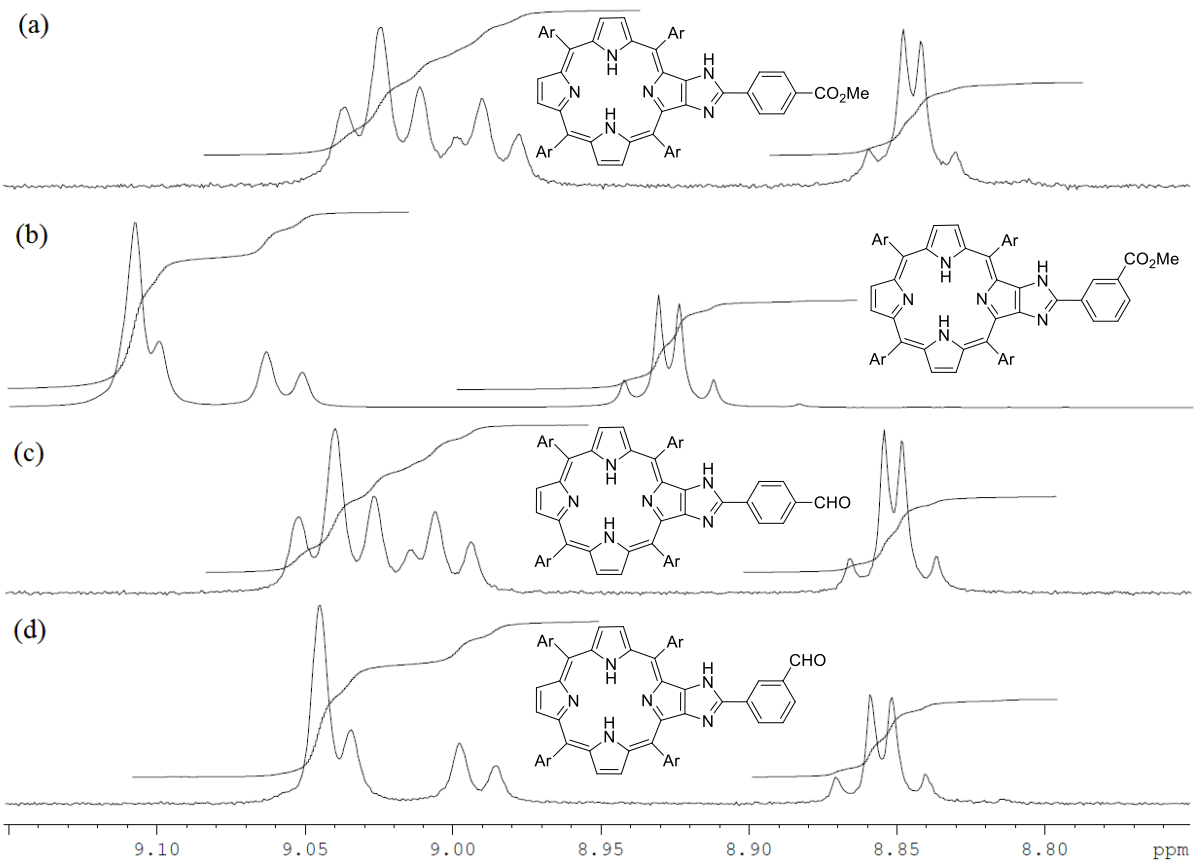

Figure 2.3: A section of the 400 MHz ^{1}H NMR spectra in $CDCl_3$ at 298 K showing the β-pyrrolic protons of (a) **32** (*p*-methylester phenyl imidazole porphyrin), (b) **33** (*m*-methyl ester phenyl imidazole porphyryrin), (c) **38** (*p*-formylphenyl imidazole porphyrin) and (d) **39** (*m*-formylphenyl imidazole porphyrin).

It appears that equilibration is *not* rapid on the ^{1}H NMR timescale, at least not at 298 K. While variable temperature work was not performed as part of this thesis, it would be interesting to see if the appearance of the spectra change to the expected pattern (Figure 2.1 (b)) upon heating. The compounds have very poor solubility in DMSO, however d_6-benzene may be an appropriate solvent for such studies. A possible explanation for the observed behavior may be the formation of a hydrogen bond from the imidazole NH to the π-system of an adjacent *meso*-aryl ring, which may slow the rate of tautomer interconversion.

2.5 Synthesis of Quinoxaline-fused Porphyrins

Nitroquinoxaline porphyrin **41** was synthesized by stirring 4-nitro-1,2-diaminobenzene with **21** and pyridine in chloroform for 5 days (Scheme 2.7). Reduction to afford the 6-amino derivative **42** proceeded in good yield.

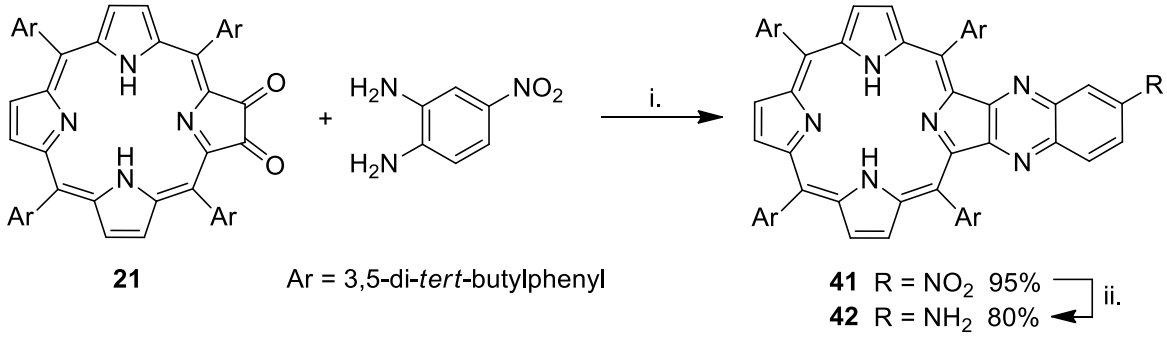

Scheme 2.7: i $CHCl_3$, pyridine; ii. $SnCl_2$, conc. HCl, CH_2Cl_2.

The synthesis of ester-functionalised quinoxaline porphyrin **43** and its conversion to the alcohol **44** and formyl **45** derivatives is shown in Scheme 2.8. **43** was synthesized by stirring methyl 3,4-diaminobenzoate with **21** and pyridine in chloroform for 5 days. The alcohol-functionalised quinoxaline porphyrin **44** was synthesized by refluxing **43** and sodium borohydride in tetrahydrofuran followed by addition of methanol. As for the previous oxidation reactions to afford formyl functionalisation, the aldehyde-functionalised quinoxaline porphyrin **45** was synthesized by oxidation of alcohol **44** with manganese oxide.

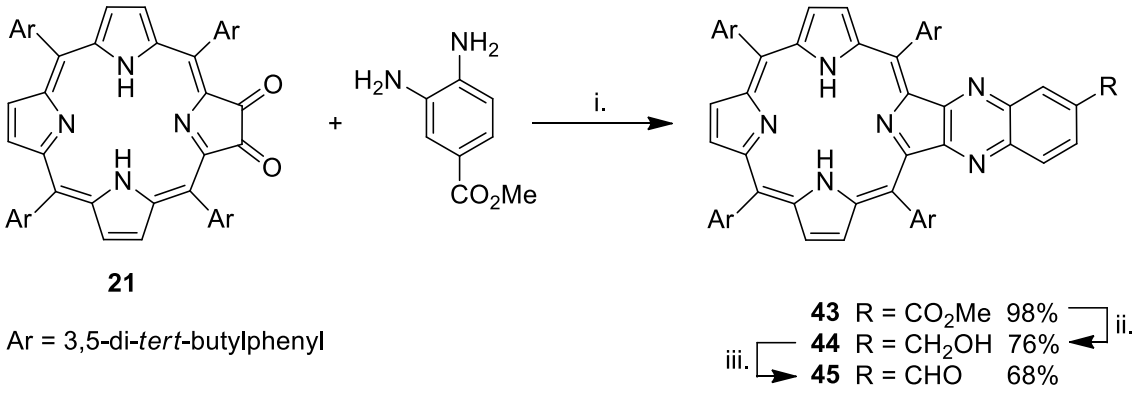

Scheme 2.8: i. $CHCl_3$, pyridine; ii. $NaBH_4$, THF; iii. MnO_2, CH_2Cl_2.

2.6 Conclusion

In summary, several of the compounds reported in this Chapter have been reported previously. The compounds reported for the first time include nitro/amino/ester/alcohol/formyl functionalised phenyl-imidazole porphyrins and the 6'- ester/alcohol/formyl quinoxaline porphyrins. A considerable amount of time and effort was required to prepare and characterize the appropriately functionalised compounds as starting materials for the synthesis of new dyads, that are described in Chapters Three and Four.

2.7 Experimental

2.7.1 Materials and Methods

Solvents and reagents were purified using standard techniques. All commercial solvents were either routinely distilled prior to use or purchased in high-purity form (HPLC quality). Hexane refers to the fraction of b.p. 60-80 °C. Where solvent mixtures are used, the portions are given by volume. Column chromatography was routinely carried out using the gravity feed column techniques on Merck silica gel type 9385 (230-400 mesh) with the stated solvent systems. All reactions were monitored by using Thin Layer Chromatography (TLC) on 0.25 mm E-Merck silica gel 60 F254 pre-coated plates (0.2 mm). Melting points were recorded on Stuart Scientific SM10 and are uncorrected. ^{1}H (400 MHz) and ^{13}C (100 MHz) NMR spectra were recorded at 25 °C on a Bruker DPX400 spectrometer using $CDCl_3$ (7.26 ppm for ^{1}H and 77 ppm for ^{13}C) and DMSO d_6 (2.49 ppm for ^{1}H and 39.5 ppm for ^{13}C) as solvent and also as internal standards. Signals were recorded in terms of chemical shifts, multiplicity, relative integral values and coupling constants (in Hz), in that order. The following abbreviations for multiplicity are used: app., apparent; s, singlet; d, doublet; t, triplet; m, multiplet; dd, doublet of doublets; br, broad; q, quartet; qn, quintet; ABq, AB quartet. IR spectra were recorded on a Nicolet iS10 FT-IR spectrometer at 298 K unless otherwise stated. The following abbreviations for peak

characteristics are used; s, strong; m, medium; w, weak; br, broad. Microanalyses were performed on a Perkin Elmer 2400 Series II CHNS/O Analyzer at Macquarie University.

3,5-Di-*tert*-butylbenzaldehyde 1

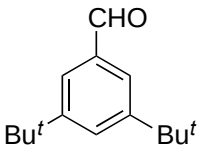

In a mixture of 3,5-di-*tert*-butyltoluene (38.7 g, 0.19 mol) and *N*-bromosuccinimide (51.6 g, 0.29 mol) in benzene (350 mL) was added benzoyl peroxide (2.1 g, 0.85 mmol). The reaction mixture was heated at reflux under constant stirring for 4 h. On cooling, the reaction mixture was filtered and benzene was removed under *vacuo* obtaining crude 1-(bromomethyl)-3,5-di-*tert*-butylbenzene. The crude product was dissolved in a mixture of ethanol/water (120 mL, 1:1), hexamine (80.0 g, 0.57 mol) was added and the reaction mixture was heated at reflux for 4 h. Hydrochloric acid (10 M, 35 mL) was added in the reaction mixture over a 30 min period and then refluxing was continued for another 30 min. On cooling, ethanol was removed under *vacuo*. The aqueous layer obtained was extracted in diethyl ether (2 x 100 mL). The combined diethyl ether layers were washed with brine (150 mL), dried over anhydrous sodium sulfate, filtered and the solvent was removed under *vacuo* affording a yellow oily product. The crude product was washed with dry ice chilled ethanol to afford white crystals of **1** (20.5 g, 50%). m.p. 86-87 °C (lit.[1] 86 °C). ^{1}H NMR (400 MHz, $CDCl_3$) δ 1.37 (s, 18H, CH_3), 7.71-7.73 (m, 3H, ArH), 10.01 (s, 1H, CHO) ppm. The spectroscopic data are in agreement with those reported in the literature.[1]

2.7.2 Preparation of *meso*-Aminophenyl Porphyrins

Nitrophenyl Porphyrins 3-5

General Procedure: To a mixture of substituted nitrobenzaldehyde (using either the *o*-, *m*- or *p*-nitrobenzaldehyde isomer) (0.38 g, 2.5 mmol) and 3,5-di-*tert*-butylbenzaldehyde **1** (1.64 g, 7.5

mmol) in chloroform (700 mL) was added pyrrole (0.67 g, 10 mmol) under an argon atmosphere. After 15 min, a catalytic amount of boron trifluoride diethyl etherate (0.02 mL) was added very slowly and the reaction mixture was stirred for 1 h. *p*-Chloranil (1.82 g, 7.4 mmol) was added and the reaction mixture was heated to reflux in air for 1.5 h. On completion, the reaction mixture was concentrated, fluorosil (5.0 g) was added and the dried powder of the reaction mixture adsorbed onto fluorosil was purified by column chromatography (silica gel, dichloromethane/hexane 1:1) to afford the desired mono-nitrophenyl porphyrin. The first compound eluted was 5,10,15,20-tetrakis(3,5-di-*tert*-butylphenyl)porphyrin **2** (117 mg, 6%), as purple microcrystals. m.p. > 300 °C. ^{1}H NMR (400 MHz, $CDCl_3$) δ -2.67 (br s, 2H, NH), 1.52 (s, 72H, CH_3), 7.78 (t, 4H, *J* = 1.8 Hz, ArH), 8.08 (d, 8H, *J* = 1.8 Hz, ArH), 8.89 (br s, 8H, β-pyrrolic H) ppm. The spectroscopic data are in agreement with those reported in the literature.[9] In each case the second compound was the desired mono-nitrophenyl porphyrin **3-5**, and all other porphyrins were collected together, evaporated to dryness and not used further in the current work.

10,15,20-Tris(3,5-di-*tert*-butylphenyl)-5-(4-nitrophenyl)porphyrin 3

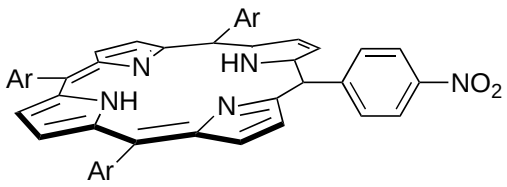

Starting with 4-nitrobenzaldehyde, **3** (0.54 g, 22%) was obtained as a purple microcrystalline solid. m.p. > 300 °C. ^{1}H NMR (400 MHz, $CDCl_3$) δ -2.69 (br s, 2H, NH), 1.52 (s, 18H, CH_3), 1.53 (s, 36H, CH_3), 7.79-7.82 (m, 3H, ArH), 8.07-8.09 (m, 6H, ArH), 8.42 (d, 2H, *J* = 8.0 Hz, ArH), 8.64 (d, 2H, *J* = 8.7 Hz, ArH), 8.73 (ABq, 2H, J_{AB} = 4.7 Hz, β-pyrrolic H), 8.91- 8.93 (m, 6H, β-pyrrolic H) ppm. The spectroscopic data are in agreement with those reported in the literature.[2]

10,15,20-Tris(3,5-di-*tert*-butylphenyl)-5-(3-nitrophenyl)porphyrin 4

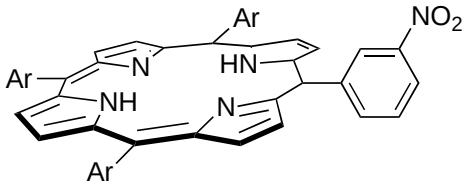

Starting with 3-nitrobenzaldehyde, **4** (0.37 g, 15%) was obtained as a purple microcrystalline solid. m.p. > 300 °C. ^{1}H NMR (400 MHz, $CDCl_3$) δ -2.69 (br s, 2H, NH), 1.52-1.54 (m, 54H, CH_3), 7.80-7.82 (m, 3H, ArH), 7.94 (app. t, 1H, J = 7.8 Hz, ArH), 8.07-8.09 (m, 6H, ArH), 8.57-8.59 (m, 1H, ArH), 8.65-8.68 (m, 1H, ArH), 8.72 (ABq, 2H, J_{AB} = 4.8 Hz, β-pyrrolic H), 8.92-8.94 (m, 6H, β-pyrrolic H), 9.10 (app. t, 1H, J = 1.9 Hz, ArH) ppm. The spectroscopic data are in agreement with those reported in the literature.[2]

10,15,20-Tris(3,5-di-*tert*-butylphenyl)-5-(2-nitrophenyl)porphyrin 5

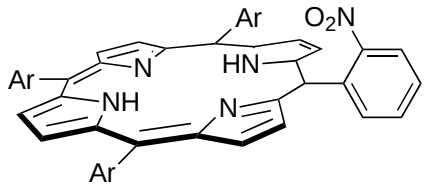

Starting with 2-nitrobenzaldehyde, **5** (0.44 g, 17%) was obtained as a purple microcrystalline solid. m.p. > 300 °C. ^{1}H NMR (400 MHz, $CDCl_3$) δ -2.64 (br s, 2H, ArH), 1.50-1.56 (m, 54H, CH_3), 7.78-7.80 (m, 3H, ArH), 7.93-7.97 (m, 2H, ArH), 8.02-8.04 (m, 2H, ArH), 8.06-8.08 (m, 2H, ArH), 8.11-8.13 (m, 2H, ArH), 8.27-8.30 (m, 1H, ArH), 8.43-8.46 (m, 1H, ArH), 8.63 (ABq, 2H, J_{AB} = 4.7 Hz, β-pyrrolic H), 8.87-8.88 (m, 6H, β-pyrrolic H) ppm. The spectroscopic data is in agreement with that reported in the literature.[2]

Aminophenyl Porphyrins 6-8

General Procedure: To a mixture of mono-nitrophenyl porphyrin (using either the mono *o*-, *m*- or *p*-nitrophenyl porphyrin isomer) **3-5** (500 mg, 0.50 mmol) and anhydrous stannous chloride (0.95 g, 5.0 mmol) in dichloromethane (50 mL), was added hydrochloric acid (10 M, 2.5 mL) under an argon atmosphere. The reaction mixture was stirred for 4 days. The organic layer was

washed with water (2 x 50 mL), sodium hydroxide solution (3 M, 2 x 50 mL), water (50 mL) and brine (50 mL), dried over anhydrous sodium sulfate, filtered and evaporated to dryness under vacuum. The crude compound obtained was purified by column chromatography (silica gel, dichloromethane/hexane 1:1) to give pure aminophenyl porphyrin **6-8**.

5-(4-Aminophenyl)-10,15,20-tris(3,5-di-*tert*-butylphenyl)porphyrin 6

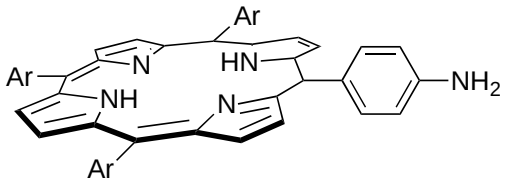

Starting with **3**, **6** (430 mg, 89%) was obtained as a purple microcrystalline solid. m.p. > 300 °C. ^{1}H NMR (400 MHz, $CDCl_3$) δ -2.67 (br s, 2H, NH), 1.52 (s, 18H, CH_3), 1.53 (s, 36H, CH_3), 4.01 (br s, 2H, NH_2), 7.07 (d, 2H, *J* = 8.2 Hz, ArH), 7.78-7.81 (m, 3H, ArH), 8.02 (d, 2H, *J* = 8.2 Hz, ArH), 8.08 (d, 2H, *J* = 1.8 Hz, ArH), 8.09 (d, 4H, *J* = 1.8 Hz, ArH), 8.86-8.90 (m, 6H, β-pyrrolic H) 8.94 (ABq, 2H, J_{AB} = 4.7 Hz, β-pyrrolic H) ppm. The spectroscopic data are in agreement with those reported in the literature.[2]

5-(3-Aminophenyl)-10,15,20-tris(3,5-di-*tert*-butylphenyl)porphyrin 7

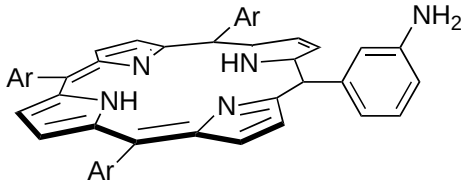

Starting with **4**, **7** (258 mg, 60%) was obtained as a purple microcrystalline solid. m.p. > 300 °C. ^{1}H NMR (400 MHz, $CDCl_3$) δ -2.68 (br s, 2H, NH), 1.54 (s, 18H, CH_3), 1.55 (s, 36H, CH_3), 3.91 (br s, 2H, NH_2), 7.06-7.10 (m, 1H, ArH), 7.51 (app. t, 1H, *J* = 7.8 Hz, ArH), 7.57-7.59 (m, 1H, ArH), 7.65-7.68 (m, 1H, ArH), 7.80-7.82 (m, 3H, ArH), 8.09-8.12 (m, 6H, ArH), 8.89 and 8.96 (ABq, 4H, J_{AB} = 4.7 Hz, β-pyrrolic H), 8.91 (s, 4H, β-pyrrolic H), ppm. The spectroscopic data is in agreement with that reported in the literature.[2]

5-(2-Aminophenyl)-10,15,20-tris(3,5-di-*tert*-butylphenyl)porphyrin 8

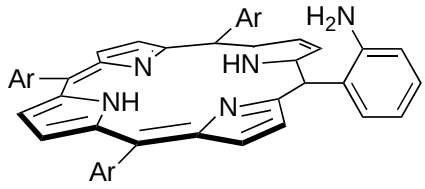

Starting with **5**, **8** (387 mg, 90%) was obtained as a purple microcrystalline solid. m.p. > 300 °C. ^{1}H NMR (400 MHz, $CDCl_3$) δ -2.63 (br s, 2H, NH), 1.53-1.55 (m, 54H, CH_3), 3.60 (br s, 2H, NH_2), 7.11-7.15 (m, 1H, ArH), 7.16-7.21 (m, 1H, ArH), 7.58-7.63 (m, 1H, ArH), 7.80-7.82 (m, 3H, ArH), 7.90-7.93 (m, 1H, ArH), 8.08-8.12 (m, 6H, ArH), 8.90-8.92 (app. s, 8H, β-pyrrolic H) ppm. The spectroscopic data is in agreement with that reported in the literature.[2]

2.7.3 Preparation of *meso*-Formylphenyl Porphyrins

Preparation of Methyl Formylbenzoates

Methyl 4-formylbenzoate 9

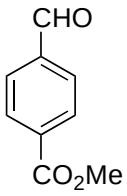

4-Formylbenzoic acid (10.0 g, 66.7 mmol) was dissolved in methanol (100 mL) followed by addition of conc. sulfuric acid (4 mL). The reaction mixture was heated to reflux overnight. On cooling, methanol was removed under vacuum. The residue was dissolved in ethyl acetate (100 mL), washed with sodium hydroxide (3 M, 3 x 100 mL), brine (100 mL), dried over anhydrous sodium sulfate, filtered and evaporated to dryness under vacuum. Crude methyl 4-formylbenzoate **9** (8.8 g, 81%) was obtained as a white solid and used without further purification. m.p. 60-62 °C (lit.[3] 61-62 °C). ^{1}H NMR (400 MHz, $CDCl_3$) δ 3.94 (s, 3H, CH_3), 7.95 (d, 2H, *J* = 8.2 Hz, ArH), 8.20 (d, 2H, *J* = 8.2 Hz, ArH), 10.08 (s, 1H, CHO) ppm. The spectroscopic data are in agreement with those reported in the literature.[3]

Methyl 3-formylbenzoate 10

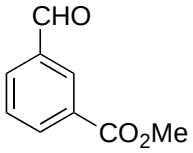

As described above, starting with 3-formylbenzoic acid. Crude methyl 3-formylbenzoate **10** (9.1 g, 83%) was obtained as a white solid and used without further purification. m.p. 50-52 °C (lit.[3] 51-52 °C). ^{1}H NMR (400 MHz, $CDCl_3$) δ 3.96 (s, 3H, CH_3), 7.62 (app. t, 1H, *J* = 7.4 Hz, ArH), 8.06-8.10 (m, 1H, ArH), 8.28-8.32 (m, 1H, ArH), 8.58 (app. t, 1H, *J* = 1.7 Hz, ArH), 10.07 (s, 1H, CHO) ppm. The spectral data are in agreement with those reported in the literature.[3]

Methyl 2-formylbenzoate 11

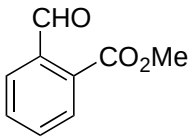

2-Formylbenzoic acid (6.0 g, 40 mmol) was dissolved in DMF (30 mL), followed by addition of methyl iodide (5.0 mL, 11.36 g, d 2.28 g/mL, 100 mmol) and potassium carbonate (2.76 g, 200 mmol). The reaction mixture was heated to reflux for 1 h. On cooling, water (40 mL) was added in the reaction mixture and extracted in dichloromethane (100 mL). The organic layer was washed with water (2 x 100 mL), saturated sodium bicarbonate (3 x 100 mL), brine (100 mL), dried over anhydrous sodium sulfate, filtered and evaporated to dryness under vacuum. Crude methyl 2-formylbenzoate **11** (5.73 g, 88%) was obtained as a colorless liquid and used without further purification. b.p. 220-221 °C (lit.[10] b.p. 220-222 °C). ^{1}H NMR (400 MHz, $CDCl_3$) δ 3.85 (s, 3H, CH_3), 7.51-7.53 (m, 2H, ArH), 7.78-7.80 (m, 1H, ArH), 7.82-7.85 (m, 1H, ArH), 10.49 (s, 1H, CHO) ppm. The spectral data are in agreement with those reported in the literature.[3]

Preparation of Ester-Functionalised Porphyrins 12-14

General Procedure: Under an argon atmosphere, pyrrole (670 mg, 10.0 mmol) was added to a mixture of methyl formylbenzoate **9-11** (410 mg, 2.5 mmol) and 3,5-di-*tert*-butylbenzaldehyde **1** (1.64 g, 7.5 mmol) in chloroform (700 mL). After 15 min, boron trifluoride diethyl etherate (0.2 mL) was added dropwise and the reaction mixture was stirred for 1 h. *p*-Chloranil (1.82 g, 7.4 mmol) was added and reaction mixture was heated to reflux in air for 1.5 h. On completion, the reaction mixture was concentrated, fluorosil (5.0 g) was added and dried powder was purified by column chromatography (silica gel, dichloromethane:hexane 1:1) to afford the desired porphyrin. The first compound eluted was 5,10,15,20-tetrakis(3,5-di-*tert*-butylphenyl)porphyrin **2** (194 mg, 10%), as purple microcrystals. m.p. > 300 °C. ^{1}H NMR (400 MHz, $CDCl_3$) δ -2.67 (br s, 2H, NH), 1.52 (s, 72H, CH_3), 7.78 (t, 4H, J = 1.8 Hz, ArH), 8.08 (d, 8H, J = 1.8 Hz, ArH), 8.89 (br s, 8H, β-pyrrolic H) ppm. The spectroscopic data are in agreement with those reported in the literature.[9] In each case the second compound was the desired mono-methyl ester porphyrin **12-14** (see below for details), and all other porphyrins were subsequently eluted, evaporated to dryness and not used further in the current work.

5-(4-Methoxycarbonyl)phenyl-10,15,20-tris(3,5-di-*tert*-butylphenyl)porphyrin 12

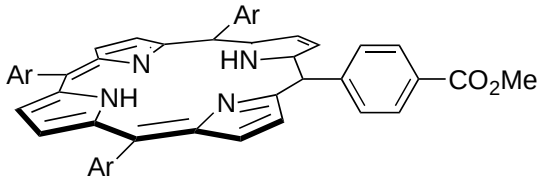

Starting with methyl 4-formylbenzoate **9**, chromatography (silica gel, dichloromethane/hexane 1:1) afforded **12** (440 mg, 17%) as a purple microcrystalline solid. m.p. > 300 °C. ^{1}H NMR (400 MHz, $CDCl_3$) δ -2.49 (br s, 2H, NH), 1.52-1.54 (m, 56H, CH_3), 4.11 (s, 3H, CO_2CH_3), 7.78-7.81 (m, 3H, ArH), 8.07-8.10 (m, 6H, ArH), 8.33 (d, 2H, J = 8.1 Hz, ArH), 8.44 (d, 2H, J = 8.1 Hz, ArH), 8.78 (ABq, 2H, J_{AB} = 4.7 Hz, β-pyrrolic H), 8.88-8.93 (m, 6H, β-pyrrolic H) ppm. The spectroscopic data are in agreement with those reported in the literature.[4]

5-(3-Methoxycarbonyl)phenyl-10,15,20-tris(3,5-di-*tert*-butylphenyl)porphyrin 13

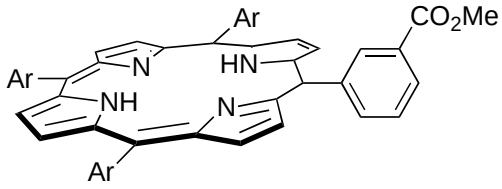

Starting with methyl 3-formylbenzoate **10**, chromatography (silica gel, dichloromethane/hexane 1:1) afforded **13** (500 mg, 19%) as a purple microcrystalline solid. m.p. > 300 °C. ^{1}H NMR (400 MHz, $CDCl_3$) δ -2.67 (br s, 2H, NH), 1.54 (app. s, 54H, CH_3), 3.99 (s, 3H, CO_2CH_3), 7.80-7.82 (m, 3H, ArH), 7.84 (app. t, 1H, J = 7.7 Hz, ArH), 8.07-8.12 (6H, m, ArH), 8.42-8.51 (m, 2H, ArH), 8.78 (ABq, 2H, J_{AB} = 4.7 Hz, β-pyrrolic H), 8.90-8.94 (m, 6H, β-pyrrolic H) ppm. The spectroscopic data are in agreement with those reported in the literature.[6]

5-(2-Methoxycarbonyl)phenyl-10,15,20-tris(3,5-di-*tert*-butylphenyl)porphyrin 14

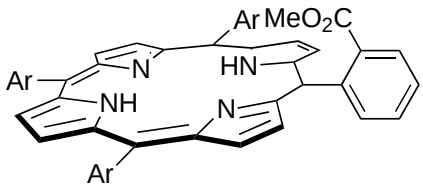

Starting with methyl 2-formylbenzoate **11**, chromatography (silica gel, dichloromethane/hexane 1:1) afforded **14** (540 mg, 21%) as a purple microcrystalline solid. m.p. > 300 °C. ^{1}H NMR (400 MHz, $CDCl_3$), δ -2.58 (br s, 2H, NH), 1.53 (s, 18H, CH_3), 1.54-1.55 (m, 18H, CH_3), 1.56 (s, 18H, CH_3), 2.82 (s, 3H, CO_2CH_3), 7.80-7.81 (m, 3H, ArH), 7.83-7.91 (m, 2H, ArH), 8.04-8.06 (m, 2H, ArH), 8.07-8.09 (m, 1H, ArH), 8.11-8.13 (m, 1H, ArH) 8.14-8.16 (m, 2H, ArH), 8.19-8.23 (m, 1H, ArH), 8.40-8.44 (m, 1H, ArH), 8.67 and 8.87 (ABq, 4H, J_{AB} = 4.7 Hz, β-pyrrolic H), 8.90 (s, 4H, β-pyrrolic H) ppm. The spectroscopic data are in agreement with those reported in the literature.[6]

Preparation of Alcohol-Functionalised Porphyrins 15-17

General Procedure: Methyl ester porphyrin **12-14** (500 mg, 0.5 mmol) was added to a mixture of lithium aluminium hydride (380 mg, 10.0 mmol) in THF (100 mL) at 0 °C, under an argon

atmosphere. The reaction mixture was allowed to reach room temperature and stirred overnight. On completion, water (2 mL) was added and the mixture was stirred for 1 h. The organic layer was washed with sodium hydroxide solution (3 M, 2 x 50 mL), brine solution (50 mL), dried over magnesium sulfate, filtered and evaporated under *vacuo*. The crude product obtained was purified using chromatography (silica gel).

5-(4-Hydroxymethylene)phenyl-(10,15,20-tris(3,5-di-*tert*-butylphenyl)porphyrin 15

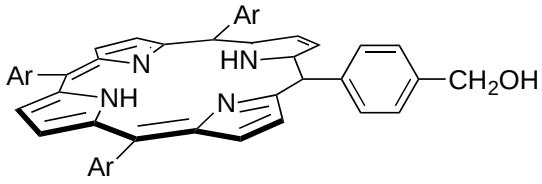

Starting with **12**, the crude material was chromatographed (silica gel, dichloromethane/hexane 2:1) to afford **15** (470 mg, 98%) as a purple microcrystals. m.p. > 300 °C. ^{1}H NMR (400 MHz, $CDCl_3$) δ -2.67 (br s, 2H, NH), 1.54 (s, 18H, CH_3), 1.55 (s, 36H, CH_3), 5.05 (d, 2H, J = 4.9 Hz, CH_2), 7.75 (d, 2H, J = 8.0 Hz, ArH), 7.80-7.82 (m, 3H, ArH), 8.10 (d, 2H, J = 1.8 Hz, ArH), 8.11 (d, 4H, J = 1.8 Hz, ArH), 8.25 (d, 2H, J = 8.0 Hz, ArH), 8.86 and 8.91 (ABq, 4H, J_{AB} = 4.7 Hz, β-pyrrolic H), 8.92 (s, 4H, β-pyrrolic H) ppm. The exchangeable OH proton was not observed. The spectroscopic data are in agreement with those reported in the literature.[4]

5-(3-Hydroxymethylene)phenyl-10,15,20-tris(3,5-di-*tert*-butylphenyl)porphyrin 16

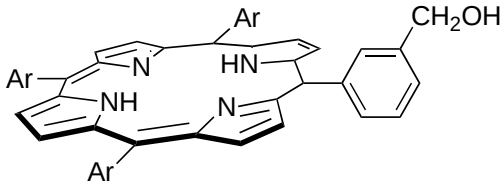

Starting with **13**, the crude material was chromatographed (silica gel, dichloromethane/hexane 1:1) to afford **16** (390 mg, 80%) as a purple microcrystalline solid. m.p. > 300 °C. ^{1}H NMR (400 MHz, $CDCl_3$) δ -2.67 (br s, 2H, NH), 1.55 (app. s, 54H, CH_3), 4.99 (s, 2H, CH_2), 7.73-7.84 (m, 5H, ArH), 8.09-8.14 (m, 6H, ArH), 8.19-8.24 (m, 2H, ArH), 8.86 and 8.92 (ABq, 4H, J_{AB} =

4.7 Hz, β-pyrrolic H), 8.94 (s, 4H, β-pyrrolic H) ppm. The exchangeable OH proton was not observed. The spectroscopic data are in agreement with those reported in the literature.[6]

5-(2-Hydroxymethylene)phenyl-10,15,20-tris(3,5-di-*tert*-butylphenyl)porphyrin 17

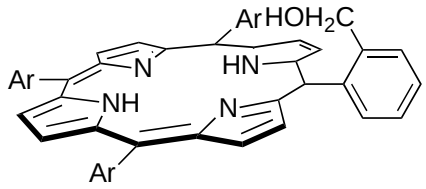

Starting with **14**, the crude material was chromatographed (silica gel, dichloromethane/hexane 2:1) to afford **17** (363 mg, 75%) as a purple microcrystals. m.p. > 300 °C. ^{1}H NMR (400 MHz, $CDCl_3$) δ -2.71 (br s, 2H, NH), 1.52-1.56 (m, 56H, CH_3), 4.40 (s, 2H, CH_2), 7.63-7.68 (m, 1H, ArH), 7.79-7.86 (m, 4H, ArH), 7.91-7.95 (m, 1H, ArH), 8.04-8.14 (m, 7H, ArH), 8.69 and 8.88 (ABq, 2H, J_{AB} = 4.7 Hz, β-pyrrolic H), 8.91 (s, 4H, β-pyrrolic H) ppm. The exchangeable OH proton was not observed. The spectroscopic data are in agreement with those reported in the literature.[6]

Preparation of Aldehyde-Functionalised Porphyrins 18-20

General Procedure: Manganese oxide (1.77 g, 20.4 mmol) was added to a mixture of mono-alcohol porphyrin **15-17** (400 mg, 0.41 mmol) in dichloromethane (100 mL) and the resulting mixture was stirred overnight. On completion, the reaction mixture was filtered over silica gel and the organic layer was evaporated to dryness to afford crude product that was purified using column chromatography (silica gel).

5-(4-Formylphenyl)-10,15,20-tris(3,5-di-*tert*-butylphenyl)porphyrin 18

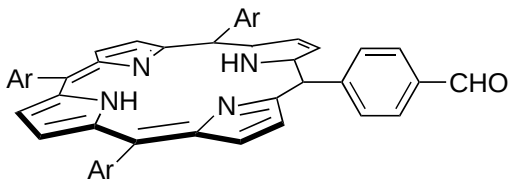

Starting with **15**, the crude material was chromatographed (silica gel, dichloromethane/hexane 1:1) to afford **18** (350 mg, 91%) as a purple microcrystals. m.p. > 300 °C. ^{1}H NMR (400 MHz,

$CDCl_3$) δ -2.66 (br s, 2H, NH), 1.52 (app. s, 54H, CH_3), 7.80-7.84 (m, 3H, ArH), 8.08-8.12 (m, 6H, ArH), 8.28 (d, 2H, *J* = 7.9 Hz, ArH), 8.44 (d, 2H, *J* = 7.9 Hz, ArH), 8.79 (ABq, 2H, J_{AB} = 4.7 Hz, β-pyrrolic H), 8.91-8.96 (m, 6H, β-pyrrolic H), 10.38 (s, 1H, CHO) ppm. The spectroscopic data are in agreement with those reported in the literature.[5]

5-(3-Formylphenyl)-10,15,20-tris(3,5-di-*tert*-butylphenyl)porphyrin 19

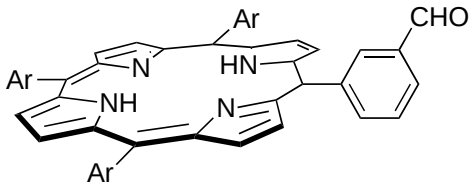

Starting with **16**, the crude material was chromatographed (silica gel, dichloromethane/hexane 1:1) to afford **19** (320 mg, 67%) as a purple microcrystalline solid. m.p. > 300 °C. ^{1}H NMR (400 MHz, $CDCl_3$) δ -2.62 (br s, 2H, NH), 1.58 (app. s, 54H, CH_3), 7.84-7.87 (m, 3H, ArH), 7.96 (app. t, 1H, *J* = 7.6 Hz, ArH), 8.13-8.17 (m, 6H, ArH), 8.32-8.36 (m, 1H, ArH), 8.54-8.58 (m, 1H, ArH), 8.77-8.79 (m, 1H, ArH), 8.81 (ABq, 2H, J_{AB} = 4.7 Hz, β-pyrrolic H), 8.96-9.00 (m, 6H, β-pyrrolic H), 10.33 (s, 1H, CHO) ppm. The spectroscopic data are in agreement with those reported in the literature.[6]

5-(2-Formylphenyl)-10,15,20-tris(3,5-di-*tert*-butylphenyl)porphyrin 20

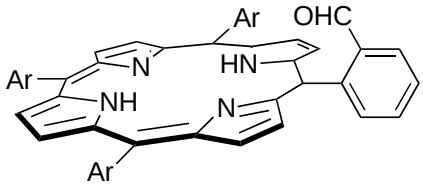

Starting with **17**, the crude material was chromatographed (silica gel, dichloromethane/hexane, 1:1) to afford **20** (320 mg, 79%) as a purple microcrystalline solid. m.p. > 300 °C. ^{1}H NMR (400 MHz, $CDCl_3$) δ -2.58 (br s, 2H, NH), 1.54-1.58 (m, 54H, CH_3), 7.81-7.84 (m, 3H, ArH), 7.92-7.97 (m, 2H, ArH), 8.08-8.15 (m, 6H, ArH), 8.27-8.31 (m, 1H, ArH), 8.42-8.46 (m, 1H, ArH), 8.68 (ABq, 2H, J_{AB} = 4.7 Hz, β-pyrrolic H), 8.91-8.97 (m, 6H, β-pyrrolic H), 9.57 (s, 1H, CHO) ppm. The spectroscopic data are in agreement with those reported in the literature.[6]

2.7.4 Preparation of 2,3-dioxo-5,10,15,20-tetrakis(3,5-di-*tert*-butylphenyl)porphyrin 21

5,10,15,20-Tetrakis(3,5-di-*tert*-butylphenyl)porphyrin 2

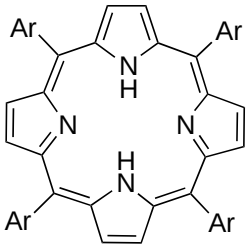

To a stirred mixture of 3,5-di-*tert*-butylbenzaldehyde **1** (31.4 g 14.4 mmol) in propanoic acid (150 mL) was added pyrrole (9.65 g, 14.4 mmol). The reaction was heated at reflux for 1 h and the reaction mixture was stirred at room temperature overnight. The reaction mixture was then filtered and washed with ice-cold hexane (20 mL) to afford **2** (7.4 g, 19%) as violet microcrystals that were used without purification. m.p. > 300 °C. ^{1}H NMR (400 MHz, $CDCl_3$) δ -2.67 (br s, 2H, NH), 1.52 (s, 72H, CH_3), 7.78 (t, 4H, *J* = 1.8 Hz, ArH), 8.08 (d, 8H, *J* = 1.8 Hz, ArH), 8.89 (br s, 8H, β-pyrrolic) ppm. FTIR (cm^{-1}) 3315 (NH). The spectroscopic data are in agreement with those reported in the literature.[9]

[5,10,15,20-Tetrakis(3,5-di-*tert*-butylphenyl)porphyrinato]copper(II) 22

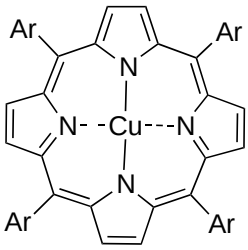

A mixture of 5,10,15,20-tetrakis(3,5-di-*tert*-butylphenyl)porphyrin **2** (7.0 g, 6.5 mmol) and copper(II) acetate monohydrate (2.5 g, 12.6 mmol) in dichloromethane (800 mL) was heated at reflux for 1 h. On cooling, the organic layer was washed with water (2 x 200 mL), brine (200 mL), dried over sodium sulfate, filtered and evaporated under *vacuo*. The crude product was purified by column chromatography (silica gel, dichloromethane/hexane 1:4) to afford pure **22**

(6.16 g, 83%) as a purple-red microcrystalline solid. m.p. > 300 °C. The spectroscopic data are in agreement with those reported in the literature.[9]

[2-Nitro-5,10,15,20-tetrakis(3,5-di-*tert*-butylphenyl)-porphyrinato]copper(II) 23

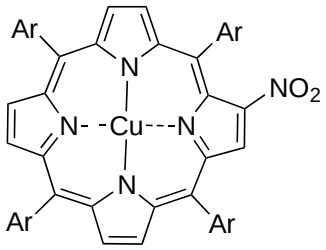

In a mixture of [5,10,15,20-tetrakis(3,5-di-*tert*-butylphenyl)porphyrinato]copper (II) **22** (2.0 g, 1.78 mmol) in dichloromethane (100 mL) was added nitrogen oxide (0.5% in hexane). The progress of the reaction was followed by TLC (dichloromethane/hexane 1:4). On completion, the reaction mixture was filtered through a silica bed and washed with hexane to remove impurities. The organic layer was evaporated to dryness and purified by column chromatography (silica gel, dichloromethane/hexane 1:4) to afford pure **23** (1.85 g, 93%). m.p. > 300 °C. FTIR (cm^{-1}) 1526 (NO_2). The spectroscopic data are in agreement with those reported in the literature.[9]

2-Nitro-5,10,15,20-tetrakis(3,5-di-*tert*-butylphenyl)porphyrin 24

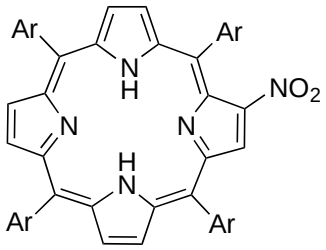

In a mixture of [2-nitro-5,10,15,20-tetrakis(3,5-di-*tert*-butylphenyl)porphyrinato]copper(II) **23** (4.0 g, 3.42 mmol) in dichloromethane (80 mL) was added sulfuric acid (18 M, 8 mL) slowly. The reaction mixture was stirred for 5 min and quenched over ice (100 mL). The two layers were allowed to reach room temperature and then separated. The organic layer was washed with sodium hydroxide (3 M, 2 x 100 mL), brine (100 mL), dried over anhydrous sodium sulfate,

filtered and evaporated under *vacuo* to afford crude product. The crude product was purified by column chromatography (silica gel, dichloromethane/hexane 1:4) to afford pure **24** (3.4 g, 90%). m.p. > 300 °C. ^{1}H NMR (400 MHz, $CDCl_3$) δ -2.54 (br s, 2H, NH), 1.53-1.56 (m, 72H, CH_3), 7.77-7.85 (m, 4H, ArH), 8.06-8.08 (m, 6H, ArH), 8.09-8.11 (m, 2H, ArH), 8.77-8.80 (ABq, 2H, J_{AB} = 4.7 Hz, β-pyrrolic H), 8.94-8.97 (m, 3H, β-pyrrolic H), 9.06-9.09 (m, 2H, β-pyrrolic H) ppm. The spectroscopic data are in agreement with those reported in the literature.[9]

2-Amino-5,10,15,20-tetrakis(3,5-di-*tert*-butylphenyl)porphyrin 25

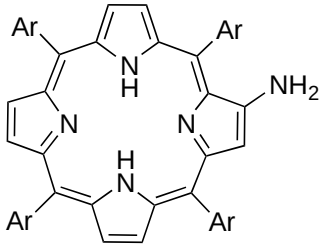

In a mixture of 2-nitro-5,10,15,20-tetrakis(3,5-di-*tert*-butylphenyl)porphyrin **24** (0.9 g, 0.81 mmol), anhydrous tin chloride (1.22 g, 6.48 mmol), dichloromethane (30 mL) was added hydrochloric acid (10 M, 2 mL). The reaction mixture was stirred for 24 h in dark under an argon atmosphere. On completion, the reaction mixture was diluted with dichloromethane (150 mL). The organic layer was washed with water (100 mL), sodium hydrogen carbonate (saturated, 2 x 150 mL), brine (200 mL), dried over anhydrous sodium sulfate, filtered and evaporated to dryness under *vacuo* to afford crude **25** (0.7 g, 80%) that was used without further purification. m.p. > 300 °C. ^{1}H NMR (400 MHz, $CDCl_3$) δ -2.60 (br s, 2H, NH), 1.50-1.54 (m, 72H, CH_3), 4.46 (br s, 2H, NH_2), 7.75-7.81 (m, 5H, ArH), 7.86 (t, 1H, *J* = 1.8 Hz, ArH), 8.00 (d, 2H, *J* = 1.8 Hz, ArH), 8.01-8.03 (m, 1H, ArH), 8.04 (d, 2H, *J* = 1.8 Hz, ArH), 8.09 (app. t, 3H, *J* = 1.8 Hz, ArH), 8.57 (d, 1H, *J* = 4.7 Hz, β-pyrrolic H), 8.71 (d, 1H, *J* = 4.7 Hz, β-pyrrolic H), 8.80-8.87 (m, 5H, β-pyrrolic H) ppm. The spectroscopic data are in agreement with those reported in the literature.[9]

2,3-Dioxo-5,10,15,20- tetrakis(3,5-di-*tert*-butylphenyl)porphyrin 21

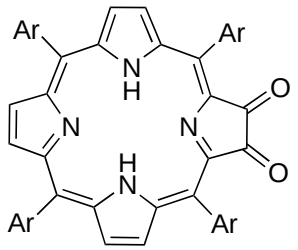

A mixture of 2-amino-5,10,15,20-tetrakis(3,5-di-*tert*-butylphenyl)porphyrin **25** (200 mg, 0.185 mmol) in dichloromethane (200 mL) was stirred under UV light for 3 h. Dichloromethane was removed under *vacuo* affording crude product. The crude product was purified by column chromatography (silica gel, dichloromethane/hexane 1:3) to afford **21** (178 mg, 87%). m.p. > 300 °C. ^{1}H NMR (400 MHz, $CDCl_3$) δ -1.94 (br s, 2H, NH), 1.46 (s, 36H, CH_3), 1.50 (s, 36H, CH_3), 7.72 (d, 4H, *J* = 1.7 Hz, ArH), 7.75 (t, 2H, *J* = 1.7 Hz, ArH), 7.77 (t, 2H, *J* = 1.7 Hz, ArH), 7.98 (d, 4H, *J* = 1.7 Hz, ArH), 8.61 and 8.78 (ABq, 4H, J_{AB} = 4.7 Hz, β-pyrrolic H), 8.62 (s, 2H, β-pyrrolic H) ppm. The spectroscopic data are in agreement with those reported in the literature.[11]

2.7.5 Preparation of Imidazole-fused Porphyrins

Preparation of Nitro-functionalised Phenyl-Imidazolo-Porphyrins 14-16

General Procedure: To a mixture of **21** (500 mg, 0.46 mmol) and (*o*-, *m*- or *p*- isomer) nitrobenzaldehydes (69 mg, 0.46 mmol) in chloroform/glacial acetic acid mixture (1:1, 30 mL), was added ammonium acetate (140 mg, 1.84 mmol). The resulting reaction mixture was heated at reflux overnight under an argon atmosphere. On cooling, the reaction mixture was diluted with chloroform (20 mL) and washed with water (50 mL). The organic layer was washed with sodium hydroxide solution (3 M, 2 x 50 mL), water (50 mL) and brine (50 mL), dried over anhydrous sodium sulfate, filtered and evaporated to dryness under vacuum. The crude compounds obtained were purified by column chromatography (silica gel, dichloromethane/hexane 1:1) to give pure nitro-functionalised imidazole porphyrin **26-28**.

(5,10,15,20-Tetrakis(3,5-di-*tert*-butylphenyl)porphyrin[2,3-*b*]-1'*H*-imidazol-2'-yl)-4''-nitrophenyl 26

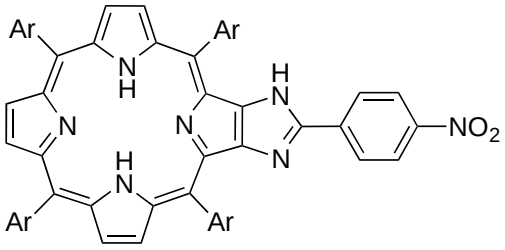

Starting with 4-nitrobenzaldehyde, **26** (288 mg, 51%) was obtained as a purple microcrystalline solid. m.p. > 300 °C. ^{1}H NMR (400 MHz, $CDCl_3$) δ -2.81 (br s, 2H, NH), 1.52-1.54 (m, 72H, CH_3), 7.80-7.81 (m, 2H, ArH), 7.83 (d, 2H, *J* = 8.9 Hz, ArH), 7.89 (t, 1H, *J* = 1.8 Hz, ArH), 8.09-8.11 (m, 5H, ArH), 8.12-8.14 (m, 4H, ArH), 8.31 (d, 2H, *J* = 8.9 Hz, ArH), 8.40 (br s, 1H, NH), 8.83 and 8.85 (ABq, 2H, J_{AB} = 4.6 Hz, β-pyrrolic H), 8.99-9.06 (m, 4H, β-pyrrolic H) ppm. ^{13}C NMR (100 MHz, $CDCl_3$) δ 31.7, 31.8, 35.0, 115.5, 121.1, 121.3, 122.2, 124.1, 125.1, 127.0, 127.2, 129.3, 129.6, 129.7, 133.5, 133.8, 137.5, 141.1, 141.4, 148.6, 148.80, 148.84, 151.2 ppm. FTIR 1107 (w), 1166 (w), 1248 (m), 1346 (m), 1361 (m), 1394 (w), 1424 (w), 1476 (m), 1524 (m, NO_2), 1594 (m), 1714 (w), 2867 (m), 2958 (s), 3436 (w, NH) cm^{-1}. Anal Calcd for $C_{83}H_{97}N_7O_2$: C, 81.40; H, 7.98; N, 8.01. Found: C, 79.13 ; H, 8.21; N, 7.45. Anal Calcd for $C_{83}H_{97}N_7O_2$.½ CH_2Cl_2: C, 79.14; H, 7.80; N, 7.74.

(5,10,15,20-Tetrakis(3,5-di-*tert*-butylphenyl)porphyrin[2,3-*b*]-1'*H*-imidazol-2'-yl)-3''-nitrophenyl 27

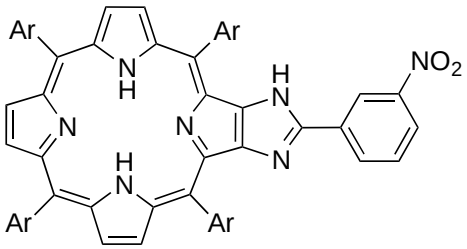

Starting with 3-nitrobenzaldehyde, **27** (375 mg, 67%) was obtained as a purple microcrystalline solid. m.p. > 300 °C. ^{1}H NMR (400 MHz, $CDCl_3$) δ -2.80 (br s, 2H, NH), 1.53-1.57 (m, 72H,

CH_3), 7.62 (app. t, 1H, J = 8.0 Hz, ArH), 7.80-7.83 (m, 2H, ArH), 7.91-7.93 (m, 1H, ArH), 8.10-8.24 (m, 11H, ArH), 8.32 (br s, 1H, NH), 8.43-8.45 (m, 1H, ArH), 8.84 and 8.87 (ABq, 2H, J_{AB} = 4.7 Hz, β-pyrrolic H), 9.01 (ABq, 1H, J_{AB} = 4.7 Hz, β-pyrrolic H), 9.05-9.09 (m, 3H, β-pyrrolic H) ppm. ^{13}C NMR (100 MHz, $CDCl_3$) δ 31.7, 31.8, 35.0, 35.1, 115.4, 118.9, 119.3, 121.0, 121.3, 122.2, 122.3, 122.5, 123.0, 127.1, 128.4, 129.0, 129.3, 129.6, 129.7, 129.9, 130.8, 133.0, 133.3, 133.8, 139.6, 141.1, 141.5, 142.2, 148.1, 148.6, 148.8, 148.8, 151.2 ppm. FTIR 1108 (w), 1165 (w), 1246 (m), 1343 (m), 1363 (m), 1392 (w), 1425 (w), 1477 (m), 1523 (m, NO_2), 1595 (m), 1713 (w), 2869 (m), 2956 (s), 3434 (w, NH) cm^{-1}. Anal Calcd for $C_{83}H_{97}N_7O_2$: C, 81.40; H, 7.98; N, 8.01. Found: C, 79.12; H, 7.19; N, 7.63. Anal Calcd for $C_{83}H_{97}N_7O_2.½\ CH_2Cl_2$: C, 79.14; H, 7.80; N, 7.74.

(5,10,15,20-Tetrakis(3,5-di-*tert*-butylphenyl)porphyrin[2,3-*b*]-1'*H*-imidazol-2'-yl)-2''-nitrophenyl 28

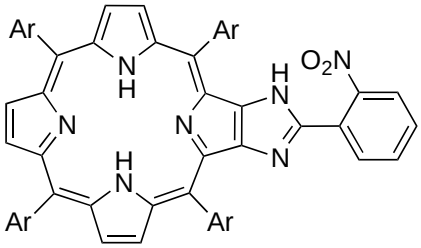

Starting with 2-nitrobenzaldehyde, **28** (325 mg, 58%) was obtained as a purple microcrystalline solid. m.p. > 300 °C. ^{1}H NMR (400 MHz, $CDCl_3$) δ -2.81 (br s, 2H, NH), 1.52 (s, 18H, CH_3), 1.53 (s, 18H, CH_3), 1.54 (app. s, 36H, CH_3), 7.44-7.50 (m, 1H, ArH), 7.59-7.65 (m, 1H, ArH), 7.80-7.83 (m, 3H, ArH), 7.86 (t, 1H, J = 1.7 Hz, ArH), 8.04 (t, 1H, J = 1.7 Hz, ArH), 8.07-8.09 (m, 2H, ArH), 8.11-8.14 (m, 6H, ArH), 8.43-8.46 (m, 1H, ArH), 8.84 and 8.87 (ABq, 2H, J_{AB} = 4.7 Hz, β-pyrrolic H), 8.93 (ABq, 1H, J_{AB} = 4.7 Hz, β-pyrrolic H), 8.89-9.05 (m, 3H, β-pyrrolic H), 9.48 (br s, 1H, NH) ppm. ^{13}C NMR (100 MHz, $CDCl_3$) δ 31.66, 31.75, 31.82, 35.04, 35.06, 35.3, 116.3, 118.8, 121.0, 121.2, 122.2, 122.3, 122.7, 124.8, 125.3, 127.2, 128.8, 129.1, 129.6, 129.7, 132.3, 132.8, 140.0, 141.0, 141.2, 141.5, 145.9, 147.5, 148.58, 148.63, 148.7, 150.5 ppm.

FTIR 1109 (w), 1167(w), 1247 (m), 1345 (m), 1362 (m), 1393 (w), 1424 (w), 1475 (m), 1525 (m, NO_2), 1592 (m), 1716 (w), 2868 (m), 2959 (s), 3435 (w, NH) cm^{-1}. Anal Calcd for $C_{83}H_{97}N_7O_2$: C, 81.40; H, 7.98; N, 8.01. Found: C, 79.65; H, 7.21; N, 7.56. Anal Calcd for $C_{83}H_{97}N_7O_2.½\ CH_2Cl_2$: C, 79.14; H, 7.80; N, 7.74.

Preparation of Amino-functionalised Phenyl-Imidazolo-Porphyrins 29-31

General Procedure: To a mixture of nitro-functionalised imidazole porphyrin (using either *o*-, *p*- or *m*- isomer) **26-28** (350 mg, 0.285 mmol) and anhydrous stannous chloride (0.54 g, 2.85 mmol) in dichloromethane (40 mL), was added hydrochloric acid (10 M, 2.0 mL) under an argon atmosphere. The reaction mixture was stirred at room temperature for 4 days. The organic layer was washed with water (2 x 50 mL), sodium hydroxide solution (3 M, 2 x 50 mL), water (50 mL) and brine (50 mL), dried over anhydrous sodium sulfate, filtered and evaporated to dryness under vacuum. The crude compound obtained was purified by column chromatography (silica gel, dichloromethane/hexane 1:1) to give pure amino-functionalised imidazole porphyrin **29-31**.

(5,10,15,20-Tetrakis(3,5-di-*tert*-butylphenyl)porphyrin[2,3-*b*]-1'*H*-imidazol-2'-yl)-4''-aminophenyl 29

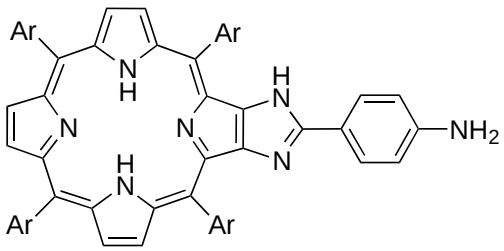

Starting with **26**, **29** (280 mg, 82%) was obtained as a purple microcrystalline solid. m.p. > 300 °C. ^{1}H NMR (400 MHz, $CDCl_3$) δ -2.78 (br s, 2H, NH), 1.53 (app. s, 36H, CH_3), 1.54 (s, 18H, CH_3), 1.55 (s, 18H, CH_3), 3.86 (br s, 2H, NH_2) 6.74 (d, 2H, *J* = 8.5 Hz, ArH), 7.58 (d, 2H, *J* = 8.5 Hz, ArH), 7.80 (app. t, 2H, *J* = 1.7 Hz, ArH), 7.86 (t, 1H, *J* = 1.7 Hz, ArH), 8.06 (t, 1H, *J* = 1.7 Hz, ArH), 8.11-8.14 (m, 6H, ArH), 8.19 (d, 2H, *J* = 1.7 Hz, ArH), 8.26 (br s, 1H, NH),

8.86 and 8.88 (ABq, 2H, J_{AB} = 4.7 Hz, β-pyrrolic H), 8.94-9.01 (m, 4H, β-pyrrolic H) ppm. FTIR 644 (m), 712 (s), 753 (m), 799 (m), 881 (m), 899 (m), 922 (m), 1162 (m), 1246 (m), 1362 (m), 1425 (m), 1471 (m), 1592 (m), 2955 (m), 3308 (w, NH_2), 3434 (w, NH) cm^{-1}. Anal Calcd for $C_{83}H_{99}N_7$: C, 83.44; H, 8.35; N, 8.21. Found: C, 81.67; H, 7.33; N, 8.00. Anal Calcd for $C_{83}H_{99}N_7.½\ CH_2Cl_2$: C, 81.06; H, 8.15; N, 7.92.

(5,10,15,20-Tetrakis(3,5-di-*tert*-butylphenyl)porphyrin[2,3-*b*]-1'*H*-imidazol-2'-yl)-3''-aminophenyl 30

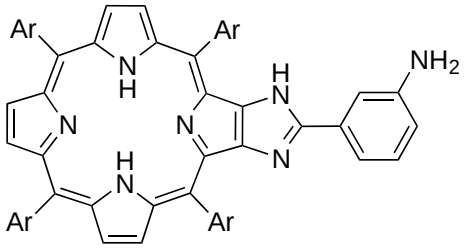

Starting with **27**, **30** (246 mg, 72%) was obtained as a purple microcrystalline solid. m.p. > 300 °C. ^{1}H NMR (400 MHz, $CDCl_3$) δ -2.76 (br s, 2H, NH), 1.54-1.58 (m, 72H, CH_3), 3.75 (br s, 2H, NH_2), 6.70-6.74 (m, 1H, ArH), 6.96-6.99 (m, 1H, ArH), 7.23 (app. t, 1H, J = 7.8 Hz, ArH), 7.34-7.36 (m, 1H, ArH), 7.82 (app. t, 2H, J = 1.7 Hz, ArH), 7.88-7.90 (m, 1H, ArH), 8.07-8.09 (1H, m, ArH), 8.12-8.16 (m, 6H, ArH), 8.19-8.22 (m, 2H, ArH), 8.39 (br s, 1H, NH), 8.87 and 8.89 (ABq, 2H, J_{AB} = 4.6 Hz, β-pyrrolic H), 8.98-9.05 (m, 4H, β-pyrrolic H) ppm. ^{13}C NMR (100 MHz, $CDCl_3$) δ 31.76, 31.82, 31.9, 35.0, 35.1, 35.4, 122.5, 114.7, 115.4, 115.7, 115.4, 115.7, 119.1, 121.0, 121.1, 122.0, 122.3, 127.3, 127.8, 129.1, 129.6, 129.7, 132.2, 132.8, 139.8, 141.2, 141.7, 142.3, 146.8, 148.5, 148.6, 148.7, 150.9, 151.3 ppm. FTIR 645 (m), 713 (s), 754 (m), 798 (m), 880 (m), 899 (m), 921 (m), 1163 (m), 1245 (m), 1361 (m), 1423 (m), 1473 (m), 1590 (m), 2956 (m), 3305 (w, NH_2), 3437 (w, NH) cm^{-1}. Anal Calcd for $C_{83}H_{99}N_7$: C, 83.44; H, 8.35; N, 8.21. Found: C, 82.11; H, 7.89; N, 7.89. Anal Calcd for $C_{83}H_{99}N_7.1/3\ CH_2Cl_2$: C, 81.84; H, 8.21; N, 8.02.

(5,10,15,20-Tetrakis(3,5-di-*tert*-butylphenyl)porphyrin[2,3-*b*]-1'*H*-imidazol-2'-yl)-2''-aminophenyl 31

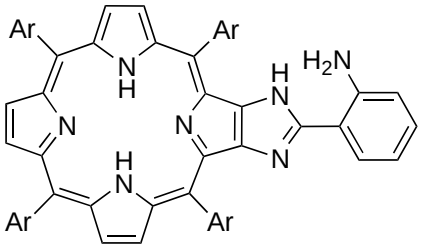

Starting with **28**, **31** (312 mg, 82%) was obtained as a purple microcrystalline solid. m.p. > 300 °C. ^{1}H NMR (400 MHz, $CDCl_3$) δ -2.85 (br s, 2H, NH), 1.52-1.56 (m, 72H, CH_3), 5.99 (br s, 2H, NH_2), 6.64-6.69 (m, 1H, ArH), 6.72-6.76 (m, 1H, ArH), 7.06-7.10 (m, 1H, ArH), 7.11-7.16 (m, 1H, ArH), 7.79-7.81 (m, 2H, ArH), 7.82-7.84 (m, 1H, ArH), 8.06-8.09 (m, 3H, ArH), 8.11-8.14 (m, 6H, ArH), 8.42 (br s, 1H, NH), 8.86 (app. s, 2H, β-pyrrolic H), 8.98-9.04 (m, 4H, β-pyrrolic H) ppm. ^{13}C NMR (100 MHz, $CDCl_3$) δ 31.7, 31.8, 31.9, 111.8, 115.7, 115.8, 116.6, 118.6, 120.7, 121.0, 122.1, 122.4, 124.3, 127.2, 128.4, 129.6, 129.67, 129.70, 140.7, 141.3, 141.5, 142.1, 147.1, 148.6, 148.7, 148.9, 151.1 ppm. FTIR 644 (m), 713 (s), 733 (s), 753 (m), 800 (s), 880 (m), 900 (m), 922 (m), 1158 (m), 1202 (m), 1245 (m), 1362 (m), 1425 (m), 1475 (m), 1591 (m), 2958 (m), 3302 (w, NH_2), 3431 (w, NH) cm^{-1}. Anal Calcd for $C_{83}H_{99}N_7$: C, 83.44; H, 8.35; N, 8.21. Found: C, 81.24; H, 7.87; N, 7.72. Anal Calcd for $C_{83}H_{99}N_7.½\ CH_2Cl_2$: C, 81.06; H, 8.15; N, 7.92.

Preparation of Ester-functionalised Phenyl-Imidazolo-Porphyrins 32-34

General Procedure: To a mixture of 2,3-dioxo-5,10,15,20-tetrakis(3,5-di-*tert*-butylphenyl)chlorin **21** (500 mg, 0.46 mmol) and methyl 2-, 3- or 4-formylbenzoate **9-11** (75 mg, 0.46 mmol) in a mixture of chloroform and glacial acetic acid (1:1 (v/v), 30 mL), was added ammonium acetate (140 mg, 1.84 mmol). The resulting mixture was refluxed overnight under an argon atmosphere. On cooling, the reaction mixture was diluted with chloroform (20 mL)

and washed with water (50 mL). The organic layer was washed with sodium hydroxide solution (3 M, 2 x 50 mL), water (50 mL) and brine (50 mL), dried over anhydrous sodium sulfate, filtered and evaporated to dryness under vacuum. The crude compound obtained was purified by column chromatography (silica gel, dichloromethane/hexane 1:1) to give pure ester-functionalised imidazole porphyrin **32-34**.

(5,10,15,20-Tetrakis(3,5-di-*tert*-butylphenyl)porphyrin[2,3-*b*]-1'*H*-imidazol-2'-yl)-4''-methoxycarbonylphenyl 32

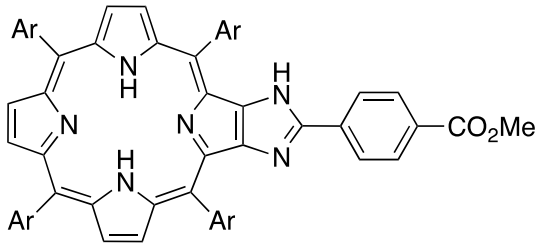

Starting with **9,** the crude material was chromatographed (silica gel, dichloromethane/hexane 3:1) to afford **32** (300 mg, 52%) as a purple microcrystalline solid. m.p. > 300 °C. ^{1}H NMR (400 MHz, $CDCl_3$) δ -2.80 (br s, 2H, NH), 1.52-1.54 (m, 72H, CH_3), 3.98 (s, 3H, CO_2CH_3) 7.77-7.81 (m, 4H, ArH), 7.87-7.89 (m, 1H, ArH), 8.08-8.14 (m, 9H, ArH), 8.15 (d, 2H, J = 1.7 Hz, ArH), 8.39 (br s, 1H, NH), 8.84-8.85 (ABq, 2H, J_{AB} = 4.7 Hz, β-pyrrolic H), 8.97-9.05 (m, 4H, β-pyrrolic H) ppm. ^{13}C NMR (100 MHz, $CDCl_3$) δ 31.7, 31.81, 31.85, 35.0, 35.1, 35.4, 52.2, 115.4, 119.2, 121.0, 121.2, 122.08, 122.12, 122.5, 127.2, 128.6, 129.1, 129.5, 129.6, 129.7, 129.8, 130.1, 133.0, 133.5, 135.4, 139.7, 141.2, 141.6, 142.2, 148.6, 148.76, 148.81, 149.6, 151.1 ppm. FTIR 714 (s), 732 (m), 754 (s), 801 (s), 880 (m), 924 (m), 1169 (m), 1202 (m), 1244 (m), 1262 (m), 1360 (m), 1426 (m), 1474 (m), 1593 (m), 1728 (m, C=O), 2952 (m), 3313 (w, NH), 3425 (w, NH) cm^{-1}. Anal Calcd for $C_{85}H_{100}N_6O_2$: C, 82.48; H, 8.14; N, 6.79. Found: C, 80.12; H, 8.39; N, 6.52. Anal Calcd for $C_{85}H_{100}N_6O_2.½\ CH_2Cl_2$: C, 80.21; H, 7.95; N, 6.56.

(5,10,15,20-Tetrakis(3,5-di-*tert*-butylphenyl)porphyrin[2,3-*b*]-1'*H*-imidazol-2'-yl)-3''-methoxycarbonylphenyl 33

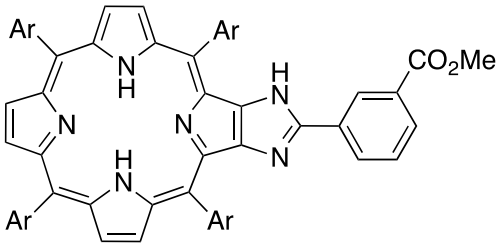

Starting with **10**, the crude material was chromatographed (silica gel, dichloromethane/hexane 2:1) to afford **33** (315 mg, 55%) as a purple microcrystalline solid. m.p. > 300 °C. ^{1}H NMR (400 MHz, $CDCl_3$) δ -2.73 (br s, 2H, NH), 1.59 (s, 18H, CH_3), 1.60 (s, 18H, CH_3), 1.61 (s, 18H, CH_3), 1.62 (s, 18H, CH_3), 4.13 (s, 3H, CO_2CH_3), 7.59 (app. t, 1H, *J* = 7.7 Hz, ArH), 7.85-7.88 (m, 2H, ArH), 7.95 (t, 1H, *J* = 1.7 Hz, ArH), 8.11-8.15 (m, 1H, ArH), 8.17-8.22 (m, 8H, ArH), 8.24 (d, 2H, *J* = 1.8 Hz, ArH), 8.30-8.31 (m, 1H, ArH), 8.41 (br s, 1H, NH), 8.92 and 8.94 (ABq, 2H, J_{AB} = 4.7 Hz, β-pyrrolic H), 9.06 (d, 1H, *J* = 4.9 Hz, β-pyrrolic H), 9.10-9.12 (m, 3H, β-pyrrolic H) ppm. ^{13}C NMR (100 MHz, $CDCl_3$) δ 31.8, 31.9, 35.07, 35.14, 35.4, 52.3, 115.4, 119.2, 121.0, 121.2, 122.1, 122.2, 122.5, 125.0, 127.2, 127.5, 128.7, 129.0, 129.3, 129.5, 129.6, 129.7, 129.9, 130.0, 130.8, 131.5, 132.9, 133.4, 139.8, 141.2, 141.6, 142.3, 148.6, 148.7, 148.8, 149.9, 151.1, 166.5 ppm. FTIR 713 (s), 733 (m), 754 (s), 800 (s), 881 (m), 922 (m), 1167 (m), 1201 (m), 1246 (m), 1263 (m), 1361 (m), 1428 (m), 1472 (m), 1591 (m), 1726 (m, C=O), 2956 (m), 3310 (w, NH), 3422 (w, NH) cm^{-1}. Anal Calcd for $C_{85}H_{100}N_6O_2$: C, 82.48; H, 8.14; N, 6.79. Found: C, 79.92; H, 8.37; N, 6.53. Anal Calcd for $C_{85}H_{100}N_6O_2$.½ CH_2Cl_2: C, 80.21; H, 7.95; N, 6.56.

(5,10,15,20-Tetrakis(3,5-di-*tert*-butylphenyl)porphyrin[2,3-*b*]-1'*H*-imidazol-2'-yl)-2''-methoxycarbonylphenyl 34

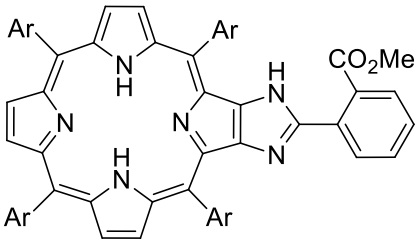

Starting with **11**, the crude material was chromatographed (silica gel, dichloromethane/hexane 2:1) to afford **34** (407 mg, 71%) as a purple microcrystalline solid. m.p. > 300 °C. ^{1}H NMR (400 MHz, $CDCl_3$) δ -2.79 (br s, 2H, NH), 1.49 (s, 36H, CH_3), 1.52 (s, 36H, CH_3), 3.82 (s, 3H, $COOCH_3$), 7.36-7.41 (m, 1H, ArH), 7.53-7.58 (m, 1H, ArH), 7.77-7.79 (m, 2H, ArH), 7.92-7.98 (m, 2H, ArH), 8.07-8.14 (m, 9H, ArH), 8.56-8.60 (m, 1H, ArH), 8.80-8.8.84 (m, 3H, β-pyrrolic H), 8.93-8.96 (m, 2H, β-pyrrolic H), 8.97-9.00 (m, 1H, β-pyrrolic H), 11.52 (br s, 1H, NH) ppm. ^{13}C NMR (100 MHz, $CDCl_3$) δ 31.13, 31.5, 32.0, 32.4, 35.0, 103.2, 116.4, 118.6, 120.8, 121.1, 122.0, 127.0, 127.9, 128.0, 128.5, 129.2, 129.3, 129.6, 129.7, 131.15, 131.6, 132.4, 140.3, 141.1, 141.4, 141.6, 148.6, 150.1 ppm. FTIR 714 (s), 732 (m), 753 (s), 803 (s), 882 (m), 924 (m), 1164 (m), 1203 (m), 1244 (m), 1261 (m), 1365 (m), 1423 (m), 1474 (m), 1592 (m), 1727 (m, C=O), 2952 (m), 3311 (w, NH), 3423 (w, NH) cm^{-1}. Anal Calcd for $C_{85}H_{100}N_6O_2$: C, 82.48; H, 8.14; N, 6.79. Found: C, 75.61; H, 7.65; N, 6.22. Anal Calcd for $C_{85}H_{100}N_6O_2$. 3/2 CH_2Cl_2: C, 76.10; H, 7.60; N, 6.16. Found: C, 75.61; H, 7.65; N, 6.22.

Preparation of Hydroxymethylene-functionalised Phenyl-Imidazolo-Porphyrins 35-37

General Method: Ester porphyrin **32-34** (300 mg, 0.24 mmol) was added to a mixture of lithium aluminium hydride (277 mg, 7.28 mmol) in THF (100 mL) at 0 °C, under an argon atmosphere. The reaction mixture was allowed to reach room temperature and stirred overnight. On completion, water (2 mL) was added and the mixture was stirred for 1 h. The organic layer was washed with sodium hydroxide solution (3 M, 2 x 50 mL), brine solution (50 mL), dried

over magnesium sulfate, filtered and evaporated under *vacuo*. The crude product obtained was purified using column chromatography (silica gel).

(5,10,15,20-Tetrakis(3,5-di-*tert*-butylphenyl)porphyrin[2,3-*b*]-1'*H*-imidazol-2'-yl)-4''-hydroxymethylenephenyl 35

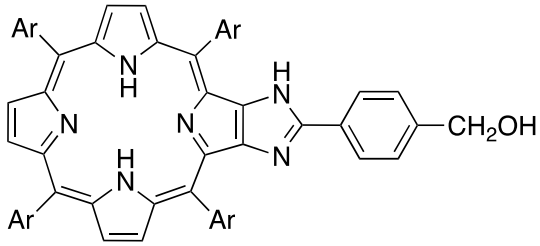

Starting with **32**, the crude material was chromatographed (silica gel, dichloromethane/hexane 3:1) to afford **35** (266 mg, 91%) as a purple microcrystalline solid. m.p. > 300 °C. ^{1}H NMR (400 MHz, $CDCl_3$) δ -2.79 (br s, 2H, NH), 1.52-1.55 (m, 72H, CH_3), 4.77 (d, 2H, J = 5.2 Hz, CH_2), 7.45 (d, 2H, J = 8.1 Hz, ArH), 7.75 (d, 2H, J = 8.1 Hz, ArH), 7.79-7.81 (m, 2H, ArH), 7.86-7.89 (m, 1H, ArH), 8.07-8.09 (m, 1H, ArH), 8.10-8.14 (m, 6H, ArH), 8.17-8.18 (m, 1H, ArH), 8.37 (br s, 1H, NH), 8.85 and 8.87 (ABq, 2H, J_{AB} = 4.7 Hz, β-pyrrolic H), 8.96-9.03 (m, 4H, β-pyrrolic H) ppm. The exchangeable OH proton was not observed. ^{13}C NMR (100 MHz, $CDCl_3$) δ 31.7, 31.8, 31.9, 35.0, 35.1, 35.4, 65.0, 115.3, 119.2, 121.0, 121.1, 122.0, 122.4, 125.2, 127.2, 127.3, 129.58, 129.62, 129.7, 130.6, 139.7, 141.2, 141.4, 141.6, 142.3, 148.5, 148.7, 150.8, 150.9 ppm. FTIR 713 (s), 753 (m), 799 (s), 881 (m), 922 (m), 1203 (m), 1246 (m), 1362 (m), 1424 (m), 1474 (m), 1591 (m), 2957 (m), 3316 (w, NH), 3424 (w, NH) cm^{-1}. Anal Calcd for $C_{84}H_{100}N_6O$: C, 83.40; H, 8.33; N, 6.95. Found: C, 81.21; H, 8.43; N, 6.71. Anal Calcd for $C_{84}H_{100}N_6O.½\ CH_2Cl_2$: C, 81.05; H, 8.13; N, 6.71.

(5,10,15,20-Tetrakis(3,5-di-*tert*-butylphenyl)porphyrin[2,3-*b*]-1'*H*-imidazol-2'-yl)-3''-hydroxymethylenephenyl 36

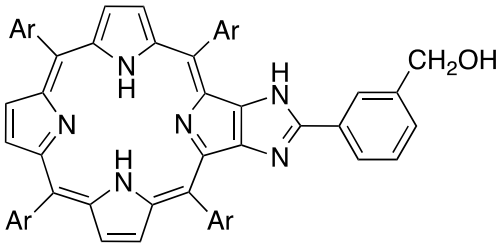

Starting with **33**, the crude material was chromatographed (silica gel, dichloromethane/hexane 3:1) to afford **36** (253 mg, 86%) as a purple microcrystalline solid. m.p. > 300 °C. ^{1}H NMR (400 MHz, $CDCl_3$) δ -2.79 (br s, 2H, NH), 1.54 (app. s, 72H, CH_3), 4.78 (s, 2H, CH_2), 7.37-7.57 (m, 2H, ArH), 7.65-7.69 (m, 1H, ArH), 7.78-7.81 (m, 3H, ArH), 7.86-7.91 (m, 1H, ArH), 8.09-8.18 (m, 9H, ArH), 8.37 (br s, 1H, NH), 8.83-8.87 (m, 2H, β-pyrrolic H), 8.96-9.04 (m, 4H, β-pyrrolic H) ppm. The exchangeable OH proton was not observed. ^{13}C NMR (100 MHz, $CDCl_3$) δ 31.7, 31.8, 35.0, 65.2, 121.0, 121.2, 122.07, 122.10, 123.7, 124.1, 127.16, 127.21, 127.7, 129.0, 129.6, 129.7, 131.4, 139.2, 139.8, 141.2, 141.6, 142.2, 142.3, 148.5, 148.7, 150.8, 151.0 ppm. FTIR 712 (s), 752 (m), 800 (s), 882 (m), 924 (m), 1201 (m), 1247 (m), 1361 (m), 1423 (m), 1476 (m), 1592 (m), 2956 (m), 3318 (w, NH), 3423 (w, NH) cm^{-1}. Anal Calcd for $C_{84}H_{100}N_6O$: C, 83.40; H, 8.33; N, 6.95. Found: C, 81.13; H, 7.13; N, 6.49. Anal Calcd for $C_{84}H_{100}N_6O.½\ CH_2Cl_2$: C, 81.05; H, 8.13; N, 6.71.

(5,10,15,20-Tetrakis(3,5-di-*tert*-butylphenyl)porphyrin[2,3-*b*]-1'*H*-imidazol-2'-yl)-2''-hydroxymethylenephenyl 37

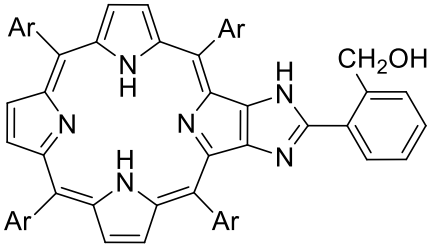

Starting with **34**, TLC analysis of the reaction mixture revealed the presence of a spot co-eluting with the starting material. Nevertheless, the reaction was work-up as described above, to afford

the crude material that was chromatographed (silica gel, dichloromethane/hexane 3:1) to afford unchanged **34** in essentially quantitative yield that had identical spectral properties to authentic material. A similar result was obtained when the further equivalents of either lithium aluminium hydride or sodium borohydride were used, and also when the reaction was allowed to run for extended time periods.

Preparation of Formyl-functionalised Phenyl-Imidazolo-Porphyrin 38 and 39

General Method: Manganese oxide (548 mg, 6.3 mmol) was added to a mixture of alcohol-functionalised imidazolo-porphyrin **35** and **36** (250 mg, 0.21 mmol) in dichloromethane (70 mL) and the resulting mixture was stirred overnight. On completion, the reaction mixture was filtered over silica gel and the organic layer was evaporated to dryness to afford crude product that was purified using column chromatography (silica gel).

(5,10,15,20-Tetrakis(3,5-di-*tert*-butylphenyl)porphyrin[2,3-*b*]-1'*H*-imidazol-2'-yl)-4''-formylphenyl 38

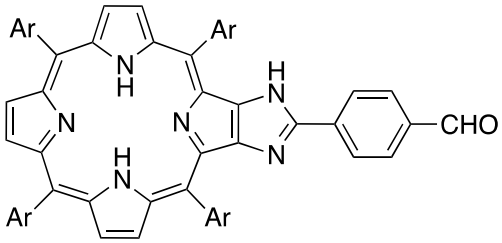

Starting with **35**, the crude material was chromatographed (silica gel, dichloromethane/hexane 3:1) to afford **38** (235 mg, 95%) as a purple microcrystalline solid. m.p. > 300 °C. ^{1}H NMR (400 MHz, $CDCl_3$) δ -2.80 (br s, 2H, NH), 1.52-1.55 (m, 72H, CH_3), 7.80-7.82 (m, 2H, ArH), 7.86-7.90 (m, 3H, ArH), 7.97 (d, 2H, J = 8.3 Hz, ArH), 8.09-8.14 (m, 7H, ArH), 8.16 (d, 2H, J = 1.7 Hz, ArH), 8.42 (br s, 1H, NH), 8.84 and 8.86 (ABq, 2H, J_{AB} = 4.7 Hz, β-pyrrolic H), 8.98-9.06 (m, 4H, β-pyrrolic H), 10.06 (s, 1H, CHO) ppm. ^{13}C NMR (100 MHz, $CDCl_3$) δ 31.7, 31.80, 31.84, 35.0, 35.1, 35.4, 115.4, 119.2, 121.0, 121.3, 122.1, 122.2, 122.5, 125.1, 127.2, 127.2, 128.5, 129.0, 129.3, 129.5, 129.6, 129.7, 130.3, 133.7, 135.9, 136.7, 139.6, 141.1, 141.5,

142.2, 148.6, 148.7, 148.8, 149.2, 151.1, 191.5 ppm. FTIR 713 (m), 723 (m), 800 (s), 1206 (m), 1246 (m), 1362 (m), 1474 (m), 1572 (m), 1700 (m, C=O), 3280 (w, NH), 3435 (w, NH) cm^{-1}. Anal Calcd for $C_{84}H_{98}N_6O$: C, 83.54; H, 8.18; N, 6.96. Found: C, 81.76; H, 8.54; N, 6.21. Anal Calcd for $C_{84}H_{98}N_6O.½\ CH_2Cl_2$: C, 81.18; H, 7.98; N, 6.72.

(5,10,15,20-Tetrakis(3,5-di-*tert*-butylphenyl)porphyrin[2,3-*b*]-1'*H*-imidazol-2'-yl)-3''-formylphenyl 39

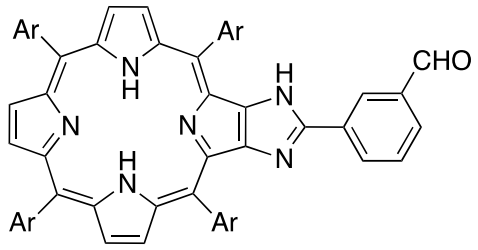

Starting with **36**, the crude material was chromatographed (silica gel, dichloromethane/hexane 3:1) to afford **39** (210 mg, 84%) as a purple microcrystalline solid. m.p. > 300 °C. ^{1}H NMR (400 MHz, $CDCl_3$) δ -2.80 (br s, 2H, NH), 1.52-1.55 (m, 72H, CH_3), 7.62 (app. t, 1H, J = 7.6 Hz, ArH), 7.79-7.82 (m, 2H, ArH), 7.85-7.91 (m, 2H, ArH), 8.09-8.19 (m, 11H, ArH), 8.36 (br s, 1H, NH), 8.85 and 8.87 (ABq, 2H, J_{AB} = 4.7 Hz, β-pyrrolic H), 8.89 (d, 2H, J = 4.7 Hz, β-pyrrolic H), 9.03-9.05 (m, 3H, β-pyrrolic H), 10.11 (s, 1H, CHO) ppm. ^{13}C NMR (100 MHz, $CDCl_3$) δ 31.7, 31.9, 35.0, 35.1, 35.4, 115.4, 119.2, 120.3, 121.0, 121.2, 122.1, 122.3, 122.5, 125.2, 127.1, 127.3, 128.6, 129.1, 129.5, 129.6, 129.7, 130.8, 132.3, 133.5, 137.0, 139.7, 141.1, 141.6, 142.3, 148.6, 148.75, 148.82, 149.3, 151.1, 191.5 ppm. FTIR 713 (m), 713 (m), 798 (s), 1202 (m), 1247 (m), 1391 (m), 1474 (m), 1590 (m), 1703 (m, C=O), 3281 (w, NH), 3434 (w, NH) cm^{-1}. Anal Calcd for $C_{84}H_{98}N_6O$: C, 83.54; H, 8.18; N, 6.96. Found: C, 81.23; H, 8.48; N, 6.47. Anal Calcd for $C_{84}H_{98}N_6O.½\ CH_2Cl_2$: C, 81.18; H, 7.98; N, 6.72.

2.7.6 Preparation of Quinoxaline-fused Porphyrins

5,10,15,20-Tetrakis(3,5-di-*tert*-butylphenyl)porphyrin[2,3-*b*]-6'-nitroquinoxaline 41

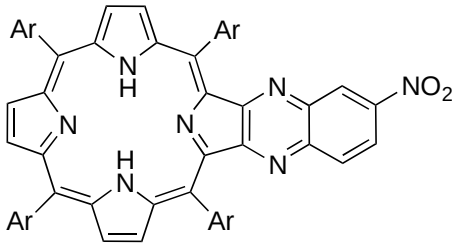

A mixture of 2,3-dioxo-5,10,15,20-tetrakis(3,5-di-*tert*-butylphenyl)chlorin **21** (600 mg, 0.54 mmol), 4-nitro-1,2-diaminobenzene (116 mg, 0.76 mmol) and pyridine (5 mL) in dichloromethane (35 mL) was stirred at room temperature for 5 days. The reaction mixture was diluted with dichloromethane (30 mL). The organic layer was washed with hydrochloric acid (3 M, 3 x 50 mL), water (50 mL), saturated sodium carbonate (2 x 50 mL), brine (50 mL), dried over anhydrous sodium sulfate, filtered and evaporated to dryness under vacuum. The crude product obtained was chromatographed (silica gel, dichloromethane/hexane 1:1) to afford pure **41** (635 mg, 95%) as a purple microcrystalline solid. m.p. > 300 °C. ^{1}H NMR (400 MHz, $CDCl_3$) δ -2.48 (br s, 2H, NH), 1.48 (s, 18H, CH_3), 1.50 (s, 18H, CH_3), 1.54 (app. s, 36H, CH_3), 7.81-7.83 (m, 2H, ArH), 7.91-7.99 (m, 6H, ArH), 8.00-8.02 (m, 1H, ArH), 8.09-8.11 (m, 4H, ArH), 8.52 (dd, 1H, *J* = 2.5, 9.1 Hz, ArH), 8.74 (d, 1H, *J* = 2.5 Hz, ArH), 8.80 (app. s, 2H, β-pyrrolic H), 9.00-9.03 (m, 2H, β-pyrrolic H), 9.08-9.13 (m, 2H, β-pyrrolic H) ppm. ^{13}C NMR (100 MHz, $CDCl_3$) δ 31.7, 31.9, 35.0, 35.1, 118.6, 118.8, 121.0, 121.2, 121.3, 122.1, 123.1, 123.2, 127.0, 128.2, 128.3, 128.6, 128.7, 129.6, 131.7, 134.2, 134.6, 138.5, 138.6, 139.1, 139.4, 139.6, 140.4, 140.6, 140.9, 144.2, 144.4, 147.2, 148.9, 149.1, 149.2, 153.9, 154.2, 155.3, 155.4 ppm. FTIR 711 (m), 762 (m), 801 (s), 822 (m), 1153 (m), 1224 (m), 1247 (m), 1344 (m), 1535 (m, NO_2), 1592 (m), 3347 (w, NH) cm^{-1}. Anal Calcd for $C_{82}H_{95}N_7O_2$: C, 81.35; H, 7.91; N, 8.10. Found: C, 79.48; H, 8.24; N, 7.78. Anal Calcd for $C_{82}H_{95}N_7O_2$.½ CH_2Cl_2: C, 79.07; H, 7.72; N, 7.82. The spectroscopic data are in agreement with those reported in the literature.[12]

5,10,15,20-Tetrakis(3,5-di-*tert*-butylphenyl)porphyrin[2,3-*b*]-6'-aminoquinoxaline 42

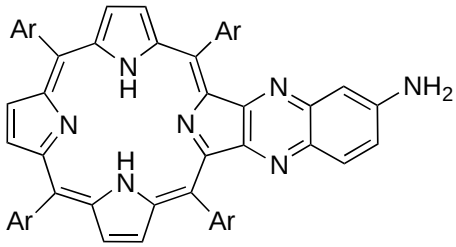

To a mixture of **41** (635 mg, 0.52 mmol) and anhydrous stannous chloride (0.99 g, 5.2 mmol) in dichloromethane (50 mL), was added hydrochloric acid (10 M, 2.5 mL) under an argon atmosphere. The reaction mixture was stirred at room temperature for 2 days. The organic layer was washed with water (2 x 50 mL), sodium hydroxide solution (3 M, 2 x 50 mL), water (50 mL) and brine (50 mL), dried over anhydrous sodium sulfate, filtered and evaporated to dryness under vacuum. The crude compound obtained was purified by column chromatography (silica gel, dichloromethane/hexane 1:1) to afford pure **42** (500 mg, 80%) as a purple microcrystalline solid. m.p. > 300 °C. ^{1}H NMR (400 MHz, $CDCl_3$) δ -2.48 (br s, 2H, NH), 1.47 (s, 18H, CH_3), 1.49 (s, 18H, CH_3), 1.53 (app. s, 36H, CH_3), 4.12 (br s, 2H, NH_2), 6.88 (d, 1H, *J* = 2.5 Hz, ArH), 7.17 (dd, 1H, *J* = 2.5, 8.9 Hz, ArH), 7.59 (d, 1H, *J* = 8.9 Hz, ArH), 7.79 (app. t, 2H, *J* = 1.6 Hz, ArH), 7.89 (app. t, 2H, *J* = 1.6 Hz, ArH), 7.96 (app. d, 4H, *J* = 1.6 Hz, ArH), 8.09 (app. d, 4H, *J* = 1.6 Hz, ArH), 8.77 (app. s, 2H, β-pyrrolic H), 8.94-9.05 (m, 4H, β-pyrrolic H) ppm. ^{13}C NMR (100 MHz, $CDCl_3$) δ 31.7, 31.88, 31.91, 34.97, 35.05, 109.4, 117.7, 118.1, 120.5, 120.6, 121.0, 121.6, 122.4, 122.6, 127.8, 127.9, 128.0, 128.1, 128.5, 129.6, 131.5, 133.9, 134.0, 131.5, 133.9, 134.0, 136.1, 137.8, 137.9, 139.7, 141.0, 141.1, 141.2, 142.7, 146.3, 147.0, 147.1, 148.7, 148.8, 150.4, 153.4, 154.5, 154.7 ppm. FTIR 714 (m), 799 (s), 923 (m), 1124 (m), 1221 (m), 1247 (m), 1361 (m), 1591 (m), 1630 (m), 2362 (m), 3308 (w, NH_2), 3394 (w, NH) cm^{-1}. Anal Calcd for $C_{82}H_{97}N_7$: C, 83.42; H, 8.28; N, 8.30. Found: C, 81.18; H, 8.49; N, 8.01. Anal Calcd for $C_{82}H_{97}N_7$.½ CH_2Cl_2: C, 81.01; H, 8.08; N, 8.02. The spectroscopic data are in agreement with those reported in the literature.[12]

5,10,15,20-Tetrakis(3,5-di-*tert*-butylphenyl)porphyrin[2,3-*b*]-6'-methoxycarbonyl-quinoxaline 43

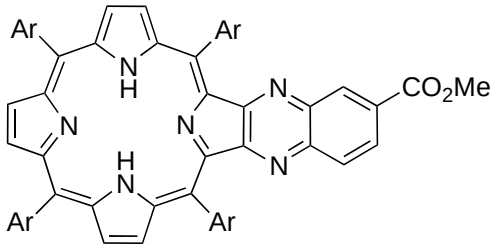

In a mixture of 2,3-dioxo-5,10,15,20-tetrakis(3,5-di-*tert*-butylphenyl)chlorin **21** (500 mg, 0.45 mmol) and methyl 3,4-diaminobenzoate (108 mg, 0.65 mmol) in dichloromethane (30 mL) was added pyridine (5 mL) and stirred for 5 days. The reaction mixture was diluted with dichloromethane (30 mL). The organic layer was washed with hydrochloric acid (3 M, 3 x 50 mL), water (50 mL), saturated sodium carbonate (2 x 50 mL), brine (50 mL), dried over anhydrous sodium sulfate and evaporated under vacuum. The crude product obtained was chromatographed (silica gel, dichloromethane/hexane 1:1) to afford pure **43** (550 mg, 98%). m.p. > 300 °C. ^{1}H NMR (400 MHz, $CDCl_3$) δ -2.48 (br s, 2H, NH), 1.49 (s, 18H, CH_3), 1.50 (s, 18H, CH_3), 1.54 (app. s, 36H, CH_3), 4.06 (s, 3H, CO_2CH_3), 7.81-7.83 (m, 2H, ArH), 7.86 (d, 1H, *J* = 8.7 Hz, ArH), 7.94-7.96 (m, 1H, ArH), 7.97-8.00 (m, 5H, ArH), 8.10-8.12 (m, 4H, ArH), 8.33 (dd, 1H, *J* = 1.8, 8.7 Hz, ArH), 8.60 (d, 1H, *J* = 1.8 Hz, ArH), 8.80 (app. s, 2H, β-pyrrolic H), 8.99-9.02 (m, 2H, β-pyrrolic H), 9.07-9.12 (m, 2H, β-pyrrolic H) ppm. ^{13}C NMR (100 MHz, $CDCl_3$) δ 31.7, 31.9, 35.02, 35.06, 52.5, 118.3, 118.5, 120.9, 121.1, 121.2, 122.9, 123.0, 128.0, 128.1, 128.4, 129.6, 130.1, 130.5, 133.6, 134.3, 134.4, 138.2, 138.3, 139.5, 139.6, 139.8, 140.6, 140.7, 141.0, 142.7, 145.1, 145.3, 148.8, 149.0, 153.4, 153.7, 155.0, 155.1, 166.8 ppm. FTIR 641 (w), 711 (m), 721 (m), 760 (m), 800 (s), 848 (w), 879 (w), 899 (w), 921 (m), 990 (w), 1087 (w), 1122 (m), 1149 (m), 1223 (m), 1248 (s), 1291 (w), 1361 (m), 1392 (w), 1429 (w), 1475 (w), 1592 (m), 1729 (m, C=O), 2956 (m), 3336 (w, NH) cm^{-1}. Anal Calcd for $C_{84}H_{98}N_6O_2$: C, 82.45;

H, 8.07; N, 6.87. Found: C, 80.88; H, 8.47; N, 6.65. Anal Calcd for $C_{84}H_{98}N_6O_2$.½ CH_2Cl_2: C, 80.15; H, 7.88; N, 6.64.

5,10,15,20-Tetrakis(3,5-di-*tert*-butylphenyl)porphyrin[2,3-*b*]-6'-hydroxymethylene-quinoxaline 44

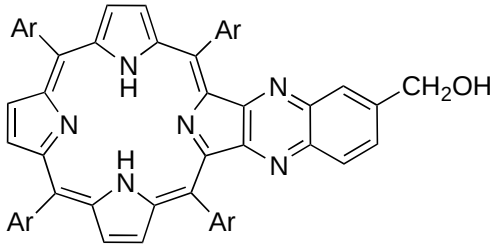

A mixture of **43** (610 mg, 0.74 mmol) and sodium borohydride (483 mg, 14.22 mmol) in THF (100 mL) was heated to reflux for 24 h. On completion, methanol (20 mL) was added to reaction mixture and reflux for overnight. On cooling reaction mixture was washed with sodium hydroxide solution (3 M, 2 x 75 mL), water (75 mL), brine (75 mL), dried over anhydrous sodium sulfate and evaporated under vacuum. The crude product obtained was chromatographed (silica gel, dichloromethane/hexane 2:1) to afford pure **44** (455 mg, 76%). m.p. > 300 °C. ^{1}H NMR (400 MHz, $CDCl_3$) δ -2.47 (br s, 2H, NH), 1.48-1.51 (m, 36H, CH_3), 1.55 (app. s, 36H, CH_3), 4.97 (d, 2H, *J* = 5.6 Hz, CH_2), 7.75-7.85 (m, 5H, ArH), 7.93-7.95 (m, 2H, ArH), 7.97-7.80 (m, 4H, ArH), 8.10-8.13 (m, 4H, ArH), 8.81 (app. s, 2H, β-pyrrolic H), 8.98-9.02 (m, 3H, β-pyrrolic H), 9.05-9.10 (m, 3H, β-pyrrolic H) ppm. The exchangeable OH proton was not observed. ^{13}C NMR (100 MHz, $CDCl_3$) δ 31.7, 31.9, 35.0, 35.1, 65.3, 118.18, 118.23, 120.8, 120.9, 121.1, 122.74, 122.76, 127.7, 128.0, 128.1, 128.3, 128.4, 128.5, 129.6, 130.8, 134.2, 138.06, 138.09, 139.60, 139.65, 140.3, 140.7, 140.8, 140.9, 141.1, 141.7, 145.8, 145.9, 148.8, 148.88, 148.93, 152.8, 153.0, 154.87, 154.89 ppm. FTIR 642 (w), 713 (m), 722 (m), 763 (m), 801 (s), 849 (w), 878 (w), 897 (w), 922 (m), 991 (w), 1088 (w), 1120 (m), 1148 (m), 1223 (m), 1291 (w), 1361 (m), 1392 (w), 1429 (w), 1475 (w), 1592 (m), 2952 (m), 3334 (w,

NH) cm^{-1}. Anal Calcd for $C_{83}H_{98}N_6O$: C, 83.37; H, 8.26; N, 7.03. Found: C, 82.10; H, 8.64; N, 6.80. Anal Calcd for $C_{83}H_{98}N_6O.1/4\ CH_2Cl_2$: C, 82.16; H, 8.16; N, 6.91.

5,10,15,20-Tetrakis(3,5-di-*tert*-butylphenyl)porphyrin[2,3-*b*]-6'-formylquinoxaline 45

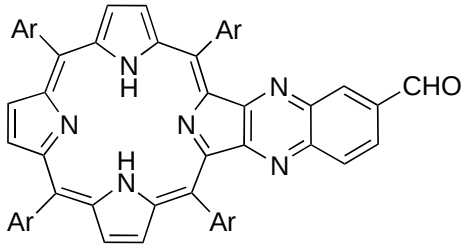

Manganese oxide (404 mg, 4.65 mmol) was added to a mixture of alcohol quinoxaline porphyrin **44** (400 mg, 0.31 mmol) in dichloromethane (150 mL) and the resulting mixture was stirred overnight. On completion, the reaction mixture was filtered over silica gel and the organic layer was evaporated to dryness. The crude product obtained was chromatographed (silica gel, dichloromethane/hexane 1:1) to afford pure **45** (270 mg, 68%). m.p. > 300 °C. ^{1}H NMR (400 MHz, $CDCl_3$) δ -2.61 (br s, 2H, NH), 1.53-1.55 (m, 72H, CH_3), 7.79-7.83 (m, 4H, ArH), 7.90-7.96 (m, 2H, ArH), 8.05-8.12 (m, 7H, ArH), 8.25-8.29 (m, 1H, ArH), 8.40-8.44 (m, 1H, ArH), 8.65 (d, 2H, *J* = 4.7 Hz, β-pyrrolic H), 8.90 (d, 2H, *J* = 4.7 Hz, β-pyrrolic H), 8.92 (app. s, 2H, β-pyrrolic H) 9.53 (s, 1H, CHO) ppm. ^{13}C NMR (100 MHz, $CDCl_3$) δ 31.7, 31.8, 31.9, 35.01, 35.04, 35.1, 118.4, 118.7, 120.99, 121.03, 121.2, 122.9, 123.1, 125.2, 128.1, 128.2, 128.4, 128.5, 128.6, 129.6, 131.6, 134.4, 134.5, 136.3, 136.9, 138.37, 138.40, 139.5, 139.6, 140.2, 140.7, 141.0, 143.8, 144.8, 145.0, 148.9, 149.06, 149.09, 153.5, 154.0, 155.2, 155.3, 191.8 ppm. FTIR 711 (s), 738 (m), 762 (m), 801 (s), 879 (m), 923 (m), 1118 (m), 1226 (m), 1247 (m), 1361 (m), 1475 (m), 1593 (m), 1701 (m, C=O), 2959 (m), 3331 (w, NH) cm^{-1}. Anal Calcd for $C_{83}H_{96}N_6O$: C, 83.51; H, 8.11; N, 7.04. Found: C, 79.99; H, 8.46; N, 6.50. Anal Calcd for $C_{83}H_{96}N_6O.2/3\ CH_2Cl_2$: C, 80.37; H, 7.85; N, 6.72.

2.8 References

1. Megiatto, J. D.; Schuster, D. I.; Abwandner, S.; de Miguel, G.; Guldi, D. M. *J. Am. Chem. Soc.* **2010**, *132* (11), 3847-3861.
2. Imahori, H.; Hagiwara, K.; Aoki, M.; Akiyama, T.; Taniguchi, S.; Okada, T.; Shirakawa, M.; Sakata, Y. *J. Am. Chem. Soc.* **1996**, *118* (47), 11771-11782.
3. Baillargeon, V. P.; Stille, J. K. *J. Am. Chem. Soc.* **1986**, *108*, 452-461.
4. Salom-Roig, X. J.; Chambron, J.-C.; Goze, C.; Heitz, V.; Sauvage, J.-P. *Eur. J. Org. Chem.* **2002**, *2002* (19), 3276-3280.
5. Urbani, M.; Iehl, J.; Osinska, I.; Louis, R.; Holler, M.; Nierengarten, J.-F. *Eur. J. Org. Chem.* **2009**, *2009* (22), 3715-3725.
6. Tkachenko, N. V.; Lemmetyinen, H.; Sonoda, J.; Ohkubo, K.; Sato, T.; Imahori, H.; Fukuzumi, S. *J. Phys. Chem. A* **2003**, *107* (42), 8834-8844.
7. Crossley, M. J.; Burn, P. L. *J. Chem. Soc., Chem. Commun.* **1987**, 39-40.
8. Crossley, M. J.; McDonald, J. A. *J. Chem. Soc., Perkin Trans. 1* **1999**, (17).
9. Promarak, V.; Burn, P. L. *J. Chem. Soc., Perkin Trans. 1* **2001**, (1), 14-20.
10. Gabriel, S. *Ber. Dtsch. Chem. Ges.* **1916**, *49* (2), 1608-1613.
11. Beavington, R.; Rees, P. A.; Burn, P. L. *J. Chem. Soc., Perkin Trans. 1* **1998**, (17), 2847-2852.
12. Try, A. C., PhD Thesis, The University of Sydney, **1994**.

Chapter Three

Porphyrin-Boranil Conjugates

3.1 Background

Recently, Ziessel and coworkers[1,2] introduced new fluorescent N-B-O complexes, called boranils, with the ligands named "anils", from a contraction of "aniline imines". The ligands are readily prepared *via* reaction of aniline and a 2-hydroxybenzaldehyde. The boranils, with high quantum yields, are synthesized by forming boron complexes of the Schiff base (anil) ligands.[1, 3,4] Some representative boranils are shown in Figure 3.1.

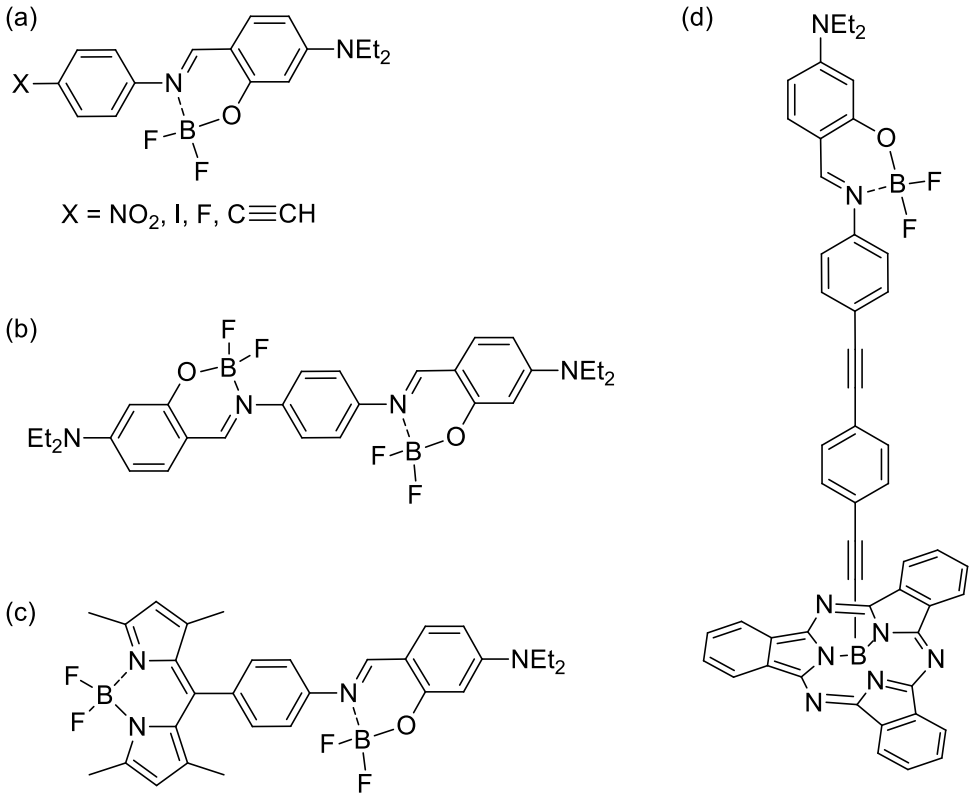

Figure 3.1: Examples of (a) simple boranils, (b) a bis-boranil, (c) a boranil-BODIPY dyad and (d) a boranil-subphthalocyanine dyad.[1]

As can be seen in Figure 3.1, several dyads where prepared, where the boranil unit was linked to other chromophores (as well as itself), such as a BODIPY unit and a subphthalocyanine unit (Figure 3.1, (c) and (d), respectively). The reported photo-physical properties of the dyads showed that the boranil-BODIPY system (Figure 3.1 (c)) shows the linear combination in absorption spectra, as expected from the fact that the two chromophores are not coplanar. When excited at 380 nm (boranil absorption maxima), quantitative energy transfer occurs; leading to

fluorescence of BODIPY at 514 nm. Similar results were observed in case of boranil-subphthalocyanine dyads (Figure 3.1 (d)), where the boranil unit served as input energy antenna for a cascade energy transfer to the subphthalocyanine residue.[1]

In this Chapter, the three amino-functionalised porphyrin frameworks shown in Figure 1.30 (see Chapter Two, Section 2.2 for their synthetic schemes) were reacted with salicylaldehyde (2-hydroxybenzaldehyde) and 2-hydroxy-1-naphthaldehyde to form new porphyrin anils. These compounds were converted to the corresponding porphyrin-boranils, and their zinc(II) complexes. The three series of compounds that are the subject of this Chapter are depicted in Figure 3.2.

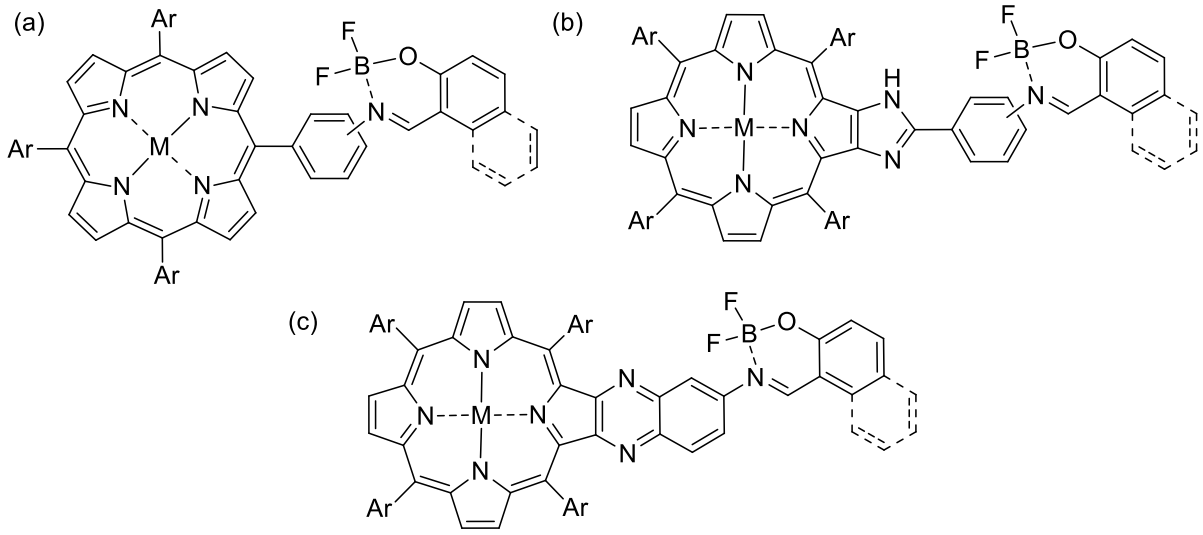

Figure 3.2: Porphyrin-boranil conjugates; (a) *meso*-phenyl porphyrin boranil conjugates, (b) imidazoloporphyrin-boranil conjugates and (c) quinoxalinoporphyrin-boranil conjugates. M = 2H (free-base porphyrins) or Zn (zinc(II) porphyrins).

As a preliminary investigation of the photo-physical properties of these compounds, the UV-visible absorption and fluorescence emission spectra of the free-base porphyrin-anils, free-base porphyrin-boranils and zinc(II) porphyrin-boranils were recorded, and their quantum yields were calculated. The porphyrins were converted to their zinc(II) chelates as zinc(II) porphyrins are known to be suitable donors in electron and energy transfer studies.[5]

3.2 Synthesis

The synthetic routes for *meso*-phenyl porphyrin boranil conjugates, imidazoloporphyrin-boranil conjugates and quinoxalinoporphyrin-boranil conjugates are shown in Schemes 3.1, 3.2 and 3.3, respectively, with each involving three steps. The first step is the condensation of substituted free-base porphyrin amines with either salicylaldehyde or 2-hydroxy-1-naphthaldehyde, in the presence of a catalytic amount of *p*-toluenesulfonic acid to afford the porphyrin-anil conjugates. The second step involves the formation of the boron complexes *via* reaction of the free anil ligands with boron trifluoride diethyl etherate in the presence of triethylamine, to afford the porphyrin-boranil conjugates. The last step involves zinc(II) complexation by the porphyrin macrocycle. The crude products from steps two and three were purified by column chromatography with small columns, as the products tend to decompose if they spend a prolonged period of time on silica. It was found that the best yields could be obtained following the reaction sequence shown in the schemes below, *i.e.*, formation of the boranil followed by zinc(II) complexation, rather than initial zinc(II) complexation, then boranil formation as the final step. This may be the result of triethylamine (a reagent use in the boranil synthesis reaction) coordinating to the zinc(II) porphyrin, hindering purification of the desired material.

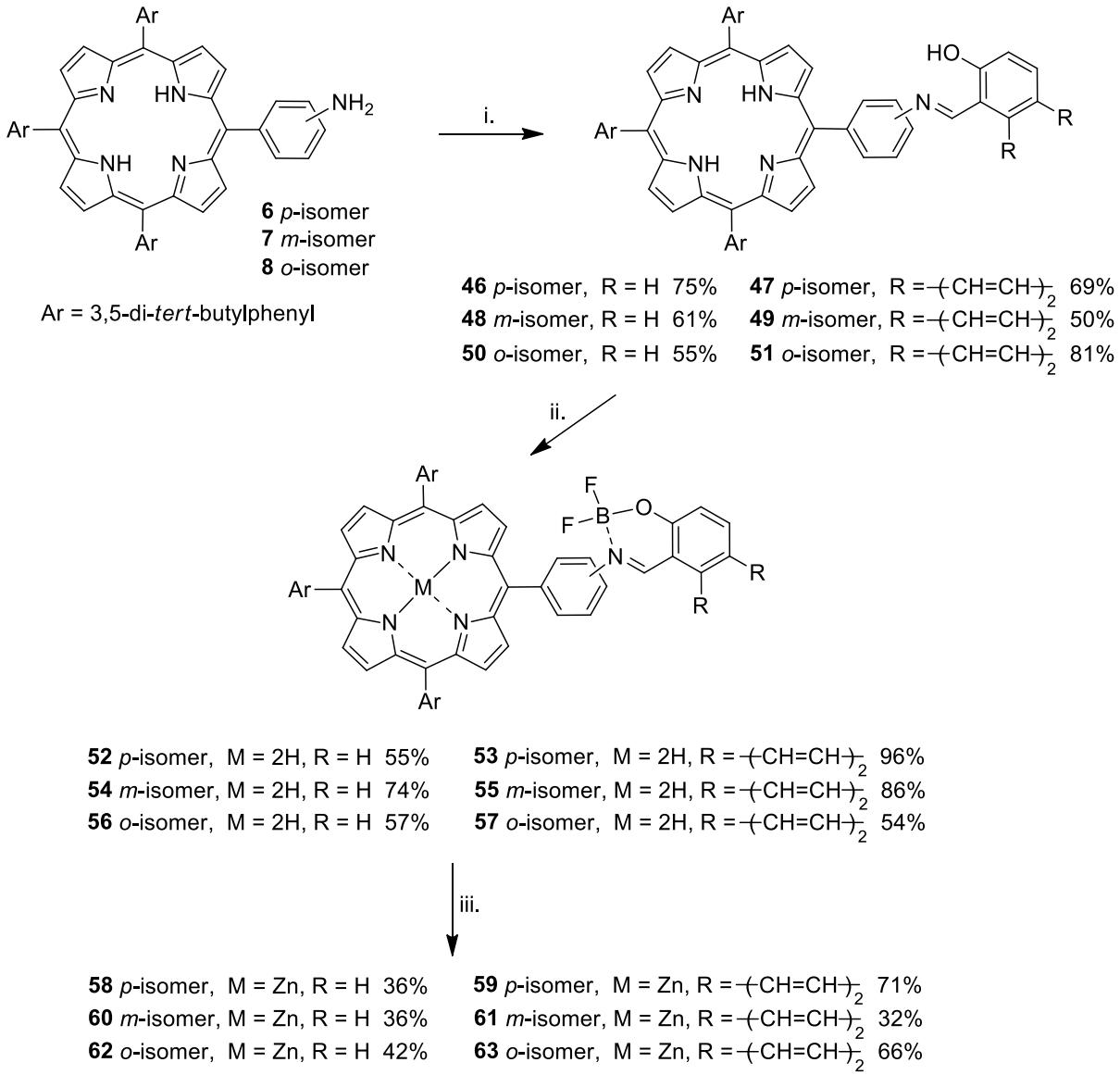

Scheme 3.1: i. Salicylaldehyde or 2-hydroxy-1-naphthaldehyde, *p*-TSA, EtOH; ii. BF_3OEt_2, TEA, DCE; iii. $Zn(OAc)_2$, CH_2Cl_2.

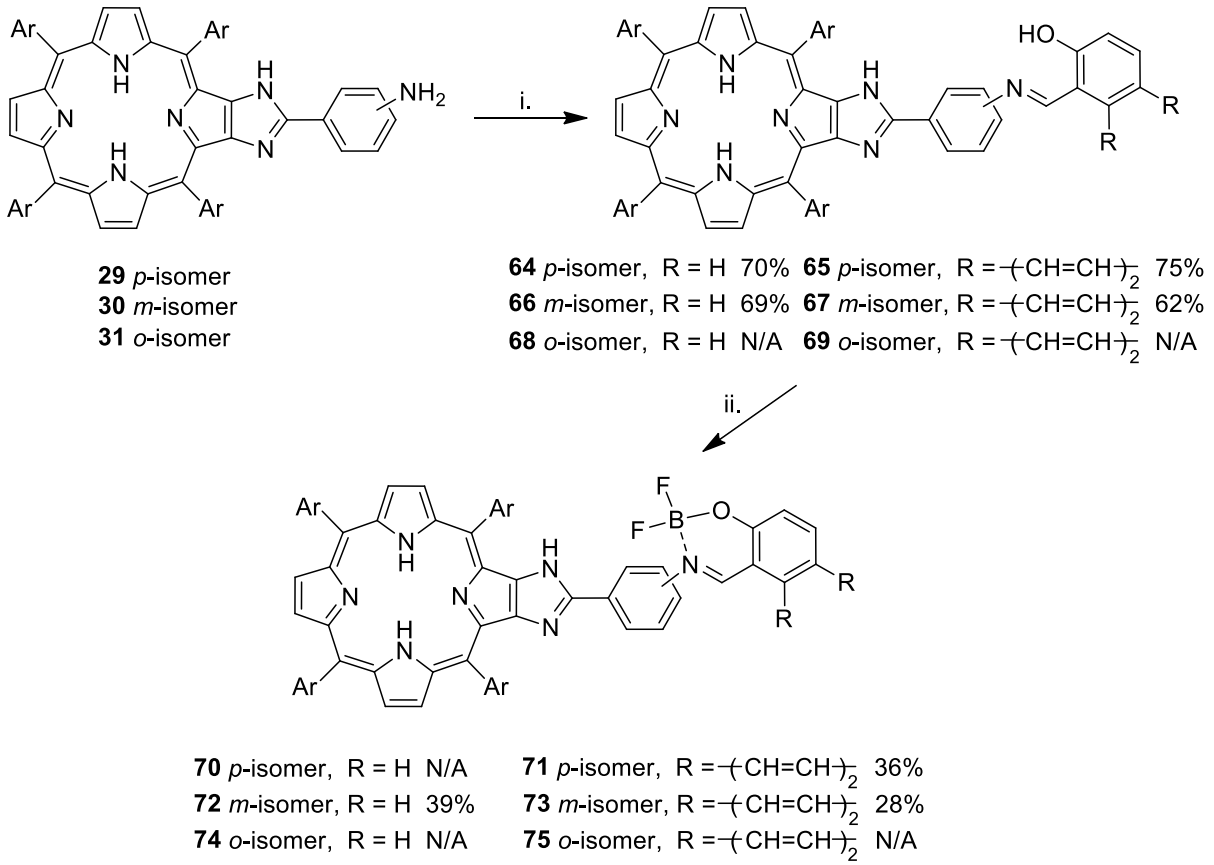

29 *p*-isomer
30 *m*-isomer
31 *o*-isomer

64 *p*-isomer, R = H 70% **65** *p*-isomer, R = $-(CH=CH)_2-$ 75%
66 *m*-isomer, R = H 69% **67** *m*-isomer, R = $-(CH=CH)_2-$ 62%
68 *o*-isomer, R = H N/A **69** *o*-isomer, R = $-(CH=CH)_2-$ N/A

70 *p*-isomer, R = H N/A **71** *p*-isomer, R = $-(CH=CH)_2-$ 36%
72 *m*-isomer, R = H 39% **73** *m*-isomer, R = $-(CH=CH)_2-$ 28%
74 *o*-isomer, R = H N/A **75** *o*-isomer, R = $-(CH=CH)_2-$ N/A

Scheme 3.2: i. Salicylaldehyde or 2-hydroxy-1-naphthaldehyde, *p*-TSA, EtOH; ii. BF_3OEt_2, TEA, DCE.

The attempted syntheses of **68** and **69** under various conditions proved unsuccessful; the reaction mixture was stirred for 30 days and also heated at reflux for 8 days, but in all cases unconverted amino porphyrins were recovered in near quantitative yields. This lack of reactivity may be related to an interaction between the *o*-amino group and the imidazole nitrogen / NH group, as noted for the *o*-nitro group and the *o*-ester functionality in Section 2.4.

In another reaction that ultimately would be classed as unsuccessful, isolation of compound **70** in analytically pure form was problematic, with the compound proving to be more prone to decomposition than other free-base porphyrin-boranils formed in this work. Due to time constraints (and the fact that only three members of free-base imidazoloporphyrin-boranil conjugates were prepared) no zinc(II) adducts of this family were prepared in the current work.

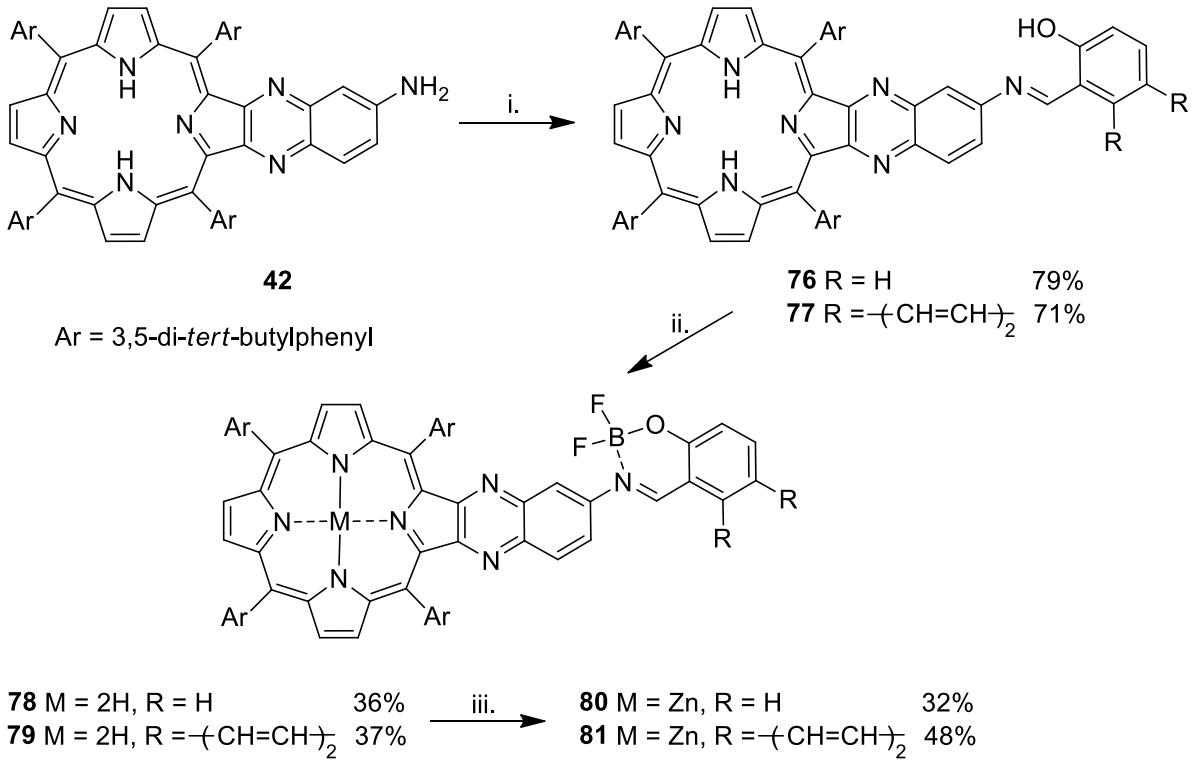

Scheme 3.3: i. Salicylaldehyde or 2-hydroxy-1-naphthaldehyde, *p*-TSA, EtOH; ii. BF_3OEt_2, TEA, DCE; iii. $Zn(OAc)_2$, CH_2Cl_2.

The appearance (or disappearance) of key signals in the ^{1}H NMR spectra of crude materials after work-up provided support for the formation of the desired products. In the case of the anils, this came in the form of the imine CH proton as a singlet in the region of δ 8.66-8.99 ppm (for salicylaldehyde derived anils) or δ 9.35-9.70 ppm (for 2-hydroxy-1-naphthaldehyde derived anils), together with the OH proton as a broad signal at δ 11.27-15.78 ppm, most likely a result of intramolecular H-bonding with the imine nitrogen.

Upon formation of the boranil, the OH signal is no longer present, and the imine CH proton signal undergoes a slight shift and broadens. Upon formation of the zinc(II) porphyrin complexes the inner NH proton signal is no longer present, whilst the previously mentioned features associated with boranils remain.

Some features of the ^{1}H NMR spectra of selected examples of these compounds are discussed below.

As noted in Chapter Two, with reference to the proton signals of the methyl ester group located at the *o*-position of *meso*-phenyl ring, the effect of placement of the anil unit over the face of the porphyrin ring is readily apparent, with the porphyrin ring current exerting a strong effect on the signals of the salicylaldehyde-derived unit.

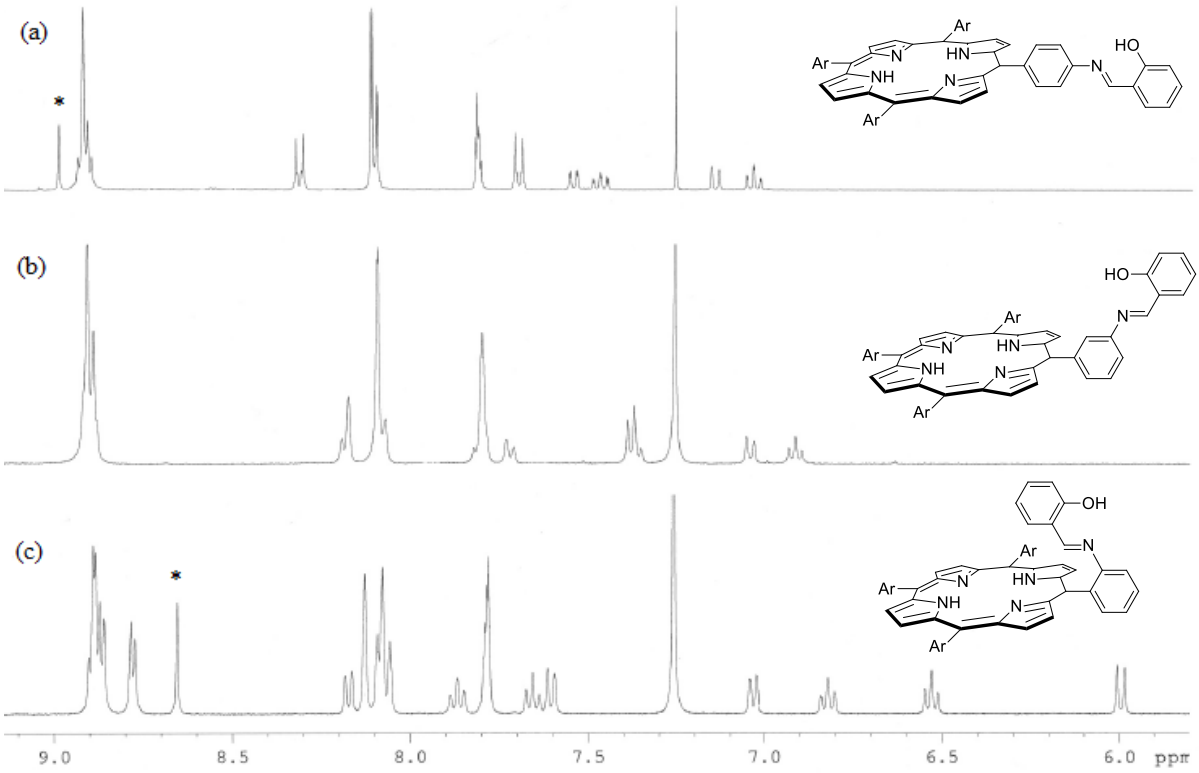

Figure 3.3: A section of the 400 MHz ^{1}H NMR spectra in $CDCl_3$ at 298 K of the anils derived from free-base *meso*-phenyl porphyrins bearing amino groups at (a) the *p*-position, compound **46**, (b) the *m*-position, compound **48** and (c) the *o*-position, compound **50**. The asterisk (*) shows the position of the imine proton, which is located in the same region as the β-pyrrolic proton signals (8.75-8.83 ppm) for (b).

This effect is equally striking with all compounds in the series, and another example is shown in Figure 3.4 below, with the *p*-, *m*-, *o*-series of boranils derived from the products of the reaction of the amino-substituted *meso*-phenyl porphyrin series of compounds (**6**, **7** and **8**) with 2-hydroxy-1-naphthaldehyde.

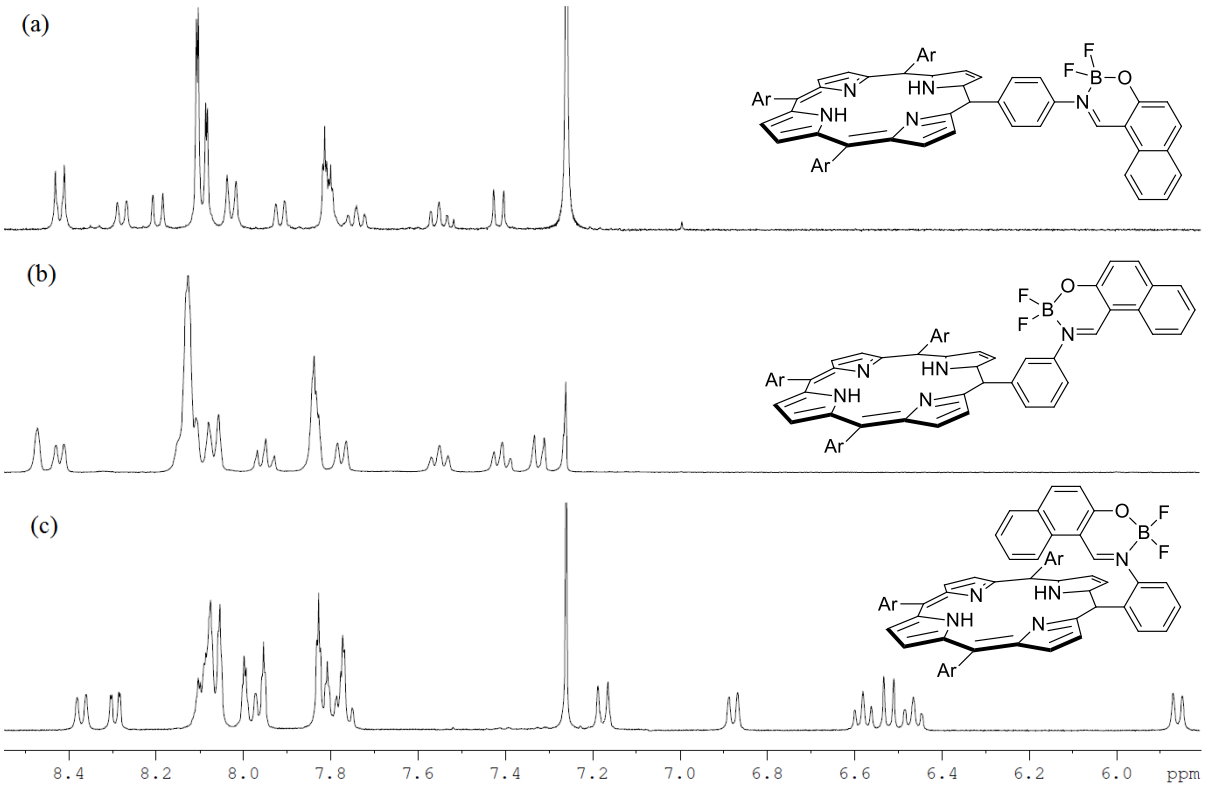

Figure 3.4: A section of the 400 MHz ^{1}H NMR spectra in $CDCl_3$ at 298 K of the boranils derived from free-base *meso*-phenyl porphyrins bearing amino groups at (a) the *p*-position, compound **53** (b) the *m*-position, compound **55** and (c) the *o*-position, compound **57**.

When boranil **56** is formed from anil **50** (both compounds have the boranil / anil unit oriented toward the porphyrin macrocycle by virtue of attachment *via* the *ortho* position of a *meso* phenyl ring), further upfield chemical shifts are observed, as shown in Figure 3.5. This may be a result of rigidification of the organic ligand over the porphyrin ring, as formation of other boranils leads to a general *downfield* chemical shift of signals associated with the anil portion of the spectrum, as exemplified in Figure 3.6 for the corresponding free-base *meso*-phenyl porphyrin *with p*-substituted systems, **46** and **52**.

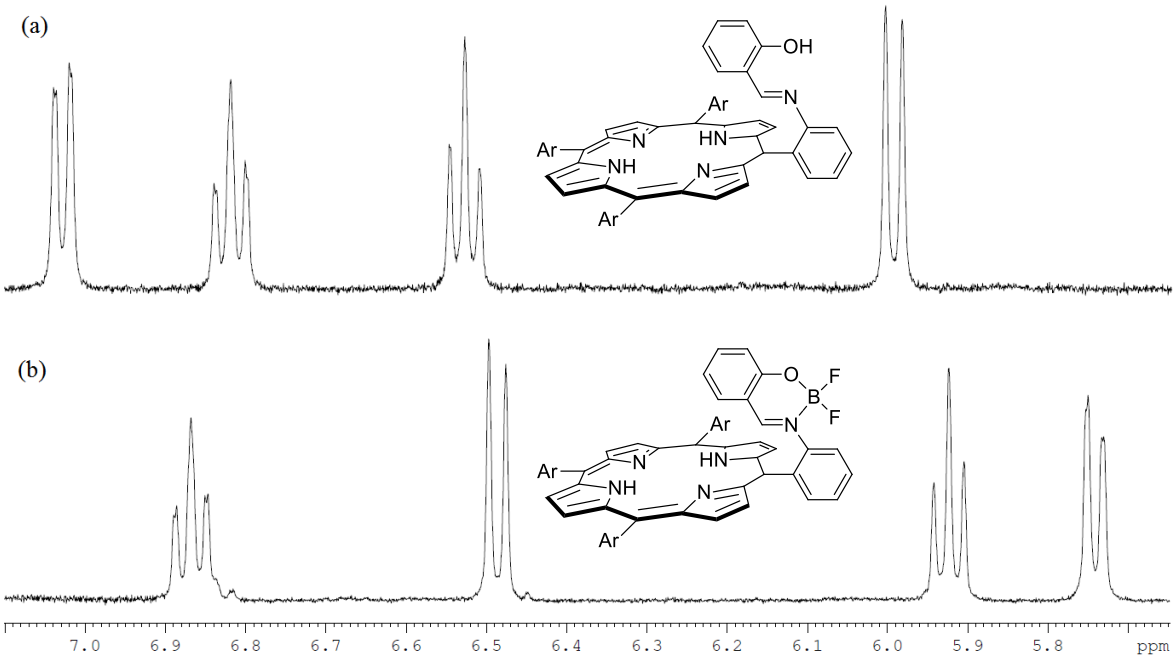

Figure 3.5: A section of the 400 MHz ^{1}H NMR spectra in $CDCl_3$ at 298 K of (a) the anil, compound **50** and (b) the boranil, compound **56**, derived from a free-base *meso*-phenyl porphyrin bearing an *o*-amino group.

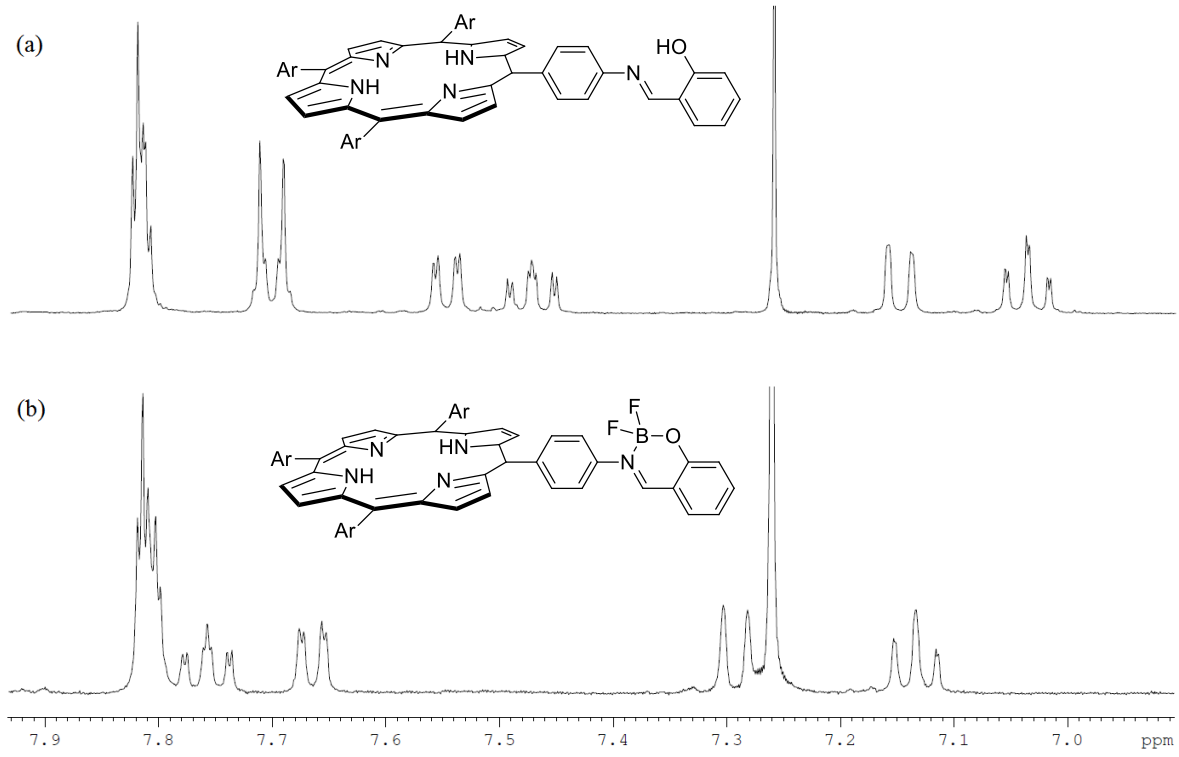

Figure 3.6: A section of the 400 MHz ^{1}H NMR spectra in $CDCl_3$ at 298 K of (a) the anil, compound **46** and (b) the boranil, compound **52**, derived from a free-base *meso*-phenyl porphyrin bearing an *p*-amino group.

Finally, asymmetry of ^{1}H NMR spectra associated with all imidazole-fused porphyrins in this work (noted in Section 2.4 and Figures 2.1 - 2.3) is exemplified with the spectrum of compound **65**, shown in Figure 3.7.

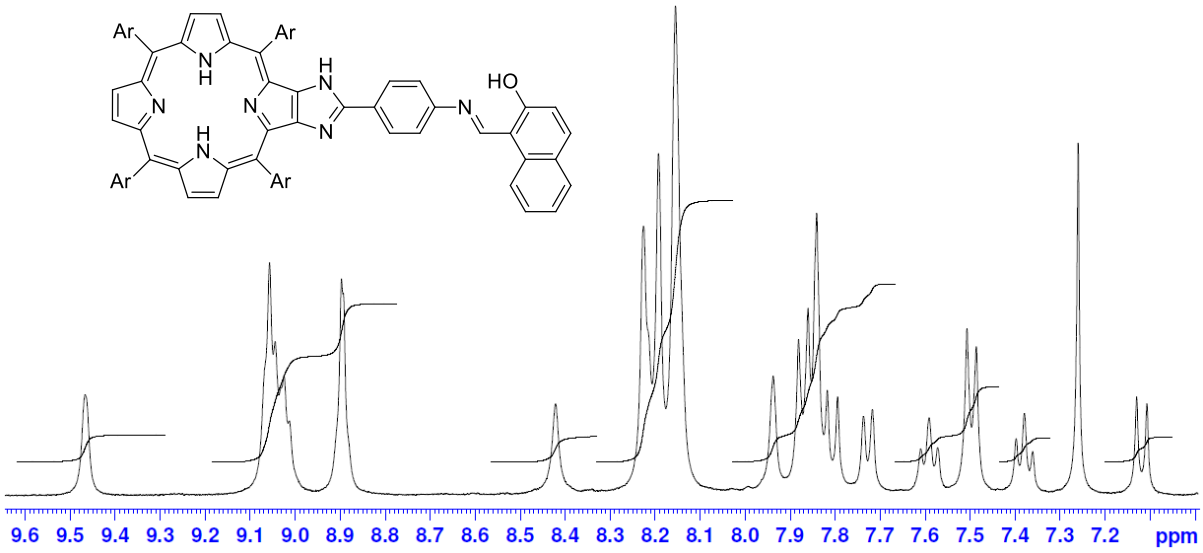

Figure 3.7: A section of the 400 MHz ^{1}H NMR spectra in $CDCl_3$ at 298 K of compound **65**, a free-base imidazoloporphyrin *p*-anil, from a reaction with 2-hydroxy-1-naphthaldehyde and **29**, showing the aromatic region; note the lack of symmetry in the spectrum. Minimum integral height represents 1 proton.

As discussed previously, assuming rapid tautomeric equilibrium of the imidazole ring on the ^{1}H NMR timescale, compounds of this type should exhibit a plane of symmetry, dissecting the imidazole ring and the opposing pyrrole ring in the porphyrin macrocycle. If this were the case, three β-pyrrolic proton environments are expected, but this is clearly not the case in the region of δ 8.5-9.1 ppm in Figure 3.7. The ^{1}H NMR spectrum of the β-pyrrolic region of compound **73**

(Figure 3.8) shows the best resolved signals of all imidazoloporphyrin compounds prepared in this work, with six distinct environments present in the form of three AB quartets.

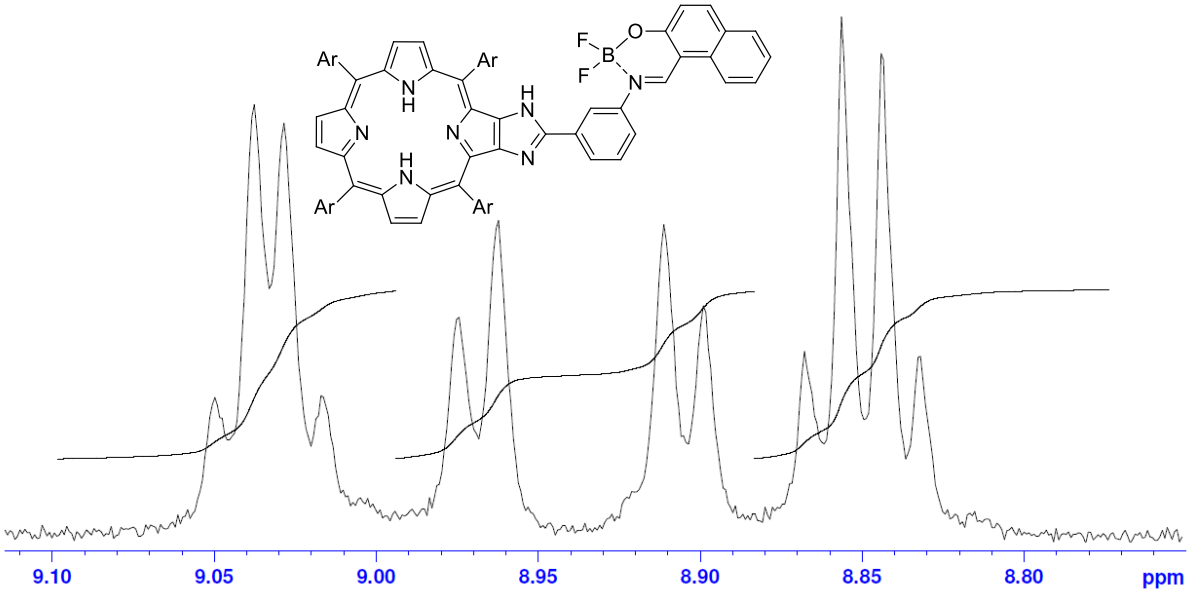

Figure 3.8: A section of the 400 MHz ^{1}H NMR spectra in $CDCl_3$ at 298 K of compound **73**, a free-base imidazoloporphyrin *m*-boranil, from a reaction with 2-hydroxy-1-naphthaldehyde showing the β-pyrrolic region, highlighting the asymmetry of the molecule; all β-pyrrolic protons appear in well resolved and unique environments, with three AB quartets clearly visible.

3.3 Photo-physical Properties

The UV-visible absorption, fluorescence emission and relative quantum yield of free-base porphyrin-anils and boranils, and zinc(II) porphyrin-boranils were recorded in de-acidified chloroform. The relative quantum yields of free-base porphyrin-anils and boranils were compared with tetraphenylporphyrin (TPP). In the case of zinc(II) porphyrin-boranils, ZnTPP was used as the reference standard. The photo-physical properties of *meso*-phenyl porphyrin-anils and boranils are summarised in Table 3.1.

Table 3.1: Absorption maxima wavelength (λ_{abs}, nm); molar extinction coefficient (ε, x 10^4, $Lmol^{-1}cm^{-1}$); fluorescence maxima wavelength (λ_{em}, nm); relative quantum yield (ϕ) of **46-63** in chloroform

No.	λ_{abs} (nm)	ε ($Lmol^{-1}cm^{-1}$)/10^4	λ_{em} (nm)	ϕ
Free-base porphyrin meso-*phenyl anil* ϕ^1				
46	422	52.75	651	0.099
47	423	37.20	653	0.124
48	422	59.27	651	0.068
49	422	43.13	650	0.100
50	423	39.90	652	0.085
51	423	40.25	652	0.098
Free-base porphyrin meso-*phenyl boranil* ϕ^1				
52	422	48.16	655	0.117
53	422	36.00	655	0.122
54	422	47.63	654	0.101
55	422	41.71	654	0.099
56	423	44.55	655	0.100
57	423	40.09	654	0.088
Zinc(II) porphyrin meso-*phenyl boranil* ϕ^2				
58	427	44.30	607	0.052
59	427	37.43	608	0.042
60	427	44.15	606	0.050
61	427	30.23	604	0.028
62	427	37.91	604	0.023
63	427	36.13	606	0.024

[1]relative quantum yield compared to TPP, [2]relative quantum yield compared to ZnTPP

The UV-visible spectra of free-base *meso*-phenyl porphyrin-anils **46-51**, free-base *meso*-phenyl porphyrin-boranils **52-57** and zinc(II) *meso*-phenyl porphyrin-boranils **58-63** are shown in Figure 3.9, Figure 3.10 and Figure 3.11, respectively. The free-base porphyrins showed a Soret band at around 422 nm and four Q-bands at around 525, 560, 600 and 650 nm. The zinc(II) boranil complexes showed a bathochromic shift of 4-5 nm compared with the free-base porphyrins, with a Soret band at 427 nm and two Q-bands at around 560 and 600 nm. The molar extinction coefficients of the free-base *meso*-phenyl porphyrin anils were observed in the range of 372,000-600,000 $Lmol^{-1}cm^{-1}$, whilst the values for the corresponding boranils were in the range of 360,000-480,000 $Lmol^{-1}cm^{-1}$, and the zinc(II) complexes show a further reduction, in the range of 300,000-440,000 $Lmol^{-1}cm^{-1}$. Essentially, the molar extinction coefficients generally decreased from free-base *meso*-phenyl porphyrin anil to free-base *meso*-phenyl porphyrin boranil to zinc(II) *meso*-phenyl porphyrin boranil.

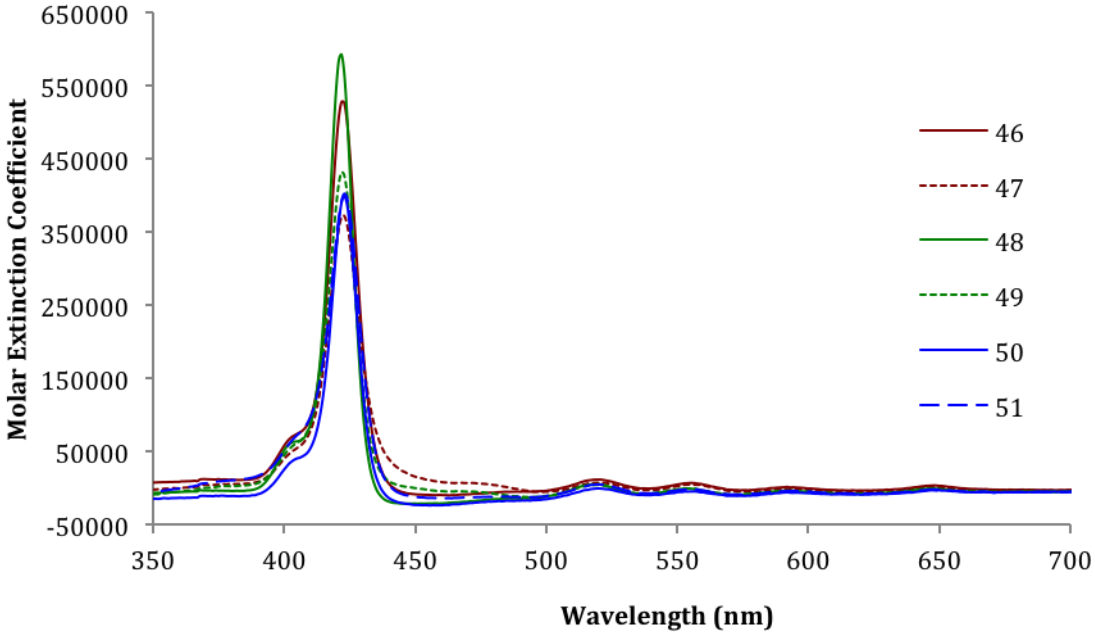

Figure 3.9: UV-visible spectra of free-base *meso*-phenyl porphyrin anils **46-51** in $CHCl_3$.

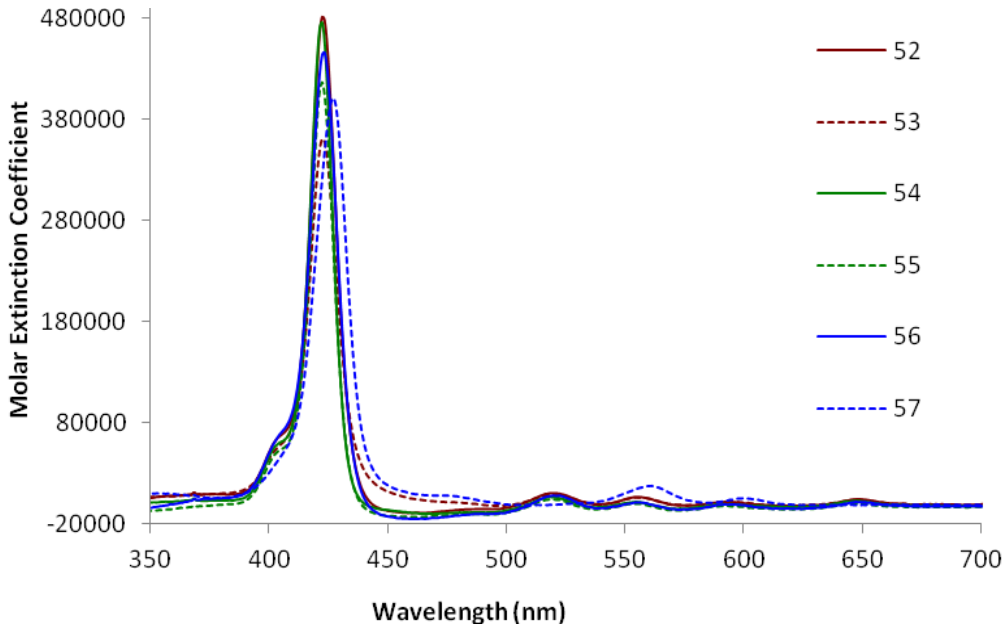

Figure 3.10: UV-visible spectra of free-base *meso*-phenyl porphyrin boranils **52-57** in $CHCl_3$.

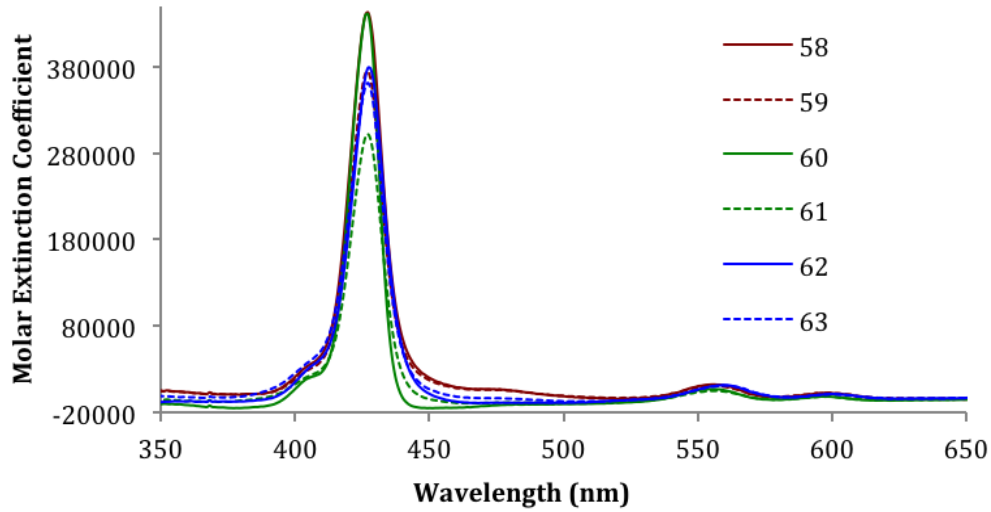

Figure 3.11: UV-visible spectra of zinc(II) *meso*-phenyl porphyrin boranils **58-63** in $CHCl_3$.

The normalised fluorescence emission spectra of free-base *meso*-phenyl porphyrin anils, free-base *meso*-phenyl porphyrin boranils and zinc(II) *meso*-phenyl porphyrin boranils in chloroform are shown in Figure 3.12, Figure 3.13 and Figure 3.14, respectively. The fluorescence emission and quantum yields of *meso*-phenyl porphyrin anils and boranils are summarised in Table 3.1. Typical fluorescence emission spectra for the zinc(II) complexes (Figure 3.14) were observed at

shorter wavelength (around 600 nm) compared to free-base porphyrins (around 650 nm), and the quantum yield of the zinc(II) complexes were considerably weaker than the free-base porphyrins.

In general, the quantum yield of all compounds decreases from *para* to *meta* to *ortho* substitution. The reduction of fluorescence intensity may indicate an interaction between the two chromophores in the excited state.[6]

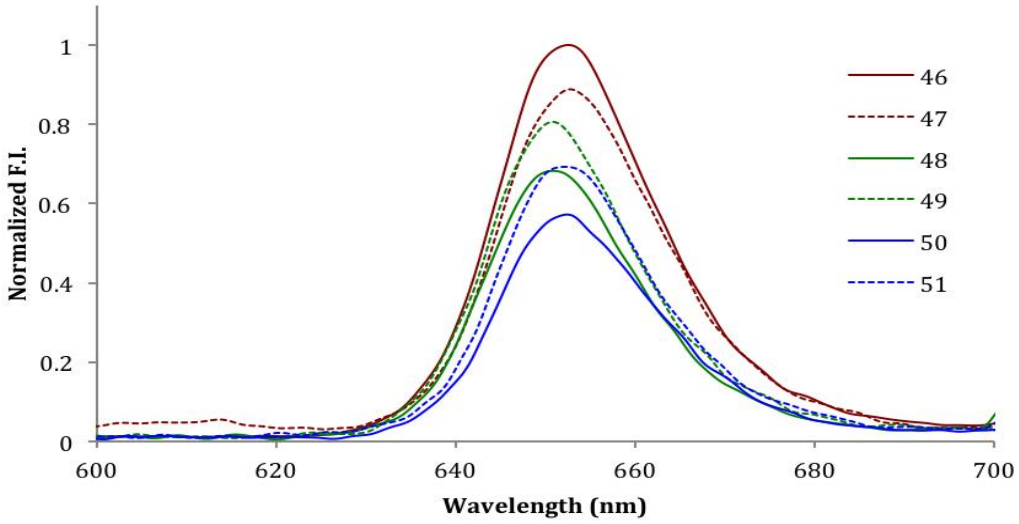

Figure 3.12: Normalised fluorescence spectra of free-base *meso*-phenyl porphyrin anils **46-51** in $CHCl_3$.

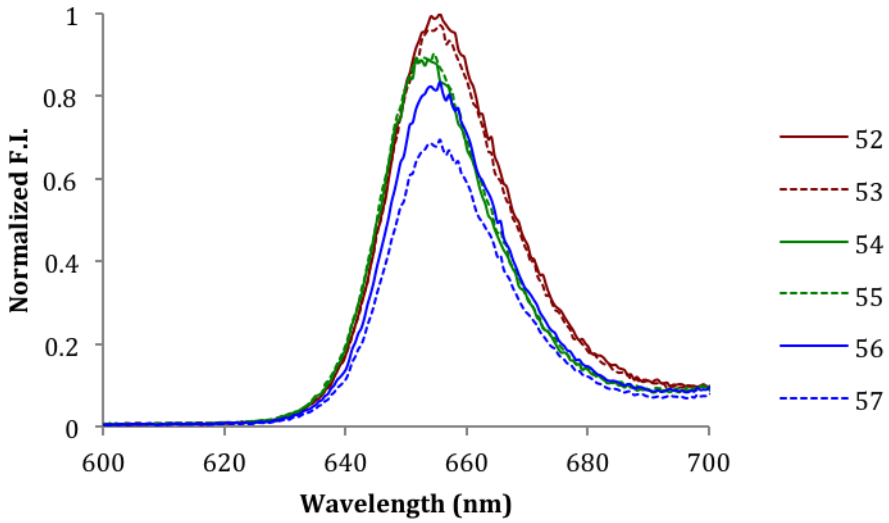

Figure 3.13: Normalised fluorescence spectra of free-base *meso*-phenyl porphyrin boranils **52-57** in $CHCl_3$.

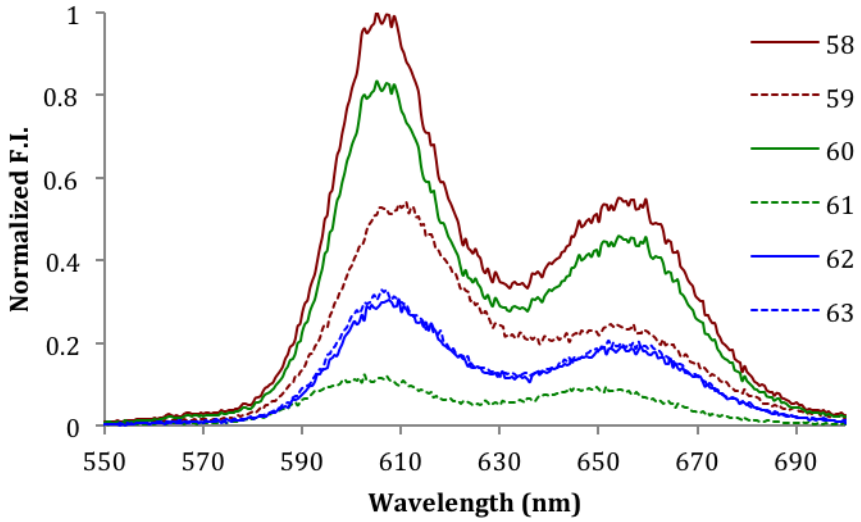

Figure 3.14: Normalised fluorescence spectra of zinc(II) *meso*-phenyl porphyrin boranils **58-63** in $CHCl_3$.

The photo-physical properties of free-base imidazoloporphyrin anils and boranils, free-base quinoxalinoporphyrin anils and boranils and zinc(II) quinoxalinoporphyrin boranils are summarised in Table 3.2.

The UV-visible spectra of free-base imidazolo- and quinoxalino-porphyrin anils **64-67**, **76** and **77**, respectively, are shown in Figure 3.15. The UV-visible spectra of free-base imidazolo- and quinoxalino-porphyrin boranils, **71-73**, **78** and **79**, respectively, are shown in Figure 3.16. The UV-visible spectra of zinc(II) quinoxalino-porphyrin boranils, **80** and **81** are shown in Figure 3.17.

Table 3.2: Absorption maxima wavelength (λ_{abs}, nm); molar extinction coefficient (ε x 10^4, $Lmol^{-1}cm^{-1}$); fluorescence maxima wavelength (λ_{em}, nm); relative quantum yield (ϕ) of **64-67**, **71-73**, and **76-81** in chloroform

No.	λ_{abs} (nm)	ε ($Lmol^{-1}cm^{-1}$)/10^4	λ_{em} (nm)	ϕ
Free-base imidazolo- and quinoxalino- porphyrin anils [1]				
64	423	22.43	650	0.114
65	423	26.96	650	0.127
66	422	31.26	652	0.115
67	422	31.90	650	0.110
76	437	17.07	656	0.027
77	436	14.87	658	0.032
Free-base imidazolo- and quinoxalino- porphyrin boranils [1]				
71	422	27.56	653	0.090
72	422	31.93	652	0.063
73	423	28.42	653	0.065
78	437	17.38	658	0.030
79	436	15.09	658	0.023
Zinc(II) quinoxalinoporphyrin boranils [2]				
80	429	9.12	629	0.023
81	427	11.13	630	0.007

[1]relative quantum yield compared to TPP, [2]relative quantum yield compared to ZnTPP

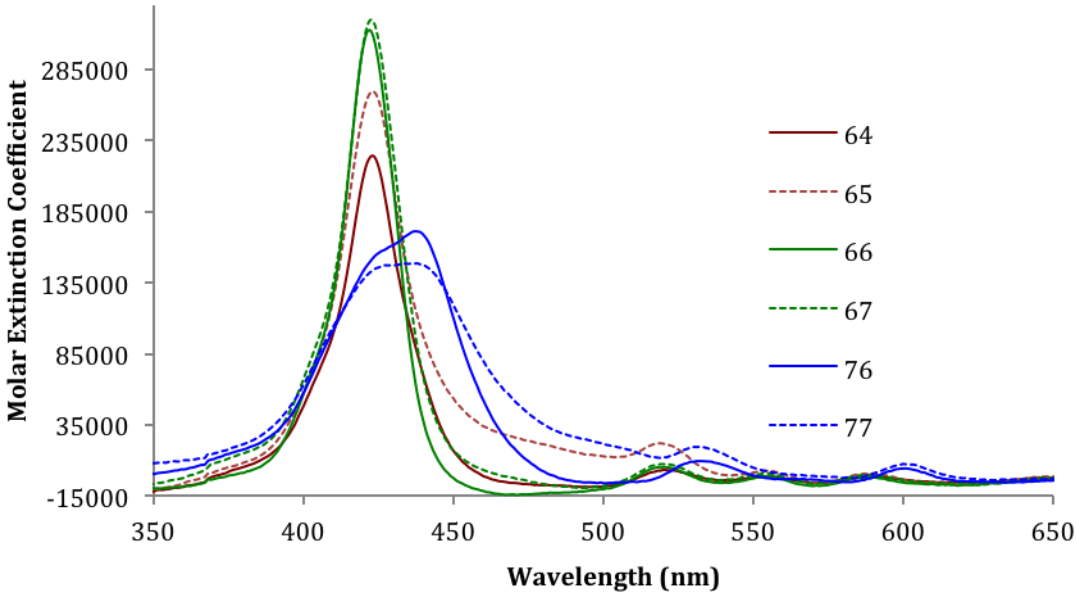

Figure 3.15: UV-visible spectra of free-base imidazoloporphyrin anils **64-67** and free-base quinoxalinoporphyrin anils **76** and **77** in $CHCl_3$.

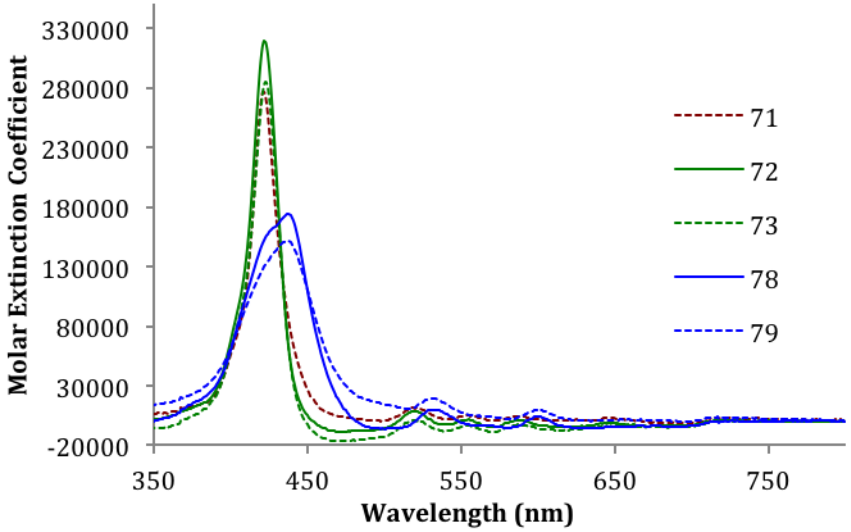

Figure 3.16: UV-visible spectra of free-base imidazoloporphyrin boranils **71-73** and free-base quinoxalinoporphyrin boranils **78** and **79** in $CHCl_3$.

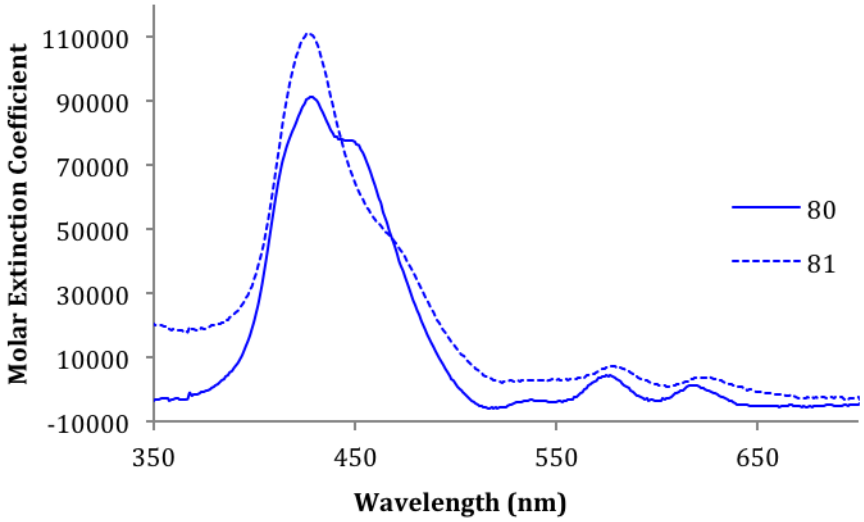

Figure 3.17: UV-visible spectra of zinc(II) quinoxalinoporphyrin boranils **80** and **81** in $CHCl_3$.

The free-base imidazoloporphyrin anils and boranils exhibit a Soret band at 422-423 nm and two Q-bands at 540 and 610 nm, while the free-base quinoxalinoporphyrin anils and boranils absorb at longer wavelength of 436-437 nm. The molar extinction coefficients of free-base imidazoloporphyrin anils are observed in the range of 224,000-320,000 $Lmol^{-1}cm^{-1}$. The molar extinction coefficients of free-base imidazoloporphyrin boranils are observed in the range of 275,000-320,000 $Lmol^{-1}cm^{-1}$.

The molar extinction coefficients of quinoxalinoporphyrins were observed at lower values compared to the *meso*-phenyl porphyrin and imidazoloporphyrin anils and boranils. The molar extinction coefficients of free-base quinoxalinoporphyrin anils were determined to be 148,000-171,000 $Lmol^{-1}cm^{-1}$; for the free-base quinoxalinoporphyrin boranils they were 151,000-174,000 $Lmol^{-1}cm^{-1}$ and for zinc(II) quinoxalinoporphyrin boranils 91,000-111,000 $Lmol^{-1}cm^{-1}$.

In summary, the zinc(II) complexes of quinoxalinoporphyrin boranils absorbed relatively poorly compared to the free-base imidazolo- and quinoxalino-porphyrin boranils.

The fluorescence emission and quantum yield of imidazolo- and quinoxalino-porphyrin anils and boranils are summarised in Table 3.2. The fluorescence emission spectra of imidazolo- and quinoxalino-porphyrin anils **64**-**67**, **76** and **77**, respectively are shown in Figure 3.18.

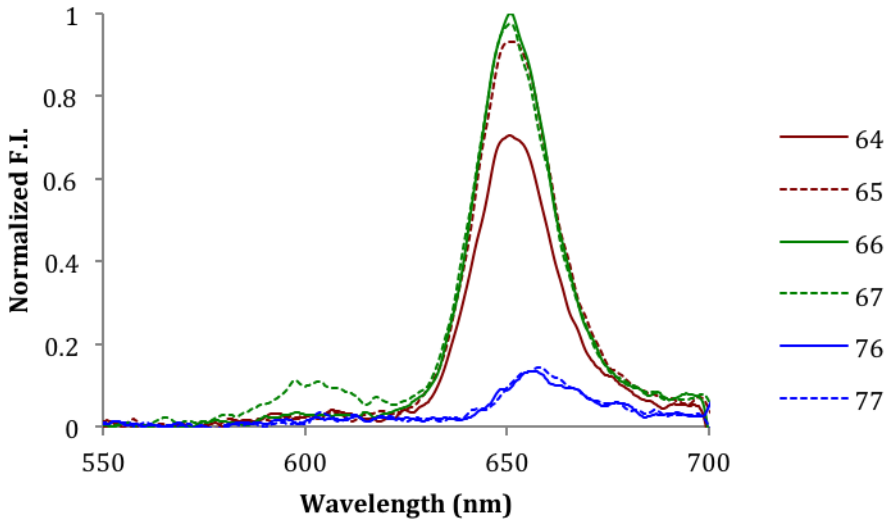

Figure 3.18: Normalised fluorescence spectra of free-base imidazoloporphyrin anils **64-67** and free-base quinoxalinoporphyrin anils **76** and **77** in $CHCl_3$.

The fluorescence emission spectra of imidazolo- and quinoxalino-porphyrin boranils **71-73**, **78** and **79** and zinc(II) quinoxalinoporphyrin boranils **80** and **81** are shown in Figure 3.19 and Figure 3.20, respectively.

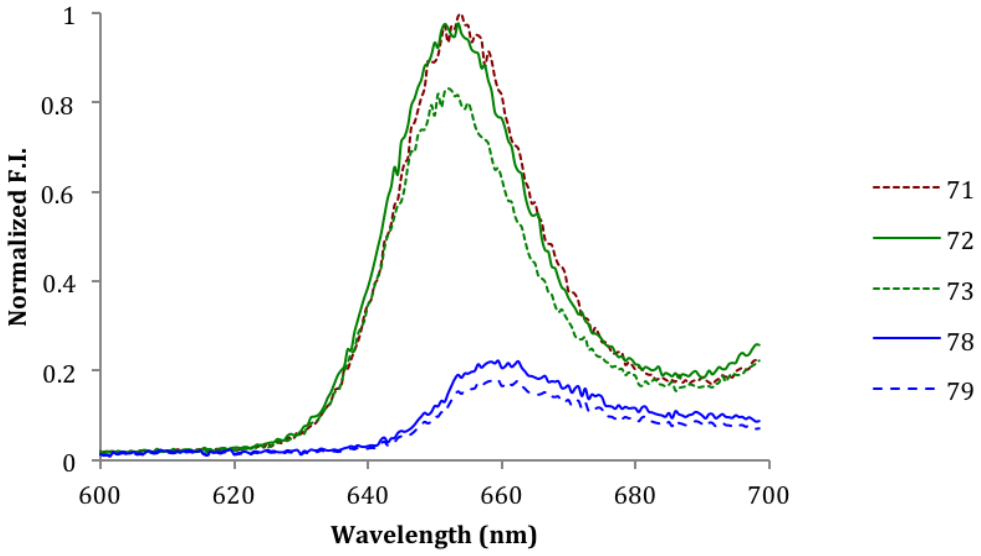

Figure 3.19: Normalised fluorescence spectra of free-base imidazoloporphyrin boranils **71-73** and free-base quinoxalinoporphyrin boranils **78** and **79** in $CHCl_3$.

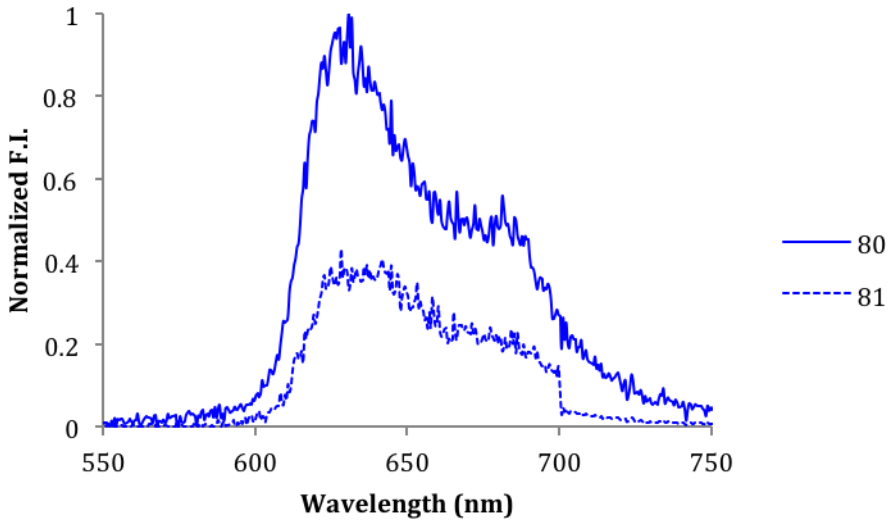

Figure 3.20: Normalised fluorescence spectra of zinc(II) quinoxalinoporphyrin boranils **80** and **81** in $CHCl_3$.

The relative quantum yields of free-base imidazole-fused porphyrin anils were observed in the range of 0.110-0.127. The relative quantum yields of all quinoxalinoporphyrins were observed at lower values in the range of 0.007-0.032. This is the result of different structural framework. Noticeably, the molar extinction coefficients (UV-vis spectra) of these quinoxaline porphyrins are also significantly reduced. It is likely the result of different electronic delocalisation pathways (HOMO – LUMO band gaps) of the parent fused quinoxalinoporphyrin system. The imidazolo- and quinoxalino-porphyrins fail to show any trends in terms of their photo-physical behaviour.

3.4 Conclusion

In summary, zinc(II) porphyrin-boranil conjugates were prepared in three steps. Three series were synthesised with *meso*-phenyl porphyrin-boranils, fused-imidazoloporphyrin-boranils and fused-quinoxalinoporphyrin-boranils. The structure of all porphyrin-conjugates were confirmed and characterised with ^{1}H and ^{13}C NMR spectroscopy, FTIR and elemental analysis. In the case of *meso*-phenyl porphyrin-conjugates bearing the anils / boranils at the *ortho*-position, the ^{1}H NMR spectra shows evidence of a strong porphyrin ring current effect on the anil / boranil units

with large upfield chemical shifts observed for signals associated with these fragments of the compounds. ^{1}H NMR of the fused imidazoloporphyrin reveals a lack of symmetry in the molecules, that is particularly evident in the β-pyrrolic regions.

Preliminary photo-physical characterisation was performed, in the form of recording the UV-visible absorption and fluorescence emission properties of the compounds. The relative quantum yield of free-base porphyrin-boranil conjugates and zinc(II) porphyrin-boranil conjugates were compared with TPP and ZnTPP, respectively. In the case of *meso*-porphyrin-conjugates, the relative quantum yield gradually decreases as the boranil unit is moved from the *para* to *meta* to *ortho* position, which indicates that there maybe an interaction between the two chromophores. The quinoxalinoporphyrin-boranil conjugates show relatively weak UV-visible absorption profiles and quantum yields in comparison with the other series studied in this work.

3.5 Experimental

3.5.1 Materials and Methods

The materials and methods used in this Chapter are the same as discussed in Section 2.7.1, with the following additions.

UV-visible absorbances were recorded on a Varian Cary 1 Bio UV-visible spectrophotometer using a UV-visible spectroscopy cell. Fluorescence emission spectra were recorded on a Perkin Elmer Luminescence spectrometer LS50B using a fluorescence spectroscopy cell.

The relative quantum yield (Φ) of free-base porphyrins and zinc(II) porphyrin complexes were calculated by using 5,10,15,20-tetraphenylporphyrin (TPP) and [5,10,15,20-tetraphenylporphyrin] zinc(II) (ZnTPP) as references, respectively. Both compounds were purchased from Sigma-Aldrich. TPP (Φ_{ST} = 0.11, $\lambda_{excitation}$ 419 nm) and ZnTPP (Φ_{ST} = 0.033, $\lambda_{excitation}$ 419 nm)[7] was dissolved in toluene (refractive index: 1.49)[8] and all the compounds were dissolved in de-acidified chloroform (refractive index: 1.44)[8]. The relative quantum yield was calculated according to the following equation:

$$\Phi_X = \Phi_{ST}\left(\frac{m_X}{m_{ST}}\right)\left(\frac{\eta_X^2}{\eta_{ST}^2}\right)$$

Where Φ is the fluorescence quantum yield, 'm' is the slope of the plot of integrated fluorescence intensity versus absorbance, and 'η' is the refractive index of the solvent. The subscripts ST and X refer to the reference (standard) and sample compounds, respectively. Excitation and emission slit widths were set at 5.0 nm when recording their fluorescence spectra.

3.5.2 General Preparation Procedures

General Preparation of Free-Base Porphyrin-Anils: In a mixture of amine porphyrin (150 mg, 0.155 mmol) and salicylaldehyde (18.9 mg, 0.155 mmol) or 2-hydroxy-1-naphthaldehyde (26.7 mg, 0.155 mmol) in anhydrous ethanol (50 mL) was added *p*-toluenesulfonic acid (5 mg, 0.03 mmol). The reaction mixture was stirred for 3 days and monitored by TLC. Upon completion, the reaction mixture was filtered and the residue was washed with ethanol and hexane. The crude product obtained was recrystallised from a mixture of dichloromethane and hexane.

General Preparation of Free-Base Porphyrin-Boranils: A mixture of ligand (100 mg, 1 eq.) in 1,2-dichloroethane (20 mL) was heated to reflux. Boron trifluoride diethyl etherate (10 eq.) was added. The reaction mixture was heated at reflux for 2 days. On cooling, the reaction mixture was washed with saturated sodium bicarbonate (3 x 25 mL), brine (50 mL), dried over anhydrous sodium sulfate, filtered and the solvent was removed under *vacuo*. The crude product obtained was purified by column chromatography (silica gel).

General Preparation of Zinc(II) Boranils: The free-base porphyrin of boranil (40 mg, 1 eq.) and zinc acetate (2.5 eq.) in dichloromethane (5 mL) was heated to reflux for 4 h. On cooling, dichloromethane (20 mL) was added to the reaction mixture. The organic layer was washed with water (2 x 20 mL) and brine (20 mL), dried over sodium sulfate, filtered and evaporated to dryness under vacuum. The crude product obtained was purified by column chromatography

(silica gel).

3.5.3 Preparation of Free-Base *meso*-Phenyl Porphyrin Anils

5-([(2-Hydroxyphenyl)methylidene]-4-aminophenyl)-10,15,20-tris(3,5-di-*tert*-butylphenyl)porphyrin 46

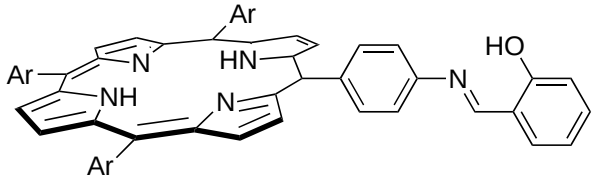

Starting with **6** and salicylaldehyde, **46** (125 mg, 75%) was obtained as a purple microcrystalline solid. m.p. > 300 °C. ^{1}H NMR (400 MHz, $CDCl_3$) δ -2.64 (br s, 2H, NH), 1.55 (app. s, 54H, CH_3), 7.01-7.07 (m, 1H, ArH), 7.13-7.16 (m, 1H, ArH), 7.45-7.50 (m, 1H, ArH), 7.53-7.57 (m, 1H, ArH), 7.70 (d, 2H, *J* = 8.3 Hz, ArH), 7.81-7.83 (m, 3H, ArH), 8.10 (d, 2H, *J* = 1.8 Hz, ArH), 8.12 (d, 4H, *J* = 1.8 Hz, ArH), 8.32 (d, 2H, *J* = 8.3 Hz, ArH), 8.90-8.95 (m, 8H, β-pyrrolic H), 8.99 (s, 1H, CH), 13.48 (br s, 1H, OH) ppm. ^{13}C NMR (100 MHz, $CDCl_3$) δ 31.5, 35.0, 117.4, 118.5, 119.2, 119.4, 119.48, 119.51, 121.0, 121.5, 129.7, 129.8, 132.5, 133.3, 135.5, 141.2, 141.3, 147.8, 148.68, 148.72, 161.4, 163.1 ppm. FTIR 712 (m), 730 (m), 754 (m), 800 (s), 913 (m), 1246 (m), 1361 (m), 1474 (m), 1592 (m), 2961 (m), 3325 (br, NH) cm^{-1}. λ_{max} ($CHCl_3$) 407sh, 422, 520, 555, 592, 648 nm (log ε 4.89, 5.72, 4.28, 4.16, 3.96, 4.05). Anal Calcd for $C_{75}H_{83}N_5O$. 1/10 CH_2Cl_2: C, 83.60; H, 7.77; N, 6.49. Found: C, 83.50; H, 8.05; N, 6.57.

5-([(2-Hydroxynaphthyl)methylidene]-4-aminophenyl)-10,15,20-tris(3,5-di-*tert*-butylphenyl)porphyrin 47

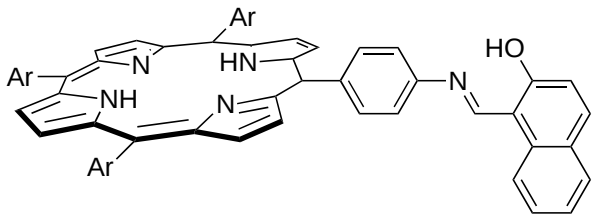

Starting with **6** and 2-hydroxy-1-naphthaldehyde, **47** (123 mg, 69%) was obtained as a purple microcrystalline solid. m.p. > 300 °C. ^{1}H NMR (400 MHz, $CDCl_3$) δ -2.66 (br s, 2H, NH), 1.55 (app. s, 54H, CH_3), 7.19 (d, 1H, *J* = 9.0 Hz, ArH), 7.38-7.43 (m, 1H, ArH), 7.57-7.63 (m, 1H, ArH), 7.75-7.85 (m, 6H, ArH), 7.87 (d, 1H, *J* = 9.0 Hz, ArH), 8.07-8.17 (m, 6H, ArH), 8.26-8.31 (m, 1H, ArH), 8.36 (d, 2H, *J* = 7.8 Hz, ArH), 8.87-8.98 (m, 8H, β-pyrrolic H), 9.70 (s, 1H, CH), 15.78 (br s, 1H, OH) ppm. ^{13}C NMR (100 MHz, $CDCl_3$) δ 31.7, 35.02, 35.05, 109.1, 118.4, 118.6, 119.0, 121.0, 121.5, 121.7, 122.4, 123.7, 127.4, 128.2, 129.5, 129.7, 129.8, 133.4, 135.7, 136.9, 140.9, 141.2, 141.3, 148.64, 148.70, 148.74, 167.04 ppm. FTIR 715 (m), 732 (m), 800 (s), 883 (m), 913 (m), 970 (m), 1245 (m), 1361 (m), 1473 (m), 1591 (m), 2958 (m), 3318 (br, NH) cm^{-1}. λ_{max} ($CHCl_3$) 406sh, 423, 520, 555, 593, 649 nm (log ε 4.76, 5.57, 4.04, 3.93, 3.37, 3.68). Anal Calcd for $C_{79}H_{85}N_5O$. 1/2 CH_2Cl_2: C, 82.10; H, 7.45; N, 6.02. Found: C, 82.21; H, 7.28; N, 6.10.

5-([(2-Hydroxyphenyl)methylidene]-3-aminophenyl)-10,15,20-tris(3,5-di-*tert*-butylphenyl)porphyrin 48

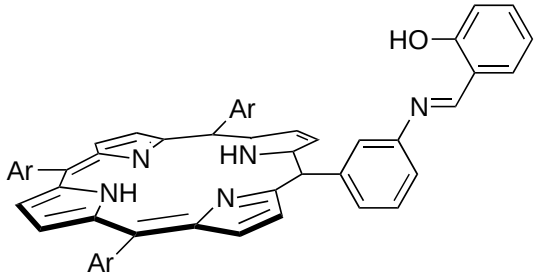

Starting with **7** and salicylaldehyde, **48** (101 mg, 61%) was obtained as a purple microcrystalline solid. m.p. > 300 °C. ^{1}H NMR (400 MHz, $CDCl_3$) δ -2.67 (br s, 2H, NH), 1.53 (app. s, 54H, CH_3), 6.89-6.94 (m, 1H, ArH), 7.03-7.06 (m, 1H, ArH), 7.35-7.40 (m, 2H, ArH), 7.71-7.75 (m, 1H, ArH), 7.78-7.82 (m, 4H, ArH), 8.06-8.12 (m, 6H, ArH), 8.18-8.21 (m, 2H, ArH), 8.87-8.93 (m, 9H, β-pyrrolic H and CH), 13.37 (br s, 1H, OH) ppm. ^{13}C NMR (100 MHz, $CDCl_3$) δ 31.7, 35.04, 35.06, 117.3, 118.4, 119.1, 119.3, 121.0, 121.2, 121.5, 121.7, 126.6, 127.6, 129.67, 129.71, 129.82, 129.84, 132.4, 133.0, 133.3, 141.2, 141.3, 143.9, 146.8, 148.69, 148.72, 148.75, 161.2, 163.4 ppm. FTIR 708 (m), 739 (m), 759 (m), 790 (m), 802 (s), 879 (m), 913 (m), 979 (m), 1152 (m), 1245 (m), 1277 (m), 1361 (m), 1474 (m), 1592 (m), 1620 (m), 2957 (m), 3315 (br, NH) cm^{-1}. λ_{max} ($CHCl_3$) 411sh, 422, 520, 554, 594, 647 nm (log ε 5.00, 5.77, 4.42, 4.31, 4.24, 4.31). Anal Calcd for $C_{75}H_{83}N_5O$. 1/5 CH_2Cl_2: C, 83.05; H, 7.73; N, 6.44. Found: C, 82.84; H, 7.62; N, 6.45.

5-([(2-Hydroxynaphthyl)methylidene]-3-aminophenyl)-10,15,20-tris(3,5-di-*tert*-butylphenyl)porphyrin 49

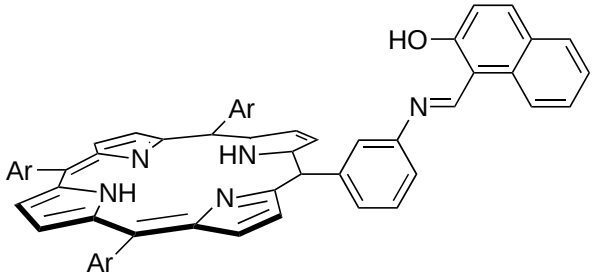

Starting with **7** and 2-hydroxy-1-naphthaldehyde, **49** (87 mg, 50%) was obtained as a purple microcrystalline solid. m.p. > 300 °C. m.p. > 300 °C. ^{1}H NMR (400 MHz, $CDCl_3$) δ -2.68 (br s, 2H, NH), 1.50-1.54 (m, 54H, CH_3), 7.06-7.10 (m, 1H, ArH), 7.34-7.40 (m, 1H, ArH), 7.63-7.67 (m, 1H, ArH), 7.75-7.85 (m, 6H, ArH), 8.00-8.04 (m, 2H, ArH), 8.05-8.11 (m, 6H, ArH), 8.16-8.20 (m, 1H, CH), 8.25-8.27 (m, 1H, ArH), 8.88-8.94 (m, 8H, β-pyrrolic H), 9.56 (s, 1H, CH), 13.14 (br s, 1H, OH) ppm. ^{13}C NMR (100 MHz, $CDCl_3$) δ 31.7, 35.1, 109.1, 118.2, 118.6, 118.8, 119.2, 120.2, 121.0, 121.6, 121.8, 122.3, 123.5, 124.5, 125.7, 127.1, 127.3, 127.9, 128.1, 129.1, 129.3, 129.67, 129.69, 129.8, 129.9, 136.9, 139.1, 141.2, 141.3, 143.6, 144.2, 148.70, 148.74, 148.77, 155.0 ppm. FTIR 678 (m), 725 (s), 800 (s), 881 (m), 914 (m), 1157 (m), 1245 (m), 1311 (m), 1361 (m), 1471 (m), 1560 (m), 1590 (m), 2958 (m), 3322 (br, NH) cm^{-1}. λ_{max} ($CHCl_3$) 406sh, 422, 520, 554, 593, 647 nm (log ε 4.80, 5.63, 4.00, 3.69, 3.23, 3.64). Anal Calcd for $C_{79}H_{85}N_5O$. 1/2 CH_2Cl_2: C, 82.10; H, 7.45; N, 6.02. Found: C, 82.49; H, 7.77; N, 5.78.

5-([(2-Hydroxyphenyl)methylidene]-2-aminophenyl)-10,15,20-tris(3,5-di-*tert*-butylphenyl)porphyrin 50

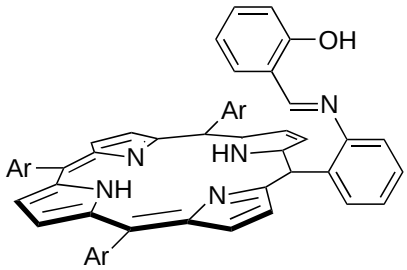

Starting with **8** and salicylaldehyde, **50** (92 mg, 55%) was obtained as a purple microcrystalline solid. m.p. > 300 °C. ^{1}H NMR (400 MHz, $CDCl_3$) δ -2.62 (br s, 2H, NH), 1.53 (app. s, 54H, CH_3), 5.98-6.02 (m, 1H, ArH), 6.50-6.56 (m, 1H, ArH), 6.79-6.85 (m, 1H, ArH), 7.01-7.05 (m, 1H, ArH), 7.58-7.62 (m, 1H, ArH), 7.63-7.68 (m, 1H, ArH), 7.77-7.80 (m, 3H, ArH), 7.84-7.90 (m, 1H, ArH), 8.05-8.11 (m, 4H, ArH), 8.11-8.14 (m, 2H, ArH), 8.16-8.19 (m, 1H, ArH), 8.66 (s, 1H, CH), 8.78 (ABq, 2H, J_{AB} = 4.7 Hz, β-pyrrolic H), 8.85-8.91 (m, 6H, β-pyrrolic H), 11.27 (br s, 1H, OH) ppm. ^{13}C NMR (100 MHz, $CDCl_3$) δ 31.7, 35.0, 115.7, 116.5, 117.9, 118.2, 18.7, 120.8, 120.9, 121.4, 121.6, 125.1, 129.5, 129.6, 129.7, 129.9, 130.0, 131.7, 132.5, 135.7, 137.1, 141.2, 141.4, 148.5, 148.6, 149.9, 160.2, 162.4 ppm. FTIR 712 (m), 734 (m), 801 (s), 913 (m), 1245 (m), 1361 (m), 1473 (m), 1590 (m), 2959 (m), 3325 (br, NH) cm^{-1}. λ_{max} ($CHCl_3$) 410sh, 423, 520, 557, 592, 648 nm (log ε 4.73, 5.60, 4.31, 4.22, 4.19, 4.26). Anal Calcd for $C_{75}H_{83}N_5O$. 1/3 CH_2Cl_2: C, 82.34; H, 7.67; N, 6.37. Found: C, 82.19; H, 7.40; N, 6.09.

5-([(2-Hydroxynaphthyl)methylidene]-2-aminophenyl)-10,15,20-tris(3,5-di-*tert*-butylphenyl)porphyrin 51

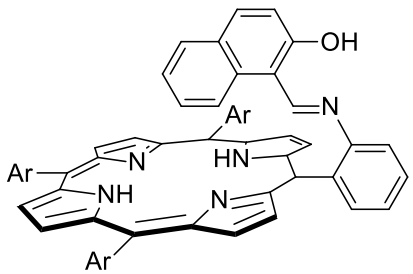

Starting with **8** and 2-hydroxy-1-naphthaldehyde, **51** (145 mg, 81%) was obtained as a purple microcrystalline solid. m.p. > 300 °C. ^{1}H NMR (400 MHz, $CDCl_3$) δ -2.60 (br s, 2H, NH),

1.49-1.56 (m, 54H, CH_3), 6.10-6.16 (m, 1H, ArH), 6.98-7.08 (m, 2H, ArH), 7.20-7.24 (m, 1H, ArH), 7.29-7.35 (m, 1H, ArH), 7.38-7.44 (m, 1H, ArH), 7.63-7.69 (m, 1H, ArH), 7.55-7.82 (m, 4H, ArH), 7.88-7.94 (m, 1H, ArH), 8.05-8.13 (m, 6H, ArH), 8.18-8.23 (m, 1H, ArH), 8.81-8.85 (m, 2H, β-pyrrolic H), 8.86-8.93 (m, 6H, β-pyrrolic H), 9.35 (s, 1H, CH), 13.84 (br s, 1H, OH) ppm. ^{13}C NMR (100 MHz, $CDCl_3$) δ 31.7, 35.0, 108.6, 115.0, 118.6, 118.7, 120.7, 120.9, 121.0, 121.5, 121.8, 122.9, 124.8, 126.8, 127.4, 128.8, 129.6, 129.72, 129.74, 129.9, 130.0, 132.6, 135.3, 136.0, 136.2, 141.1, 141.4, 148.0, 148.6, 148.7, 156.4, 166.8 ppm. FTIR 715 (m), 731 (m), 801 (s), 914 (m), 1245 (m), 1361 (m), 1470 (m), 1590 (m), 2958 (m), 3321 (br, NH) cm^{-1}. λ_{max} ($CHCl_3$) 408sh, 423, 521, 557, 592, 648 nm (log ε 4.92, 5.60, 4.26, 4.07, 3.98, 4.06). Anal Calcd for $C_{79}H_{85}N_5O$: C, 84.68; H, 7.65; N, 6.25. Found: C, 84.35; H, 7.29; N, 5.98

3.5.4 Preparation of Free-Base *meso*-Phenyl Porphyrin Boranils

5-([(2-Hydroxyphenyl)methylidene]-4-aminophenyl)-10,15,20-tris(3,5-di-*tert*-butylphenyl)porphyrin boron difluoride chelate 52

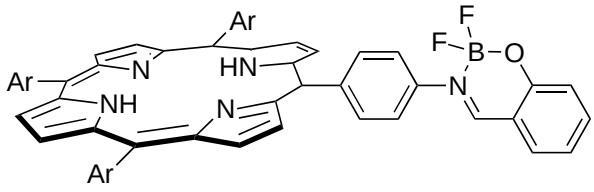

Starting with **46**, the crude material was chromatographed (dichloromethane/hexane 1:1) to afford **52** (55 mg, 55%) as a purple microcrystalline solid. m.p. > 300 °C. ^1H NMR (400 MHz, $CDCl_3$) δ -2.69 (br s, 2H, NH), 1.52-1.55 (m, 54H, CH_3), 7.11-7.16 (m, 1H, ArH), 7.28-7.31 (m, 1H, ArH), 7.65-7.68 (m, 1H, ArH), 7.73-7.78 (m, 1H, ArH), 7.79-7.82 (m, 3H, ArH), 7.99 (d, 2H, J = 8.2 Hz, ArH), 8.08 (d, 2H, J = 1.7 Hz, ArH), 8.10 (d, 4H, J = 1.7 Hz, ArH), 8.40 (d, 2H, J = 8.2 Hz, ArH), 8.84 (ABq, 2H, J_{AB} = 4.7 Hz, β-pyrrolic H), 8.90-8.94 (m, 7H, β-pyrrolic H and CH) ppm. ^{13}C NMR (100 MHz, $CDCl_3$) δ 31.7, 35.0, 117.4, 118.6, 119.2, 119.4, 119.5, 120.9, 121.0, 121.5, 121.6, 129.7, 129.8, 132.5, 133.4, 135.5, 141.2, 141.25, 141.30, 147.9,

148.6, 148.7, 161.3, 163.1 ppm. FTIR 670 (m), 713 (s), 799 (s), 881 (m), 913 (m), 973 (m), 1151 (m), 1245 (m), 1361 (m), 1474 (m), 1591 (m), 2956 (m), 3281 (br, NH) cm^{-1}. λ_{max} ($CHCl_3$) 406sh, 422, 518, 555, 594, 648 nm (log ε 4.84, 5.68, 4.28, 4.19, 4.04, 4.13). Anal Calcd for $C_{75}H_{82}BF_2N_5O$. 1/2 CH_2Cl_2: C, 78.12; H, 7.21; N, 6.03. Found: C, 77.97; H, 7.56; N, 6.02.

5-([(2-Hydroxynaphthyl)methylidene]-4-aminophenyl)-10,15,20-tris(3,5-di-*tert*-butylphenyl)porphyrin boron difluoride chelate 53

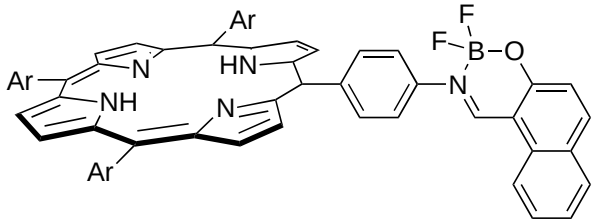

Starting with **47**, the crude material was chromatographed (dichloromethane/hexane 1:1) to afford **53** (100 mg, 96%) as a purple microcrystalline solid. m.p. > 300 °C. ^{1}H NMR (400 MHz, $CDCl_3$) δ -2.67 (br s, 2H, NH), 1.52-1.55 (m, 54H, CH_3), 7.41 (d, 1H, *J* = 9.1 Hz, ArH), 7.53-7.58 (m, 1H, ArH), 7.71-7.77 (m, 1H, ArH), 7.78-7.83 (m, 3H, ArH), 7.90-7.93 (m, 1H, ArH), 8.03 (d, 2H, *J* = 8.3 Hz, ArH), 8.08 (d, 2H, *J* = 1.7 Hz, ArH), 8.11 (d, 4H, *J* = 1.7 Hz, ArH), 8.20 (d, 1H, *J* = 9.1 Hz, ArH), 8.26-8.30 (m, 1H, ArH), 8.42 (d, 2H, *J* = 8.3 Hz, ArH), 8.88-8.96 (m, 8H, β-pyrrolic H), 9.51 (br s, 1H, CH) ppm. ^{13}C NMR (100 MHz, $CDCl_3$) δ 31.7, 35.1, 118.6, 119.3, 120.7, 121.1, 121.5, 121.7, 121.9, 122.4, 123.7, 124.5, 125.3, 128.2, 129.7, 129.8, 129.9, 131.6, 135.6, 141.1, 141.2, 141.4, 143.7, 148.7, 148.8, 154.9, 158.4 ppm. FTIR 714 (m), 747 (m), 799 (s), 913 (m), 973 (m), 1156 (m), 1246 (m), 1361 (m), 1465 (m), 1553 (m), 1591 (m), 2956 (m), 3292 (br, NH) cm^{-1}. λ_{max} ($CHCl_3$) 406sh, 422, 520, 555, 595, 649 nm (log ε 4.79, 5.56, 4.03, 3.89, 3.54, 3.77). Anal Calcd for $C_{79}H_{84}BF_2N_5O$. 1 CH_2Cl_2: C, 76.67; H, 6.92; N, 5.59. Found: C, 76.61; H, 7.26; N, 5.77.

5-([(2-Hydroxyphenyl)methylidene]-3-aminophenyl)-10,15,20-tris(3,5-di-*tert*-butylphenyl)porphyrin boron difluoride chelate 54

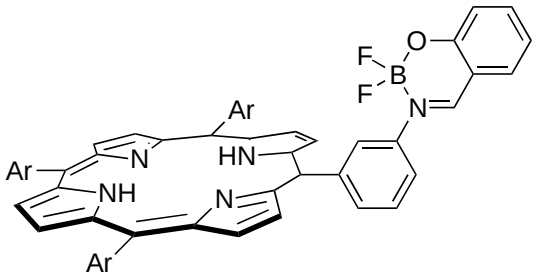

Starting with **48**, the crude material was chromatographed (dichloromethane/hexane 1:1) to afford **54** (77 mg, 74%) as a purple microcrystalline solid. m.p. > 300 °C. ^{1}H NMR (400 MHz, $CDCl_3$) δ -2.70 (br s, 2H, NH), 1.53 (app. s, 54H, CH_3), 6.97-7.02 (m, 1H, ArH), 7.17-7.21 (m, 1H, ArH), 7.46-7.50 (m, 1H, ArH), 7.62-7.68 (m, 1H, ArH), 7.78-7.82 (m, 3H, ArH), 7.88-7.94 (m, 1H, ArH), 8.05-8.12 (m, 7H, ArH), 8.36-8.40 (m, 2H, ArH), 8.72 (br s, 1H, CH), 8.84-8.96 (m, 8H, β-pyrrolic H). ^{13}C NMR (100 MHz, $CDCl_3$) δ 31.7, 35.0, 117.3, 118.4, 119.1, 119.2, 121.0, 121.1, 121.5, 1221.7, 126.6, 127.6, 129.6, 129.8, 132.4, 133.0, 133.2, 141.2, 141.3, 143.9, 146.8, 148.67, 148.70, 161.2, 163.3 ppm. FTIR 713 (s), 753 (m), 799 (s), 881 (m), 914 (m), 979 (m), 1245 (m), 1362 (m), 1473 (m), 1591 (m), 2958 (m), 3295 (br, NH) cm^{-1}. λ_{max} ($CHCl_3$) 407sh, 422, 518, 554, 594, 646 nm (log ε 4.81, 5.68, 4.18, 4.01, 3.90, 4.05). Anal Calcd for $C_{75}H_{82}BF_2N_5O$: C, 80.55; H, 7.39; N, 6.26. Found: C, 80.55; H, 7.78; N, 6.13.

5-([(2-Hydroxynaphthyl)methylidene]-3-aminophenyl)-10,15,20-tris(3,5-di-*tert*-butylphenyl)porphyrin boron difluoride chelate 55

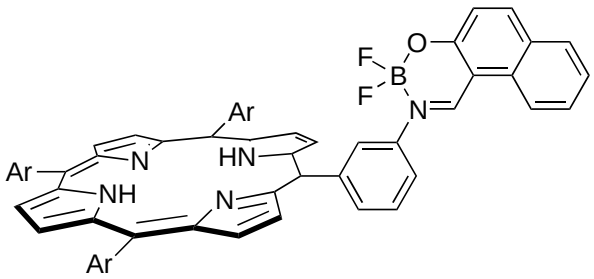

Starting with **49**, the crude material was chromatographed (dichloromethane/hexane 1:1) to afford **55** (90 mg, 86%) as a purple microcrystalline solid. m.p. > 300 °C. ^{1}H NMR (400 MHz,

$CDCl_3$) δ -2.65 (br s, 2H, NH), 1.54-1.58 (m, 54H, CH_3), 7.30-7.34 (m, 1H, ArH), 7.38-7.43 (m, 1H, ArH), 7.52-7.58 (m, 1H, ArH), 7.75-7.79 (m, 1H, ArH), 7.82-7.86 (m, 3H, ArH), 7.92-7.98 (m, 1H, ArH), 8.04-8.09 (m, 2H, ArH), 8.10-8.16 (m, 7H, ArH), 8.40-8.44 (m, 1H, ArH), 8.45-8.49 (m, 1H, ArH), 8.92-9.00 (m, 8H, β-pyrrolic H), 9.40 (br s, 1H, CH) ppm. ^{13}C NMR (100 MHz, $CDCl_3$) δ 31.8, 35.1, 117.2, 119.2, 120.5, 121.1, 121.7, 122.0, 123.3, 125.1, 127.98, 128.02, 129.1, 129.5, 129.67, 129.70, 129.81, 129.84, 131.4, 135.0, 141.1, 141.22, 141.25, 141.4, 148.7, 148.8, 158.4, 163.0 ppm. FTIR 714 (m), 799 (s), 880 (m), 914 (m), 979 (m), 1051 (m), 1246 (m), 1361 (m), 1473 (m), 1591 (m), 2959 (m), 3291 (br, NH) cm^{-1}. λ_{max} ($CHCl_3$) 406sh, 427, 521, 556, 594, 648 nm (log ε 4.71, 5.60, 4.24, 4.15, 4.10, 4.16). Anal Calcd for $C_{79}H_{84}BF_2N_5O$. 1 CH_2Cl_2: C, 76.67; H, 6.92; N, 5.59. Found: C, 76.62; H, 7.01; N, 5.80.

5-([(2-Hydroxyphenyl)methylidene]-2-aminophenyl)-10,15,20-tris(3,5-di-*tert*-butylphenyl)porphyrin boron difluoride chelate 56

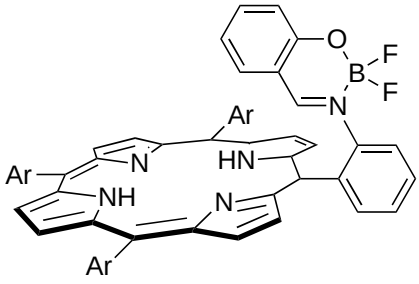

Starting with **50**, the crude material was chromatographed (dichloromethane/hexane 1:1) to afford **56** (59 mg, 57%) as a purple microcrystalline solid. m.p. > 300 °C. ^1H NMR (400 MHz, $CDCl_3$) δ -2.74 (br s, 2H, NH), 1.53-1.54 (m, 54H, CH_3), 5.72-5.76 (m, 1H, ArH), 5.90-5.95 (m, 1H, ArH), 6.47-6.50 (m, 1H, ArH), 6.84-6.89 (m, 1H, ArH), 7.77-7.85 (m, 4H, ArH), 7.96-7.99 (m, 2H, ArH), 8.03-8.06 (m, 2H, ArH), 8.08-8.13 (m, 3H, ArH), 8.27-8.37 (m, 3H, ArH and CH), 8.88-8.94 (m, 6H, β-pyrrolic H), 8.95-8.98 (m, 2H, β-pyrrolic H) ppm. ^{13}C NMR (100 MHz, $CDCl_3$) δ 31.7, 35.0, 111.8, 114.4, 115.2, 116.6, 117.9, 118.2, 118.8, 119.3, 120.8, 121.0, 121.2, 121.9, 126.9, 129.4, 129.7, 129.8, 129.9, 130.1, 131.8, 132,5, 134.8, 135.8, 136.9, 138.1,

140.8, 141.1, 141.2, 148.59, 148.68, 148.79, 148.82, 162.4, 164.6 ppm. FTIR 713 (s), 799 (s), 880 (m), 913 (m), 973 (m), 1052 (m), 1152 (m), 1199 (m), 1245 (m), 1362 (m), 1474 (m), 1591 (m), 2956 (m), 3292 (br, NH) cm^{-1}. λ_{max} ($CHCl_3$) 407sh, 423, 520, 555, 595, 647 nm (log ε 4.88, 5.65, 4.35, 4.20, 4.14, 4.21). Anal Calcd for $C_{75}H_{82}BF_2N_5O$: C, 80.55; H, 7.39; N, 6.26. Found: C, 80.21; H, 7.70; N, 6.24.

5-([(2-Hydroxynaphthyl)methylidene]-2-aminophenyl)-10,15,20-tris(3,5-di-*tert*-butylphenyl)porphyrin boron difluoride chelate 57

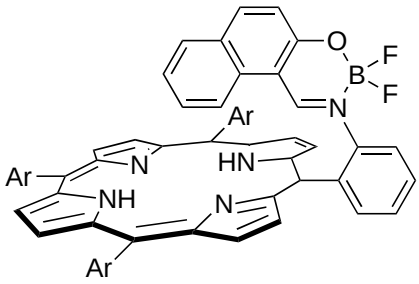

Starting with **51**, the crude material was chromatographed (dichloromethane/hexane 1:1) to afford **57** (56 mg, 54%) as a purple microcrystalline solid. m.p. > 300 °C. ^{1}H NMR (400 MHz, $CDCl_3$) δ -2.85 (br s, 2H, NH), 1.48-1.58 (m, 54H, CH_3), 5.83-5.88 (m, 1H, ArH), 6.43-6.49 (m, 1H, ArH), 6.50-6.54 (m, 1H, ArH), 6.55-6.60 (m, 1H, ArH), 6.86-6.89 (m, 1H, ArH), 7.14-7.19 (m, 1H, ArH), 7.74-7.84 (m, 4H, ArH), 7.94-8.01 (m, 2H, ArH), 8.04-8.12 (m, 5H, ArH), 8.26-8.31 (m, 1H, ArH), 8.35-8.39 (m, 1H, ArH), 8.80-8.86 (m, 3H, β-pyrrolic H), 8.89-9.01 (m, 1H, β-pyrrolic H), 9.00 and 9.06 (ABq, 2H, J_{AB} = 4.8 Hz, β-pyrrolic H), 9.32 (br s, 1H, CH) ppm. ^{13}C NMR (100 MHz, $CDCl_3$) δ 31.7, 31.8, 34.9, 35.0, 113.8, 117.8, 120.4, 120.5, 122.2, 123.3, 123.8, 124.7, 125.9, 128.3, 129.2, 129.5, 129.6, 129.8, 129.9, 130.2, 131.8, 132.1, 132.8, 133.2, 134.9, 136.3, 142.8, 148.2, 148.3, 149.5, 150.2, 150.3, 150.6 ppm. FTIR 715 (m), 799 (s), 882 (m), 916 (m), 979 (m), 1050 (m), 1242 (m), 1364 (m), 1472 (m), 1593 (m), 2957 (m), 3293 (br, NH) cm^{-1}. λ_{max} ($CHCl_3$) 406 sh, 427, 521, 556, 594, 648 nm (log ε 4.71, 5.60, 4.24, 4.15, 4.10, 4.16). Anal Calcd for $C_{79}H_{84}BF_2N_5O$: C, 81.21; H, 7.25; N, 5.99. Found: C, 81.11; H, 7.04; N, 5.69.

3.5.5 Preparation of Zinc(II) *meso*-Phenyl Porphyrin Boranils

{5-([(2-Hydroxyphenyl)methylidene]-4-aminophenyl)-10,15,20-tris(3,5-di-*tert*-butylphenyl)porphyrin} zinc(II) boron difluoride chelate 58

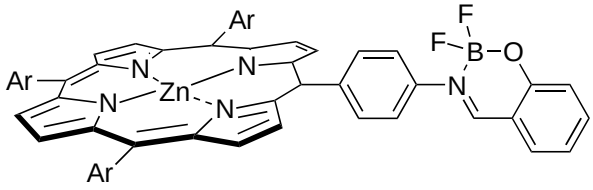

Starting with **52**, the crude material was chromatographed (dichloromethane/hexane 1:1) to afford **58** (15 mg, 36%) as a purple microcrystalline solid. m.p. > 300 °C. ^{1}H NMR (400 MHz, $CDCl_3$) δ 1.50-1.56 (app. s, 54H, CH_3), 7.12-7.16 (m, 1H, ArH), 7.27-7.31 (m, 1H, ArH), 7.66-7.70 (m, 1H, ArH), 7.70-7.82 (m, 4H, ArH), 7.99 (d, 2H, *J* = 8.0 Hz, ArH), 8.07-8.12 (m, 6H, ArH), 8.40 (d, 2H, *J* = 8.0 Hz, ArH), 8.95 (ABq, 1H, J_{AB} = 4.6 Hz, β-pyrrolic H), 9.00-9.06 (m, 7H, β-pyrrolic H and CH) ppm. ^{13}C NMR (100 MHz, $CDCl_3$) δ 31.7, 31.9, 35.0, 35.1, 113.6, 117.2, 119.0, 120.4, 120.6, 121.8, 129.6, 129.7, 129.8, 131.8, 131.9, 132.2, 132.3, 142.3, 148.2, 148.3, 148.5, 149.2, 149.9, 150.1, 150.4 ppm. FTIR 716 (m), 747 (m), 796 (s), 822 (m), 999 (m), 1361 (m), 1590 (m), 2957 (m) cm^{-1}. λ_{max} ($CHCl_3$) 427, 556, 599 nm (log ε 5.65, 4.08, 3.40). Anal Calcd for $C_{75}H_{80}BF_2N_5OZn$. 1/2 CH_2Cl_2: C, C, 74.08; H, 6.67; N, 5.72. Found: C, 73.88; H, 6.42; N, 5.32.

{5-([(2-Hydroxynaphthyl)methylidene]-4-aminophenyl)-10,15,20-tris(3,5-di-*tert*-butylphenyl)porphyrin} zinc(II) boron difluoride chelate 59

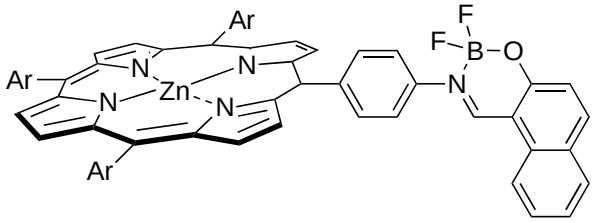

Starting with **53**, the crude material was chromatographed (dichloromethane/hexane 1:1) to afford **59** (30 mg, 71%) as a purple microcrystalline solid. m.p. > 300 °C. ^{1}H NMR (400 MHz,

$CDCl_3$) δ 1.51-1.55 (m, 54H, CH_3), 7.41 (d, 1H, *J* = 9.1 Hz, ArH), 7.50-7.56 (m, 1H, ArH), 7.67-7.73 (m, 1H, ArH), 7.78-7.82 (m, 3H, ArH), 7.88-7.92 (m, 1H, ArH), 8.02 (d, 2H, *J* = 8.3 Hz, ArH), 8.09-8.13 (m, 6H, ArH), 8.18 (d, 1H, *J* = 9.1 Hz, ArH), 8.30-8.34 (m, 1H, ArH), 8.42 (d, 2H, *J* = 8.3 Hz, ArH), 8.98-9.06 (m, 8H, β-pyrrolic H), 9.50 (br s, 1H, ArH) ppm. ^{13}C NMR (100 MHz, $CDCl_3$) δ 31.8, 35.1, 118.3, 120.8, 121.7, 122.4, 122.6, 122.7, 123.6, 125.3, 128.1, 129.6, 129.7, 129.8, 131.3, 131.4, 132.3, 132.4, 132.6, 135.4, 135.6, 141.81, 141.83, 148.5, 148.6, 149.7, 150.5, 150.6, 158.3 ppm. FTIR 716 (m), 796 (s), 1000 (m), 1207 (m), 1247 (m), 1361 (m), 1464 (m), 1591 (m), 2959 (m) cm^{-1}. λ_{max} ($CHCl_3$) 427, 556, 599 nm (log ε 5.57, 4.07, 3.57). Anal Calcd for $C_{79}H_{82}BF_2N_5OZn$. 1/2 CH_2Cl_2: C, 74.94; H, 6.57; N, 5.50. Found: C, 74.64; H, 6.43; N, 5.54.

{5-([(2-Hydroxyphenyl)methylidene]-3-aminophenyl)-10,15,20-tris(3,5-di-*tert*-butylphenyl)porphyrin} zinc(II) boron difluoride chelate 60

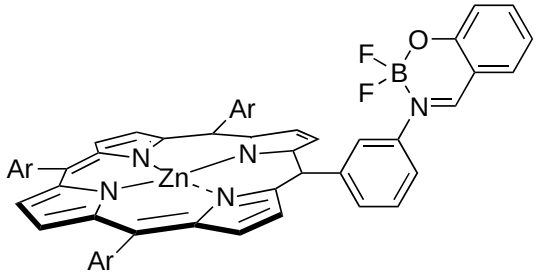

Starting with **54**, the crude material was chromatographed (dichloromethane/hexane 1:1) to afford **60** (15 mg, 36%) as a purple microcrystalline solid. m.p. > 300 °C. ^{1}H NMR (400 MHz, $CDCl_3$) δ 1.52 (app. s, 54H, CH_3), 6.84-6.88 (m, 1H, ArH), 6.97-7.02 (m, 1H, ArH), 7.77-7.83 (m, 5H, ArH), 7.96-7.98 (m, 1H, ArH), 8.08-8.12 (m, 5H, ArH), 8.21-8.23 (m, 3H, ArH), 8.26-8.28 (m, 1H, ArH), 8.89 (br s, 1H, CH), 8.98-9.05 (m, 8H, β-pyrrolic H) ppm. ^{13}C NMR (100 MHz, $CDCl_3$) δ 31.8, 35.1, 120.4, 120.8, 126.5, 129.9, 131.4, 131.9, 132.3, 132.4, 141.6, 141.8, 142.4, 142.7, 148.2, 148.3, 148.5, 149.2, 150.1, 150.4 ppm. FTIR 717 (m), 747 (m), 796 (s), 823 (m), 1000 (m), 1361 (m), 1592 (m), 2958 (m) cm^{-1}. λ_{max} ($CHCl_3$) 427, 556, 598 nm (log ε

5.64, 4.33, 4.11). Anal Calcd for $C_{75}H_{80}BF_2N_5OZn$: C, 76.23; H, 6.82; N, 5.93. Found: C, 76.11; H, 6.49; N, 5.70.

{5-([(2-Hydroxynaphthyl)methylidene]-3-aminophenyl)-10,15,20-tris(3,5-di-*tert*-butylphenyl)porphyrin} zinc(II) boron difluoride chelate 61

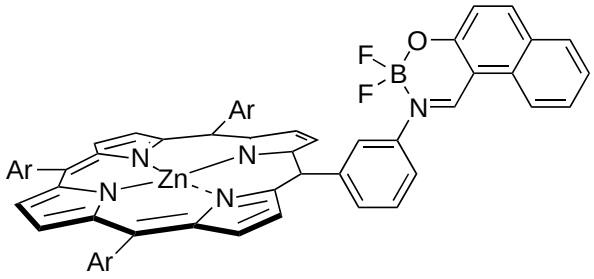

Starting with **55**, the crude material was chromatographed (dichloromethane/hexane 1:1) to afford **61** (13 mg, 32%) as a purple microcrystalline solid. m.p. > 300 °C. ^{1}H NMR (400 MHz, $CDCl_3$) δ 1.51-1.56 (m, 54H, CH_3), 7.30-7.34 (m, 1H, ArH), 7.38-7.44 (m, 1H, ArH), 7.51-7.575 (m, 1H, ArH), 7.77-7.82 (m, 4H, ArH), 7.90-7.96 (m, 1H, ArH), 8.03-8.14 (m, 7H, ArH), 8.38-8.43 (m, 1H, ArH), 8.43-8.46 (s, 1H, ArH), 9.01-9.08 (m, 8H, β-pyrrolic H), 9.38 (br s, 1H, ArH) ppm. ^{13}C NMR (100 MHz, $CDCl_3$) δ 31.8, 35.1, 118.3, 119.2, 120.6, 120.9, 122.7, 123.0, 125.1, 127.9, 128.0, 129.0, 129.5, 129.66, 129.72, 131.3, 131.54, 132.3, 132.4, 132.8, 134.8, 141.2, 141.3, 141.7, 144.9, 148.6, 149.7, 150.5, 150.6, 158.4, 162.9 ppm. FTIR 716 (m), 749 (m), 796 (s), 1005 (m), 1048 (m), 1208 (m), 1259 (m), 1361 (m), 1463 (m), 1553 (m), 1592 (m), 2959 (m) cm^{-1}. λ_{max} ($CHCl_3$) 427, 557, 598 nm (log ε 5.48, 4.16, 3.88).

{5-([(2-Hydroxyphenyl)methylidene]-2-aminophenyl)-10,15,20-tris(3,5-di-*tert*-butylphenyl)porphyrin} zinc(II) boron difluoride chelate 62

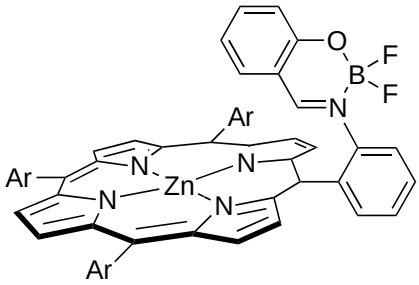

Starting with **56**, the crude material was chromatographed (dichloromethane/hexane 1:1) to afford **62** (18 mg, 42%) as a purple microcrystalline solid. m.p. > 300 °C. ^{1}H NMR (400 MHz, $CDCl_3$) δ 1.49-1.53 (m, 54H, CH_3), 5.61-5.66 (m, 1H, ArH), 5.83-5.90 (m, 1H, ArH), 6.39-6.44 (m, 1H, ArH), 6.78-6.83 (m, 1H, ArH), 7.74-7.83 (m, 4H, ArH), 7.92-8.12 (m, 7H, ArH), 8.22-8.37 (m, 3H, ArH and CH), 8.92-9.05 (m, 8H, β-pyrrolic H) ppm. ^{13}C NMR (100 MHz, $CDCl_3$) δ 31.7, 35.0, 114.4, 118.8, 119.2, 121.0, 122.9, 125.2, 126.9, 129.5, 130.7, 130.9, 132.3, 132.5, 133.4, 138.0, 141.5, 148.5, 148.6, 150.4, 150.7, 159.0, 164.3 ppm. FTIR 716 (s), 752 (s), 796 (s), 1000 (s), 1053 (m), 1202 (m), 1245 (m), 1361 (m), 1460 (m), 1475 (m), 1590 (m), 2956 (m) cm^{-1}. λ_{max} ($CHCl_3$) 427, 559, 599 nm (log ε 5.58, 4.31, 4.01). Anal Calcd for $C_{75}H_{80}BF_2N_5OZn$. 1/5 CH_2Cl_2: C, 75.35; H, 6.76; N, 5.84. Found: C, 75.21; H, 6.38; N, 5.58.

{5-([(2-Hydroxynaphthyl)methylidene]-2-aminophenyl)-10,15,20-tris(3,5-di-*tert*-butylphenyl)porphyrin} zinc(II) boron difluoride chelate 63

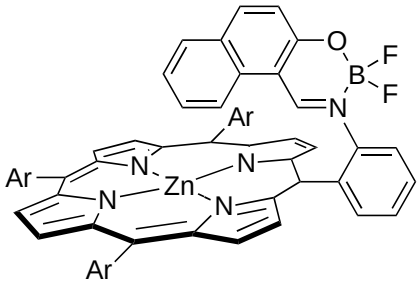

Starting with **57**, the crude material was chromatographed (dichloromethane/hexane 1:1) to afford **63** (28 mg, 66%) as a purple microcrystalline solid. m.p. > 300 °C. ^{1}H NMR (400 MHz,

$CDCl_3$) δ 1.47-1.53 (m, 54H, CH_3), 5.45-5.48 (m, 1H, ArH), 6.20-6.26 (m, 1H, ArH), 6.42-6.48 (m, 1H, ArH), 6.50-6.54 (m, 1H, ArH), 6.77-6.82 (m, 1H, ArH), 7.12-7.17 (m, 1H, ArH), 7.74-7.82 (m, 4H, ArH), 7.95-8.00 (m, 3H, ArH), 8.02-8.05 (m, 2H, ArH), 8.07-8.10 (m, 2H, ArH), 8.32-8.37 (m, 2H, ArH), 8.89-8.95 (m, 3H, β-pyrrolic H), 9.00-9.02 (m, 1H, β-pyrrolic H), 9.04 and 9.14 (ABq, 4H, J_{AB} = 4.6 Hz, β-pyrrolic H), 9.12 (br s, 1H, CH) ppm. ^{13}C NMR (100 MHz, $CDCl_3$) δ 31.7, 31.8, 34.9, 35.0, 35.1, 117.1, 119.6, 120.9, 121.0, 122.8, 123.3, 123.5, 125.4, 126.5, 126.6, 127.6, 128.1, 129.4, 129.5, 129.6, 129.7, 129.9, 130.0, 130.2, 131.8, 132.3, 132.4, 133.6, 136.3, 137.4, 139.6, 141.5, 141.6, 143.5, 148.2, 148.5, 148.6, 148.7, 150.2, 150.3, 150.4, 150.6, 150.7, 159.0, 161.6 ppm. FTIR 718 (m), 748 (m), 798 (s), 1003 (m), 1049 (m), 1209 (m), 1260 (m), 1364 (m), 1462 (m), 1554 (m), 1590 (m), 2958 (m) cm^{-1}. λ_{max} ($CHCl_3$) 427, 560, 599 nm (log ε 5.56, 4.25, 3.87). Anal Calcd for $C_{79}H_{82}BF_2N_5OZn$. 1/2 CH_2Cl_2: C, 74.94; H, 6.57; N, 5.50. Found: C, 75.28; H, 6.40; N, 5.29.

3.5.6 Preparation of Free-Base Imidazoloporphyrin Anils

(5,10,15,20-Tetrakis(3,5-di-*tert*-butylphenyl)porphyrin[2,3-*b*]-1'*H*-imidazol-2'-yl)-([(2'''-hydroxyphenyl)methylidene]-4''-aminophenyl 64

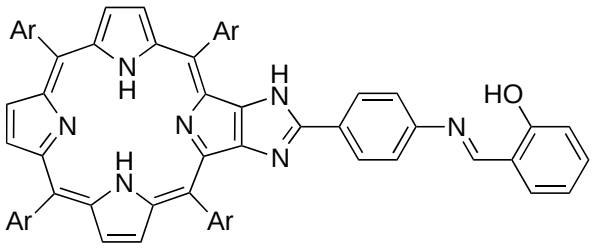

Starting with **29** and salicylaldehyde, **64** (114 mg, 70%) was obtained as a purple microcrystalline solid. m.p. > 300 °C. ^{1}H NMR (400 MHz, $CDCl_3$) δ -2.79 (br s, 2H, NH), 1.52-1.56 (m, 72H, CH_3), 6.96-7.01 (m, 1H, ArH), 7.05-7.08 (m, 1H, ArH), 7.39 (d, 2H, J = 8.3 Hz, ArH), 7.41-7.46 (m, 1H, ArH), 7.71-7.73 (m, 3H, ArH), 7.78-7.83 (m, 4H, ArH), 7.87-7.90 (m, 1H, ArH), 7.98-8.00 (m, 1H, ArH), 8.08-8.12 (m, 4H, ArH), 8.13-8.15 (m, 2H, ArH), 8.16-

8.19 (m, 2H, ArH), 8.37 (br s, 1H, NH), 8.74 (s, 1H, CH), 8.83-8.86 (m, 2H, β-pyrrolic H), 8.96-9.04 (m, 4H, β-pyrrolic H), 13.20 (br s, 1H, OH) ppm. ^{13}C NMR (100 MHz, $CDCl_3$) δ 31.75, 31.83, 35.0, 35.1, 117.4, 119.2, 121.0, 121.2, 121.8, 122.0, 126.1, 127.3, 129.2, 129.6, 129.7, 132.4, 142.3, 148.6, 148.7, 149.0, 151.0, 162.5 ppm. FTIR 642 (m), 664 (m), 713 (s), 754 (m), 798 (s), 880 (m), 921 (m), 1166 (m), 1202 (m), 1246 (m), 1361 (m), 1475 (m), 1592 (m), 2957 (m), 3335 (br, NH), 3445 (br, NH) cm^{-1}. λ_{max} ($CHCl_3$) 423, 520, 553, 591, 648 nm (log ε 5.36, 3.99, 3.70, 3.65, 3.64). Anal Calcd for $C_{90}H_{103}N_7O$: C, 83.23; H, 7.99; N, 7.55. Found: C, 83.50; H, 8.35; N, 7.57.

(5,10,15,20-Tetrakis(3,5-di-*tert*-butylphenyl)porphyrin[2,3-*b*]-1'*H*-imidazol-2'-yl)-([(2'''-hydroxynaphthyl)methylidene]-4''-aminophenyl 65

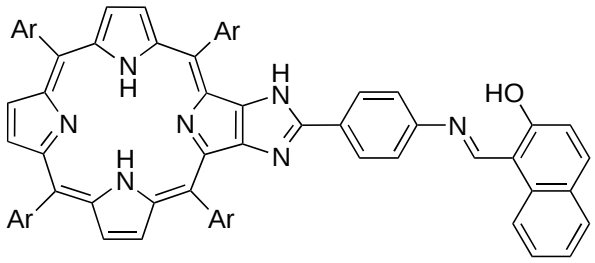

Starting with **29** and 2-hydroxy-1-naphthaldehyde, **65** (128 mg, 75%) was obtained as a purple microcrystalline solid. m.p. > 300 °C. ^{1}H NMR (400 MHz, $CDCl_3$) δ -2.74 (br s, 2H, NH), 1.57 (s, 36H, CH_3), 1.60 (s, 36H, CH_3), 7.11 (d, 1H, *J* = 9.1 Hz, ArH), 7.38 (app. t, 1H, *J* = 7.3 Hz, ArH), 7.50 (d, 2H, *J* = 8.3 Hz, ArH), 7.59 (app. t, 1H, *J* = 7.6 Hz, ArH), 7.72 (app. d, 1H, *J* = 8.0 Hz, ArH), 7.80 (d, 1H, *J* = 9.1 Hz, ArH), 7.82-7.90 (m, 5H, ArH), 7.95 (app. s, 1H, ArH), 8.12-8.25 (m, 10H, ArH), 8.42 (br s, 1H, NH), 8.88-9.02 (m, 2H, β-pyrrolic H), 9.00-9.10 (m, 4H, β-pyrrolic H), 9.46 (s, 1H, CH), 15.52 (s, 1H, OH) ppm. ^{13}C NMR (100 MHz, $CDCl_3$) δ 31.76, 31.80, 35.06, 35.15, 35.4, 109.1, 115.4, 119.0, 119.2, 120.7, 121.0, 121.2, 122.0, 122.1, 122.4, 123.7, 126.3, 127.3, 127.4, 128.2, 129.4, 129.6, 129.7, 133.2, 136.8, 139.8, 141.2, 141.6, 142.3, 145.5, 148.6, 148.8, 150.3, 151.0, 154.2 ppm. FTIR 654 (w), 713 (s), 798 (s), 820 (m), 879 (m), 899 (m), 921 (m), 1165 (m), 1245 (s), 1297 (m), 1361 (m), 1392 (m), 1424 (m), 1475

(m), 1590 (m), 1622 (w), 2867 (w), 2903 (w), 2957 (m), 3325 (br, NH), 3424 (br, NH) cm^{-1}. λ_{max} ($CHCl_3$) 423, 519, 554, 589, 648 nm (log ε 5.44, 4.44, 3.92, 3.80, 3.63). Anal Calcd for $C_{94}H_{105}N_7O$. 1/3 CH_2Cl_2: C, 81.93; H, 7.83; N, 7.30. Found: C, 82.10; H, 7.72; N, 6.91.

(5,10,15,20-Tetrakis(3,5-di-*tert*-butylphenyl)porphyrin[2,3-*b*]-1'*H*-imidazol-2'-yl)-([(2'''-hydroxyphenyl)methylidene]-3''-aminophenyl 66

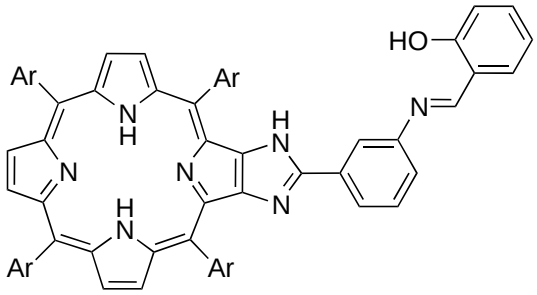

Starting with **30** and salicylaldehyde, **66** (113 mg, 69%) was obtained as a purple microcrystalline solid. m.p. > 300 °C. ^1H NMR (400 MHz, $CDCl_3$) δ -2.78 (br s, 2H, NH), 1.54 (app. s, 72H, CH_3), 7.04-7.09 (m, 1H, ArH), 7.13-7.17 (m, 1H, ArH), 7.30-7.33 (m, 1H, ArH), 7.47-7.54 (m, 3H, ArH), 7.58-7.61 (m, 1H, ArH), 7.75-7.77 (m, 1H, ArH), 7.80-7.83 (m, 2H, ArH), 7.87-7.90 (m, 1H, ArH), 8.10-8.16 (m, 7H, ArH), 8.17-8.20 (m, 2H, ArH), 8.40 (br s, 1H, NH), 8.74 (s, 1H, CH), 8.85-8.88 (m, 2H, β-pyrrolic H), 8.98-9.05 (m, 4H, β-pyrrolic H), 13.14 (s, 1H, OH) ppm. ^{13}C NMR (100 MHz, $CDCl_3$) δ 31.75, 31.82, 31.9, 35.05, 35.13, 35.4, 115.4, 117.5, 117.9, 119.1, 121.0, 121.2, 121.7, 122.1, 122.4, 122.9, 127.2, 127.5, 128.8, 129.5, 129.6, 129.7, 129.8, 132.4, 132.6, 133.4, 139.8, 141.2, 141.6, 142.3, 148.6, 148.7, 148.8, 149.2, 150.3, 151.1, 161.4, 163.2 ppm. FTIR 687 (m), 714 (s), 751 (s), 798 (s), 879 (m), 921(m), 1173 (m), 1202 (m), 1246 (m), 1280 (m), 1361 (m), 1393 (m), 1425 (m), 1475 (m), 1572 (m), 1591 (m), 2867 (m), 2961 (m), 3320 (br, NH), 3416 (br, NH) cm^{-1}. λ_{max} ($CHCl_3$) 422, 520, 555, 589, 651 nm (log ε 5.51, 4.28, 4.09, 4.08, 4.03). Anal Calcd for $C_{90}H_{103}N_7O$. 1/2 CH_2Cl_2: C, 81.04; H, 7.82; N, 7.31. Found: C, 81.12; H, 7.51; N, 6.97.

(5,10,15,20-Tetrakis(3,5-di-*tert*-butylphenyl)porphyrin[2,3-*b*]-1'*H*-imidazol-2'-yl)-([(2'''-hydroxynaphthyl)methylidene]-3''-aminophenyl 67

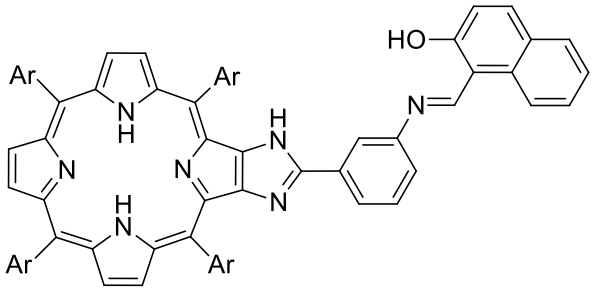

Starting with **30** and 2-hydroxy-1-naphthaldehyde, **67** (105 mg, 62%) was obtained as a purple microcrystalline solid. m.p. > 300 °C. ^{1}H NMR (400 MHz, $CDCl_3$) δ -2.76 (br s, 2H, NH), 1.52-1.56 (m, 72H, CH_3), 7.25 (d, 1H, *J* = 9.1 Hz, ArH), 7.35-7.40 (m, 1H, ArH), 7.42-7.46 (m, 1H, ArH), 7.51-7.58 (m, 2H, ArH), 7.62-7.68 (m, 1H, ArH), 7.80-7.83 (m, 3H, ArH), 7.89-7.93 (m, 3H, ArH), 8.11-8.22 (m, 9H, ArH), 8.25 (d, 1H, *J* = 9.1 Hz, ArH), 8.43 (br s, 1H, NH), 8.87 (app. s, 2H, β-pyrrolic H), 9.00-9.05 (m, 4H, β-pyrrolic H), 9.50 (s, 1H, CH), 15.44 (s, 1H, OH) ppm. ^{13}C NMR (100 MHz, $CDCl_3$) δ 31.75, 31.84, 35.0, 109.2, 117.7, 119.3, 121.0, 121.1, 121.7, 122.5, 123.7, 127.2, 127.5, 128.1, 128.7, 129.4, 129.7, 130.0, 132.7, 133.3, 136.5, 147.2, 148.7, 150.2, 156.6, 168.7 ppm. FTIR 713 (m), 728 (m), 800 (s), 820 (m), 880 (m), 922 (m), 1247 (m), 1361 (m), 1474 (m), 1567 (m), 1592 (m), 2960 (m), 3315 (br, NH), 3426 (br, NH) cm^{-1}. λ_{max} ($CHCl_3$) 422, 520, 554, 588, 647 nm (log ε 5.50, 4.05, 3.69, 3.59, 3.28). Anal Calcd for $C_{94}H_{105}N_7O$. 1/3 CH_2Cl_2: C, 81.93; H, 7.83; N, 7.30. Found: C, 81.62; H, 7.48; N, 6.95.

3.5.7 Preparation of Free-Base Imidazoloporphyrin Boranils

Attempted Preparation of (5,10,15,20-Tetrakis(3,5-di-*tert*-butylphenyl)porphyrin[2,3-*b*]-1'*H*-imidazol-2'-yl)-([(2'''-hydroxyphenyl)methylidene]-4''-aminophenyl boron difluoride chelate 70

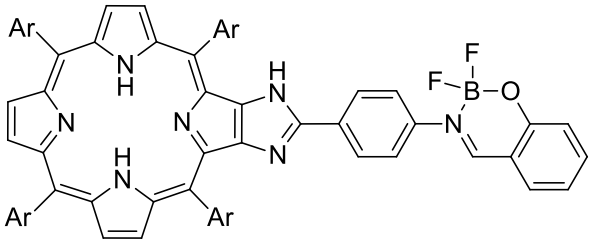

Starting with **64**, **70** could only be prepared in crude form and was inseparable from impurities. Characterisation data of the major peaks are not included here.

(5,10,15,20-Tetrakis(3,5-di-*tert*-butylphenyl)porphyrin[2,3-*b*]-1'*H*-imidazol-2'-yl)-([(2'''-hydroxynaphthyl)methylidene]-4''-aminophenyl boron difluoride chelate 71

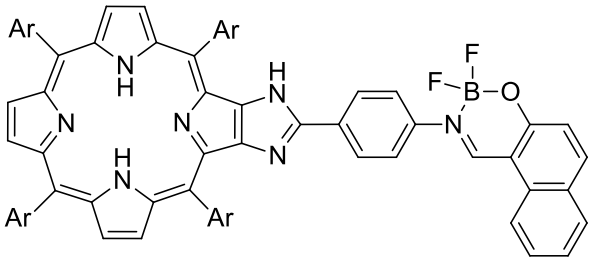

Starting with **65**, the crude material was chromatographed (dichloromethane/hexane 3:1) to afford **71** (30 mg, 36%) as a purple microcrystalline solid. m.p. > 300 °C. ^{1}H NMR (400 MHz, $CDCl_3$) δ -2.78 (br s, 2H, NH), 1.54 (s, 36H, CH_3), 1.56 (s, 36H, CH_3), 7.34 (d, 1H, J = 9.1 Hz, ArH), 7.50-7.55 (m, 1H, ArH), 7.67-7.73 (m, 3H, ArH), 7.80-7.82 (m, 2H, ArH), 7.86-7.92 (m, 4H, ArH), 8.09-8.19 (m, 11H, ArH), 8.43 (br s, 1H, NH), 8.84-8.89 (m, 2H, β-pyrrolic H), 8.98-9.06 (m, 4H, β-pyrrolic H), 9.20 (br s, 1H, CH) ppm. ^{13}C NMR (100 MHz, $CDCl_3$) 31.7, 31.9, 35.0, 35.1, 35.4, 115.5, 119.2, 119.3, 120.5, 121.0, 121.1, 122.0, 122.2, 122.5, 124.1, 125.3, 126.1, 127.3, 128.2, 129.5, 129.59, 129.65, 129.70, 129.9, 131.5, 132.0, 139.8, 141.1, 141.4, 141.6, 142.2, 142.7, 148.6, 148.7, 148.8, 149.4, 151.1, 157.5, 162.9 ppm. FTIR 713 (s), 750 (s),

799 (s), 1048 (m), 1163 (m), 1205 (m), 1245 (m), 1361 (m), 1464 (m), 1553 (m), 1591 (m), 2956 (m), 3317 (br, NH), 3422 (br, NH) cm^{-1}. λ_{max} ($CHCl_3$) 422, 519, 555, 588, 646 nm (log ε 5.44, 4.04, 3.64, 3.59, 3.42). Anal Calcd for $C_{94}H_{104}BF_2N_7O$. 1/2 CH_2Cl_2: C, 78.87; H, 7.35; N, 6.81. Found: C, 78.67; H, 6.95; N, 6.54.

(5,10,15,20-Tetrakis(3,5-di-*tert*-butylphenyl)porphyrin[2,3-*b*]-1'*H*-imidazol-2'-yl)-([(2'''-hydroxyphenyl)methylidene]-3''-aminophenyl boron difluoride chelate 72

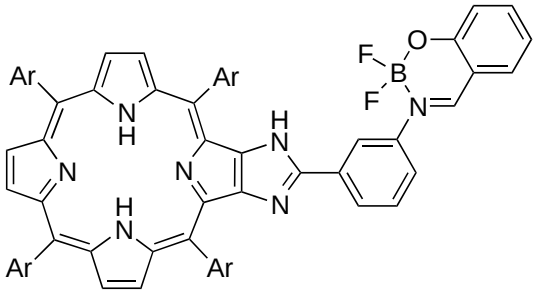

Starting with **66**, the crude material was chromatographed (dichloromethane/hexane 3:1) to afford **72** (32 mg, 39%) as a purple microcrystalline solid. m.p. > 300 °C. ^{1}H NMR (400 MHz, $CDCl_3$) δ -2.77 (br s, 2H, NH), 1.50-1.58 (m, 72H, CH_3), 7.15-7.20 (m, 1H, ArH), 7.28-7.32 (m, 1H, ArH), 7.56-7.64 (m, 2H, ArH), 7.68-7.73 (m, 2H, ArH), 7.76-7.82 (m, 1H, ArH), 7.82-7.85 (m, 3H, ArH), 8.01-8.04 (m, 1H, ArH), 8.11-8.17 (m, 7H, ArH), 8.18-8.21 (2H, m, ArH), 8.42 (s, 1H, NH), 8.68 (s, 1H, CH), 8.86-8.90 (m, 2H, β-pyrrolic H), 8.99-9.09 (m, 4H, β-pyrrolic H) ppm. ^{13}C NMR (100 MHz, $CDCl_3$) δ 31.75, 31.83, 35.0, 35.1, 35.4, 115.6, 115.9, 119.0, 119.9, 120.4, 120.5, 121.0, 122.2, 122.5, 124.0, 125.0, 127.2, 128.5, 129.6, 129.7, 130.0, 132.3, 132.9, 139.6, 140.0, 141.1, 141.6, 142.0, 143.0, 148.6, 148.8, 148.9, 149.4, 151.1, 160.2, 163.8 ppm. FTIR 714 (m), 755 (s), 799 (s), 879 (m), 1055 (m), 1155 (m), 1203 (m), 1246 (s), 1362 (m), 1474 (m), 1554 (m), 1590 (m), 1626 (m), 2958 (s), 3323 (br, NH), 3423 (br, NH) cm^{-1}. λ_{max} ($CHCl_3$) 422, 519, 555, 588, 647 nm (log ε 5.51, 4.21, 3.99, 3.96, 3.84). Anal Calcd for $C_{90}H_{102}BF_2N_7O$. 1/2 CH_2Cl_2: C, 78.87; H, 7.35; N, 6.81. Found: C, 79.12; H, 7.52; N, 6.55.

(5,10,15,20-Tetrakis(3,5-di-*tert*-butylphenyl)porphyrin[2,3-*b*]-1'*H*-imidazol-2'-yl)-[(2'''-hydroxynaphthyl)methylidene]-3''-aminophenyl boron difluoride chelate 73

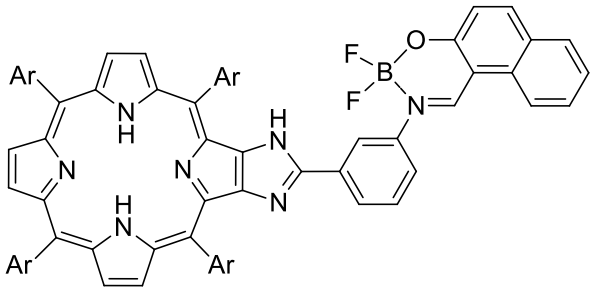

Starting with **67**, the crude material was chromatographed (dichloromethane/hexane 1:1) to afford **73** (23 mg, 28%) as a purple microcrystalline solid. m.p. > 300 °C. ^{1}H NMR (400 MHz, $CDCl_3$) δ -2.81 (br s, 2H, NH), 1.51-1.54 (app. s, 72H, CH_3), 7.40 (d, 1H, J = 9.1 Hz, ArH), 7.56-7.62 (m, 3H, ArH), 7.64-7.68 (m, 3H, ArH), 7.71-7.76 (m, 3H, ArH), 7.79-7.82 (m, 3H, ArH), 8.07-8.19 (m, 9H, ArH), 8.21 (d, J = 9.1 Hz, ArH), 8.41 (br s, 1H, NH), 8.83 and 8.86 (ABq, 2H, J_{AB} = 4.6 Hz, β-pyrrolic H), 8.90 and 8.97 (ABq, 2H, J_{AB} = 4.9 Hz, β-pyrrolic H), 9.02 and 9.05 (ABq, 2H, J_{AB} = 4.6 Hz, β-pyrrolic H), 9.36 (br s, 1H, CH) ppm. ^{13}C NMR (100 MHz, $CDCl_3$) δ 31.70, 31.74, 35.0, 35.4, 115.5, 119.8, 120.6, 121.0, 122.2, 122.5, 124.2, 124.7, 125.2, 127.2, 127.5, 128.1, 128.5, 129.6, 129.67, 129.71, 129.8, 130.0, 131.7, 132.8, 140.0, 141.1, 141.3, 141.6, 142.0, 143.6, 158.9, 163.0 ppm. FTIR 713 (m), 751 (s), 799 (s), 1049 (m), 1162 (m), 1206 (m), 1247 (m), 1361 (m), 1393 (m), 1424 (w), 1463 (m), 1552 (s), 1591 (m), 2956 (s), 3329 (br, NH), 3421 (br, NH) cm^{-1}. λ_{max} ($CHCl_3$) 423, 519, 554, 587, 652 nm (log ε 5.48, 4.23, 4.11, 4.12, 4.12). Anal Calcd for $C_{94}H_{104}BF_2N_7O$. 1/2 CH_2Cl_2: C, 78.87; H, 7.35; N, 6.81. Found: C, 78.71; H, 7.23; N, 6.78.

3.5.8 Preparation of Free-Base Quinoxalinoporphyrin Anils

5,10,15,20-Tetrakis(3,5-di-*tert*-butylphenyl)porphyrin[2,3-*b*]-[(2''-hydroxyphenyl)-methylidene]-6'-aminoquinoxaline 76

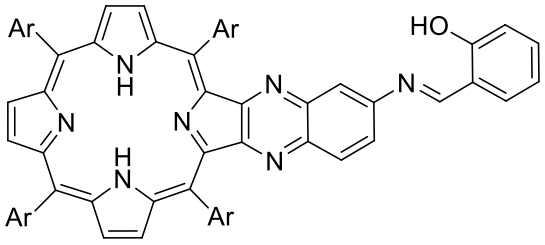

Starting with **42** and salicylaldehyde, **76** (129 mg, 79%) was obtained as a purple microcrystalline solid. m.p. > 300 °C. ^{1}H NMR (400 MHz, $CDCl_3$) δ -2.47 (br s, 2H, NH), 1.49-1.58 (m, 72H, CH_3), 7.03-7.09 (m, 1H, ArH), 7.11-7.15 (m, 1H, ArH), 7.45-7.51 (m, 2H, ArH), 7.61-7.65 (m, 1H, ArH), 7.73-7.78 (m, 1H, ArH), 7.80-7.84 (m, 2H, ArH), 7.85-7.89 (m, 1H, ArH), 7.93-7.97 (m, 2H, ArH), 7.98-8.02 (m, 4H, ArH), 8.09-8.14 (m, 4H, ArH), 8.76 (s, 1H, CH), 8.81 (app. s, 2H, β-pyrrolic H), 8.98-9.12 (m, 4H, β-pyrrolic H), 13.17 (br s, 1H, OH) ppm. ^{13}C NMR (100 MHz, $CDCl_3$) δ 31.8, 31.89, 31.92, 35.0, 35.1, 117.4, 118.2, 118.3, 119.4, 119.9, 120.9, 121.0, 121.1, 122.8, 124.6, 128.01, 128.04, 128.32, 128.34, 128.45, 128.50, 129.6, 131.51, 132.6, 133.7, 134.22, 134.24, 134.26, 138.1, 138.2, 139.60, 139.62, 139.9, 140.8, 140.9, 141.10, 141.12, 141.3, 148.8, 148.95, 148.97, 161.3, 162.1, 163.8 ppm. FTIR 711 (m), 741 (m), 801 (s), 879 (m), 922 (m), 1123 (m), 1151 (m), 1167 (m), 1222 (m), 1246 (m), 1361 (m), 1593 (m), 2956 (m), 3335 (br, NH) cm^{-1}. λ_{max} ($CHCl_3$) 437, 533, 601 nm (log ε 5.23, 3.96, 3.59). Anal Calcd for $C_{89}H_{101}N_7O$. 1/3 CH_2Cl_2: C, 81.71; H, 7.80; N, 7.47. Found: C, 81.90; H, 7.72; N, 7.27.

5,10,15,20-Tetrakis(3,5-di-*tert*-butylphenyl)porphyrin[2,3-*b*]-[(2''-hydroxynaphthyl)-methylidene]-6'-aminoquinoxaline 77

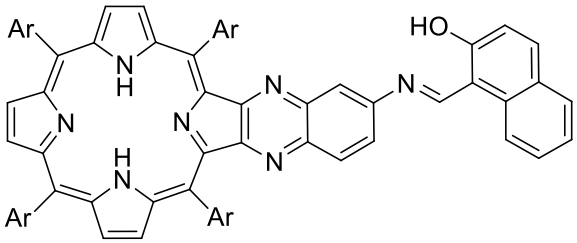

Starting with **42** and 2-hydroxy-1-naphthaldehyde, **77** (120 mg, 71%) was obtained as a purple microcrystalline solid. m.p. > 300 °C. ^{1}H NMR (400 MHz, $CDCl_3$) δ -2.46 (br s, 2H, NH), 1.51-1.56 (m, 72H, CH_3), 7.17 (d, 1H, *J* = 9.1 Hz, ArH), 7.42-7.47 (m, 1H, ArH), 7.62-7.67 (m, 1H, ArH), 7.72-7.75 (m, 1H, ArH), 7.77-7.83 (m, 4H, ArH), 7.87-7.90 (m, 1H, ArH), 7.89-7.91 (m, 1H, ArH), 7.95-7.98 (m, 2H, ArH), 7.99-8.03 (m, 4H, ArH), 8.10-8.13 (m, 4H, ArH), 8.22 (d, 1H, *J* = 9.1 Hz, ArH), 8.78-8.83 (m, 2H, β-pyrrolic H), 9.00-9.03 (m, 2H, β-pyrrolic), 9.07-9.12 (m, 2H, β-pyrrolic H), 9.53 (s, 1H, CH), 15.36 (br s, 1H, OH) ppm. ^{13}C NMR (100 MHz, $CDCl_3$) δ 31.9, 32.07, 32.14, 110.0, 118.6, 118.89, 118.91, 119.6, 121.5, 121.8, 122.8, 123.5, 124.6, 125.0, 128.2, 128.7, 128.8, 129.0, 129.1, 129.2, 130.3, 132.5, 134.0, 134.9, 135.0, 138.0, 138.9, 139.0, 140.4, 141.6, 141.7, 141.9, 142.2, 146.2, 146.6, 146.9, 149.5, 149.6 149.79, 149.82, 153.3, 154.3, 155.8, 155.9, 156.2 ppm. FTIR 711 (m), 740 (m), 800 (s), 921 (m), 1124 (m), 1161 (m), 1247 (m), 1361 (m), 1591 (m), 2954 (m), 3325 (br, NH) cm^{-1}. λ_{max} ($CHCl_3$) 436, 532, 600 nm (log ε 5.17, 4.29, 3.89). Anal Calcd for $C_{93}H_{103}N_7O$. 1/2 CH_2Cl_2: C, 81.53; H, 7.61; N, 7.12. Found: C, 81.74; H, 7.42; N, 6.77.

3.5.9 Preparation of Free-Base Quinoxalinoporphyrin Boranils

5,10,15,20-Tetrakis(3,5-di-*tert*-butylphenyl)porphyrin[2,3-*b*]-[(2''-hydroxyphenyl)-methylidene]-6'-aminoquinoxaline boron difluoride chelate78

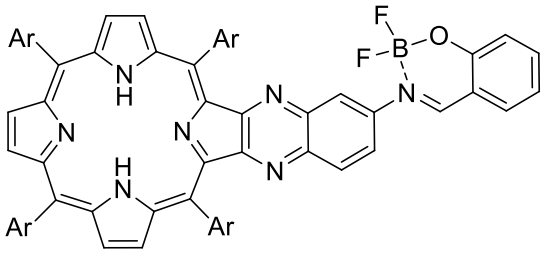

Starting with **76**, the crude material was chromatographed (dichloromethane/hexane 1:1) to afford **78** (44 mg, 36%) as a purple microcrystalline solid. m.p. > 300 °C. ^{1}H NMR (400 MHz, $CDCl_3$) δ -2.48 (br s, 2H, NH), 1.50-1.56 (m, 72H, CH_3), 7.11-7.16 (m, 1H, ArH), 7.26-7.29 (m, 1H, ArH), 7.55-7.58 (m, 1H, ArH), 7.73-7.79 (m, 1H, ArH), 7.81-7.84 (m, 2H, ArH), 7.94-7.97 (m, 2H, ArH), 7.98-8.01 (m, 3H, ArH), 8.01-8.05 (m, 3H, ArH), 8.11-8.13 (m, 4H, ArH), 8.58 (br s, 1H, CH), 8.80-8.84 (m, 2H, β-pyrrolic H), 9.00-9.04 (m, 2H, β-pyrrolic H), 9.10-9.13 (m, 2H, β-pyrrolic H) ppm. FTIR 643 (m), 714 (s), 802 (s), 879 (m), 902 (m), 921 (m), 988 (w), 1034 (w), 1079 (w), 1125 (m), 1161 (m), 1219 (m), 1245 (m), 12897 (m), 1362 (m), 1395 (w), 1424 (w), 1472 (m), 1552 (w), 1591 (m), 1625 (w), 2338 (w), 2362 (w), 2955 (m), 3335 (br, NH). λ_{max} ($CHCl_3$) 437, 530, 619 nm (log ε 5.24, 4.15, 3.95). Anal Calcd for $C_{89}H_{100}BF_2N_7O$. 1/3 CH_2Cl_2: C, 78.84; H, 7.46; N, 7.20. Found: C, 79.01; H, 7.29; N, 6.87.

5,10,15,20-Tetrakis(3,5-di-*tert*-butylphenyl)porphyrin[2,3-*b*]-[(2''-hydroxynaphthyl)-methylidene]-6'-aminoquinoxaline boron difluoride chelate 79

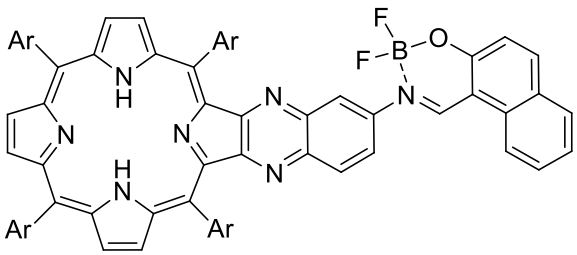

Starting with **77**, the crude material was chromatographed (dichloromethane/hexane 1:1) to afford **79** (31 mg, 37%) as a purple microcrystalline solid. mp > 300 °C. ^{1}H NMR (400 MHz,

$CDCl_3$) δ -2.48 (br s, 2H, NH), 1.51-1.56 (m, 76H, CH_3), 7.39 (m, 1H, *J* = 8.7 Hz, ArH), 7.45-7.50 (m, 1H, ArH), 7.55-7.60 (m, 2H, ArH), 7.70-7.75 (m, 1H, ArH), 7.81-7.84 (m, 3H, ArH), 7.90-7.92 (m, 1H, ArH), 7.98-8.04 (m, 3H, ArH), 8.06 (d, 1H, *J* = 1.8 Hz, ArH), 8.10-8.14 (m, 4H, ArH), 8.16 (d, 1H, *J* = 1.8 Hz, ArH), 8.19-8.22 (m, 1H, ArH), 8.27-8.32 (m, 2H, ArH), 8.80-8.85 (m, 2H, β-pyrrolic H), 9.00-9.06 (m, 4H, β-pyrrolic H), 9.30 (br s, 1H, CH) ppm. ^{13}C NMR (100 MHz, $CDCl_3$) δ 31.7, 31.9, 35.1, 35.2, 114.9, 118.4, 119.1, 119.6, 120.7, 121.0, 121.2, 121.4, 122.8, 122.9, 123.7, 123.9, 124.1, 124.7, 125.4, 125.6, 127.1, 127.3, 128.2, 128.3, 128.6, 129.04, 129.3, 129.6, 130.0, 130.2, 131.6, 131.9, 132.1, 132.3, 133.1, 134.4, 134.8, 137.5, 138.3, 138.5, 139.7, 140.4, 140.7, 141.0, 141.6, 147.3, 148.8, 149.2, 150.7, 153.1, 155.2, 156.7, 158.1 ppm. FTIR 641 (m), 719 (s), 800 (s), 880 (m), 901 (m), 922 (m), 989 (w), 1036 (w), 1077 (w), 1123 (m), 1160 (m), 1220 (m), 1247 (m), 1289 (m), 1361 (m), 1392 (w), 1425 (w), 1472 (m), 1551 (w), 1592 (m), 1624 (w), 2339 (w), 2360 (w), 2957 (m), 3336 (br, NH). λ_{max} ($CHCl_3$) 436, 532, 601 nm (log ε 5.18, 4.27, 3.98). Anal Calcd for $C_{93}H_{102}BF_2N_7O$. 1/2 CH_2Cl_2: C, C, 78.80; H, 7.28; N, 6.88. Found: C, 78.87; H, 6.95; N, 6.52.

3.5.10 Preparation of Zinc(II) Quinoxalinoporphyrin Boranils

5,10,15,20-Tetrakis(3,5-di-*tert*-butylphenyl)porphyrin[2,3-*b*]-[(2''-hydroxyphenyl)-methylidene]-6'-aminoquinoxaline boron difluoride chelate 80

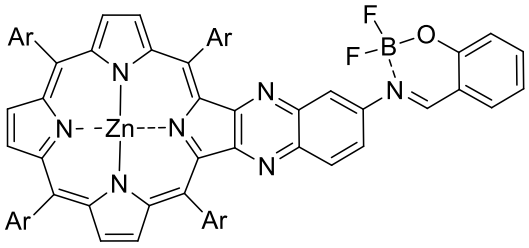

Starting with **78**, the crude material was chromatographed (dichloromethane/hexane 1:1) to afford **80** (10 mg, 32%) as a purple microcrystalline solid. m.p. > 300 °C. ^{1}H NMR (400 MHz, $CDCl_3$) δ 1.49-1.53 (m, 72H, CH_3), 6.84 (d, 1H, *J* = 2.3 Hz, ArH), 6.97-7.04 (m, 1H, ArH), 7.08 (dd, 1H, *J* = 9.1, 2.3 Hz, ArH), 7.62 (d, 2H, *J* = 9.1 Hz, ArH), 7.77-7.80 (m, 3H, ArH), 7.85-

7.89 (m, 2H, ArH), 7.92-7.96 (m, 4H, ArH), 8.07-8.10 (m, 4H, ArH), 8.88-8.90 (m, 3H, β-pyrrolic H and CH), 8.97-9.03 (m, 4H, β-pyrrolic H) ppm. ^{13}C NMR (100 MHz, $CDCl_3$) δ 31.7, 31.9, 35.0, 117.8, 120.8, 120.9, 124.9, 128.2, 129.3, 131.6, 131.7, 132.5, 132.6, 132.7, 141.5, 141.6, 141.7, 148.6, 148.8, 150.0, 151.2, 152.6, 161.6, 163.9 ppm. FTIR 711 (m), 752 (m), 796 (s), 813 (m), 879 (m), 938 (m), 1005 (m), 1222 (m), 1247 (m), 1361 (m), 1459 (m), 1592 (m), 2956 (m) cm^{-1}. λ_{max} ($CHCl_3$) 429, 448, 575, 620 nm (log ε 4.96, 4.89, 3.63, 3.07). Anal Calcd for $C_{89}H_{98}BF_2N_7OZn$. 2/3 CH_2Cl_2: C, 74.14; H, 6.89; N, 6.75. Found: C, 74.18; H, 6.77; N, 6.57.

{5,10,15,20-Tetrakis(3,5-di-*tert*-butylphenyl)porphyrin[2,3-*b*]-[(2''-hydroxynaphthyl)-methylidene]-6'-aminoquinoxaline} zinc(II) boron difluoride chelate 81

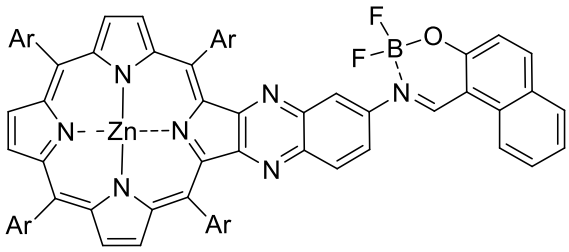

Starting with **79**, the crude material was chromatographed (dichloromethane/hexane 1:1) to afford **81** (15 mg, 48%) as a purple microcrystalline solid. m.p. > 300 °C. ^{1}H NMR (400 MHz, $CDCl_3$) δ 1.49-1.57 (m, 72H, CH_3), 6.99 (d, 1H, *J* = 8.9 Hz, ArH), 7.41-7.45 (m, 1H, ArH), 7.61-7.64 (m, 1H, ArH), 7.75-7.82 (m, 4H, ArH), 7.83-7.86 (m, 1H, ArH), 7.93-8.01 (m, 7H, ArH), 8.07-8.12 (m, 5H, ArH), 8.16-8.20 (m, 1H, ArH), 8.90-8.93 (m, 2H, β-pyrrolic H), 9.00-9.08 (m, 4H, β-pyrrolic H), 9.48 (br s, 1H, CH) ppm. ^{13}C NMR (100 MHz, $CDCl_3$) δ 31.7, 31.9, 35.0, 35.1, 120.6, 120.9, 122.1, 123.9, 128.2, 129.3, 131.5, 131.6, 131.7, 132.4, 137.4, 138.4, 139.8, 141.3, 141.4, 141.6, 148.6, 148.8, 148.9, 155.0 ppm. FTIR 712 (m), 753 (s), 796 (m), 814 (m), 938 (m), 1003 (m), 1058 (m), 1152 (m), 1189 (m), 1221 (m), 1246 (m), 1361 (m), 1459 (m), 1476 (m), 1555 (m), 1592 (m), 1615 (m), 2865 (m), 2954 (s) cm^{-1}. λ_{max} ($CHCl_3$) 427, 470, 579, 621 nm (log ε 5.04, 4.66, 3.86, 3.59). Anal Calcd for $C_{93}H_{100}BF_2N_7OZn$. 2/3 CH_2Cl_2: C, 74.87; H, 6.80; N, 6.52. Found: C, 74.89; H, 6.61; N, 6.40.

3.6 References

1. Frath, D.; Azizi, S. Å.; Ulrich, G.; Retailleau, P.; Ziessel, R. *Org. Lett.* **2011**, *13* (13), 3414-3417.
2. Frath, D.; Azizi, S. Å.; Ulrich, G.; Ziessel, R. *Org. Lett.* **2012**, *14* (18), 4774-4777.
3. Chibani, S.; Charaf-Eddin, A.; Le Guennic, B.; Jacquemin, D. *J. Chem. Theory Comput.* **2013**, *9* (7), 3127-3135.
4. Telitel, S.; Blanchard, N.; Schweizer, S.; Morlet-Savary, F.; Graff, B.; Fouassier, J. P.; Lalevee, J. *Polym.* **2013**, *54* (8), 2071-2076.
5. Chardon-Noblat, S.; Sauvage, J.-P.; Mathis, P. *Angew. Chem. Int. Ed.* **1989**, *28* (5), 593-595.
6. Toa, M.; Liu, L.; Liu, D.; Zhou, X. *Dyes Pigm.* **2010**, *85*, 21-26.
7. Seybold, P. G.; Gouterman, M. *J. Mol. Spectrosc.* **1969**, *31*, 1-13.
8. Reichardt, C. *Chem. Rev.* **1994**, *94* (8), 2319-2358.

Chapter Four

Porphyrin-α-Cyanostilbene Conjugates

4.1 Background

Some structures and their associated photo-physical properties related to the compounds described in this Chapter were briefly discussed in Section 1.3.6.3.

In this Chapter, the syntheses of porphyrin-α-cyanostilbene conjugates, using the three frameworks shown in Figure 1.30, are described. Photo-physical properties, in the form of UV-visible absorption and fluorescence emission spectra, are also reported.

4.2 Synthesis of Porphyrin-α-Cyanostilbene Conjugates

The synthetic route to *meso*-phenyl linked α-cyanostilbene porphyrins is shown in Scheme 4.1. Closely related chemistry used to afford the α-cyanostilbene chromophore attached *via* a phenyl appended imidazole-fused porphyrin and *via* the quinoxaline unit in a quinoxaline-fused porphyrin is shown in Schemes 4.2 and 4.3, respectively.

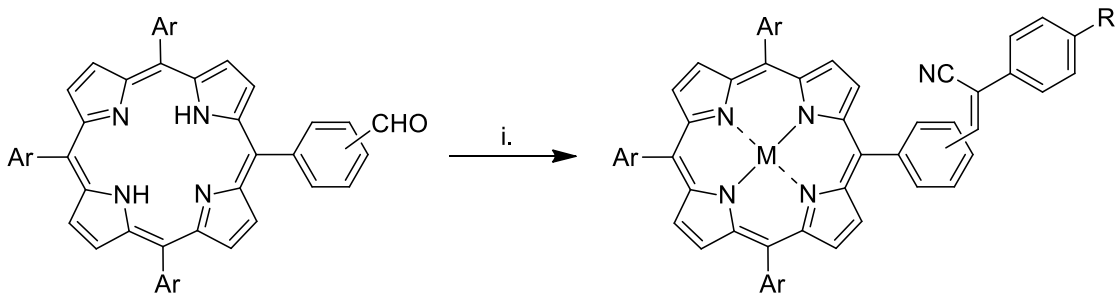

18 *p*-isomer
19 *m*-isomer
20 *o*-isomer

82 *p*-isomer, M = 2H, R = H 59%
83 *p*-isomer, M = 2H, R = Br 50%
84 *p*-isomer, M = 2H, R = NO_2 64%
85 *m*-isomer, M = 2H, R = H 63%
86 *m*-isomer, M = 2H, R = Br 88%
87 *m*-isomer, M = 2H, R = NO_2 58%

88 *o*-isomer, M = 2H, R = H 33%
89 *o*-isomer, M = 2H, R = Br 75%
90 *o*-isomer, M = 2H, R = NO_2 80%

ii.

91 *p*-isomer, M = Zn, R = H 68%
92 *p*-isomer, M = Zn, R = Br 72%
93 *p*-isomer, M = Zn, R = NO_2 87%
94 *m*-isomer, M = Zn, R = H 76%
95 *m*-isomer, M = Zn, R = Br 80%
96 *m*-isomer, M = Zn, R = NO_2 83%

97 *o*-isomer, M = Zn, R = H 57%
98 *o*-isomer, M = Zn, R = Br 72%
99 *o*-isomer, M = Zn, R = NO_2 61%

Scheme 4.1: i. Piperidine or NaOMe, benzyl cyanide or 4'-bromophenylacetonitrile or 4'-nitrophenylacetonitrile, EtOH / CH_2Cl_2; ii. $Zn(OAc)_2$, CH_2Cl_2.

In all cases the chemistry involves the reaction of the formyl group present in **18-20** (Scheme 4.1), **38-39** (Scheme 4.2) and **45** (Scheme 4.3) in a Knoevenagel condensation with the reactive methylene group present in benzyl cyanide, 4'-bromophenylacetonitrile and 4'-nitrophenylacetonitrile, in a dichloromethane / ethanol mixture, followed by zinc(II) complexation in dichloromethane. As for Chapter Three, the reactions are shown over three schemes to help visualise the structures of the products from the three different porphyrin building blocks.

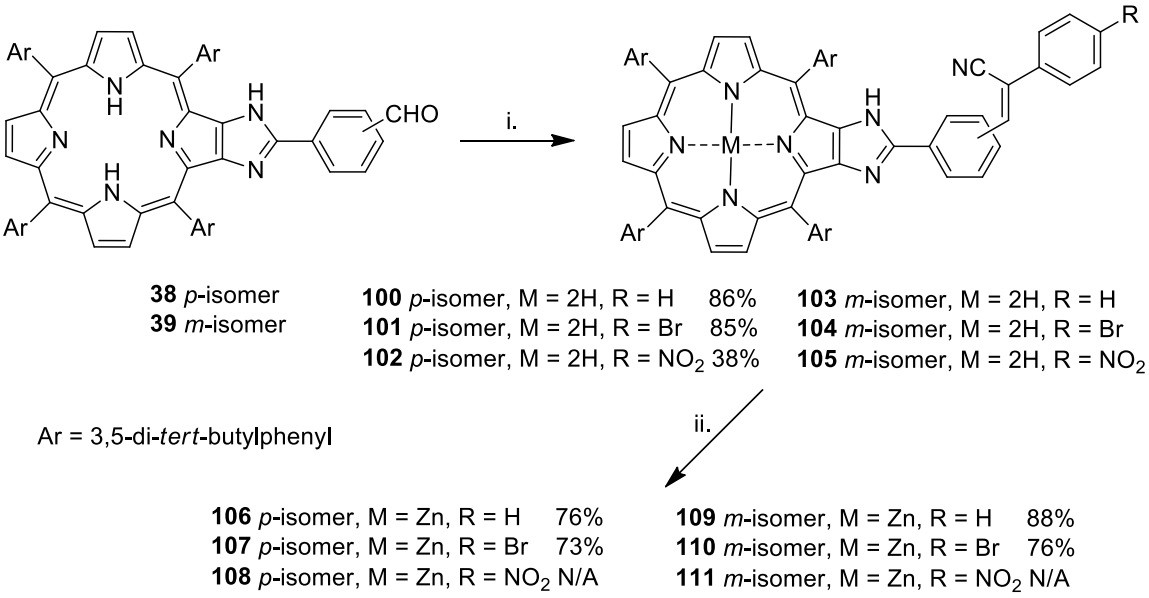

Scheme 4.2: i. Piperidine or NaOMe, benzyl cyanide or 4'-bromophenylacetonitrile or 4'-nitrophenylacetonitrile, EtOH / CH_2Cl_2; ii. $Zn(OAc)_2$, CH_2Cl_2.

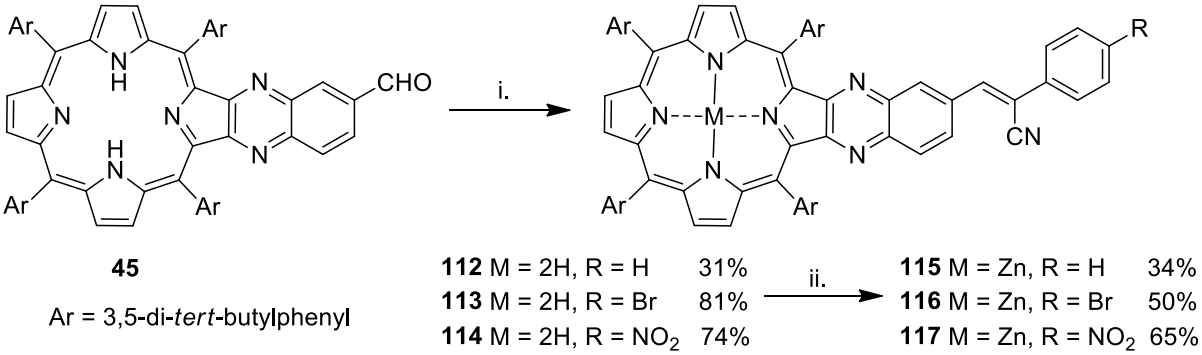

Scheme 4.3: i. Piperidine or NaOMe, benzyl cyanide or 4'-bromophenylacetonitrile or 4'-nitrophenylacetonitrile, EtOH / CH_2Cl_2; ii. $Zn(OAc)_2$, CH_2Cl_2.

The syntheses of the formyl-functionalised porphyrins were discussed in Chapter Two (Schemes 2.3, 2.6 and 2.8). Nitro substituted α-cyanostilbene-porphyrins **84**, **87**, **90**, **102** and **114** were synthesised from the formyl-functionalised porphyrins and 4'-nitrophenylacetonitrile under refluxing conditions overnight, with piperidine as a base. The methylene protons of benzyl cyanide and 4'-bromophenylacetonitrile are less acidic than those of 4'-nitrophenylacetonitrile, and for the Knoevenagel reactions of these compounds a stronger base, sodium methoxide, was required. For an unknown reason, the synthesis of **105** was unsuccessful. The reaction was attempted with an excess of piperidine and also with the use of sodium methoxide but the desired product was never observed in ^{1}H NMR analyses of the products. Zinc(II) complexes were obtained by refluxing a dichloromethane solution of the free-base porphyrins with zinc(II) acetate overnight.

An attempt to synthesise **108** was made, starting with **102**, in which the reaction mixture was refluxed for 1 h and the reaction was monitored by TLC. A new pink spot was observed on the TLC plate, as was the case for successful zinc(II) porphyrin complexation reactions in this series, however, upon work-up a grey mass was obtained that was insoluble in $CDCl_3$ and DMSO d_6, and this material has not been characterised any further.

^{1}H NMR, ^{13}C NMR and IR spectroscopy verified the molecular structures. Most noticeably, there was a loss of the aldehyde signal in the ^{1}H NMR spectra of all products, and the alkene CH proton of the α-cyanostilbene was generally observed as a singlet (although in some compounds it was overlayed by other signals). In the IR spectra, a weak nitrile absorption band was observed for all compounds.

As was the case with the *meso*-phenyl porphyrin boranil conjugates described in Chapter Three, for the *o*-substituted isomers the proximity of the second chromophore (in this case the α-cyanostilbene units) to the porphyrin ring was evident in ^{1}H NMR spectra and this exemplified in Figure 4.1.

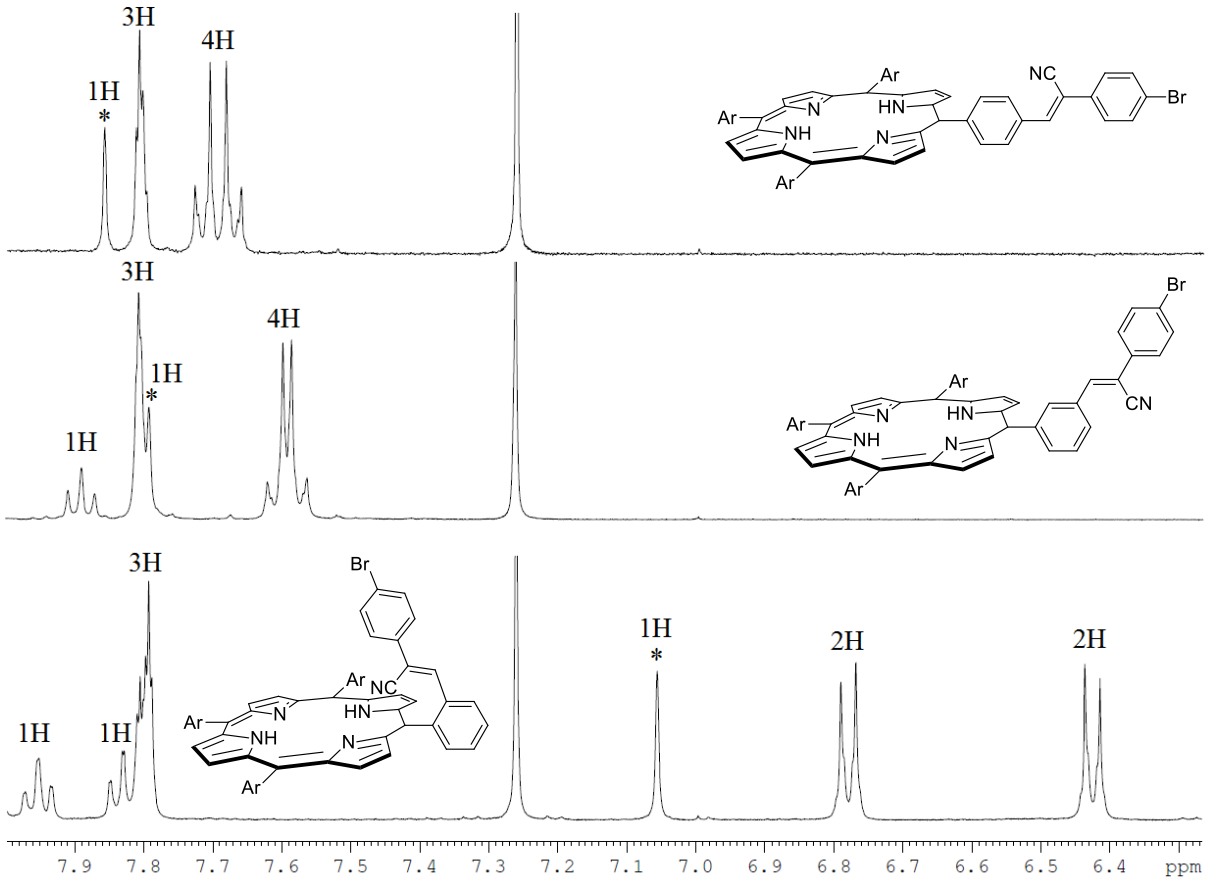

Figure 4.1: A section of the 400 MHz ^{1}H NMR spectra in $CDCl_3$ at 298 K of the α-cyanostilbenes derived from 4'-bromophenylacetonitrile and free-base *meso*-phenyl porphyrins bearing formyl groups at (a) the *p*-position, compound **83** (b) the *m*-position, compound **86** and (c) the *o*-position, compound **89**. The alkene CH proton is indicated with an asterisk (*).

The AB quartet systems of the four protons on the *p*-bromo substituted phenyl rings are apparent in each spectrum in Figure 4.1 and the alkene CH proton is indicated with an asterisk (*). The upfield chemical shifts of these protons for **89** (Figure 4.1 (c)) is indicative of the α-cyanostilbene unit being located over the porphyrin and experiencing the effects of the ring current of the macrocycle.

4.3 Photo-physical Properties

The UV-visible absorption, fluorescence emission and relative quantum yield of free-base and zinc(II) complex of all prepared porphyrin-α-cyanostilbene conjugates were recorded in de-

acidified chloroform. The relative quantum yields of free-base porphyrin-α-cyanostilbenes were compared with 5,10,15,20-tetraphenylporphyrin (TPP). In the case of zinc(II) porphyrin-α-cyanostilbenes, ZnTPP was used as the reference standard. The photo-physical properties of *meso*-phenyl linked α-cyanostilbene porphyrins are reported in Table 4.1.

Table 4.1: Absorption maxima wavelength (λ_{abs}, nm); molar extinction coefficient (ε, x 10^4, $Lmol^{-1}cm^{-1}$); fluorescence maxima wavelength (λ_{em}, nm); relative quantum yield (ϕ) of **82-90** and **91-99** in chloroform

	Free Base					Zinc(II) Complex			
	λ_{max}	$\varepsilon/10^4$	λ_{em}	ϕ^1		λ_{max}	$\varepsilon/10^4$	λ_{em}	ϕ^2
82	423	10.78	653	0.138	**91**	427	11.08	612	0.066
83	423	8.46	653	0.134	**92**	427	8.55	612	0.078
84	422	12.4	654	0.056	**93**	426	9.49	609	0.008
85	422	10.56	650	0.104	**94**	427	10.02	605	0.059
86	423	7.58	650	0.111	**95**	427	11.07	605	0.053
87	422	13.08	651	0.052	**96**	426	5.47	603	0.002
88	424	8.05	655	0.120	**97**	429	6.42	609	0.046
89	425	5.80	654	0.099	**98**	429	7.56	608	0.051
90	423	7.53	654	0.039	**99**	426	8.92	608	0.004

[1]relative quantum yield compared to TPP, [2]relative quantum yield compared to ZnTPP

The UV-visible absorption spectra of *meso*-phenyl linked porphyrin-α-cyanostilbenes **82-90** are shown in Figure 4.2. A typical porphyrin absorption spectrum was observed in each case, with the presence of a Soret band at around 422 nm, accompanied by four weak Q-bands. The four Q bands were located at around 520 nm, 560 nm, 600 nm and 650 nm. The Soret peak is designated to π-π* transitions. The molar extinction coefficients for **82-90** were observed in the range of 58,000 to 130,000 $Lmol^{-1}cm^{-1}$.

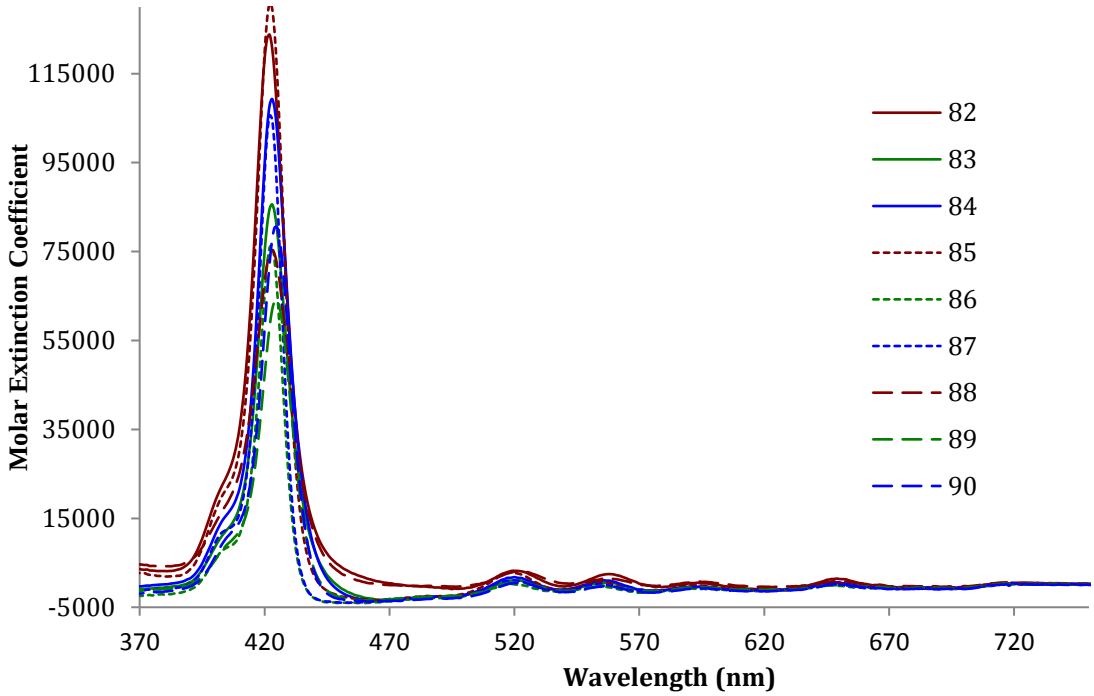

Figure 4.2: UV-visible absorption spectra of free-base *meso*-phenyl linked porphyrin-α-cyanostilbenes **82-90** in $CHCl_3$.

The UV-visible absorption spectra of *meso*-phenyl linked zinc(II) porphyrin-α-cyanostilbenes **91-99** are shown in Figure 4.3. Again, a typical porphyrin absorption spectrum was observed in each case, with a bathochromic shift of 3-6 nm in comparison to the free-base analogues, and the presence of two Q-bands. The Soret band was observed at around 426-429 nm and the two Q bands were observed at around 500 nm and 600 nm. The molar extinction coefficients for **91-99** were observed in the range of 75,600 to 110,800 $Lmol^{-1}cm^{-1}$.

Porphyrin bromo-substituted-α-cyanostilbenes show a weak molar extinction coefficient compared to the unsubstituted and nitro-substituted α-cyanostilbenes. In general, the molar extinction coefficient decreases for all three substitution types (H, Br, NO_2) from *para* to *meta* to *ortho* porphyrin-α-cyanostilbene conjugates in both the free-base and zinc(II) series.

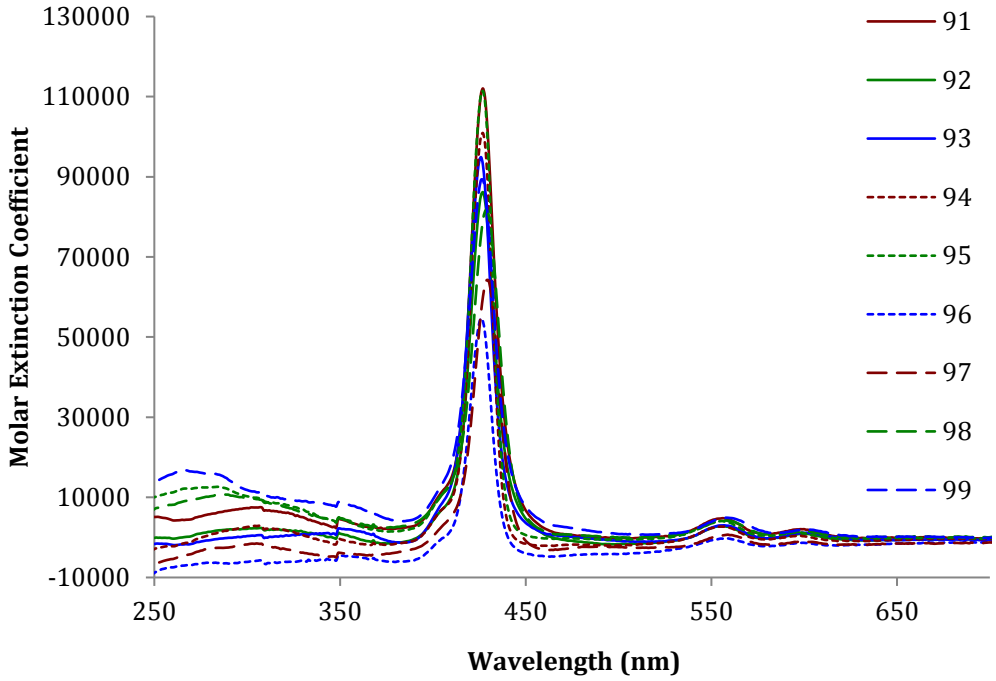

Figure 4.3: UV-visible absorption of *meso*-phenyl linked zinc(II) porphyrin-α-cyanostilbenes **91-99** in $CHCl_3$.

The normalised fluorescence emission of free-base and zinc(II) *meso*-phenyl linked porphyrin-α-cyanostilbenes in chloroform are shown in Figure 4.4 and Figure 4.5, respectively. The features of the fluorescence emission spectra and quantum yields are summarised in Table 4.1. The porphyrin nitro-substituted-α-cyanostilbenes show weak fluorescence emissions compared with unsubstituted and bromo-substituted α-cyanostilbene compounds. For the zinc(II) complexes, a typical fluorescence emission spectrum was observed with emission bands at 605-612 nm and 660 nm.

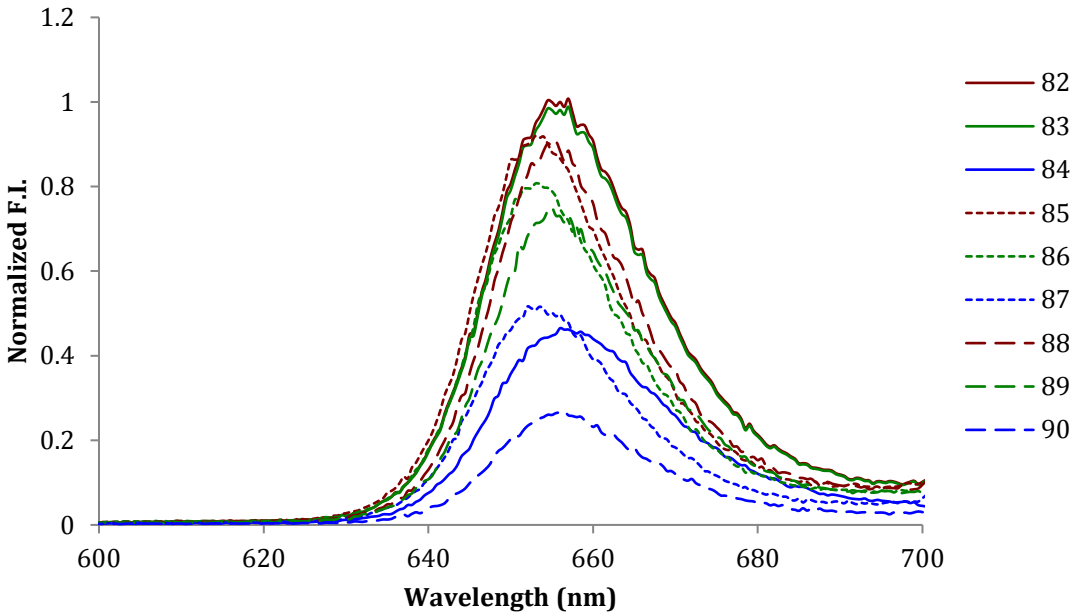

Figure 4.4: Normalised fluorescence spectra of free-base *meso*-phenyl linked porphyrin-α-cyanostilbenes **82-90** in $CHCl_3$.

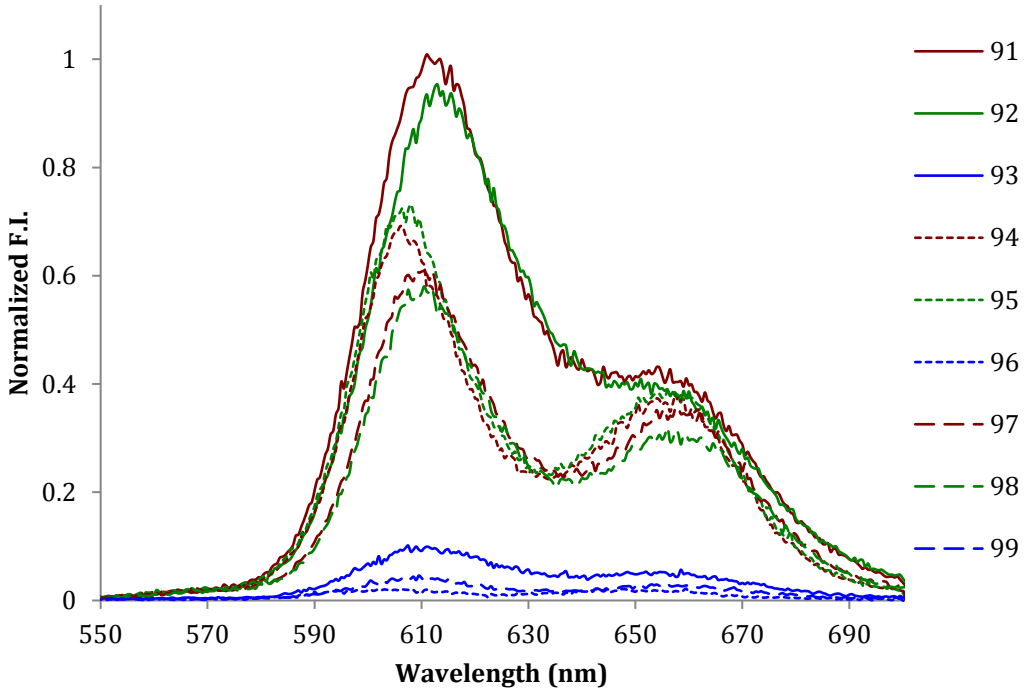

Figure 4.5: Normalised fluorescence spectra of *meso*-phenyl linked zinc(II) porphyrin-α-cyanostilbenes **91-99** in $CHCl_3$.

The quantum yield generally decreases from *para* to *meta* to *ortho* in all three substitutent types (H, Br, NO_2) in the *meso*-phenyl linked porphyrin-α-cyanostilbene series, and this may be the result of photo-induced intramolecular electron and / or energy transfer processes.[1]

The photo-physical properties of α-cyanostilbene imidazole-porphyrins and quinoxaline α-cyanostilbene-porphyrins are summarised in Table 4.2. The UV-visible absorption spectra of free-base and zinc(II) α-cyanostilbene imidazole-porphyrins and α-cyanostilbene quinoxaline-porphyrins are shown in Figure 4.6 and Figure 4.7, respectively.

Table 4.2: Absorption maxima wavelength (λ_{abs}, nm); molar extinction coefficient (ε x 10^4); fluorescence maxima wavelength (λ_{em}, nm); relative quantum yield (ϕ) of **100-104**, **112-114** and **106**, **107**, **109**, **110** and **115-117** in chloroform

	Free Base					Zinc(II) Complex			
	λ_{max}	$\varepsilon/10^4$	λ_{em}	ϕ^1		λ_{max}	$\varepsilon/10^4$	λ_{em}	ϕ^2
100	426	21.47	655	0.072	**106**	429	19.24	605	0.107
101	426	31.45	655	0.073	**107**	430	32.10	604	0.082
102	424	24.81	651	0.021	**108**	-	-	-	-
103	423	27.92	652	0.090	**109**	430	20.70	607	0.100
104	422	32.82	653	0.077	**110**	430	34.18	603	0.080
112	428	16.13	661	0.018	**115**	435	16.49	661	0.006
113	428	18.77	662	0.026	**116**	433	20.42	666	0.006
114	430	30.44	665	0.007	**117**	435	17.00	647	0.0008

[1]relative quantum yield compared to TPP, [2]relative quantum yield compared to ZnTPP

The Soret band was observed around 423-426 nm for imidazole-porphyrin-α-cyanostilbenes with molar extinction coefficients in the range of 214,000 to 314,000 $Lmol^{-1}cm^{-1}$. The Soret band of quinoxaline-porphyrin-α-cyanostilbenes was observed at 427-435 nm with molar extinction coefficient values in the range of 160,000 to 300,000 $Lmol^{-1}cm^{-1}$. A bathochromic

shift of ~10 nm in the Soret band was observed in the case of quinoxaline-porphyrin-α-cyanostilbenes in comparison with imidazole-porphyrin-α-cyanostilbenes, indicating electronic interaction of the fused quinoxaline ring with the porphyrin macrocycle. For the imidazole-porphyrin-α-cyanostilbene compounds, a bathchromic shift of ~8 nm was observed from free-base to zinc(II) complexes.

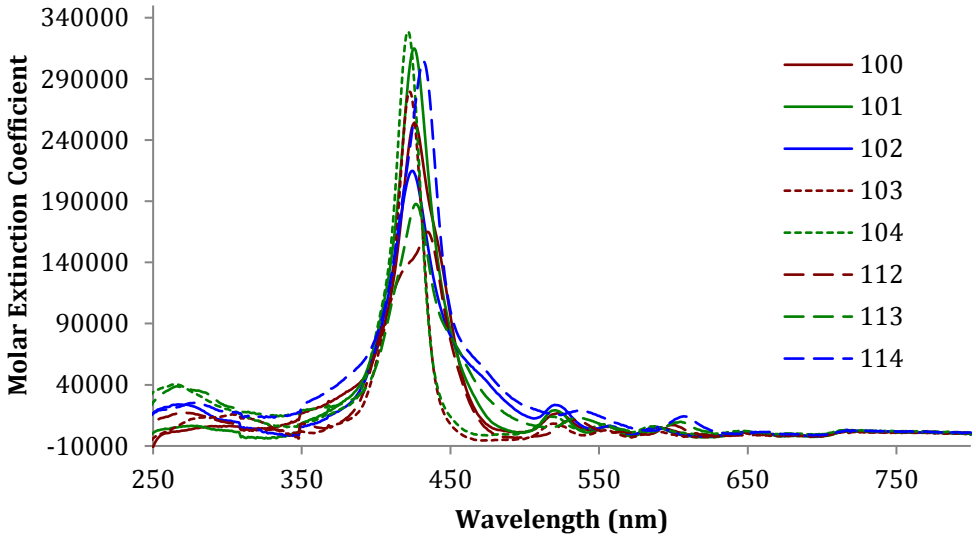

Figure 4.6: UV-visible absorption of free-base porphyrins **100**-**104** and **112**-**114** in $CHCl_3$.

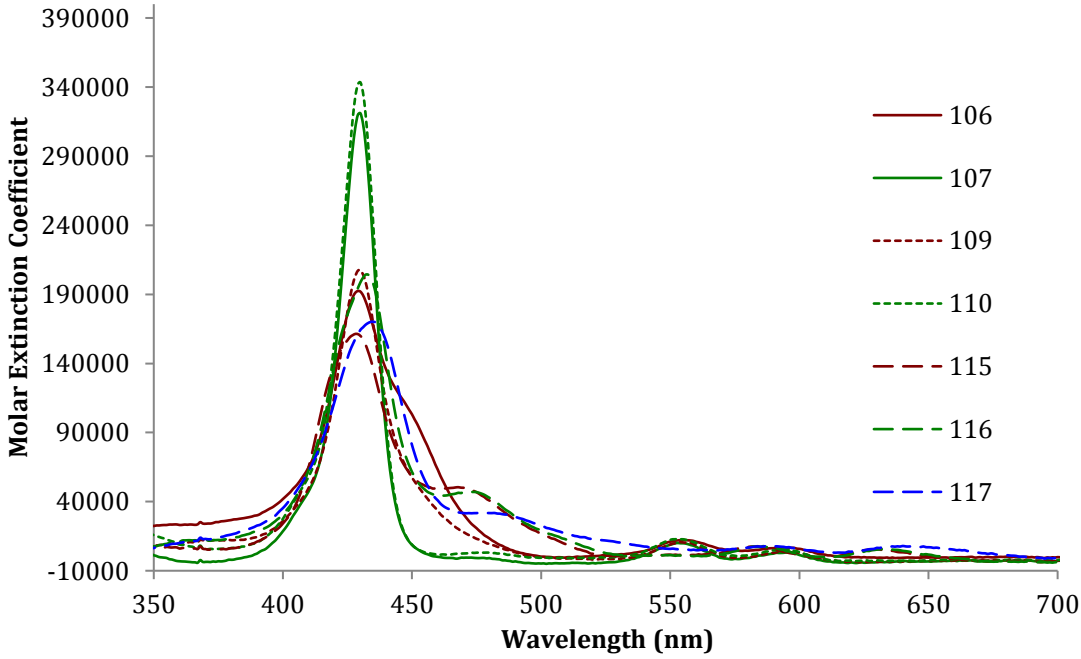

Figure 4.7: UV-visible absorption of zinc(II) porphyrins **106**, **107**, **109**, **110** and **115**-**117** in $CHCl_3$.

The fluorescence emission spectra of free-base and zinc(II) imidazole- and quinoxaline-porphyrin-α-cyanostilbenes are shown in Figure 4.8 and Figure 4.9. Both free-base and zinc(II) complexes of imidazole- and quinoxaline-porphyrin α-cyanostilbenes show dual fluorescence. The imidazole-porphyrin-α-cyanostilbenes show emission at 650 and 710 nm and quinoxaline-porphyrin-α-cyanostilbenes show emission at 660 and 730 nm. The relative quantum yields of quinoxaline-porphyrin-α-cyanostilbenes were poor compared to imidazole-porphyrin-α-cyanostilbenes. As noted in Chapter 3, Section 3.3, this is the result of different structural framework. It is likely the result of different electronic delocalisation pathways (HOMO – LUMO band gaps) of the parent fused quinoxalinoporphyrin system.

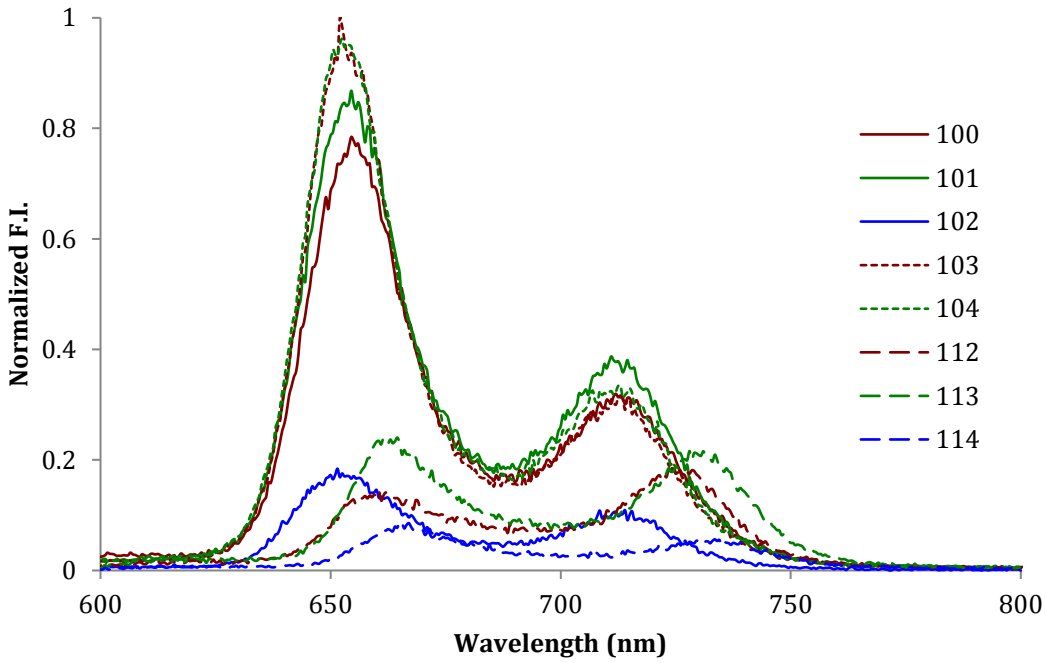

Figure 4.8: Normalised fluorescence spectra of free-base porphyrins **100-104** and **112-114** in $CHCl_3$.

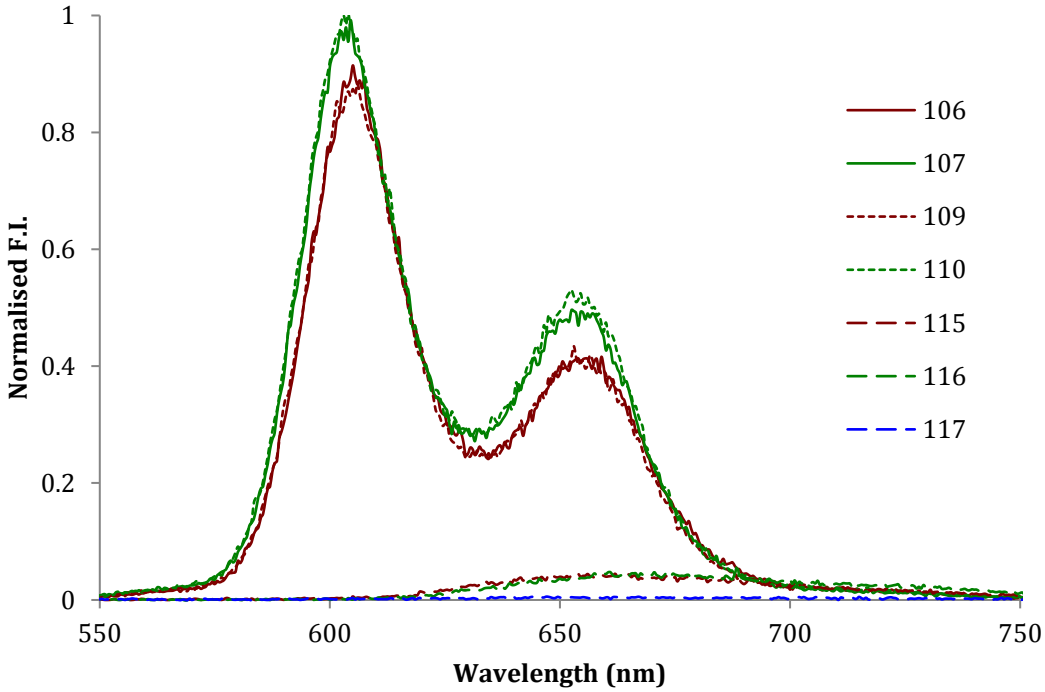

Figure 4.9: Normalised fluorescence spectra of zinc(II) porphyrins **106**, **107**, **109**, **110** and **115-117** in $CHCl_3$.

4.4 Conclusions

Three series of porphyrin-α-cyanostilbene conjugates were prepared by condensation of aldehyde-functionalised porphyrins with benzyl cyanides, followed by formation of their zinc(II) complexes. The structure of all compounds were characterised with ^{1}H and ^{13}C NMR spectroscopy, FTIR and elemental analysis. As was the case for the anils and boranils formed in Chapter Three, in the case of the *meso*-phenylporphyrins bearing the α-cyanostilbene units at the *ortho*-position, the ^{1}H NMR spectra shows evidence of a strong porphyrin ring current effect on the α-cyanostilbene portions, with large upfield chemical shifts observed for signals associated with these fragments.

The preliminary investigation of the photo-physical properties of *meso*-porphyrin-conjugates reveals possible interactions between two chromophores as the relative quantum yield decreases

from *para* to *meta* to *ortho*. Similar to quinoxalinoporphyrin-boranils, quinoxalinoporphyrin-α-cyanostilbenes show weak UV-visible absorption as well as weak relative quantum yields.

4.5 Experimental

4.5.1 Materials and Methods

The materials and methods used in this Chapter are as described in Sections 2.7.1 and 3.5.1.

4.5.2 Preparation of Free-Base *meso*-Phenyl Porphyrin-α-Cyanostilbenes

General Procedure Method A: To a mixture of formyl porphyrin (75 mg, 0.077 mmol) and substituted acetonitrile (0.077 mmol; benzyl cyanide 9.0 mg or 4'-bromophenylacetonitrile 15.1 mg) in a dichloromethane/ethanol mixture (1:9; 20 mL) was added sodium methoxide (20.8 mg, 0.38 mmol). The reaction mixture was heated at reflux overnight under an argon atmosphere. The reaction mixture was allowed to cool to room temperature and filtered. The residue obtained was washed with ethanol (10 mL) and then chromatographed (silica gel, dichloromethane/hexane 1:1) to afford the desired products.

General Procedure Method B: To a mixture of formyl porphyrin (75 mg, 0.077 mmol) and 4'-nitrophenylacetonitrile (12.5 mg, 0.077 mmol) in a dichloromethane/ethanol mixture (1:9; 20 mL) was added piperidine (13.1 mg, 0.15 mmol). The reaction mixture was refluxed overnight under an argon atmosphere. The reaction mixture was allowed to cool to room temperature and filtered. The residue obtained was washed with ethanol (10 mL) and chromatographed (silica gel, dichloromethane/hexane 1:1) to afford pure products.

5-(Phenyl-4-[(*Z*)-2-cyano-2-phenylethenyl])-10,15,20-tris(3,5-di-*tert*-butylphenyl)porphyrin 82

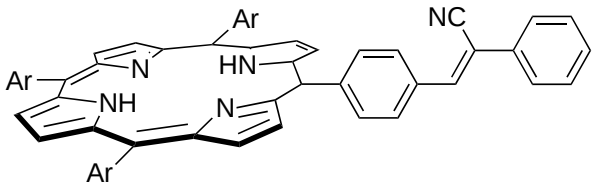

Using Method A and starting with **18** and benzyl cyanide, **82** (49 mg, 59%) was obtained as a purple microcrystalline solid. m.p. > 300 °C. ^{1}H NMR (400 MHz, $CDCl_3$) δ -2.67 (br s, 2H, NH), 1.51-1.58 (m, 54H, CH_3), 7.48-7.51 (m, 1H, ArH), 7.52-7.58 (m, 2H, ArH), 7.78-7.90 (m, 6H, ArH and CH), 8.07-8.12 (m, 6H, ArH), 8.30 and 8.37 (ABq, 2H, J_{AB} = 8.3 Hz, ArH), 8.85-8.95 (m, 8H, β-pyrrolic H) ppm. ^{13}C NMR (100 MHz, $CDCl_3$) δ 31.7, 35.1, 112.1, 118.2, 118.3, 121.0, 121.6, 121.8, 126.2, 127.6, 129.2, 129.4, 129.7, 129.9, 133.0, 134.7, 135.1, 141.18, 141.25, 142.1, 145.0, 148.7, 148.8 ppm. FTIR 681 (m), 706 (m), 728 (s), 795 (m), 913 (m), 1245 (m), 1361 (m), 1591 (m, C=C), 2228 (w, CN), 2960 (m), 3310 (br, NH) cm^{-1}. λ_{max} ($CHCl_3$) 422, 520, 558, 593, 649 nm (log ε 5.09, 3.59, 3.50, 3.10, 3.34). Anal Calcd for $C_{77}H_{83}N_5$. 3/2 CH_2Cl_2: C, 78.18.75; H, 7.19; N, 5.81. Found: C, 78.49; H, 7.54; N, 5.74.

5-(Phenyl-4-[(*Z*)-2-cyano-2-(4'-bromophenyl)ethenyl])-(10,15,20-tris(3,5-di-*tert*-butylphenyl)porphyrin 83

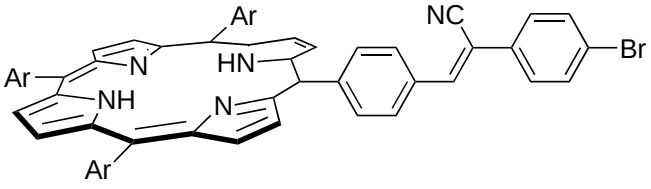

Using Method A and starting with **18** and 4'-bromophenylacetonitrile, **83** (44 mg, 50%) was obtained as a purple microcrystalline solid. m.p. > 300 °C. ^{1}H NMR (400 MHz, $CDCl_3$) δ -2.67 (br s, 2H, NH), 1.53 (s, 18H, CH_3), 1.54 (s, 36H, CH_3), 7.67 and 7.72 (ABq, 2H, J_{AB} = 8.7 Hz, ArH), 7.79-7.82 (m, 3H, ArH), 7.85 (s, 1H, CH), 8.08 (d, 2H, *J* = 1.8 Hz, ArH), 8.10 (d, 4H, *J* = 1.8 Hz, ArH), 8.29 (d, 2H, *J* = 8.2 Hz, ArH), 8.36 (d, 2H, *J* = 8.2 Hz, ArH), 8.85 and 8.92 (ABq,

4H, J_{AB} = 4.7 Hz, β-pyrrolic H), 8.91 (app. s, 4H, β-pyrrolic H) ppm. ^{13}C NMR (100 MHz, $CDCl_3$) δ 31.7, 35.0, 117.85, 117.87, 121.0, 121.6, 121.8, 127.6, 127.7, 129.7, 129.8, 132.4, 132.7, 133.8, 135.2, 141.20, 141.23, 142.4, 145.4, 148.74, 148.76 ppm. FTIR 707 (m), 734 (m), 797 (s), 879 (m), 913 (m), 1254 (m), 1362 (m), 1427 (m), 1474 (m), 1591 (m, C=C), 2229 (w, CN), 2960 (m), 3302 (br, NH) cm^{-1}. λ_{max} ($CHCl_3$) 423, 521 557, 594, 649 nm (log ε 4.94, 3.48, 3.40, 3.18, 3.38). Anal Calcd for $C_{77}H_{82}BrN_5$. 1 CH_2Cl_2: C, 75.41; H, 6.82; N, 5.64. Found: C, 75.21; H, 6.87; N, 5.68.

5-(Phenyl-4-[(*Z*)-2-cyano-2-(4'-nitrophenyl)ethenyl])-10,15,20-tris(3,5-di-*tert*-butylphenyl)porphyrin 84

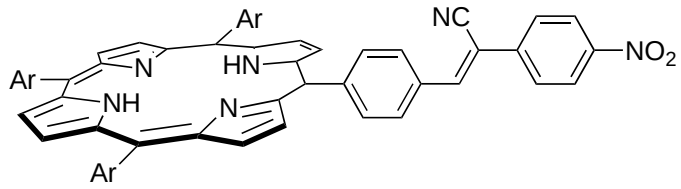

Using Method B and starting with **18** and 4'-nitrophenylacetonitrile, **84** (55 mg, 64%) was obtained as a purple microcrystalline solid. m.p. > 300 °C. ^{1}H NMR (400 MHz, $CDCl_3$) δ -2.67 (br s, 2H, NH), 1.52 (s, 18H, CH_3), 1.53 (s, 36H, CH_3), 7.80-7.82 (m, 3H, ArH), 7.79-8.02 (m, 3H, ArH), 8.01 (s, 1H, CH), 8.08 (d, 2H, *J* = 1.8 Hz, ArH), 8.10 (d, 4H, *J* = 1.8 Hz, ArH), 8.34 (d, 2H, *J* = 8.3 Hz, ArH), 8.38-8.42 (m, 4H, ArH), 8.84 and 8.93 (ABq, 4H, J_{AB} = 4.7 Hz, β-pyrrolic H), 8.91 (app. s, 4H, β-pyrrolic H) ppm. ^{13}C NMR (100 MHz, $CDCl_3$) δ 31.7, 35.0, 109.6, 117.5, 117.6, 121.1, 121.7, 122.0, 124.5, 126.9, 128.1, 129.7, 129.8, 132.1, 135.3, 140.7, 141.1, 141.2, 145.3, 146.3, 148.0, 148.7, 148.8 ppm. FTIR 709 (m), 799 (s), 855 (m), 913 (m), 1245 (m), 1341 (m), 1520 (m, NO_2), 1590 (m, C=C), 2227 (w, CN), 2958 (m), 3320 (br, NH) cm^{-1}. λ_{max} ($CHCl_3$) 423, 520, 556, 596, 648 nm (log ε 5.05, 3.58, 3.49, 3.23, 3.42). Anal Calcd for $C_{77}H_{82}N_6O_2$. 1/2 CH_2Cl_2: C, 79.83; H, 7.17; N, 7.21. Found: C, 80.12; H, 6.86; N, 7.16.

5-(Phenyl-3-[(*Z*)-2-cyano-2-phenylethenyl])-10,15,20-tris(3,5-di-*tert*-butylphenyl)porphyrin 85

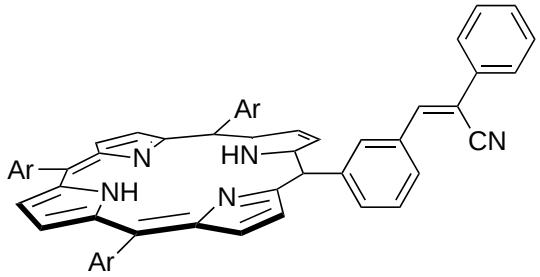

Using Method A and starting with **19** and benzyl cyanide, **85** (52 mg, 63%) was obtained as a purple microcrystalline solid. m.p. > 300 °C. ^{1}H NMR (400 MHz, $CDCl_3$) δ -2.69 (br s, 2H, NH), 1.53 (app. s, 54H, CH_3), 7.37-7.49 (m, 3H, ArH), 7.72-7.83 (m, 6H, ArH and CH), 7.85-7.92 (m, 1H, ArH), 8.06-8.14 (m, 6H, ArH), 8.30-8.35 (m, 1H, ArH), 8.51-8.57 (m, 2H, ArH), 8.84-8.96 (m, 8H, β-pyrrolic H) ppm. ^{13}C NMR (100 MHz, $CDCl_3$) δ 31.7, 35.0, 112.8, 118.0, 118.1, 121.0, 121.6, 121.8, 126.1, 127.3, 127.4, 129.1, 129.3, 129.7, 129.8, 132.3, 134.4, 135.8, 136.2, 141.15, 141.24, 142.3, 143.3, 148.67, 148.71 ppm. FTIR 695 (m), 725 (m), 754 (m), 800 (m), 880 (m), 914 (m), 1246 (m), 1362 (m), 1393 (m), 1425 (m), 1591 (m, C=C), 2958 (m), 2225 (w, CN), 3298 (br, NH) cm^{-1}. λ_{max} ($CHCl_3$) 422, 519, 555, 597, 647 nm (log ε 5.12, 3.65, 3.38, 3.16, 3.34). Anal Calcd for $C_{77}H_{83}N_5$. 2 CH_2Cl_2: C, 76.01; H, 7.02; N, 5.61. Found: C, 75.91; H, 6.94; N, 5.55.

5-(Phenyl-3-[(*Z*)-2-cyano-2-(4'-bromophenyl)ethenyl])-10,15,20-tris(3,5-di-*tert*-butylphenyl)porphyrin 86

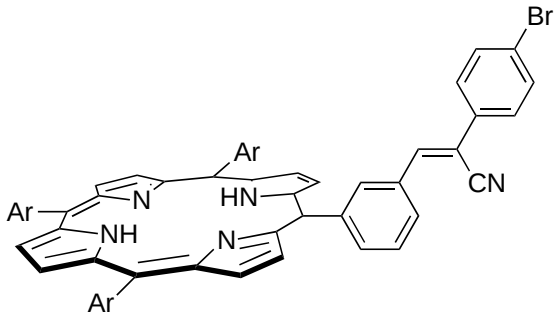

Using Method A and starting with **19** and 4'-bromophenylacetonitrile, **86** (78 mg, 88%) was obtained as a purple microcrystalline solid. m.p. > 300 °C. ^{1}H NMR (400 MHz, $CDCl_3$) δ -2.69 (br s, 2H, NH), 1.54 (app. s, 54H, CH_3), 7.57 and 7.61 (ABq, 4H, J_{AB} = 9.0 Hz, ArH), 7.77-7.82 (m, 4H, ArH and CH), 7.89 (app. t, 1H, *J* = 7.7 Hz, ArH), 8.09 (d, 2H, *J* = 1.7 Hz, ArH), 8.10 (d, 4H, *J* = 1.7 Hz, ArH), 8.32-8.36 (m, 1H, ArH), 8.50-8.55 (m, 2H, ArH), 8.85 (ABq, 2H, J_{AB} = 4.7 Hz, β-pyrrolic H), 8.91-8.94 (m, 6H, β-pyrrolic H) ppm. ^{13}C NMR (100 MHz, $CDCl_3$) δ 32.2, 35.5, 112.1, 118.1, 118.2, 121.4, 122.0, 122.3, 124.0, 127.8, 127.88, 127.93, 130.1, 130.3, 132.4, 132.7, 133.8, 136.3, 136.9, 141.55, 141.64, 143.0, 143.9, 149.10, 149.14 ppm. FTIR 637 (m), 671 (m), 711 (m), 726 (m), 799 (s), 914 (m), 979 (m), 1245 (m), 1361 (m), 1473 (m), 1591 (m, C=C), 960 (m), 2215 (w, CN), 3323 (br, NH) cm^{-1}. λ_{max} ($CHCl_3$) 423, 519, 556, 591, 648 nm (log ε 4.89, 3.35, 3.21, 3.09, 3.29). Anal Calcd for $C_{77}H_{82}BrN_5$: C, 79.90; H, 7.14; N, 6.05. Found: C, 79.48; H, 7.41; N, 6.38.

5-(Phenyl-3-[(*Z*)-2-cyano-2-(4'-nitrophenyl)ethenyl])-10,15,20-tris(3,5-di-*tert*-butylphenyl)porphyrin 87

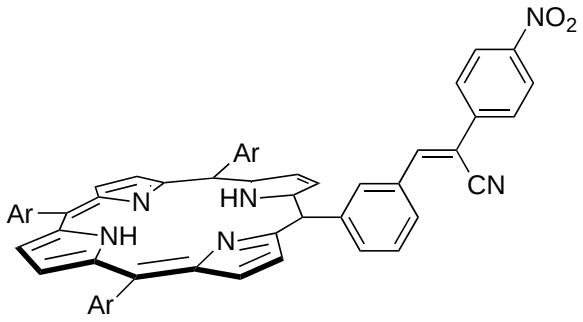

Using Method B and starting with **19** and 4'-nitrophenylacetonitrile, **87** (50 mg, 58%) was obtained as a purple microcrystalline solid. m.p. > 300 °C. ^{1}H NMR (400 MHz, $CDCl_3$) δ -2.70 (br s, 2H, NH), 1.54 (app. s, 54H, CH_3), 7.79-7.82 (m, 3H, ArH), 7.86 (d, 2H, *J* = 9.1 Hz, ArH), 7.90 (s, 1H, CH), 7.92 (app. t, 1H, *J* = 7.8 Hz, ArH), 8.07-8.11 (m, 6H, ArH), 8.27 (d, 2H, *J* = 9.1 Hz, ArH), 8.37-8.40 (m, 1H, ArH), 8.54-8.57 (m, 1H, ArH), 8.57-8.60 (m, 1H, ArH), 8.83 (ABq, 2H, J_{AB} = 4.8 Hz, β-pyrrolic H), 8.91-8.95 (m, 6H, β-pyrrolic H) ppm. ^{13}C NMR (100 MHz, $CDCl_3$) δ 32.1, 35.5, 117.6, 117.8, 121.5, 122.1, 122.4, 124.8, 127.2, 128.05, 128.10, 130.1, 130.2, 131.9, 136.6, 137.6, 140.9, 141.5, 141.6, 144.1, 146.0, 149.1, 149.2 ppm. FTIR 695 (m), 712 (m), 729 (m), 801 (s), 851 (m), 914 (m), 979 (m), 1245 (m), 1339 (m), 1362 (m), 1473 (m), 1520 (m, NO_2), 1591 (m, C=C), 2228 (w, CN), 2956 (m), 3326 (br, NH) cm^{-1}. λ_{max} ($CHCl_3$) 422, 520, 556, 592, 649 nm (log ε 5.03, 3.47, 3.29, 3.16, 3.32). Anal Calcd for $C_{77}H_{82}N_6O_2$: C, 82.32; H, 7.36; N, 7.48. Found: C, 81.96; H, 7.15; N, 7.25.

5-(Phenyl-2-[(*Z*)-2-cyano-2-phenylethenyl])-10,15,20-tris(3,5-di-*tert*-butylphenyl)porphyrin 88

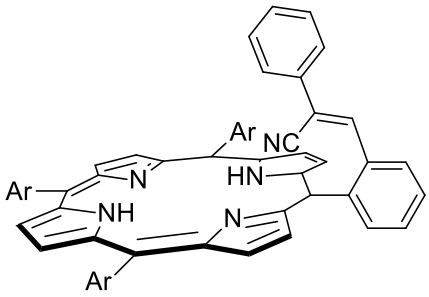

Using Method A and starting with **20** and benzyl cyanide, **88** (27 mg, 33%) was obtained as a purple microcrystalline solid. m.p. > 300 °C. ^{1}H NMR (400 MHz, $CDCl_3$) δ -2.62 (br s, 2H, NH), 1.50 (s, 18H, CH_3), 1.51-1.55 (m, 36H, CH_3), 6.57-6.62 (m, 2H, ArH), 6.67 (app. t, 2H, *J* = 7.4 Hz, ArH), 6.81 (app. t., 1H, *J* = 7.4 Hz, ArH), 7.12 (s, 1H, CH), 7.77-7.82 (m, 4H, ArH), 7.92-7.98 (m, 1H, ArH), 8.02-8.11 (m, 6H, ArH), 8.22-8.25 (m, 1H, ArH), 8.62-8.65 (m, 1H, ArH), 8.73 and 8.89 (ABq, 4H, J_{AB} = 4.6 Hz, β-pyrrolic H), 8.92 (app. s, 4H, β-pyrrolic H) ppm. ^{13}C NMR (100 MHz, $CDCl_3$) δ 31.61, 31.65, 31.8, 31.9, 109.1, 113.0, 120.5, 120.6, 121.2, 121.4, 121.8, 125.1, 126.3, 127.0, 127.4, 128.2, 128.5, 128.9, 129.17, 129.21, 129.3, 129.5, 129.7, 130.0, 131.1, 132.2, 134.6, 134.7, 136.2, 136.8, 140.4, 140.5, 140.7, 142.1, 143.9, 149.0, 149.12, 149.14, 150.9 ppm. FTIR 693 (m), 729 (s), 801 (s), 914 (m), 1246 (m), 1362 (m), 1591 (m, C=C), 2212 (w, CN), 2960 (m), 3321 (br, NH) cm^{-1}. λ_{max} ($CHCl_3$) 423, 522, 558, 595, 650 nm (log ε 4.88, 3.53, 3.25, 3.01, 3.07). Anal Calcd for $C_{77}H_{83}N_5$. 3/2 CH_2Cl_2: C, 78.18; H, 7.19; N, 5.81. Found: C, 78.23; H, 7.01; N, 6.10.

5-(Phenyl-2-[(*Z*)-2-cyano-2-(4'-bromophenyl)ethenyl])-10,15,20-tris(3,5-di-*tert*-butylphenyl)porphyrin 89

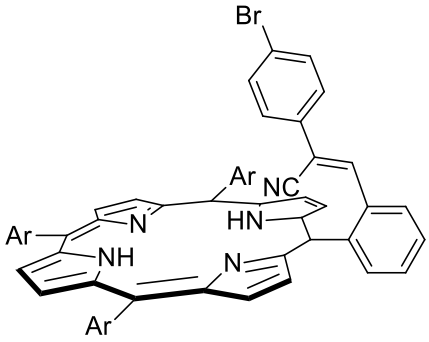

Using Method A and starting with **20** and 4'-bromophenylacetonitrile, **89** (66 mg, 75%) was obtained as a purple microcrystalline solid. m.p. > 300 °C. ^{1}H NMR (400 MHz, $CDCl_3$) δ -2.63 (br s, 2H, NH), 1.50 (s, 18H, CH_3), 1.51-1.55 (m, 36H, CH_3), 6.42 (d, 2H, *J* = 8.7 Hz, ArH), 6.78 (d, 2H, *J* = 8.7 Hz, ArH), 7.05 (s, 1H, CH), 7.77-7.86 (m, 4H, ArH), 7.92-7.98 (m, 1H, ArH), 8.01-8.03 (m, 2H, ArH), 8.03-8.05 (m, 1H, ArH), 8.07-8.11 (3H, m, ArH), 8.26-8.29 (m, 1H, ArH), 8.58-8.62 (m, 1H, ArH), 8.71 (d, 2H, *J* = 4.7 Hz, β-pyrrolic H), 8.88 (d, 2H, *J* = 4.7 Hz, β-pyrrolic H), 8.92 (app. s, 4H, β-pyrrolic H) ppm. ^{13}C NMR (100 MHz, $CDCl_3$) δ 31.68, 31.72, 34.99, 35.06, 111.9, 115.2, 117.9, 121.1, 121.8, 122.3, 122.8, 127.0, 127.1, 128.4, 128.8, 129.6, 129.7, 129.8, 129.9, 131.4, 132.8, 140.9, 141.1, 142.5, 143.1, 148.7, 148.8 ppm. FTIR 712 (m), 800 (s), 914 (m), 1246 (m), 1360 (m), 1590 (m, C=C), 2958 (m), 2219 (w, CN), 3313 (br, NH) cm^{-1}. λ_{max} ($CHCl_3$) 425, 521, 556, 595, 650 nm (log ε 4.81, 3.26, 3.04, 2.88, 3.09). Anal Calcd for $C_{77}H_{82}BrN_5$. 3/2 CH_2Cl_2: C, 73.38; H, 6.67; Br, 6.22; N, 5.45. Found: C, 73.12; H, 6.44; N, 5.05.

5-(Phenyl-2-[(*Z*)-2-cyano-2-(4'-nitrophenyl)ethenyl])-10,15,20-tris(3,5-di-*tert*-butylphenyl)porphyrin 90

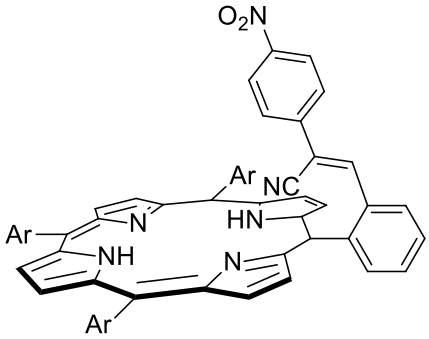

Using Method B and starting with **20** and 4'-nitrophenylacetonitrile, **90** (68 mg, 80%) was obtained as a purple microcrystalline solid. m.p. > 300 °C. ^{1}H NMR (400 MHz, $CDCl_3$) δ -2.61 (br s, 2H, NH), 1.49 (s, 18H, CH_3), 1.52-1.56 (m, 36H, CH_3), 6.71 (d, 2H, *J* = 8.9 Hz, ArH), 7.21 (s, 1H, CH), 7.50 (d, 2H, *J* = 8.9 Hz, ArH), 7.79-7.83 (m, 3H, ArH), 7.88 (app. t, 1H, *J* = 7.5 Hz, ArH), 7.97-8.02 (m, 3H, ArH), 8.03-8.05 (m, 1H, ArH), 8.07-8.12 (m, 3H, ArH), 8.32-8.36 (m, 1H, ArH), 8.64-8.68 (m, 1H, ArH), 8.71 and 8.90 (ABq, 2H, J_{AB} = 4.7 Hz, β-pyrrolic H), 8.93 (app. s, 4H, β-pyrrolic H) ppm. ^{13}C NMR (100 MHz, $CDCl_3$) δ 31.68, 31.73, 35.01, 35.04, 35.05, 110.8, 114.7, 117.4, 121.2, 121.9, 122.5, 123.6, 126.4, 127.1, 129.0, 129.1, 129.6, 129.7, 129.8, 135.5, 136.2, 140.0, 140.9, 141.1, 143.7, 145.2, 147.3, 148.79, 148.82, 148.87, 148.91 ppm. FTIR 686 (m), 722 (s), 799 (s), 852 (m), 915 (m), 975 (m), 1247 (m), 1340 (s), 1362 (m), 1467 (m), 1522 (m, NO_2), 1591 (m, C=C), 2219 (w, CN), 2955 (m), 3331 (br, NH) cm^{-1}. λ_{max} ($CHCl_3$) 425, 522, 557, 593, 649 nm (log ε 4.91, 3.38, 3.21, 3.07, 3.32). Anal Calcd for $C_{77}H_{82}N_6O_2$. 1 CH_2Cl_2: C, 77.52; H, 7.01; N, 6.95. Found: C, 77.46; H, 6.78; N, 6.97.

4.5.3 Preparation of Zinc(II) Complexes of *meso*-Phenyl Porphyrin-α-Cyanostilbenes

General Procedure: In a mixture of free-base α-cyanostilbene porphyrin (25 mg) in dichloromethane (10 mL) was added zinc(II) acetate (2.5 eq.). The reaction mixture was heated to reflux for 1 h. On cooling, the reaction mixture was washed with water (2 x 20 mL), brine

(20 mL), dried over anhydrous sodium sulfate, filtered and evaporated to dryness under vacuum. The crude product was obtained was chromatographed (silica gel, dichloromethane/hexane 1:1) to afford the pure zinc(II) complex.

{5-(Phenyl-4-[(*Z*)-2-cyano-2-phenylethenyl])-10,15,20-tris(3,5-di-*tert*-butylphenyl)porphyrinato} zinc(II) 91

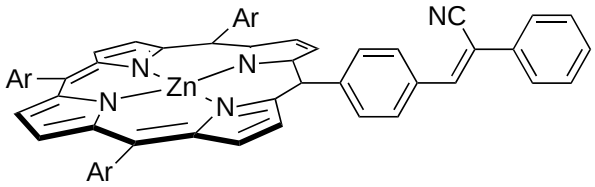

Starting with **82**, **91** (18 mg, 68%) was obtained as a purple microcrystalline solid. m.p. > 300 °C. ^{1}H NMR (400 MHz, $CDCl_3$) δ 1.54 (app. s, 54H, CH_3), 7.44-7.48 (m, 1H, ArH), 7.50-7.55 (m, 2H, ArH), 7.73-7.76 (m, 2H, ArH), 7.80-7.82 (m, 3H, ArH), 7.84 (s, 1H, CH), 8.10-8.13 (m, 6H, ArH), 8.20 (d, 2H, *J* = 8.1 Hz, ArH), 8.35 (d, 2H, *J* = 8.1 Hz, ArH), 8.97 (ABq, 2H, J_{AB} = 4.7 Hz, β-pyrrolic H), 9.02-9.05 (m, 6H, β-pyrrolic H) ppm. ^{13}C NMR (100 MHz, $CDCl_3$) δ 31.8, 35.1, 111.7, 118.1, 119.2, 120.8, 122.6, 122.9, 126.1, 127.5, 129.2, 129.3, 129.6, 129.8, 131.4, 132.2, 132.3, 132.6, 132.8, 134.6, 135.0, 141.78, 141.82, 142.2, 145.7, 148.5, 148.6, 149.6, 150.4, 150.4, 150.6 ppm. FTIR 692 (m), 713 (s), 758 (m), 794 (s), 821 (m), 879 (m), 899 (m), 931 (m), 999 (s), 1203 (m), 1220 (m), 1247 (m), 1361 (m), 1475 (m), 1591 (m, C=C), 2218 (w, CN) 2956 (m) cm^{-1}. λ_{max} ($CHCl_3$) 427, 556, 598 nm (log ε 5.04, 3.68, 3.31). Anal Calcd for $C_{77}H_{81}N_5Zn$. 1/2 CH_2Cl_2: C, 78.59; H, 6.98; N, 5.91. Found: 78.12; H, 6.61; N, 5.64.

{5-(Phenyl-4-[(*Z*)-2-cyano-2-(4'-bromophenyl)ethenyl])-10,15,20-tris(3,5-di-*tert*-butylphenyl)porphyrinato} zinc(II) 92

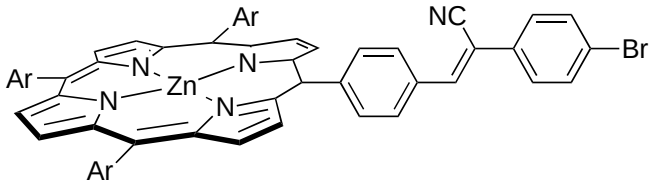

Starting with **83**, **92** (19 mg, 72%) was obtained as a purple microcrystalline solid. m.p. > 300 °C. ^{1}H NMR (400 MHz, $CDCl_3$) δ 1.53 (app. s, 54H, CH_3), 7.60-7.67 (ABq, 4H, J_{AB} = 8.3 Hz, ArH), 7.79-7.81 (m, 3H, ArH), 7.82 (s, 1H, CH), 8.08-8.12 (m, 6H, ArH), 8.19 (d, 2H, *J* = 8.0 Hz, ArH), 8.34 (d, 2H, *J* = 8.0 Hz, ArH), 8.95 (ABq, 2H, J_{AB} = 4.6 Hz, β-pyrrolic H), 9.01-9.04 (m, 6H, β-pyrrolic H) ppm. ^{13}C NMR (100 MHz, $CDCl_3$) δ 31.8, 35.0, 110.6, 117.8, 119.1, 120.8, 122.7, 122.9, 123.5, 127.5, 127.6, 129.6, 129.7, 131.3, 132.3, 132.4, 132.5, 132.6, 133.6, 135.0, 141.8, 142.5, 146.0, 148.6, 149.6, 150.4, 150.5, 150.6 ppm. FTIR 715 (s), 795 (s), 822 (m), 879 (m), 998 (m), 1203 (m), 1247 (m), 1361 (m), 1590 (m, C=C), 2218 (w, CN), 2903 (w), 2957 (m) cm^{-1}. λ_{max} ($CHCl_3$) 427, 557, 599 nm (log ε 4.93, 3.45, 2.97). Anal Calcd for $C_{77}H_{80}BrN_5Zn$. 1/2 CH_2Cl_2: C, 73.69; H, 6.46; N, 5.54. Found: 73.21; H, 6.21; N, 5.28.

{5-(Phenyl-4-[(*Z*)-2-cyano-2-(4'-nitrophenyl)ethenyl])-10,15,20-tris(3,5-di-*tert*-butylphenyl)porphyrinato} zinc(II) 93

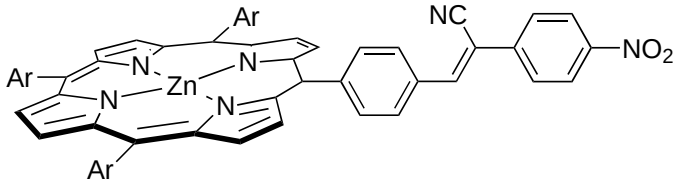

Starting with **84**, **93** (23 mg, 87%) was obtained as a purple amorphous powder. m.p. > 300 °C. ^{1}H NMR (400 MHz, $CDCl_3$) δ 1.52-1.54 (m, 54H, CH_3), 7.79-7.81 (m, 3H, ArH), 7.97 (d, 2H, *J* = 8.8 Hz, ArH), 8.00 (s, 1H, CH), 8.08-8.10 (m, 6H, ArH), 8.31 (d, 1H, *J* = 8.2 Hz, ArH), 8.38-8.42 (m, 4H, ArH), 8.93 (ABq, 2H, J_{AB} = 4.7 Hz, β-pyrrolic H), 9.00-9.04 (m, 6H, β-pyrrolic H) ppm. ^{13}C NMR (100 MHz, $CDCl_3$) δ 31.8, 35.1, 120.8, 122.7, 124.5, 126.9, 128.0, 129.6, 129.7,

131.1, 131.9, 132.3, 132.4, 132.6, 135.2, 141.7, 145.4, 147.1, 148.6, 149.4, 150.4, 150.5, 150.6 ppm. FTIR 716 (m), 750 (m), 796 (s), 822 (m), 854 (m), 999 (m), 1204 (m), 1248 (m), 1341 (s), 1521 (m, NO_2), 1589 (m, C=C), 2217 (w, CN), 2959 (m) cm^{-1}. λ_{max} ($CHCl_3$) 426, 557, 599 nm (log ε 4.98, 3.48, 3.08). Anal Calcd for $C_{77}H_{80}N_6O_2Zn$. 1 CH_2Cl_2: C, 73.66; H, 6.50; N, 6.61. Found: C, 73.84; H, 6.21; N, 6.28.

{5-(Phenyl-3-[(*Z*)-2-cyano-2-phenylethenyl])-10,15,20-tris(3,5-di-*tert*-butylphenyl)porphyrinato} zinc(II) 94

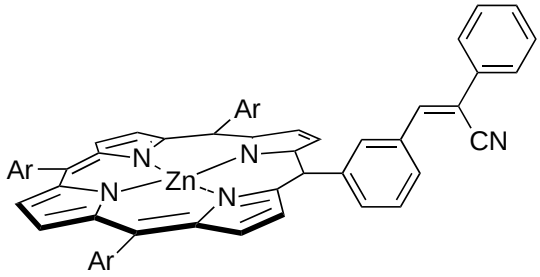

Starting with **85**, **94** (20 mg, 76%) was obtained as a purple microcrystalline solid. m.p.> 300 °C. ^{1}H NMR (400 MHz, $CDCl_3$) δ 1.55 (app. s, 54H, CH_3), 7.36-7.47 (m, 3H, ArH), 7.70-7.74 (m, 2H, ArH), 7.80-7.84 (m, 4H, ArH and CH), 7.86-7.92 (m, 1H, ArH), 8.11-8.15 (m, 6H, ArH), 8.32-8.36 (m, 1H, ArH), 8.47-8.51 (m, 1H, ArH), 8.57-8.59 (m, 1H, ArH), 8.98 (ABq, 2H, J_{AB} = 4.6 Hz, β-pyrrolic H), 9.03-9.07 (m, 6H, β-pyrrolic H) ppm. ^{13}C NMR (100 MHz, $CDCl_3$) δ 31.8, 35.0, 112.6, 118.0, 119.1, 120.8, 122.6, 122.8, 126.0, 127.3, 129.1, 129.2, 129.6, 129.7, 131.4, 132.1, 132.2, 132.3, 132.6, 134.5, 135.6, 136.1, 141.7, 141.8, 142.4, 143.9, 148.5, 148.6, 149.8, 150.4, 150.5, 150.6 ppm. FTIR 696 (m), 716 (s), 757 (s), 796 (s), 823 (m), 881 (m), 900 (m), 930 (m), 1001 (m), 1206 (m), 1247 (m), 1361 (m), 1591 (m, C=C), 2238 (w, CN), 2957 (m) cm^{-1}. λ_{max} ($CHCl_3$) 427, 555, 598 nm (log ε 5.00, 3.43, 2.64). Anal Calcd for $C_{77}H_{81}N_5Zn$. 1/4 CH_2Cl_2: C, 79.77; H, 7.06; Cl, 1.52; N, 6.02. Found: 79.34; H, 7.35; N, 5.85.

{5-(Phenyl-3-[(*Z*)-2-cyano-2-(4'-bromophenyl)ethenyl])-10,15,20-tris(3,5-di-*tert*-butylphenyl)porphyrinato} zinc(II) 95

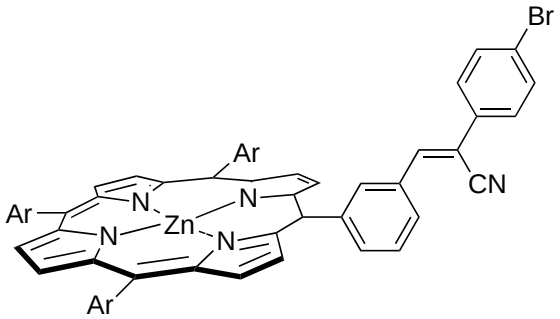

Starting with **86**, **95** (21 mg, 80%) was obtained as a purple microcrystalline solid. m.p. > 300 °C. ^{1}H NMR (400 MHz, $CDCl_3$) δ 1.53 (app. s, 54H, CH_3), 7.56 and -7.60 (ABq, 4H, J_{AB} = 9 Hz, ArH), 7.78 (s, 1H, CH), 7.79-7.81 (m, 3H, ArH), 7.88 (app. t, 1H, J = 7.8 Hz, ArH), 8.07-8.12 (m, 6H, ArH), 8.31-8.36 (m, 1H, ArH), 8.47-8.51 (m, 1H, ArH), 8.55-8.57 (m, 1H, ArH), 8.94 (ABq, 2H, J_{AB} = 4.7 Hz, β-pyrrolic H), 8.99-9.04 (m, 6H, β-pyrrolic H) ppm. ^{13}C NMR (100 MHz, $CDCl_3$) δ 32.2, 35.4, 111.9, 118.1, 119.3, 121.2, 123.0, 123.3, 123.9, 127.7, 127.9, 130.0, 130.1, 131.0, 131.5, 131.7, 132.3, 132.7, 132.8, 133.0, 133.9, 136.1, 136.7, 142.1, 143.1, 144.4, 149.0, 150.2, 150.9, 151.0 ppm. FTIR 714 (s), 764 (m), 795 (s), 822 (m), 881 (m), 899 (m), 930 (m), 1001 (m), 1072 (m), 1218 (m), 1246 (m), 1361 (m), 1475 (m), 1590 (m, C=C), 2213 (w, CN), 2958 (m) cm^{-1}. λ_{max} ($CHCl_3$) 427, 556, 598 nm (log ε 5.04, 3.61, 3.09). Anal Calcd for $C_{77}H_{80}BrN_5Zn$. 3/2 CH_2Cl_2: C, 69.93; H, 6.21; N, 5.19. Found: C, 69.65; H, 5.92; N, 4.98.

{5-(Phenyl-3-[(*Z*)-2-cyano-2-(4'-nitrophenyl)ethenyl])-10,15,20-tris(3,5-di-*tert*-butylphenyl)porphyrinato} zinc(II) 96

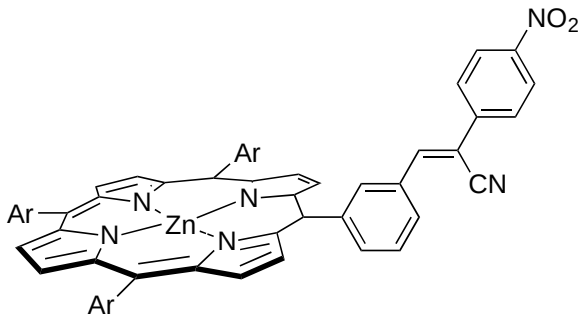

Starting with **87**, **96** (22 mg, 83%) was obtained as a purple microcrystalline solid. m.p. > 300 °C. ^{1}H NMR (400 MHz, $CDCl_3$) δ 1.53-1.55 (m, 54H, CH_3), 7.77 (d, 2H, *J* = 9.0 Hz, ArH), 7.79-7.82 (m, 3H, ArH), 7.83 (s, 1H, CH), 7.91 (app. t, 1H, *J* = 7.8 Hz, ArH), 8.08-8.13 (m, 6H, ArH), 8.22 (d, 2H, *J* = 9.0 Hz, ArH), 8.38-8.41 (m, 1H, ArH), 8.48-8.52 (m, 1H, ArH), 8.60-8.63 (m, 1H, ArH), 8.93 (ABq, 2H, J_{AB} = 4.7 Hz, β-pyrrolic H), 9.02-9.05 (m, 6H, β-pyrrolic H) ppm. ^{13}C NMR (100 MHz, $CDCl_3$) δ 31.9, 35.2, 110.8, 117.8, 119.1, 121.5, 123.3, 123.6, 125.0, 127.3, 128.2, 128.4, 130.3, 130.4, 131.9, 132.0, 133.0, 133.2, 133.4, 136.7, 137.8, 141.2, 142.5, 145.0, 146.4, 148.6, 149.4, 150.5, 151.25, 151.32, 151.4 ppm. FTIR 695 (m), 715 (s), 797 (s), 823 (m), 851 (m), 930 (m), 1003 (m), 1068 (m), 1338 (s), 1362 (m), 1521 (m, NO_2), 1591 (m, C=C), 2216 (w, CN), 2955 (m) cm^{-1}. λ_{max} ($CHCl_3$) 426, 555, 599 nm (log ε 4.76, 3.33, 3.04). Anal Calcd for $C_{77}H_{80}N_6O_2Zn$. 1 CH_2Cl_2: C, 73.66; H, 6.50; N, 6.61. Found: C, 73.61; H, 6.29; N, 6.22.

{5-(Phenyl-2-[(*Z*)-2-cyano-2-phenylethenyl])-10,15,20-tris(3,5-di-*tert*-butylphenyl)porphyrinato} zinc(II) 97

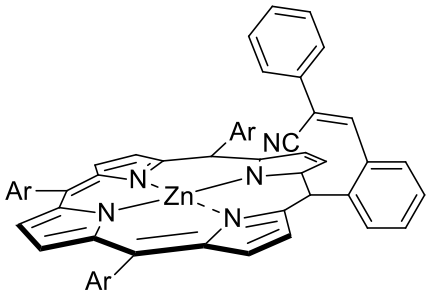

Starting with **88**, **97** (15 mg, 57%) was obtained as a purple microcrystalline solid. m.p. > 300 °C. ^{1}H NMR (400 MHz, $CDCl_3$) δ 1.49-1.56 (m, 54H, CH_3), 6.47-6.53 (m, 2H, ArH), 6.60-6.66 (m, 2H, ArH), 6.74-6.80 (m, 1H, ArH), 7.07 (s, 1H, CH), 7.76-7.83 (m, 4H, ArH), 7.91-7.96 (m, 1H, ArH), 8.03-8.13 (m, 6H, ArH), 8.23-8.28 (m, 1H, ArH), 8.57-8.62 (m, 1H, ArH), 8.82 (ABq, 2H, J_{AB} = 4.6 Hz, β-pyrrolic H), 8.97-9.05 (m, 6H, β-pyrrolic H) ppm. ^{13}C NMR (100 MHz, $CDCl_3$) δ 31.7, 35.0, 112.6, 116.6, 118.2, 120.9, 122.8, 123.1, 125.5, 126.9, 128.1, 128.2, 128.4, 128.6, 129.5, 129.7, 131.3, 132.3, 132.4, 133.0, 134.0, 135.1, 136.6, 141.5, 141.7, 142.1, 143.7, 141.5, 141.7, 142.1, 143.7, 148.5, 148.6, 150.0, 150.4, 150.7 ppm. FTIR 691 (m), 717 (s), 756 (s), 797 (s), 824 (m), 881 (m), 900 (m), 930 (m), 1000 (m), 1247 (m), 1362 (m), 1591 (m, C=C), 2214 (w, CN), 2959 (m) cm^{-1}. λ_{max} ($CHCl_3$) 429, 559, 600 nm (log ε 4.82, 3.29, 2.46). Anal Calcd for $C_{77}H_{81}N_5Zn$. 1/3 CH_2Cl_2: C, 79.37; H, 7.03; N, 5.98. Found: C, 79.61; H, 7.16; N 6.29.

{5-(Phenyl-2-[(*Z*)-2-cyano-2-(4'-bromophenyl)ethenyl])-10,15,20-tris(3,5-di-*tert*-butylphenyl)porphyrinato} zinc(II) 98

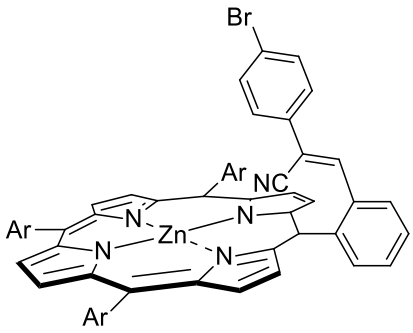

Starting with **89**, **98** (19 mg, 72%) was obtained as a purple microcrystalline solid. m.p. > 300 °C. ^{1}H NMR (400 MHz, $CDCl_3$) δ 1.52 (s, 18H, CH_3), 1.53-1.55 (m, 36H, CH_3), 6.30 (d, 2H, *J* = 8.6 Hz, ArH), 6.73 (d, 2H, *J* = 8.6 Hz, ArH), 7.00 (s, 1H, CH), 7.79-7.85 (m, 4H, ArH), 7.91-7.97 (m, 1H, ArH), 8.04-8.13 (m, 6H, ArH), 8.27-8.31 (m, 1H, ArH), 8.50-8.54 (m, 1H, ArH), 8.80 and 8.89 (ABq, 4H, J_{AB} = 4.8 Hz, β-pyrrolic H), 9.04 (app. s, 4H, β-pyrrolic H) ppm. ^{13}C NMR (100 MHz, $CDCl_3$) δ 31.7, 35.0, 111.4, 116.3, 117.8, 120.9, 122.7, 122.8, 123.3, 126.8, 127.0, 128.3, 128.7, 129.5, 129.6, 129.7, 130.5, 130.9, 131.2, 131.4, 132.3, 132.5, 133.0, 135.2, 136.5, 141.5, 141.7, 142.6, 143.7, 148.5, 148.6, 148.7, 149.9, 150.4, 150.5, 150.7 ppm. FTIR 716 (s), 764 (s), 797 (s), 823 (s), 880 (m), 900 (m), 1000 (s), 1072 (m), 1204 (m), 1248 (m), 1361 (m), 1474 (m), 1590 (m, C=C), 2219 (w, CN), 2867 (m), 2958 (m) cm^{-1}. λ_{max} ($CHCl_3$) 429, 557, 599 nm (log ε 4.88, 3.63, 3.18). Anal Calcd for $C_{77}H_{80}BrN_5Zn$. 1/4 CH_2Cl_2: C, 74.70; H, 6.53; N, 5.64. Found: C, 74.76; H, 6.75; N, 5.30.

{5-(Phenyl-2-[(*Z*)-2-cyano-2-(4'-nitrophenyl)ethenyl])-10,15,20-tris(3,5-di-*tert*-butylphenyl)porphyrinato} zinc(II) 99

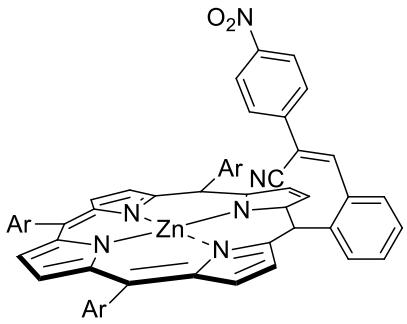

Starting with **90**, **99** (16 mg, 61%) was obtained as a purple microcrystalline solid. m.p. > 300 °C. ^{1}H NMR (400 MHz, $CDCl_3$) δ 1.50 (s, 18H, CH_3), 1.52-1.55 (m, 36H, CH_3), 6.61 (d, 2H, *J* = 8.9 Hz, ArH), 7.17 (s, 1H, CH), 7.46 (d, 2H, *J* = 8.9 Hz, ArH), 7.79-7.82 (m, 3H, ArH), 7.85-7.91 (m, 1H, ArH), 7.94-8.01 (m, 1H, ArH), 8.02-8.12 (m, 6H, ArH), 8.32-8.36 (m, 1H, ArH), 8.59-8.63 (m, 1H, ArH), 8.80 and 9.01 (ABq, 4H, J_{AB} = 4.7 Hz, β-pyrrolic H), 9.04 (app. s, 4H, β-pyrrolic H) ppm. ^{13}C NMR (100 MHz, $CDCl_3$) δ 31.69, 31.74, 35.00, 35.04, 110.3, 115.8, 117.3, 121.0, 122.9, 123.46, 123.51, 126.3, 126.9, 128.8, 129.0, 129.5, 129.6, 129.7, 129.8, 131.1, 132.4, 132.7, 133.0, 135.4, 136.0, 140.2, 141.5, 141.6, 144.4, 145.4, 147.1, 148.62, 148.65, 148.67, 148.71, 149.8, 150.4, 150.6, 150.8 ppm. FTIR 716 (s), 752 (s), 797 (s), 823 (m), 852 (m), 880 (m), 930 (m), 1000 (s), 1218 (m), 1247 (m), 1288 (m), 1340 (s), 1361 (m), 1474 (m), 1523 (m, NO_2), 1591 (m, C=C), 2216 (w, CN), 2957 (m) cm^{-1}. λ_{max} ($CHCl_3$) 426, 558, 602 nm (log ε 4.95, 3.69, 3.29). Anal Calcd for $C_{77}H_{80}N_6O_2Zn$. 1/3 CH_2Cl_2: C, 76.43; H, 6.69; N, 6.92. Found: 76.66; H, 6.98; N 6.72.

4.5.4 Preparation of Imidazoloporphyrin-α-Cyanostilbenes

General Procedure Method A: In a mixture of formyl porphyrin (75 mg, 0.062 mmol) and substituted acetonitrile (0.062 mmol; benzyl cyanide 7.2 mg or 4'-bromophenylacetonitrile 12.1 mg) in a dichloromethane / ethanol mixture (1:9; 20 mL) was added sodium methoxide (16. 7 mg, 0.31 mmol). The reaction mixture was heated at reflux overnight under an argon

atmosphere. The reaction mixture was allowed to cool to room temperature and filtered. The residue obtained was washed with ethanol (10 mL), followed by column chromatography (silica gel, dichloromethane/hexane 3:1) to afford pure products.

General Procedure Method B: In a mixture of formyl porphyrin (75 mg, 0.062 mmol) and 4'-nitrophenylacetonitrile (10.1 mg, 0.077 mmol) in dichloromethane / ethanol (1:9; 20 mL) was added piperidine (10.5 mg, 0.124 mmol). The reaction mixture was heated at reflux overnight under an argon atmosphere. The reaction mixture was allowed to cool to room temperature and filtered. The residue obtained was washed with ethanol (10 mL) followed by column chromatography (silica gel, dichloromethane/hexane 3:1) to afford pure products.

5,10,15,20-Tetrakis(3,5-di-*tert*-butylphenyl)porphyrin[2,3-*b*]imidazole-2'-phenyl-4"-[(*Z*)-2"'-cyano-2"'-phenyl)ethenyl] 100

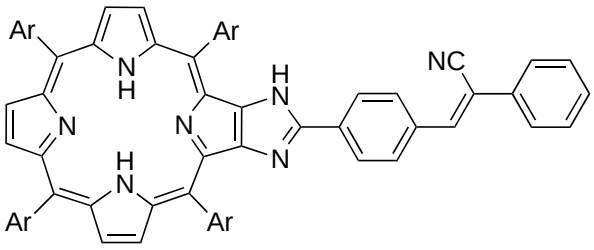

Using Method A and starting with **38** and benzyl cyanide, **100** (70 mg, 86%) was obtained as a purple microcrystalline solid. m.p. > 300 °C. ^{1}H NMR (400 MHz, $CDCl_3$) δ -2.79 (br s, 2H, NH), 1.51-1.58 (m, 72H, CH_3), 7.42-7.53 (m, 5H, ArH), 7.55-7.59 (m, 1H, ArH), 7.70-7.96 (m, 7H, ArH and CH), 7.98-8.05 (m, 2H, ArH), 8.08-8.19 (m, 7H, ArH), 8.46 (br s, 1H, NH), 8.80-8.89 (m, 2H, β-pyrrolic H), 8.98-9.07 (m, 4H, β-pyrrolic H) ppm. ^{13}C NMR (100 MHz, $CDCl_3$) δ 31.7, 31.8, 35.0, 35.1, 115.5, 118.1, 119.2, 120.1, 121.0, 121.2, 122.06, 122.08, 122.5, 123.0, 125.3, 126.0, 127.3, 128.7, 128.9, 129.2, 129.6, 129.7, 129.9, 131.1, 139.7, 141.1, 141.2, 141.4, 141.6, 142.2, 148.6, 148.7, 148.8, 149.8, 149.9, 151.1 ppm. FTIR 689 (m), 713 (m), 755 (m), 799 (s), 880 (m), 1161 (m), 1245 (s), 1361 (s), 1392 (m), 1424 (m), 1473 (m), 1591 (m, C=C), 2229 (w, CN), 2903 (m), 2957 (s), 3325 (br, NH), 3441 (br, NH) cm^{-1}. λ_{max} ($CHCl_3$) 426, 523,

557, 592, 651 nm (log ε 5.41, 4.26, 3.86, 3.82, 3.49). Anal Calcd for $C_{92}H_{103}N_7$. 1 CH_2Cl_2: C, 80.26; H, 7.60; N, 7.04. Found: C, 80.12; H, 7.21; N, 7.23.

5,10,15,20-Tetrakis(3,5-di-*tert*-butylphenyl)porphyrin[2,3-*b*]imidazole-2'-phenyl-4"-[(*Z*)-2"'-cyano-2"'-(4""-bromophenyl)ethenyl] 101

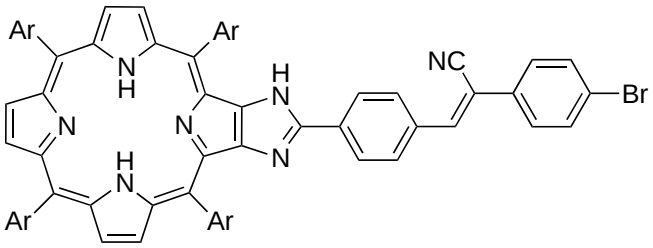

Using Method A and starting with **38** and 4'-bromophenylacetonitrile, **101** (66 mg, 85%) was obtained as a purple microcrystalline solid. m.p. > 300 °C. ^{1}H NMR (400 MHz, $CDCl_3$) δ -2.79 (br s, 2H, NH), 1.52-1.57 (s, 72H, CH_3), 7.58 and 7.62 (ABq, J_{AB} = 7.5 Hz, ArH), 7.78-7.84 (m, 4H, ArH), 7.90 (s, 1H, CH), 7.99 (d, 2H, J = 8.3 Hz, ArH), 8.08-8.19 (m, 10H, ArH), 8.46 (s, 1H, NH), 8.83-8.88 (m, 2H, β-pyrrolic H), 8.98-9.07 (m, 4H, β-pyrrolic H) ppm. ^{13}C NMR (100 MHz, $CDCl_3$) δ 31.7, 31.8, 31.9, 35.0, 35.1, 35.4, 110.1, 115.5, 117.8, 119.2, 121.0, 121.2, 122.0, 122.1, 122.4, 123.5, 125.1, 125.3, 127.2, 127.3, 127.5, 129.40, 129.43, 129.5, 129.6, 129.7, 130.0, 132.3, 133.3, 133.6, 139.7, 141.1, 141.6, 141.7, 142.1, 148.6, 148.7, 148.8, 149.7, 151.1 ppm. FTIR 712 (m), 727 (m), 754 (m), 799 (s), 819 (m), 880 (m), 921 (m), 1245 (m), 1361 (m), 1424 (m), 1461 (m), 1591 (m, C=C), 2219 (w, CN), 2959 (m), 3330 (br, NH), 3460 (br, NH) cm^{-1}. λ_{max} ($CHCl_3$) 426, 520, 556, 589, 648 nm (log ε 5.50, 4.34, 3.95, 3.92, 3.62). Anal Calcd for $C_{92}H_{102}BrN_7$. 2 CH_2Cl_2: C, 72.58; H, 6.87; N, 6.30. Found: C, 72.63; H, 7.25; N, 6.87.

5,10,15,20-Tetrakis(3,5-di-*tert*-butylphenyl)porphyrin[2,3-*b*]imidazole-2'-phenyl-4"-[(*Z*)-2"'-cyano-2"'-(4""-nitrophenyl)ethenyl] 102

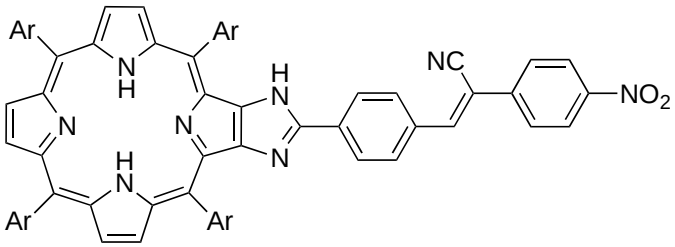

Using Method B and starting with **38** and 4'-nitrophenylacetonitrile, **102** (30 mg, 38%) was obtained as purple microcrystalline solid. m.p. > 300 °C. ^{1}H NMR (400 MHz, $CDCl_3$) δ -2.80 (br s, 2H, NH), 1.51-1.58 (s, 72H, CH_3), 7.80-7.85 (m, 6H, ArH), 7.89 (s, 1H, CH), 8.01-8.06 (m, 2H, ArH), 8.10-8.10 (m, 8H, ArH), 8.28 (d, 2H, *J* = 8.5 Hz, ArH), 8.44-8.56 (m, 3H, ArH and NH), 8.83-8.87 (m, 2H, β-pyrrolic H), 8.98-9.06 (m, 4H, β-pyrrolic H) ppm. ^{13}C NMR (100 MHz, $CDCl_3$) δ 31.7, 31.8, 35.0, 35.1, 35.4, 121.0, 121.2, 122.0, 122.5, 124.4, 125.3, 126.6, 127.3, 129.5, 129.6, 129.7, 130.5, 139.7, 140.6, 141.1, 141.5, 142.1, 144.5, 147.8, 148.6, 148.76, 148.78, 149.4, 151.1 ppm. FTIR 711 (m), 728 (m), 754 (m), 798 (s), 819 (m), 882 (m), 921 (m), 1247 (m), 1362 (m), 1427 (m), 1460 (m), 1520 (m, NO_2), 1590 (m, C=C), 2219 (w, CN), 2959 (m), 3335 (br, NH), 3462 (br, NH) cm^{-1}. λ_{max} ($CHCl_3$) 424, 521, 557, 588, 648 nm (log ε 5.33, 4.40, 3.91, 3.86, 3.47). Anal Calcd for $C_{92}H_{102}N_8O_2$. 3/2 CH_2Cl_2: C, 75.92; H, 7.15; N, 7.58. Found: C, 75.81; H, 6.80; N, 7.78.

5,10,15,20-Tetrakis(3,5-di-*tert*-butylphenyl)porphyrin[2,3-*b*]imidazole-2'-phenyl-3"-[(*Z*)-2"'-cyano-2"'-phenyl)ethenyl] 103

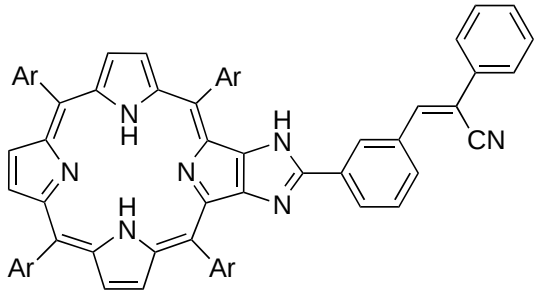

Using Method A and starting with **39** and benzyl cyanide, **103** (60 mg, 74%) was obtained as a purple microcrystalline solid. ^{1}H NMR (400 MHz, $CDCl_3$) δ -2.78 (br s, 2H, NH), 1.54-1.59 (m, 72H, ArH), 7.49-7.64 (m, 5H, ArH), 7.67-7.71 (m, 1H, ArH), 7.77-7.84 (m, 4H, ArH), 7.90 (s, 1H, CH), 8.07-8.21 (m, 10H, ArH), 8.27-8.31 (m, 1H, ArH), 8.47 (br s, 1H, NH), 8.85-8.89 (m, 2H, β-pyrrolic H), 8.99-9.06 (m, 4H, β-pyrrolic H) ppm. ^{13}C NMR (100 MHz, $CDCl_3$) δ 31.77, 31.84, 31.9, 35.06, 35.07, 35.16, 35.4, 112.6, 115.5, 117.8, 119.2, 121.0, 121.3, 122.1, 122.5, 126.0, 126.1, 127.4, 128.5, 129.3, 129.5, 129.57, 129.6, 129.7, 132.1, 134.38, 134.44, 139.8, 141.2, 141.6, 142.2, 148.6, 148.7, 148.8, 149.9, 150.9 ppm. FTIR 689 (m), 713 (m), 727 (m), 756 (s), 799 (s), 881 (m), 922 (m), 1247 (m), 1362 (m), 1591 (m, C=C), 2958 (m), 3330 (br, NH), 3440 (br, NH) cm^{-1}. λ_{max} ($CHCl_3$) 423, 519, 555, 587, 648 nm (log ε 5.45, 4.14, 3.92, 3.87, 3.80). Anal Calcd for $C_{92}H_{103}N_7$. 1/2 CH_2Cl_2: C, 82.34; H, 7.77; Cl, 2.63; N, 7.27. Found: C, 82.23; H, 7.17; N, 7.01.

5,10,15,20-Tetrakis(3,5-di-*tert*-butylphenyl)porphyrin[2,3-*b*]imidazole-2'-phenyl-3"-[(*Z*)-2"'-cyano-2"'-(4""-bromophenyl)ethenyl] 104

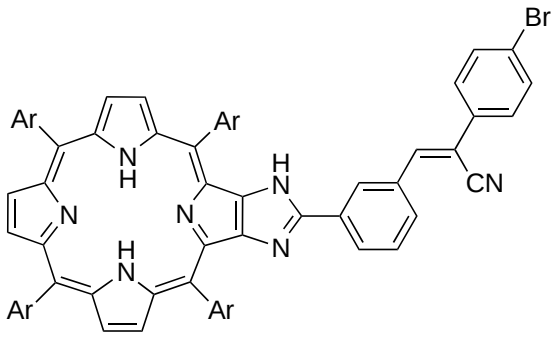

Using Method A and starting with **39** and 4'-bromophenylacetonitrile, **104** (25 mg, 32%) was obtained as a purple microcrystalline solid. m.p. > 300 °C. ^{1}H NMR (400 MHz, $CDCl_3$) δ -2.79 (br s, 2H, NH), 1.52-1.56 (m, 72H, CH_3), 7.56-7.60 (m, 2H, ArH), 7.63 (d, 2H, *J* = 8.6 Hz, ArH), 7.65-7.68 (m, 1H, ArH), 7.70 (d, 2H, *J* = 8.6 Hz, ArH), 7.79-7.82 (m, 2H, ArH), 7.88 (s, 1H, CH), 8.07-8.09 (m, 2H, ArH), 8.10-8.12 (m, 4H, ArH), 8.13-8.15 (m, 2H, ArH), 8.17-8.19 (m, 2H, ArH), 8.22-8.27 (m, 1H, ArH), 8.45 (br s, 1H, NH), 8.84 and 8.87 (ABq, 2H, J_{AB} = 4.6 Hz, β-pyrrolic H), 8.97-9.04 (m, 4H, β-pyrrolic H) ppm. ^{13}C NMR (100 MHz, $CDCl_3$) δ 31.75, 31.82, 31.9, 35.05, 35.14, 35.4, 111.5, 115.5, 117.4, 119.1, 121.0, 121.2, 122.1, 122.5, 123.8, 126.3, 127.3, 127.5, 128.6, 129.5, 129.7, 132.1, 132.5, 133.4, 134.2, 139.8, 141.2, 141.6, 141.9, 142.2, 148.6, 148.66, 148.74, 149.8, 150.9 ppm. FTIR 712 (m), 727 (m), 754 (m), 800 (s), 819 (m), 880 (m), 922 (m), 1245 (m), 1361 (m), 1424 (m), 1461 (m), 1591 (m, C=C), 2958 (m), 3332 (br, NH), 3462 (br, NH) cm^{-1}. λ_{max} ($CHCl_3$) 421, 518, 554, 587, 645 nm (log ε 5.42, 4.18, 3.95, 3.87, 3.57). Anal Calcd for $C_{92}H_{102}BrN_7$. 2 CH_2Cl_2: C, 72.58; H, 6.87; N, 6.30. Found: C, 72.58; H, 6.98; N, 6.57.

Attempted Preparation of 5,10,15,20-Tetrakis(3,5-di-*tert*-butylphenyl)porphyrin[2,3-*b*]imidazole-2'-phenyl-3"-[(*Z*)-2"'-cyano-2"'-(4""-nitrophenyl)ethenyl] 105

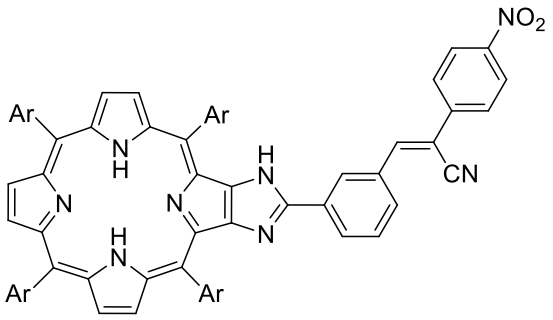

Using either Method A or Method B and starting with **39** and 4'-nitrophenylacetonitrile, a similar TLC pattern was observed when analyzing the crude material after work-up. The crude material was chromatographed (silica gel, dichloromethane/hexane 3:1) to afford unconverted **39** (20%), before the polarity was increased (neat dichloromethane) that resulted in elution of multiple closely running bands. The desired product was not observed in the ^{1}H NMR analysis of these products (after evaporation of solvent).

4.5.5 Preparation of Zinc(II) Complexes of Imidazoloporphyrin-α-Cyanostilbenes

General Procedure: To a mixture of free-base α-cyanostilbene imidazoloporphyrin (25 mg) in dichloromethane (10 mL) was added zinc(II) acetate (2.5 eq.). The reaction mixture was heated to reflux for 1 h. On cooling, the reaction mixture was washed with water (2 x 20 mL), brine (20 mL), dried over anhydrous sodium sulfate, filtered and evaporated to dryness under vacuum. The crude product obtained was chromatographed (silica gel, dichloromethane / hexane 3:1) to afford pure the zinc(II) complex.

{5,10,15,20-Tetrakis(3,5-di-*tert*-butylphenyl)porphyrinato[2,3-*b*]imidazole-2'-phenyl-4"-[(*Z*)-2"'-cyano-2"'-phenyl)ethenyl]} zinc(II) 106

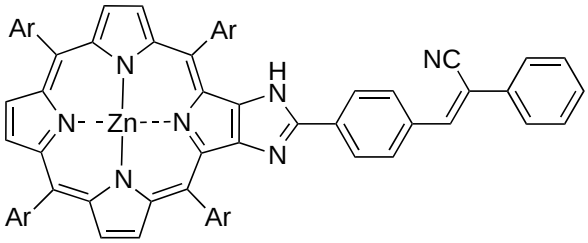

Starting with **100**, **106** (20 mg, 76%) was obtained as a purple microcrystalline solid. m.p. > 300 °C. ^{1}H NMR (400 MHz, $CDCl_3$) δ 1.52-1.58 (m, 72H, CH_3), 7.42-7.59 (m, 6H, ArH), 7.70-7.82 (m, 4H, ArH), 7.85-7.95 (m, 3H, ArH and CH), 8.00-8.04 (m, 2H, ArH), 8.08-8.18 (m, 7H, ArH), 8.64 (br s, 1H, NH), 8.99-9.11 (m, 6H, β-pyrrolic H) ppm. ^{13}C NMR (100 MHz, $CDCl_3$) δ 31.75, 31.86, 35.0, 35.1, 35.4, 111.4, 116.6, 118.1, 119.9, 120.0, 120.8, 120.9, 121.9, 123.4, 125.5, 126.0, 126.1, 128.3, 128.9, 129.1, 129.2, 129.4, 129.5, 129.9, 131.1, 131.7, 132.4, 132.6, 132.9, 133.6, 133.9, 134.6, 138.9, 140.5, 140.7, 141.4, 141.5, 141.9, 141.8, 142.5, 148.5, 148.6, 149.1, 149.2, 149.7, 150.3, 150.9, 151.9 ppm. FTIR 690 (m), 713 (m), 758 (m), 796 (s), 821 (s), 880 (m), 899 (m), 936 (m), 1002 (m), 1068 (m), 1202 (m), 1247 (s), 1361 (m), 1462 (m), 1590 (m, C=C), 2956 (s), 3439 (br, NH) cm^{-1}. λ_{max} ($CHCl_3$) 429, 555, 594 nm (log ε 5.28, 4.09, 3.84). Anal Calcd for $C_{92}H_{101}N_7Zn$. 1 CH_2Cl_2: C, 76.76; H, 7.13; N, 6.74. Found: C, 76.46; H, 7.29; N, 6.56.

{5,10,15,20-Tetrakis(3,5-di-*tert*-butylphenyl)porphyrinato[2,3-*b*]imidazole-2'-phenyl-4"-[(*Z*)-2"'-cyano-2"'-(4""-bromophenyl)ethenyl]} zinc(II) 107

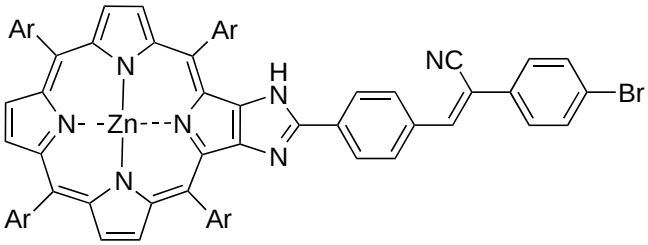

Starting with **101**, **107** (19 mg, 73%) was obtained as a purple microcrystalline solid. m.p. > 300 °C. ^{1}H NMR (400 MHz, $CDCl_3$) δ 1.57 (app. s, 36H, CH_3), 1.58 (app. s, 36H, CH_3), 7.52-

7.55 (m, 1H, ArH), 7.57-7.65 (m, 4H, ArH), 7.74-7.81 (m, 3H, ArH), 7.82-7.85 (m, 2H, ArH), 7.93 (s, 1H, CH), 8.10-8.11 (m, 1H, ArH), 8.13-8.22 (m, 8H, ArH), 8.25-8.29 (m, 1H, ArH), 8.67 (br s, 1H, NH), 9.05 (app. s, 2H, β-pyrrolic H), 9.07-9.14 (m, 4H, β-pyrrolic H) ppm. ^{13}C NMR (100 MHz, $CDCl_3$) δ 31.78, 31.85, 31.92, 35.1, 35.2, 35.4, 112.6, 116.5, 117.7, 119.9, 120.8, 121.0, 122.0, 123.4, 123.6, 126.0, 126.4, 127.3, 127.6, 128.7, 129.3, 129.4, 129.6, 130.0, 131.7, 132.0, 132.4, 132.6, 133.9, 134.3, 134.4, 138.9, 140.6, 141.4, 141.9, 142.0, 142.5, 148.49, 148.52, 149.1, 149.3, 149.77, 149.86, 150.4, 150.8, 151.9, 152.6 ppm. FTIR 690 (m), 714 (s), 758 (s), 796 (s), 823 (m), 881 (m), 899 (m), 938 (m), 1219 (m), 1246 (m), 1293 (m), 1361 (m), 1424 (m), 1474 (m), 1590 (m, C=C), 2954 (m), 3450 (br, NH) cm^{-1}. λ_{max} ($CHCl_3$) 429, 555, 594 nm (log ε 5.51, 3.99, 3.51). Anal Calcd for $C_{92}H_{100}BrN_7Zn$. 1 CH_2Cl_2: C, 72.81; H, 6.70; N, 6.39. Found: C, 72.79; H, 6.35; N, 6.64.

Attempted Preparation of {5,10,15,20-Tetrakis(3,5-di-*tert*-butylphenyl)porphyrinato-[2,3-*b*]imidazole-2'-phenyl-4"-[(*Z*)-2"'-cyano-2"'-(4""-nitrophenyl)ethenyl]} zinc(II) 108

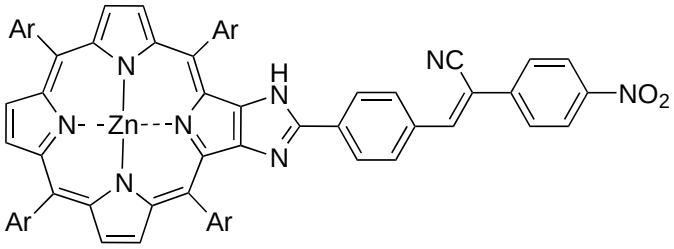

Starting with **102**, the reaction mixture was refluxed for 1h, the reaction was monitored by TLC, which indicated completion of the reaction with the formation of a new pink spot observed. However, upon work up a grey mass was obtained. The residue was insoluble in $CDCl_3$ and DMSO d_6, hence not been characterised. The procedure was repeated twice more with the same outcome. At this point it is unclear why this is the case.

{5,10,15,20-Tetrakis(3,5-di-*tert*-butylphenyl)porphyrinato[2,3-*b*]imidazole-2'-phenyl-3"-[(*Z*)-2"'-cyano-2"'-phenyl)ethenyl]} zinc(II) 109

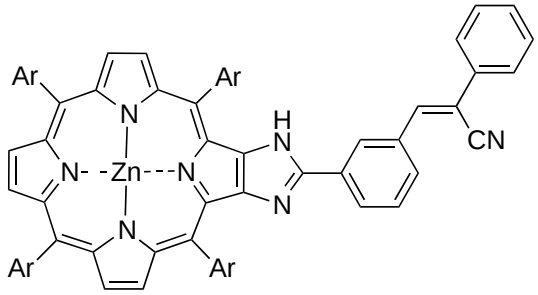

Starting with **103**, **109** (23 mg, 88%) was obtained as a purple microcrystalline solid. m.p. > 300 °C. ^{1}H NMR (400 MHz, $CDCl_3$) δ 1.52-1.57 (m, 72H, CH_3), 7.52-7.61 (m, 5H, ArH), 7.79-7.82 (m, 2H, ArH), 7.87 (d, 2H, *J* = 8.3 Hz, ArH), 7.90 (s, 1H, CH), 8.01 (d, 2H, *J* = 8.3 Hz, ArH), 8.09-8.17 (m, 9H, ArH), 8.64 (br s 1H, NH), 9.01 (app. s, 2H, β-pyrrolic H), 9.03-9.10 (m, 4H, β-pyrrolic H) ppm. ^{13}C NMR (100 MHz, $CDCl_3$) δ 31.8, 31.9, 35.06, 35.14, 35.5, 120.0, 120.8, 121.0, 121.9, 123.5, 123.6, 125.5, 127.2, 127.3, 127.5, 129.4, 129.5, 130.0, 131.8, 132.3, 134.4, 132.6, 133.2, 133.6, 139.0, 140.5, 140.8, 141.7, 141.9, 142.5, 142.6, 148.5, 148.6, 149.1, 149.3, 149.8, 150.2, 151.0, 151.9, 153.0 ppm. FTIR 672 (m), 713 (s), 757 (s), 796 (s), 822 (m), 880 (m), 899 (m), 937 (m), 1003 (m), 1077 (m), 1219 (m), 1247 (m), 1361 (m), 1591 (m, C=C), 2957 (m), 3420 (br, NH) cm^{-1}. λ_{max} ($CHCl_3$) 429, 554, 595 nm (log ε 5.32, 4.03, 3.61). Anal Calcd for $C_{92}H_{101}N_7Zn$. 2 CH_2Cl_2: C, 73.31; H, 6.87; N, 6.37. Found: C, 73.64; H, 6.54; N, 6.11.

{5,10,15,20-Tetrakis(3,5-di-*tert*-butylphenyl)porphyrinato[2,3-*b*]imidazole-2'-phenyl-3"-[(*Z*)-2"'-cyano-2"'-(4""-bromophenyl)ethenyl]} zinc(II) 110

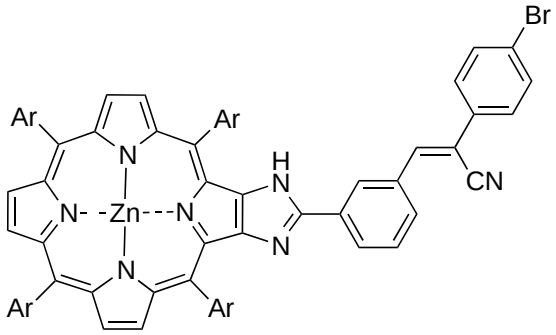

Starting with **104**, **110** (20 mg, 76%) was obtained as a purple microcrystalline solid. m.p. > 300 °C. ^{1}H NMR (400 MHz, $CDCl_3$) δ 1.52-1.58 (m, 72H, CH_3), 7.49-7.52 (m, 2H, ArH), 7.58-7.66 (m, 3H, ArH), 7.68-7.74 (m, 2H, ArH), 7.79-7.83 (m, 2H, ArH), 7.87 (s, 1H, CH), 8.10-8.19 (m, 10H, ArH), 8.21-8.26 (m, 1H, ArH), 9.00-9.03 (m, 2H, β-pyrrolic H), 9.04-9.10 (m, 4H, β-pyrrolic H) ppm (NH was absent). ^{13}C NMR (100 MHz, $CDCl_3$) δ 31.7, 31.8, 31.9, 35.0, 35.1, 35.3, 117.5, 120.8, 123.5, 123.8, 126.5, 127.4, 128.7, 129.5, 130.5, 131.8, 132.38, 132.44, 133.3, 134.2, 141.7, 141.9, 148.5, 149.2, 149.8 ppm. FTIR 671 (m), 687 (m), 713 (s), 756 (s), 796 (s), 823 (s), 881 (m), 899 (m), 937 (m), 1002 (m), 1075 (m), 1218 (m), 1246 (m), 1361 (m), 1475 (m), 1590 (m, C=C), 2955 (m), 3430 (br, NH) cm^{-1}. λ_{max} ($CHCl_3$) 430, 473, 553, 593 nm (log ε 5.53, 3.49, 4.12, 3.74). Anal Calcd for $C_{92}H_{100}BrN_7Zn$. 1 CH_2Cl_2: C, 72.81; H, 6.70; N, 6.39. Found: C, 72.89; H, 6.21; N, 6.16.

4.5.6 Preparation of Quinoxalinoporphyrin-α-Cyanostilbenes

General Procedure Method A: In a mixture of 6'-formylquinoxalinoporphyrin (75 mg, 0.063 mmol) and substituted acetonitrile (0.063 mmol; benzyl cyanide 7.4 mg or 4'-bromophenylacetonitrile 12.3 mg) in dichloromethane/ethanol (1:9; 20 mL) was added sodium methoxide (17.0 mg, 0.315 mmol). The reaction mixture was heated at reflux overnight under

an argon atmosphere. The reaction mixture was allowed to cool to room temperature and filtered. The residue obtained was washed with ethanol (10 mL) followed by column chromatography (silica gel, dichloromethane/hexane 1:1) to afford pure product.

General Procedure Method B: In a mixture of 6'-formylquinoxalinoporphyrin (75 mg, 0.063 mmol) and 4'-nitrophenylacetonitrile (10.2 mg, 0.063 mmol) in dichloromethane/ethanol mixture (1:9; 20 mL) was added piperidine (10.7 mg, 0.13 mmol). The reaction mixture was heated at reflux overnight under an argon atmosphere. On cooling, the reaction mixture was allowed to cool to room temperature and filtered. The residue obtained was washed with ethanol (10 mL) followed by column chromatography (silica gel, dichloromethane/hexane 1:1) to affording pure product.

5,10,15,20-Tetrakis(3,5-di-*tert*-butylphenyl)porphyrin[2,3-*b*]-6'((*Z*)-2"-cyano-2"-phenylethenyl)quinoxaline 112

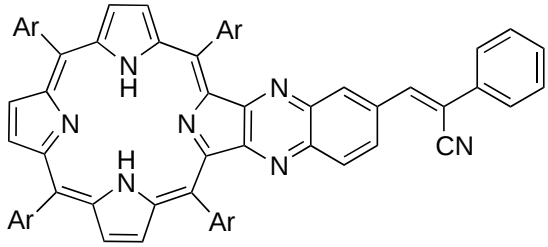

Using Method A and starting with **45** and benzyl cyanide, **112** (25 mg, 31%) was obtained as a dark green microcrystalline solid. m.p. > 300 °C. ^{1}H NMR (400 MHz, $CDCl_3$) δ -2.51 (br s, 2H, NH), 1.48 (s, 18H, CH_3), 1.50 (s, 18H, CH_3), 1.54 (app. s, 36H, CH_3), 7.35-7.37 (m, 1H, ArH), 7.40-7.49 (m, 2H, ArH), 7.63-7.71 (m, 2H, ArH), 7.80-7.86 (m, 4H, ArH and CH), 7.88-7.95 (m, 2H, ArH), 7.96-7.99 (m, 5H, ArH), 8.11 (app. d, 4H, *J* = 1.6 Hz, ArH), 8.80 (app. s, 2H, β-pyrrolic H), 8.99-9.02 (m, 2H, β-pyrrolic H), 9.07-9.12 (m, 2H, β-pyrrolic H) ppm. ^{13}C NMR (100 MHz, $CDCl_3$) δ 31.7, 31.9, 34.98, 35.00, 35.05, 117.3, 118.25, 118.34, 120.8, 121.1, 122.8, 126.0, 127.9, 128.1, 128.3, 128.36, 128.39, 129.0, 129.1, 129.26, 129.34, 129.6, 130.4, 130.5, 131.4, 134.3, 134.3, 138.15, 138.17, 139.5, 140.0, 140.5, 140.7, 140.8, 141.0, 142.3, 145.4,

148.8, 148.96, 149.04, 153.1, 153.2, 155.0 ppm. FTIR 711 (s), 756 (s), 800 (s), 922 (m), 1120 (m), 1222 (m), 1247 (m), 1361 (m), 1474 (m), 1592 (m, C=C), 2958 (s), 3330 (br, NH) cm^{-1}. λ_{max} ($CHCl_3$) 428, 468, 584, 631 nm (log ε 5.21, 4.70, 3.89, 3.73). Anal Calcd for $C_{91}H_{101}N_7$. 1/3 CH_2Cl_2: C, 83.03; H, 7.76; N, 7.42. Found: C, 83.02; H, 7.67; N, 7.41.

5,10,15,20-Tetrakis(3,5-di-*tert*-butylphenyl)porphyrin[2,3-*b*]-6'((*Z*)-2"-cyano-2"-(4"'-bromophenyl)ethenyl)quinoxaline 113

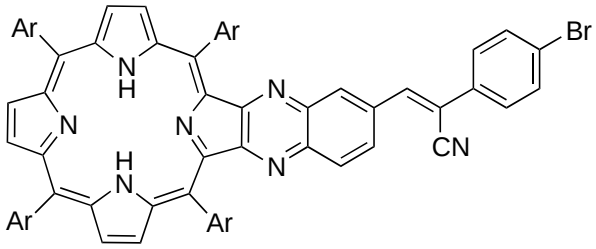

Using Method A and starting with **45** and 4'-bromophenylacetonitrile, **113** (70 mg, 81%) was obtained as a dark green microcrystalline solid. m.p. > 300 °C. ^{1}H NMR (400 MHz, $CDCl_3$) δ -2.49 (br s, NH, 2H), 1.49 (s, 18H, CH_3), 1.50 (s, 18H, CH_3), 1.54 (app. s, 36H, CH_3), 7.65-7.68 (m, 5H, ArH and CH), 7.79-7.82 (m, 2H, ArH), 7.90 (d, 1H, *J* = 8.8 Hz, QuinH), 7.94-8.00 (m, 6H, ArH), 8.09-8.12 (m, 4H), 8.20-8.22 (m, 1H, QuinH), 8.40-8.44 (m, 1H, QuinH), 8.79 (app. s, 2H, β-pyrrolic H), 8.98-9.02 (m, 2H, β-pyrrolic H), 9.05-9.10 (m, 2H, β-pyrrolic H) ppm. ^{13}C NMR (100 MHz, $CDCl_3$) δ 31.7, 31.9, 35.0, 35.1, 111.5, 117.5, 118.4, 118.5, 120.9, 121.0, 121.1, 122.9, 123.8, 127.8, 127.9, 128.1, 128.4, 128.5, 129.6, 131.3, 132.4, 133.0, 133.7, 134.3, 138.2, 128.3, 139.5, 139.6, 140.5, 140.6, 140.7, 141.0, 141.64, 141.69, 145.2, 145.3, 148.8, 148.9, 149.0, 153.3, 153.5, 155.1 ppm. FTIR 711 (m), 755 (m), 802 (s), 879 (m), 922 (m), 990 (m), 1123 (m), 1225 (m), 1247 (m), 1293 (m), 1361 (m), 1475 (m), 1593 (m, C=C), 2961 (m), 3330 (br, NH) cm^{-1}. λ_{max} ($CHCl_3$) 427, 536, 605, 656 nm (log ε 5.27, 4.11, 3.99, 2.99). Anal Calcd for $C_{91}H_{100}BrN_7$. 3/2 CH_2Cl_2: C, 74.11; H, 6.93; N, 6.54. Found: C, 74.03; H, 6.81; N, 6.59.

5,10,15,20-Tetrakis(3,5-di-*tert*-butylphenyl)porphyrin[2,3-*b*]-6'((*Z*)-2"-cyano-2"-(4"'-nitrophenyl)ethenyl)quinoxaline 114

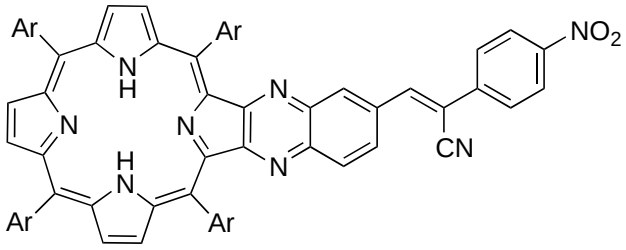

Using Method B and starting with **45** and 4'-nitrophenylacetonitrile, **114** (62 mg, 74%) was obtained as a dark green microcrystalline solid. m.p. > 300 °C. ^{1}H NMR (400 MHz, $CDCl_3$) δ -2.49 (br s, 2H, NH), 1.49 (s, 18H, CH_3), 1.50 (s, 18H, CH_3), 1.54 (app. s, 36H, CH_3), 7.79-7.84 (m, 4H, ArH and CH), 7.92 (d, 1H, *J* = 8.8 Hz, QuinH), 7.93-8.00 (m, 7H, ArH), 8.08-8.12 (m, 4H, ArH), 8.30-8.32 (m, 1H, ArH), 8.38-8.48 (m, 3H, ArH), 8.80 (app. s, 2H, β-pyrrolic H), 8.98-9.02 (m, 2H, β-pyrrolic H), 9.06-9.10 (m, 2H, β-pyrrolic H) ppm. ^{13}C NMR (100 MHz, $CDCl_3$) δ 31.7, 31.9, 35.01, 35.05, 110.3, 117.1, 120.9, 121.2, 123.0, 124.5, 127.0, 127.2, 128.0, 128.1, 128.4, 128.5, 129.6, 131.5, 133.0, 133.7, 134.4, 138.3, 139.6, 140.3, 140.6, 140.7, 140.8, 140.9, 142.0, 144.5, 148.0, 148.8, 148.9, 149.0, 153.5, 153.6, 155.2 ppm. FTIR 712 (m), 751 (s), 801 (s), 851 (m), 922 (m), 1123 (m), 1247 (m), 1341 (m), 1524 (m, NO_2), 1591 (m, C=C), 2213 (w, CN), 2955 (s), 3320 (br, NH) cm^{-1}. λ_{max} ($CHCl_3$) 432, 538, 607, 655 nm (log ε 5.48, 4.28, 4.15, 3.12). Anal Calcd for: $C_{91}H_{100}N_8O_2$. 1/3 CH_2Cl_2: C, 79.94; H, 7.37; N, 7.83. Found: C, 80.12; H, 7.56; N, 7.86.

4.5.7 Preparation of Zinc(II) Complexes of Quinoxalinoporphyrin-α-Cyanostilbenes

General Procedure: In a mixture of free-base α-cyanostilbene porphyrin-quinoxaline (25 mg) in dichloromethane (10 mL) was added zinc(II) acetate (2.5 eq.). The reaction mixture was heated at reflux overnight. On cooling, the reaction mixture was washed with water (2 x 20 mL), brine (20 mL), dried over anhydrous sodium sulfate, filtered and evaporated to dryness under

vacuum. The crude product obtained was chromatographed (silica gel, dichloromethane/hexane 1:1) to afford pure the zinc(II) complex.

{5,10,15,20-Tetrakis(3,5-di-*tert*-butylphenyl)porphyrinato[2,3-*b*]-6'((*Z*)-2"-cyano-2"-phenylethenyl)quinoxaline} zinc(II) 115

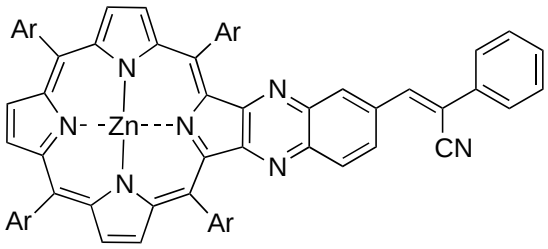

Starting with **112**, **115** (9 mg, 34%) was obtained as a dark green microcrystalline solid. m.p. > 300 °C. ^{1}H NMR (400 MHz, $CDCl_3$) δ 1.49-1.51 (m, 36H, CH_3), 1.54 (app. s, 36H, CH_3), 7.48-7.58 (m, 3H, ArH), 7.74 (s, 1H, CH), 7.79-7.84 (m, 4H, ArH), 7.94-7.99 (m, 7H, ArH), 8.08-8.11 (m, 4H, ArH), 8.25-8.27 (m, 1H, QuinH), 8.51-8.55 (m, 1H, QuinH), 8.91 (app. s, 2H, β-pyrrolic H), 9.00-9.02 (m, 2H, β-pyrrolic H), 9.03-9.08 (m, 2H, β-pyrrolic H) ppm. ^{13}C NMR (100 MHz, $CDCl_3$) δ 31.7, 31.9, 35.00, 35.03, 35.05, 112.9, 117.9, 119.2, 119.3, 120.7, 121.0, 124.97, 124.99, 126.3, 128.0, 128.1, 128.2, 129.2, 129.3, 129.6, 131.2, 131.7, 131.8, 132.5, 132.9, 134.1, 134.7, 140.7, 141.2, 141.30, 141.33, 141.4, 141.5, 141.7, 148.7, 148.8, 149.0, 149.4, 150.1, 151.2, 151.4, 152.5, 152.6 ppm. FTIR 712 (m), 754 (s), 798 (s), 938 (m), 1003 (m), 1128 (m), 1361 (m), 1592 (m, C=C), 2229 (w, CN), 2956 (s) cm^{-1}. λ_{max} ($CHCl_3$) 435, 532, 566, 598, 652 nm (log ε 5.22, 4.16, 3.69, 4.01, 3.40). Anal Calcd for $C_{91}H_{99}N_7Zn$. 1 CH_2Cl_2: C, 76.68; H, 7.06; N, 6.80. Found: C, 76.22; H, 6.81; N, 7.09.

{5,10,15,20-Tetrakis(3,5-di-*tert*-butylphenyl)porphyrinato[2,3-*b*]-6'((*Z*)-2"-cyano-2"-(4"'-bromophenyl)ethenyl)quinoxaline} zinc(II) 116

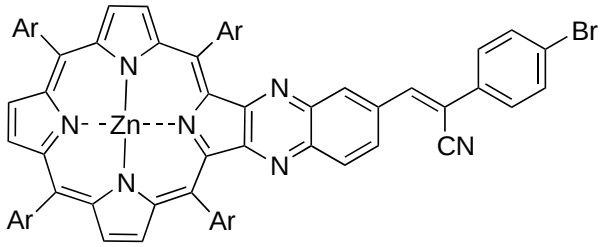

Starting with **113**, **116** (13 mg, 50%) was obtained as a dark green microcrystalline solid. m.p. > 300 °C. ^{1}H NMR (400 MHz, $CDCl_3$) δ 1.49 (s, 18H, CH_3), 1.50 (s, 18H, CH_3), 1.53 (app. s, 36H, CH_3), 7.66-7.68 (m, 2H, ArH), 7.71 (s, 1H, CH), 7.79-7.82 (m, 2H, ArH), 7.94-7.99 (m, 7H, ArH), 8.08-8.11 (m, 4H, ArH), 8.27-8.30 (m, 1H, QuinH), 8.47-8.51 (m, 1H, QuinH), 8.91 (app. s, 2H, β-pyrrolic H), 8.99-9.02 (m, 2H, β-pyrrolic H), 9.03-9.07 (m, 2H, β-pyrrolic H) ppm. ^{13}C NMR (100 MHz, $CDCl_3$) δ 31.7, 31.9, 35.00, 35.03, 35.05, 111.7, 117.5, 119.2, 119.3, 120.7, 121.0, 123.8, 124.97, 125.0, 127.8, 128.1, 128.2, 129.3, 131.3, 131.7, 131.8, 132.4, 132.5, 133.0, 133.6, 133.8, 140.6, 141.20, 141.22, 141.30, 141.35, 141.5, 141.6, 141.8, 148.6, 148.8, 149.0, 149.4, 150.1, 151.5, 152.5, 152.6 ppm. FTIR 752 (s), 800 (s), 937 (m), 1004 (m), 1129 (m), 1361 (m), 1591 (m, C=C), 2955 (s) cm^{-1}. λ_{max} ($CHCl_3$) 433, 472, 586, 632 nm (log ε 5.31, 4.67, 3.89, 3.75). Anal Calcd for $C_{91}H_{98}BrN_7Zn$. 1/2 CH_2Cl_2: C, 74.38; H, 6.75; N, 6.64. Found: C, 74.67; H, 6.39; N, 6.51.

{5,10,15,20-Tetrakis(3,5-di-*tert*-butylphenyl)porphyrinato[2,3-*b*]-6'((*Z*)-2"-cyano-2"-(4"'-nitrophenyl)ethenyl)quinoxaline} zinc(II) 117

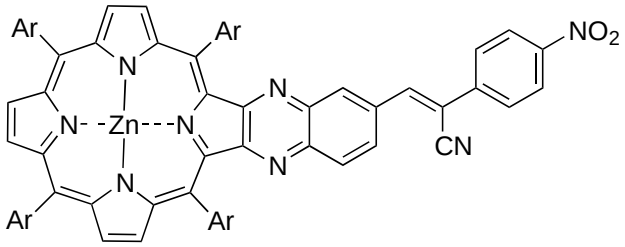

Starting with **114**, **117** (17 mg, 65%) was obtained as a dark green microcrystalline solid. m.p. > 300 °C. ^{1}H NMR (400 MHz, $CDCl_3$) δ 1.48 (s, 18H, CH_3), 1.49 (s, 18H, CH_3), 1.53 (app. s, 36H, CH_3), 7.79-7.81 (m, 2H, ArH), 7.86 (s, 1H, CH), 7.94-8.01 (m, 9H, ArH), 8.07-8.10 (m, 4H, ArH), 8.36-8.38 (m, 1H, QuinH), 8.40 (d, 2H, *J* = 8.9 Hz, ArH), 8.48-8.52 (m, 1H, QuinH), 8.91 (app. s, 2H, β-pyrrolic H), 8.99-9.07 (m, 4H, β-pyrrolic H) ppm. ^{13}C NMR (100 MHz, $CDCl_3$) δ 31.68, 31.73, 34.9, 35.0, 110.3, 115.8, 117.4, 121.0, 122.9, 123.46, 123.51, 126.2, 126.9, 128.8, 129.0, 129.50, 129.6, 129.7, 129.8, 131.11, 132.43, 132.7, 133.0, 135.3, 136.0, 140.1, 141.4, 141.6, 144.3, 145.4, 147.1, 148.60, 148.63, 148.66, 148.70, 149.8, 150.4, 150.6, 150.8 ppm. FTIR 750 (s), 799 (m), 852 (m), 939 (m), 1003 (m), 1221 (m), 1248 (m), 1340 (s), 1526 (w, NO_2), 1592 (m, C=C), 2227 (w, CN), 2956 (m) cm^{-1}. λ_{max} ($CHCl_3$) 435, 478, 587, 644 nm (log ε 5.23, 4.50, 3.89, 3.89). Anal Calcd for $C_{91}H_{98}N_8O_2Zn$. 1/2 CH_2Cl_2: C, 76.13; H, 6.91; N, 7.76. Found: C, 76.41; H, 6.80; N, 7.40.

4.6 References

1. Toa, M.; Liu, L.; Liu, D.; Zhou, X. *Dyes Pigm.* **2010**, *85*, 21-26.

Chapter Five

Boron Difluoride 1,3-Diketonates

5.1 Background

1,3-Diketones are typically prepared by a variation of a general strategy (Claisen-like condensation), involving the attack of a nucleophilic α-carbon on the carbonyl group of a carboxylic acid derivative (eg acyl halide or methyl / ethyl ester). The nucleophilic α-carbon can be generated by treatment of a methyl ketone with either sodium hydride, sodium amide, or potassium *t*-butoxide, among others. Regardless of the choice of base, the solvent used in the reaction must be anhydrous to avoid the unwanted side reaction of ester/acyl halide hydrolysis, that would result in the formation of unreactive carboxylate anions.

1,3-Diketones exist in tautomeric equilibrium with their enolic form, as shown in Figure 5.1. In cases where the two aryl rings are not the same as one another, two enolic tautomers will be present.[1] For the remainder of this thesis, the 1,3-diketones are depicted as (one of) their enol form(s), although a specific tautomer is not being implied for those cases where the two aryl rings are not the same.

The boron difluoride complexes of the compounds, known as boron difluoride 1,3-diketonates, can be prepared simply by treating a 1,3-diketone with boron trifluoride diethyl etherate. The complex is formed from the chelation to the boron atom (of the BF_2 unit) *via* the two oxygen atoms of a 1,3-diketone *via* co-ordination bonds.

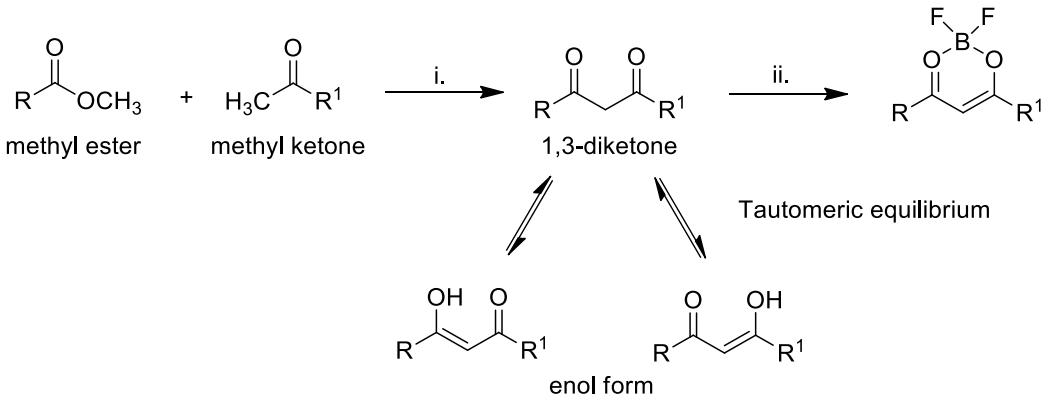

Figure 5.1: A common synthetic route to 1,3-diketones, the structures of their enolic tautomers and boron difluoride complexes. i. NaH (or CH_3ONa), DME (or THF), reflux overnight. ii. BF_3OEt_2, benzene (or CH_2Cl_2), reflux.

Boron difluoride complexes are extensively used as fluorophores due to their favourable photo-physical properties,[2] such as intense long UV-visible absorbance and high quantum yields.[3] These properties have resulted in applications in organic electroluminescence devices,[4,5] laser technology[6] and nonlinear optics[7]. The electron deficient -OBF_2O- group is reported to aid in delocalization of the electron density across the molecule.[6] The introduction of an electron donating group (eg, OMe) creates a virtual donor-π-acceptor system by lowering the HOMO/LUMO band gap. The photo-physical properties of the boron difluoride complexes can be altered by simple modifications, either synthetically or by changing their environment.[5] Mirochnik and coworkers have extensively studied the photo-physical properties of crystalline[8,9] and polymer forms[8] of boron difluoride complexes with respect to size, solvent and temperature.

At the outset of this project, it was planned to investigate boron difluoride 1,3-diaryl-1,3-diketonates as a third chromophore linked to the three porphyrin frameworks shown in Figure 1.30, complementing the worked described in Chapters Three and Four. This was to be accomplished by using the ester-functionalised porphyrins reported in this thesis, as "substituted" methyl benzoates. However, despite repeated attempts at reacting ester-functionalised porphyrins such as **12**-**14** and **43** (and indeed zinc(II) chelates of these, in case the inner NH protons were a problem) with several different substituted acetophenones, in dry solvents such as benzene, dimethoxyethane (DME) and tetrahydrofuran, with different bases (sodium hydride and sodium methoxide), with different equivalents of the acetophenones (1, 2 and 10 eq.), with different equivalents of base (2, 10 and 20 (when 10 eq. of acetophenones were used), no desired products were ever observed.

Instead, 80-90% yields of the corresponding carboxylic acids were generally recovered from the reactions, formed as a result of ester hydrolysis. These results suggest that the solvents were not as dry as required, and the bases were presumably reacting with any traces of water present to generate hydroxide ion. A range of other 1,3-diketones *were* successfully prepared using the

same solvents and experimental conditions – see below, and Chapter Seven. This aspect of the project was certainly frustrating, and it seems that the size of the "methyl ester" component of the 1,3-diketone reactions involving the ester-functionalised porphyrins greatly reduced the rate of the desired reaction, allowing time for smaller hydroxide nucleophile to attack the carbonyl group of the ester, in place of the larger deprotonated acetophenone nucleophile, *i.e.*, ester hydrolysis was more rapid than the desired condensation reaction.

In the present work, in addition to the unsuccessful work described above, it was always intended to make three simple series of boron difluoride 1,3-diaryl-1,3-diketonates as shown in Figure 5.2; a methoxy-functionalised series (for comparative purposes with the benzyloxy- and hydroxy-functionalised series) and to validate the chemistry, Scheme 5.1), and two series for future supramolecular studies. The first of the two series for supramolecular studies was a hydroxy-functionalised series (for coordination to tin(IV) porphyrins,[10] Scheme 5.3 and see Figure 1.11(b) for an example of a phenolate-tin(IV) porphyrin complex), and the second was a 4'-pyridyl-functionalised series for coordination to zinc(II) porphyrins (described in Chapter Seven, and used in Chapter Six, for some preliminary supramolecular work).

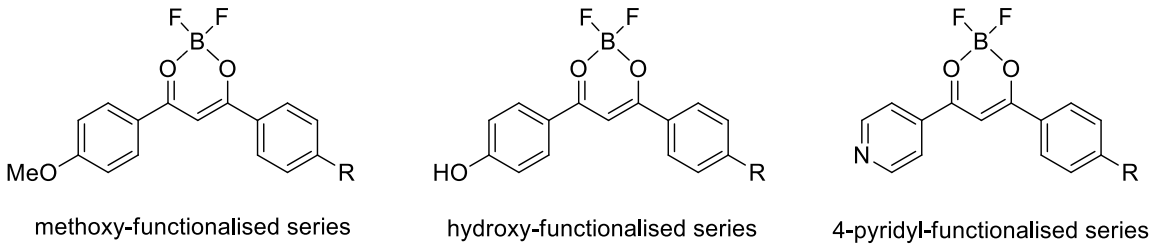

Figure 5.2: The three series of boron difluoride 1,3-diaryl-1,3-diketonates that are the focus of this Chapter.

5.2 Synthesis of Ligands and Boron Complexes

The synthetic routes to the methoxy-functionalised ligands and their boron complexes are shown in Scheme 5.1. For the benzyloxy series, 4'-benzyloxyacetophenone and methyl 4-benzyloxybenzoate were synthesised *via* benzylation of 4'-hydroxyacetophenone and methyl 4-

hydroxybenzoate, respectively, using benzyl bromide in acetone (Scheme 5.2). The synthesis of the benzyloxy-functionalised ligand series, their boron complexes, and hydroxy-functionalised boron complexes are shown in Scheme 5.3.

The methoxy diketones **118-121** and benzyloxy diketones **128-132** were prepared by condensation of substituted acetophenones with substituted methyl benzoates in dimethoxyethane, using sodium hydride (60% in oil) as a base. Refluxing the diketones with boron trifluoride diethyl etherate in dichloromethane for 30 mins afforded the corresponding methoxy diketone boron complexes **122-125**, and the benzyloxy diketone boron complexes, **133-137**.

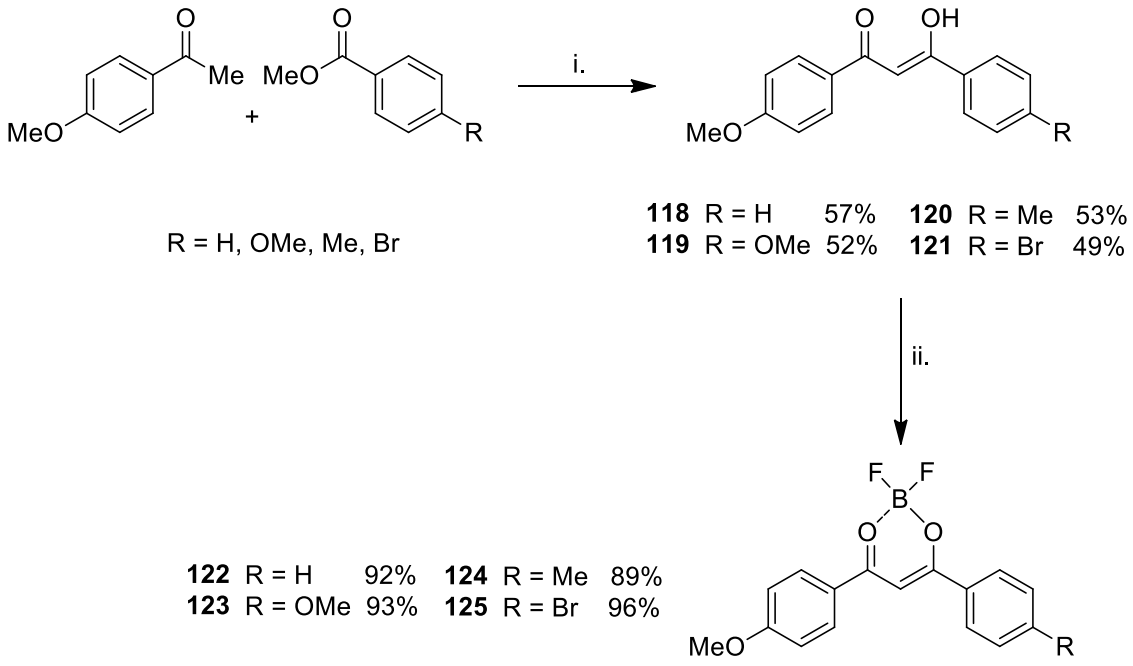

Scheme 5.1: i. NaH (60% in oil), DME; ii. BF_3OEt_2, CH_2Cl_2.

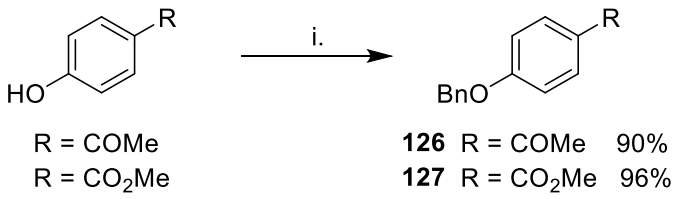

Scheme 5.2: i. BnBr, acetone.

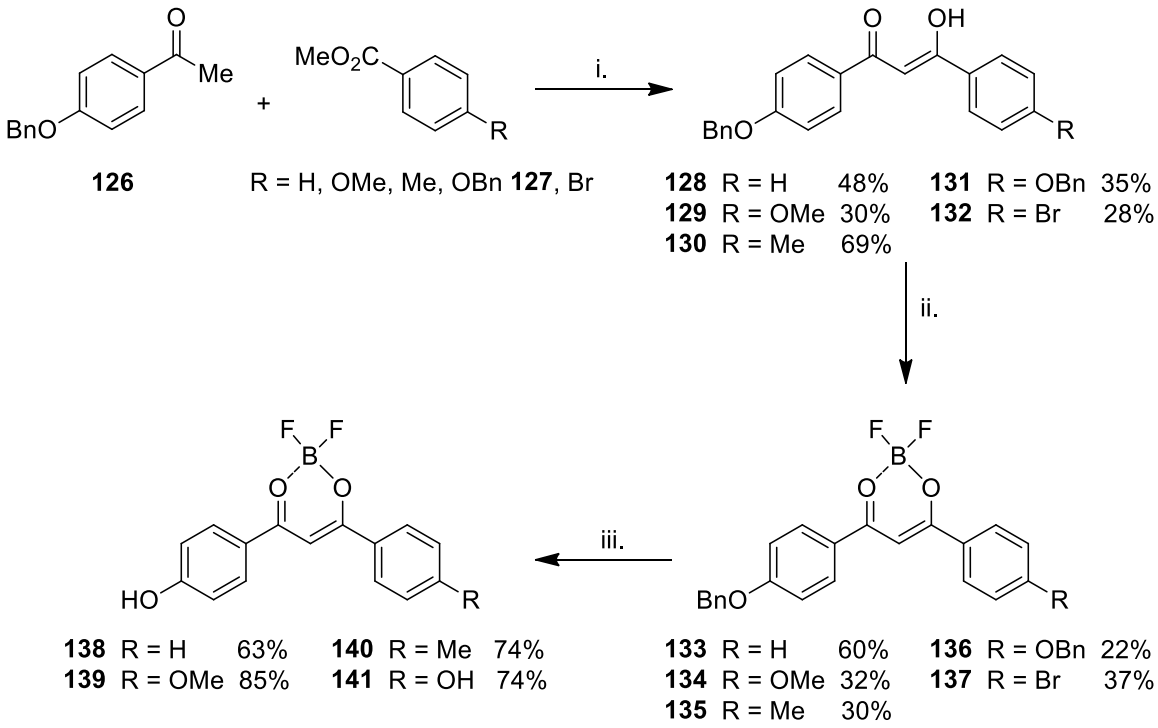

Scheme 5.3: i. NaH (60% in oil), DME; ii. BF_3OEt_2, CH_2Cl_2; iii. H_2, Pd/C, EtOH.

Hydrogenolysis of the benzyloxy diketone boron complexes, **133-136** afforded the corresponding hydroxy-functionalised boron complexes, **138-141**. All new compounds were characterised by ^{1}H and ^{13}C NMR, FTIR, mass spectrometry and elemental analysis.

In addition to the compounds described above, the unsubstituted 1,3-diphenyl-1,3-diketone **142** and the corresponding boron difluoride complex **143** were also prepared (Scheme 5.4). Compound **143** was used as the reference material for the photo-physical studies described in Section 5.3.

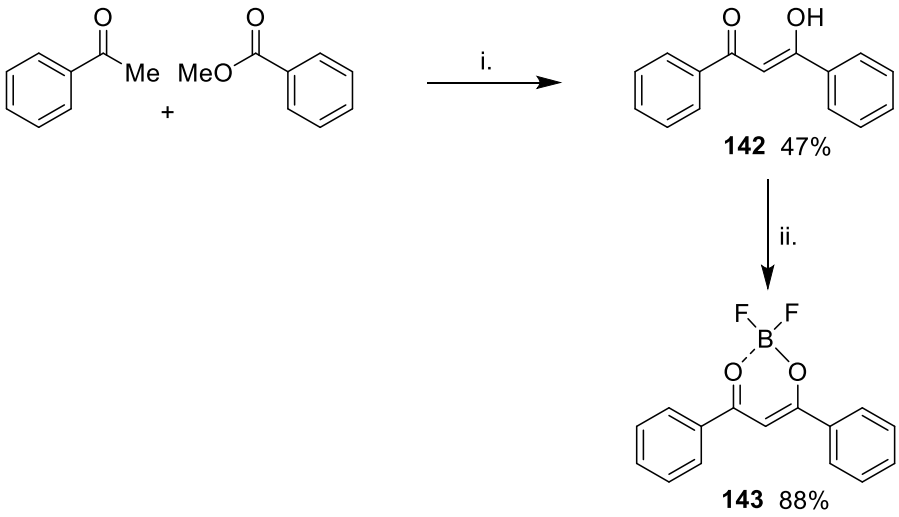

Scheme 5.4: i. NaH (60% in oil), DME; ii. BF_3OEt_2, CH_2Cl_2.

5.3 Preliminary Photo-physical Studies

The photo-physical properties; UV-visible absorption, fluorescence emission, Stokes shift, and quantum yield of the boron difluoride complexes, compounds **122-125**, **133-137** and **138-141** (and **143** as the reference material) in dichloromethane are summarised in Table 1. The quantum yields of three series were recorded against quinine sulfate in 0.1 M sulfuric acid.

Table 5.1: Absorption maxima wavelength (λ_{abs}, nm); molar extinction coefficient (ε_{max}, x 10^3 $Lmol^{-1}cm^{-1}$); fluorescence maxima wavelength (λ_{em}, nm); Stokes shift ($\Delta\lambda$, nm); relative quantum yield (ϕ) of **122-125**, **131-137**, **138-141** and **143** in dichloromethane

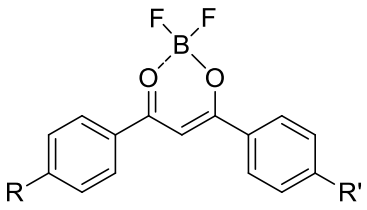

	Substituent		λ_{abs}	$\varepsilon_{max}/(10^3)$	λ_{em}	$\Delta\lambda$	ϕ
	R	**R'**					
143	H	H	364	35.18	417	53	0.18
122	OMe	H	397	54.88	433	36	0.429
123	OMe	OMe	411	62.98	440	29	0.333
124	OMe	Me	401	50.58	431	30	0.374
125	OMe	Br	404	42.80	442	38	0.238
133	OBn	H	397	61.55	430	33	0.346
134	OBn	OMe	411	62.00	440	29	0.327
135	OBn	Me	402	46.53	434	32	0.353
136	OBn	OBn	412	55.99	438	26	0.329
137	OBn	Br	404	38.98	440	36	0.345
138	OH	H	392	28.33	420	28	0.419
139	OH	OMe	406	48.04	432	27	0.444
140	OH	OH	403	39.95	428	25	0.386
141	OH	Me	396	38.62	423	26	0.328

The methoxy boron complexes absorbed in the range of 397-411 nm with molar extinction coefficients in the range of 42,000-63,000 $Lmol^{-1}cm^{-1}$ (Figure 5.3). The introduction of a strong donor (OMe) **122** results in a bathochromic shift of 33 nm when compared to the reference compound **143**. The introduction of a second OMe group in compound **123** results in a further bathochromic shift of 14 nm (411 nm) and an increase of 8,000 $Lmol^{-1}cm^{-1}$ in the molar

extinction coefficient. The introduction of two less active donor groups; Me (**124**) and Br (**125**) shows a bathochromic shift of only 4 nm and 7 nm, respectively, when compared with **122**.

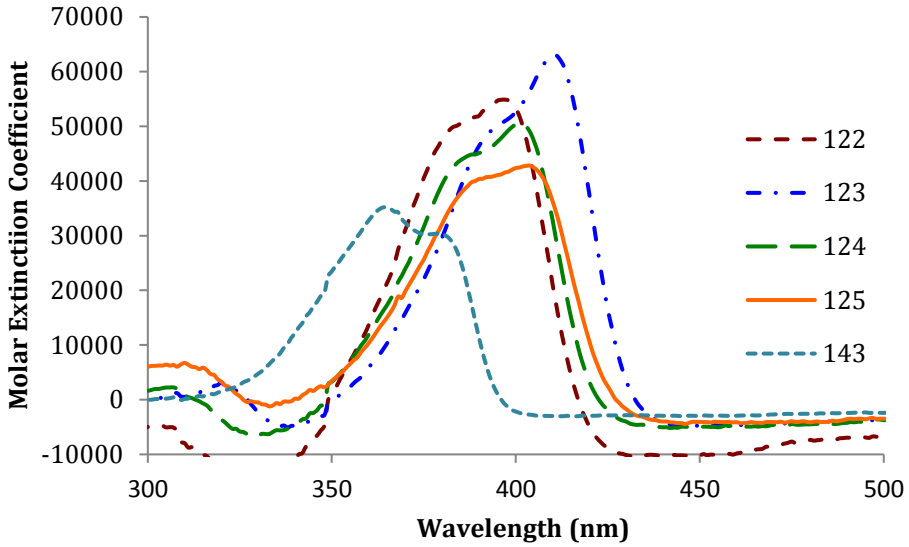

Figure 5.3: UV-visible spectra of methoxy diketone boron complexes **122-125** and **143** in CH_2Cl_2.

The UV-visible spectra of the benzyloxy boron complexes **133-137** recorded in dichloromethane are shown in Figure 5.4. The benzyloxy boron complexes exhibited similar trends to those that were observed with the methoxy series. The introduction of one OBn group (**133**) leads to an absorption maximum at 397 nm. Upon introduction of a second OBn (**136**) the absorption maximum moves to 412 nm, not surprisingly, almost the same effect as the introduction of an OMe group (**134**), that absorbs at 411 nm. The molar extinction coefficients of the benzyloxy boron complexes were observed in the same range as the methoxy series.

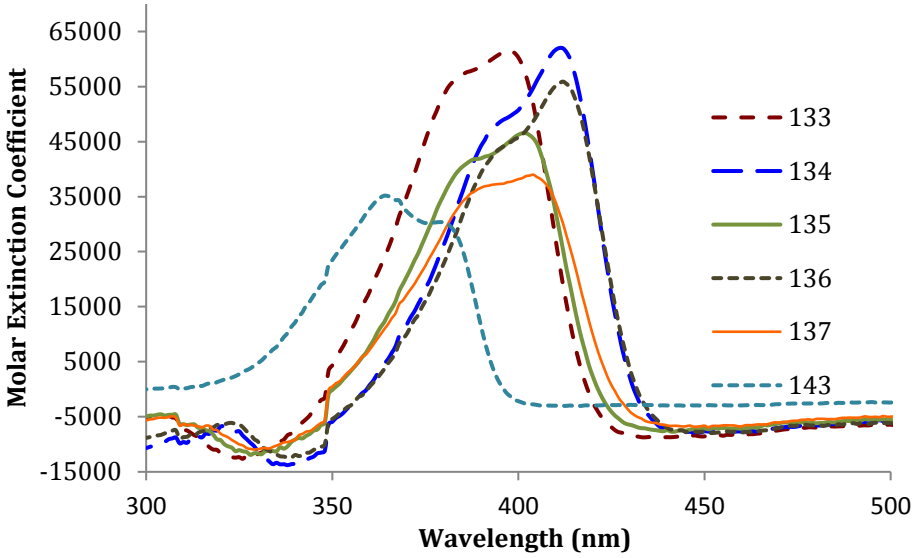

Figure 5.4: UV-visible spectra of benzyloxy diketone boron complexes **133-137** in CH_2Cl_2.

The UV-visible spectra of the hydroxy boron complexes **138-141** recorded in dichloromethane are shown in Figure 5.5. All hydroxy boron complexes show a hypsochromic shift compared to their benzyloxy and methoxy analogues. Lower molar extinction coefficients were observed compared to the corresponding members of the methoxy and benzyloxy series.

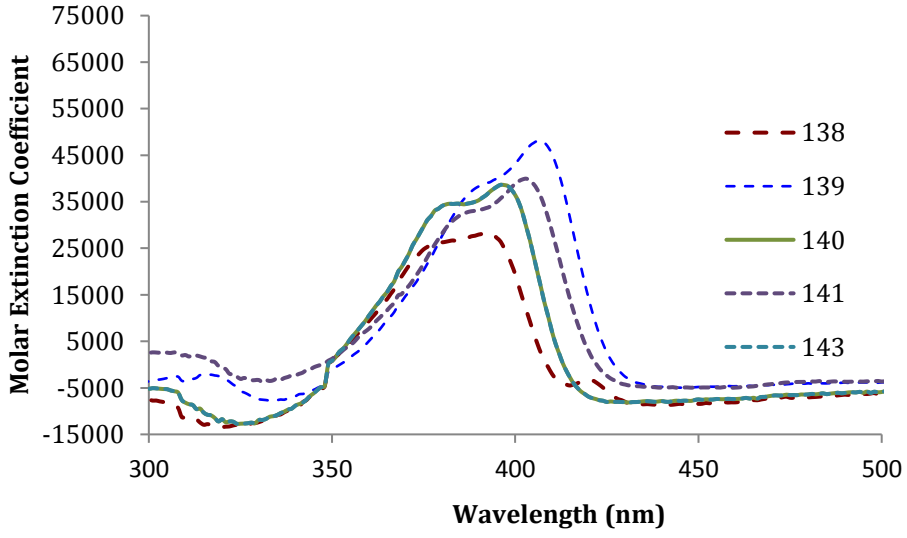

Figure 5.5: UV-visible spectra of hydroxy diketone boron complexes **138-141** in CH_2Cl_2.

The normalised fluorescence emission spectra of the methoxy series of boron complexes are shown in Figure 5.6. The fluorescence emission peaks of methoxy boron complexes **122-125**

were observed in the range of 430-440 nm with a Stokes shift of 29-34 nm. The mono-functionalised complex **122** shows the maximum quantum yield of 0.429, while the bromo complex **125** shows the lowest quantum yield of 0.238. The introduction of a second methoxy group in compound **123** lowered the quantum yield.

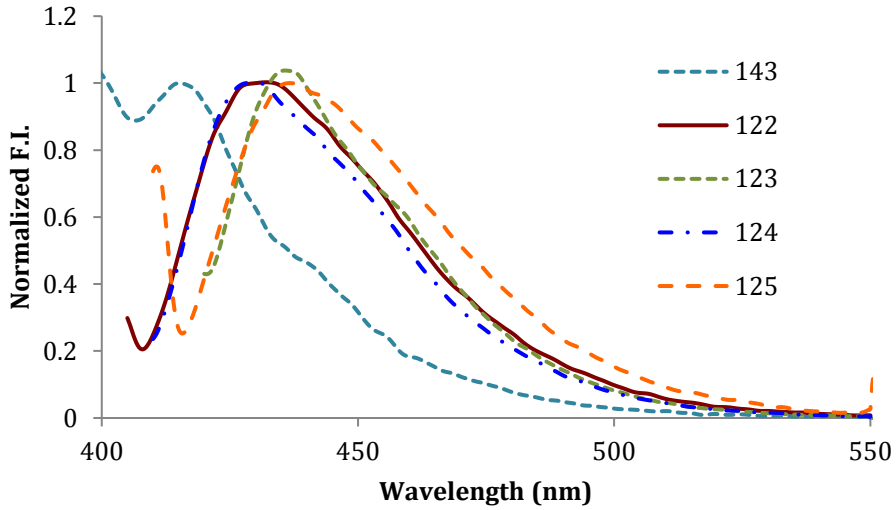

Figure 5.6: Normalised fluorescence spectra of methoxy boron complexes **122-125** in CH_2Cl_2.

The normalised fluorescence emission spectra of the benzyloxy series of boron complexes are shown in Figure 5.7. The fluorescence emission peaks of benzyloxy boron complexes **133-137** were observed in the range 434-440 nm with a Stokes shift in the range of 26-36 nm. The quantum yield of benzyloxy complexes were found in the range of 0.327-0.346. The introduction of a second strongly electron donating group, either in the form of a methoxy group **134** or benzyloxy group **136** lowered the quantum yield.

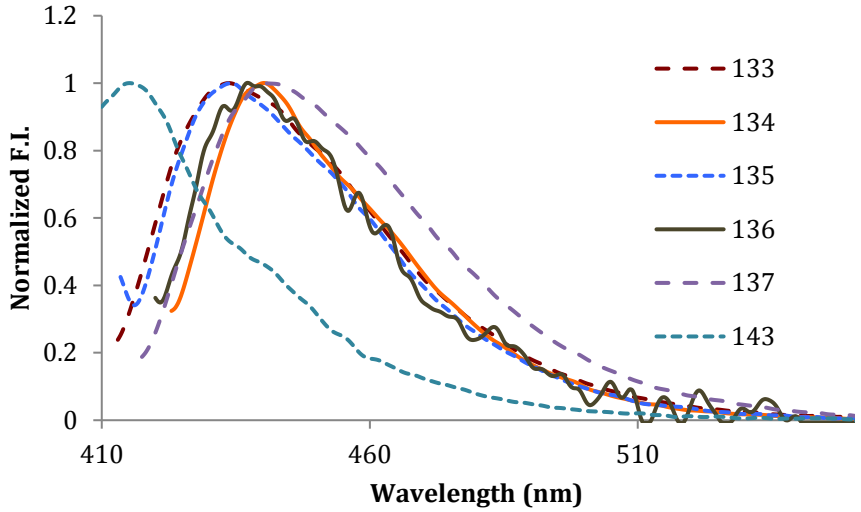

Figure 5.7: Normalised fluorescence spectra of benzyloxy boron complexes **133-137** in CH_2Cl_2.

The normalised fluorescence emission spectra of the hydroxy series of boron complexes are shown in Figure 5.8. The fluorescence emission peaks of hydroxy boron complexes **138-141** were observed at lower wavelengths (420-432 nm) compared to the two former series, with a Stokes shift of 25-28 nm. Compound **139**, bearing a methoxy substituent, emits at the longest wavelength in this series (432 nm) and shows a maximum quantum yield of 0.444.

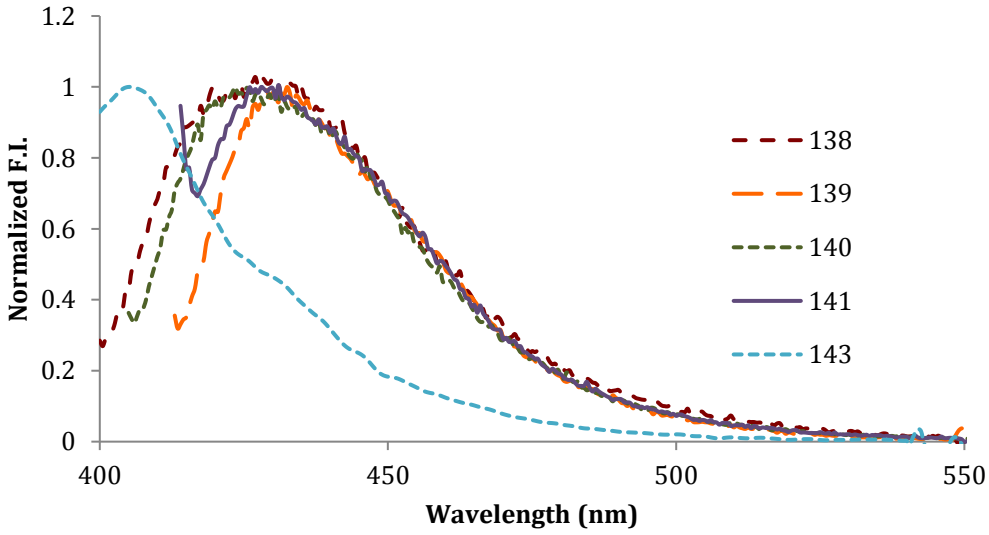

Figure 5.8: Normalised fluorescence spectra of hydroxy boron complexes **138-141** in CH_2Cl_2.

5.4 Conclusions

In this Chapter, the syntheses and absorption and emission properties of three series of 1,3-diketone boron complexes were described. The methoxy series were synthesised in order to supplement the data associated with related compounds already in the literature, and they also served as a reference series for comparisons with the benzyloxy and hydroxy series. The benzyloxy boron complexes were prepared *en route* to the synthesis of hydroxy boron complexes. The photo-physical properties such as UV-visible absorbance, fluorescence emission and relative quantum yield of all three series were studied. In the future, the binding behavior of the hydroxy boron complexes with tin(IV) porphyrins will be studied.

5.5 Experimental

5.5.1 Materials and Methods

The materials and methods used in this Chapter are as described in Sections 2.7.1 and 3.5.1, with the following variations.

The relative quantum yield (Φ) was calculated by using quinine sulfate as a reference.[11] Quinine sulfate (Φ_{ST} = 0.54, $\lambda_{excitation}$ 350 nm) was dissolved in 0.1 M H_2SO_4 (refractive index: 1.33)[12] and all the compounds were dissolved in dichloromethane (refractive index: 1.42)[12]. The relative quantum yield was calculated according to the following equation:

$$\Phi_X = \Phi_{ST}\left(\frac{m_X}{m_{ST}}\right)\left(\frac{\eta_X^2}{\eta_{ST}^2}\right)$$

Where Φ is the fluorescence quantum yield, *m* is the slope of the plot of integrated fluorescence intensity versus absorbance, and η is the refractive index of the solvent. The subscript ST and X refer to the reference and sample compounds, respectively. Excitation and emission slit widths were set at 2.5 nm when recording their fluorescence spectra.

5.5.2 Preparation of 1,3-Diketone Ligands and Their Boron Complexes

General Procedure for Ligand Preparation: A substituted acetophenone (1 eq.) was added to a mixture of sodium hydride (60% in oil, 2 eq.) in dimethoxyethane (40 mL), followed by the addition of a substituted methyl benzoate (1 eq.). The reaction mixture was heated at reflux overnight. Upon cooling to room temperature, ice (20 mL) was added to the reaction mixture, which was then acidified by the addition of hydrochloric acid (3 M, 20 mL). The aqueous layer was extracted with dichloromethane (2 x 50 mL) and the combined organic layers were washed with brine (100 mL), dried over anhydrous sodium sulfate, filtered and evaporated to dryness. The crude product was purified using column chromatography (silica gel).

General Procedure for Boron Complex Preparation: Boron trifluoride diethyl etherate (1 eq.) was added to a mixture of methoxy or benzyloxy diketone **115-118** or **125-129** in dichloromethane (15 mL), and the mixture was heated at reflux for 30 mins. On cooling, the reaction mixture was filtered and washed with hexane (20 mL) to obtain the boron complex. The crude boron difluoride methoxy diketonate **119-122** was obtained as a solid and used without purification. The crude boron difluoride benzyloxy diketonate **130-134** was purified using column chromatography (silica gel).

General Procedure for Hydroxy Boron Complex Preparation: A mixture of boron difluoride benzyloxy diketonate **130-134** and palladium on carbon (10%, 10 mg) in ethanol (5 mL) was stirred for 24 h under an atmosphere of hydrogen gas at atmospheric pressure. On completion, the reaction mixture was filtered over celite and ethanol was removed under vacuum to obtain the crude product that was purified using column chromatography (silica gel, dichloromethane / ethyl acetate 9:1).

Methoxy Series

1-(4-Methoxyphenyl)-1-phenylpropane-1,3-dione 118

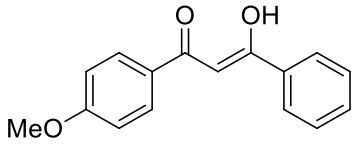

Starting with methyl benzoate (1.0 g, 7.35 mmol) and 4'-methoxyacetophenone (1.10 g, 7.35 mmol), the crude material was chromatographed (silica gel, dichloromethane/hexane 1:1) to afford **118** (1.07 g, 57%) as a beige solid. m.p. 128-129 °C (lit.[13] 127-128 °C). ^{1}H NMR (400 MHz, $CDCl_3$) δ 3.88 (s, 3H, OCH_3), 6.80 (s, 1H, CH), 6.98 (d, 2H, *J* = 9.0 Hz, ArH), 7.48-7.54 (m, 3H, ArH), 7.96-8.00 (m, 4H, ArH), 16.97 (s, 1H, OH) ppm. The spectroscopic data are in agreement with those reported in the literature.[13]

1,3-Bis(4-methoxyphenyl)propane-1,3-dione 119

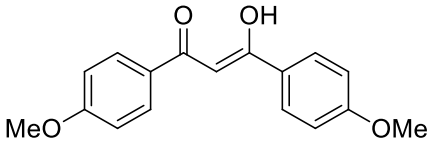

Starting with methyl 4-methoxybenzoate (1.22 g, 7.35 mmol) and 4'-methoxyacetophenone (1.1 g, 7.35 mmol), the crude material was chromatographed (silica gel, dichloromethane/hexane 1:1) to afford **119** (1.10 g, 52%) as a pale yellow solid. m.p. 114-115 °C (lit.[2] 114 °C). ^{1}H NMR (400 MHz, $CDCl_3$) δ 3.88 (s, 6H, OCH_3), 6.73 (s, 1H, CH), 6.97 (d, 4H, *J* = 8.1 Hz, ArH), 7.95 (d, 4H, *J* = 8.1 Hz, ArH), 17.12 (s, 1H, OH) ppm. The spectroscopic data are in agreement with those reported in the literature.[2]

1-(4-Methoxyphenyl)-3-(*p*-tolyl)propane-1,3-dione 120

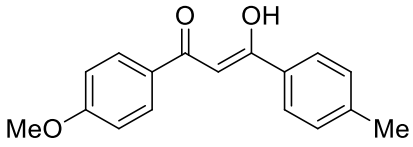

Starting with methyl 4-methylbenzoate (1.50 g, 10 mmol) and 4'-methoxyacetophenone (1.50 g, 10 mmol), the crude material was chromatographed (silica gel, dichloromethane/hexane 1:1) to

afford **120** (1.36 g, 53%) as a white solid. m.p. 103-104 °C (lit.[14] 104 °C). ^{1}H NMR (400 MHz, $CDCl_3$) δ 2.42 (s, 3H, CH_3), 3.88 (s, 3H, OCH_3), 6.77 (s, 1H, CH), 6.98 (d, 2H, *J* = 8.3 Hz, ArH), 7.28 (d, 2H, *J* = 7.9 Hz, ArH), 7.87 (d, 2H, *J* = 7.9 Hz, ArH), 7.97 (d, 2H, *J* = 8.3 Hz, ArH), 17.04 (s, 1H, OH) ppm. ^{13}C NMR (100 MHz, $CDCl_3$) δ 21.6, 55.5, 92.0, 113.9, 127.0, 128.3, 129.2, 129.3, 131.3, 132.8, 163.1, 184.4, 185.7 ppm. FTIR 615, 636, 670, 699, 733, 780, 842, 992, 1025, 1086, 1120, 1173, 1227, 1255, 1306, 1411, 1497, 1524, 1582, 3320 cm^{-1}. Elemental analysis for $C_{22}H_{16}BBrF_2O_3$: Calcd C 76.10; H 6.01. Found: C 76.27; H 6.03. Mass M^+ -19: 249.

1-(4-Bromophenyl)-3-(4-methoxyphenyl)propane-1,3-dione 121

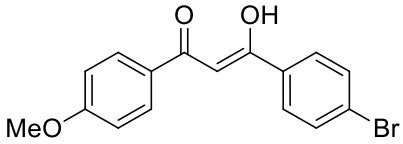

Starting with methyl 4-bromobenzoate (1.5 g, 7.0 mmol) and 4'-methoxyacetophenone (1.05 g, 7.0 mmol), the crude material was chromatographed (silica gel, dichloromethane/hexane 1:1) to afford **121** (0.82 g, 49%) as a white solid. m.p. 150-151 °C (lit.[15] 150-153 °C). ^{1}H NMR (400 MHz, $CDCl_3$) δ 3.88 (s, 3H, OCH_3), 6.74 (s, 1H, CH), 6.98 (d, 2H, *J* = 8.6 Hz, ArH), 7.61 (d, 2H, *J* = 8.2 Hz, ArH), 7.83 (d, 2H, *J* = 8.2 Hz, ArH), 7.97 (d, 2H, *J* = 8.6 Hz, ArH), 16.92 (s, 1H, OH) ppm. The spectroscopic data are in agreement with those reported in the literature.[15]

Boron difluoride 1-(4-methoxyphenyl)-1-phenylpropane-1,3-diketonate 122

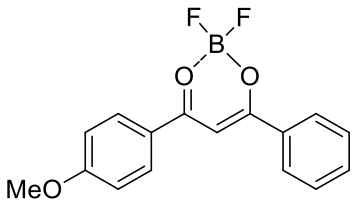

Starting with **118** (600 mg, 2.34 mmol), to afford **122** (655 mg, 92%) as a green solid. m.p. 216-217 °C (lit.[2] 216 °C). ^{1}H NMR (400 MHz, $CDCl_3$) δ 3.93 (s, 3H, OCH_3), 7.02-7.05 (m, 2H, ArH), 7.10 (s, 1H, CH), 7.54-7.66 (m, 2H, ArH), 7.65-7.70 (m, 1H, ArH), 8.11-8.16 (m, 4H,

ArH) ppm. λ_{max} (CH_2Cl_2) 397, 387 nm (log ε 4.74, 4.71). The spectroscopic data are in agreement with those reported in the literature.[2]

Boron difluoride 1,3-bis(4-methoxyphenyl)propane-1,3-diketonate 123

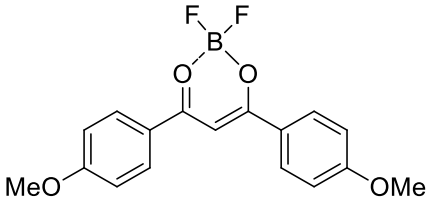

Starting with **119** (400 mg, 1.45 mmol), to afford **123** (433 mg, 93%) as a fluorescent yellow solid. m.p. 236-237 °C (lit.[2] 236 °C). ^{1}H NMR (400 MHz, $CDCl_3$) δ 3.92 (s, 6H, OCH_3), 7.17 (d, 4H, *J* = 9.0 Hz, ArH), 7.73 (s, 1H, CH), 8.12 (d, 4H, *J* = 9.0 Hz, ArH) ppm. λ_{max} (CH_2Cl_2) 411, 399 nm (log ε 4.84, 4.70). The spectroscopic data are in agreement with those reported in the literature.[2]

Boron difluoride 1-(4-methoxyphenyl)-3-(*p*-tolyl)propane-1,3-diketonate 124

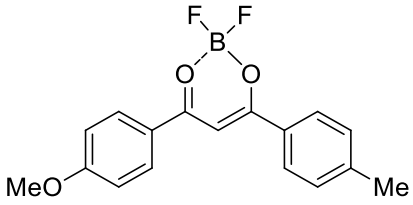

Starting with **120** (340 mg, 1.26 mmol), to afford **124** (358 mg, 89%) as a yellow solid. m.p. 230-231 °C. ^{1}H NMR (400 MHz, $CDCl_3$) δ 2.46 (s, 3H, CH_3), 3.92 (s, 3H, OCH_3), 7.01 (d, 2H, *J* = 7.8 Hz, ArH), 7.06 (s, 1H, CH), 7.33 (d, 2H, *J* = 7.7 Hz, ArH), 8.02 (d, 2H, *J* = 7.8 Hz, ArH), 8.13 (d, 2H, *J* = 7.7 Hz, ArH) ppm. ^{13}C NMR (100 MHz, $CDCl_3$) δ 21.9, 55.8, 92.1, 114.6, 124.3, 128.8, 129.6, 129.9, 131.5, 146.3, 165.6, 181.5, 181.7 ppm. FTIR 632, 701, 729, 747, 785, 842, 949, 1024, 1063, 1092, 1126, 1170, 1216, 1245, 1270, 1313, 1366, 1491, 1544, 1606 cm^{-1}. λ_{max} (CH_2Cl_2) 401, 389 nm (log ε 4.70, 4.65). Elemental analysis for $C_{22}H_{16}BBrF_2O_3$: Calcd. C 64.59; H 4.78. Found: C 64.73; H 4.83. Mass M^+ -19: 297.

Boron difluoride 1-(4-bromophenyl)-3-(4-methoxyphenyl)propane-1,3-diketonate 125

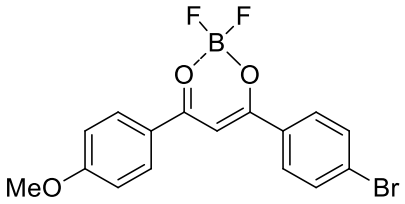

Starting with **121** (150 mg, 0.45 mmol), to afford **125** (165 mg, 96%) as a yellow solid. m.p. 219-220 °C. ^{1}H NMR (400 MHz, $CDCl_3$) δ 3.94 (s, 3H, OCH_3), 7.04 (d, 2H, *J* = 7.0 Hz, ArH), 7.05 (s, 1H, CH), 7.68 (d, 2H, *J* = 6.8 Hz, ArH), 7.97 (d, 2H, *J* = 6.8 Hz, ArH), 8.15 (d, 2H, *J* = 7.0 Hz, ArH) ppm. ^{13}C NMR (100 MHz, $CDCl_3$) δ 55.9, 92.4, 114.8, 124.0, 129.9, 130.1, 131.2, 131.8, 132.5, 166.3, 180.2, 182.8 ppm. FTIR 628, 699, 731, 759, 788, 843, 947, 1006, 1025, 1082, 1094, 1154, 1162, 1241, 1273, 1309, 1363, 1403, 1479, 1505, 1544, 1588 cm^{-1}. λ_{max} (CH_2Cl_2) 404, 393 nm (log ε 4.62, 4.61). Elemental analysis for $C_{22}H_{16}BBrF_2O_3$: Calcd. C 50.44; H 3.17. Found: C 50.65; H 3.32. Mass M^+ -19: 361.

Benzyloxy Series

4'-Benzyloxyacetophenone 126

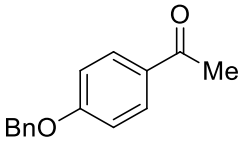

Benzyl bromide (5.13 g, 30.0 mmol) was added to a mixture of 4'-hydroxyacetophenone (5.0 g, 36.8 mmol) in acetone (50 mL). Potassium carbonate (10.0 g) was added to the reaction mixture that was heated at reflux for 4 days. On cooling, acetone was evaporated under *vacuo* and the residue was dissolved in dichloromethane (100 mL) and water (100 mL). The organic layer was washed with aqueous sodium hydroxide (3 M, 2 x 50 mL), brine (50 mL), dried over anhydrous sodium sulfate, filtered and evaporated to dryness under *vacuo*. 4'-Benzyloxyacetophenone **126** (7.47 g, 90%) was obtained as a white solid and used without any further purification. m.p. 83-84 °C (lit.[16] 82-83 °C). ^{1}H NMR (400 MHz, $CDCl_3$) δ 2.55 (s, 3H,

CH_3), 5.13 (s, 2H, OCH_2), 7.00-7.02 (m, 2H, ArH), 7.34-7.44 (m, 5H, ArH), 7.92-7.95 (m, 2H, ArH) ppm. The spectroscopic data are in agreement with those reported in the literature.[16]

Methyl 4-benzyloxybenzoate 127

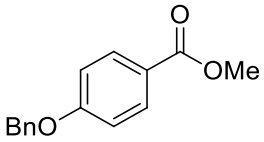

Benzyl bromide (5.63 g, 32.9 mmol) was added to methyl 4-hydroxybenzoate (5.0 g, 32.9 mmol) in acetone (50 mL). Potassium carbonate (10 g) was added to the reaction mixture that was then heated at reflux for 4 days. On cooling, acetone was evaporated under *vacuo* and the residue was dissolved in dichloromethane (100 mL) and water (100 mL). The organic layer was washed with aqueous sodium hydroxide (3M, 2 x 50 mL), brine (50 mL), dried over anhydrous sodium sulfate, filtered and evaporated to dryness under *vacuo*. Methyl 4-(benzyloxy)benzoate **127** (7.62 g, 96%) as obtained as a white solid and used without any further purification. m.p. 91-92 °C (lit.[17] 90 °C). ^{1}H NMR (400 MHz, $CDCl_3$) δ 3.88 (s, 3H, CO_2CH_3), 5.12 (s, 2H, OCH_2), 6.97-7.01 (m, 2H, ArH), 7.32-7.44 (m, 5H, ArH), 7.97-8.01 (m, 2H, ArH) ppm. The spectroscopic data are in agreement with those reported in the literature.[18]

1-(4-Benzyloxyphenyl)-3-phenylpropane-1,3-dione 128

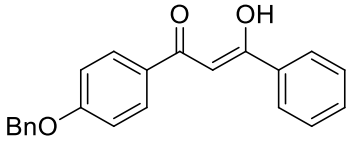

Starting with methyl benzoate (1.00 g, 7.35 mmol) and 4'-benzyloxyacetophenone **126** (1.66 g, 7.35 mmol), the crude product was chromatographed (silica gel, dichloromethane/hexane 1:1) to afford **128** (1.15 g, 48%) as a beige solid. m.p. 84-86 °C. ^{1}H NMR (400 MHz, $CDCl_3$) δ 5.15 (s, 2H, OCH_2), 6.79 (s, 1H, CH), 7.04-7.08 (m, 2H, ArH), 7.36-7.54 (m, 8H, ArH), 7.96-7.99 (m, 4H, ArH), 16.97 (s, 1H, OH) ppm. ^{13}C NMR (100 MHz, $CDCl_3$) δ 70.2, 92.4, 114.9, 127.0, 127.5, 128.2, 128.4, 128.6, 128.7, 129.3, 132.2, 135.5, 136.2, 162.3, 184.1, 186.1 ppm. FTIR 611, 634, 680, 723, 765, 798, 836, 1023, 1060, 1118, 1175, 1225, 1259, 1303, 1360, 1453, 1497,

1590 cm^{-1}. Elemental analysis for $C_{22}H_{18}O_3$: Calcd. C 79.98; H 5.49. Found: C 80.29; H 5.80. Mass M^+ +1: 331.

1-(4-Benzyloxyphenyl)-3-(4-methoxyphenyl)propane-1,3-dione 129

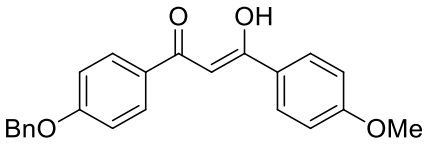

Starting with methyl 4-methoxybenzoate (1.55 g, 7.0 mmol) and 4'-benzyloxyacetophenone **126** (1.59 g, 7.0 mmol), the crude material was chromatographed (silica gel, dichloromethane/hexane 1:1) to afford **129** (0.74 g, 30%) as a white solid. m.p. 112-114 °C. ^{1}H NMR (400 MHz, $CDCl_3$) δ 3.88 (s, 3H, OCH_3), 5.14 (s, 2H, OCH_2), 6.73 (s, 1H, CH), 6.97 (d, 2H, *J* = 8.9 Hz, ArH), 7.05 (d, 2H, *J* = 8.9 Hz, ArH), 7.35-7.46 (m, 5H, ArH), 7.96 (d, 4H, *J* = 8.9 Hz, ArH), 17.09 (br s, 1H, OH) ppm. ^{13}C NMR (100 MHz, $CDCl_3$) δ 55.5, 70.2, 91.5, 113.9, 114.8, 127.5, 128.2, 128.5, 128.7, 129.0, 129.1, 136.3, 138.2, 162.2, 169.7, 184.5, 184.7 ppm. FTIR 633, 649, 696, 729, 782, 819, 847, 1023, 1114, 1174, 1227, 1255, 1308, 1385, 1401, 1453, 1497, 1601 cm^{-1}. Elemental analysis for $C_{23}H_{20}O_4$: Calcd. C 76.65; H 5.59. Found: C 76.63; H 5.36. Mass M^+ +1: 361.

1-(4-Benzyloxyphenyl)-3-(*p*-tolyl)propane-1,3-dione 130

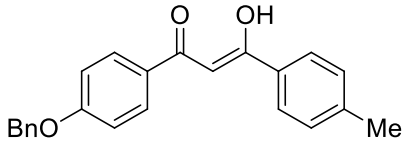

Starting with methyl 4-methylbenzoate (1.10 g, 7.35 mmol) and 4'-benzyloxyacetophenone **126** (1.66 g, 7.35 mmol), the crude material was chromatographed (silica gel, dichloromethane/hexane 1:1) to afford **130** (1.72 g, 69%) as a white solid. m.p. 126-128 °C. ^{1}H NMR (400 MHz, $CDCl_3$) δ 2.45 (s, 3H, CH_3), 5.13 (s, 2H, OCH_2), 6.77 (s, 1H, CH), 7.05 (d, 2H, *J* = 7.6 Hz, ArH), 7.28 (d, 2H, *J* = 7.6 Hz, ArH), 7.36-7.54 (m, 5H, ArH), 7.87 (d, 2H, *J* = 7.6 Hz, ArH), 7.96 (d, 2H, *J* = 7.6 Hz, ArH), 16.97 (s, 1H, OH) ppm. ^{13}C NMR (100 MHz, $CDCl_3$) δ 21.6, 70.2, 92.0, 114.8, 127.1, 127.5, 128.2, 128.5, 128.7, 129.2, 129.4, 132.9, 136.3, 142.9,

162.5, 184.5, 185.6 ppm. FTIR 647, 692, 720, 775, 835, 898, 1026, 1038, 1075, 117, 1176, 1208, 1228, 1256, 1300, 1388, 1452, 1495, 1536, 1587 cm^{-1}. Elemental analysis for $C_{23}H_{20}O_3$: Calcd. C 80.21; H 5.85. Found: C 79.78; H 5.36. Mass M^+ +1: 345.

1,3-Bis(4-benzyloxyphenyl)propane-1,3-dione 131

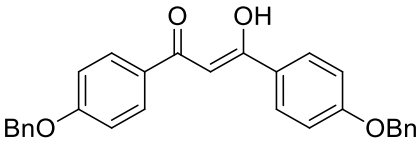

Starting with methyl 4'-benzyloxybenzoate **127** (1.5 g, 6.64 mmol) 4'-benzyloxyacetophenone **126** (1.6 g, 6.64 mmol), the crude material was chromatographed (silica gel, dichloromethane/hexane 1:1) to afford **131** (1.01 g, 35%) as a white solid. m.p. 164-166 °C. ^{1}H NMR (400 MHz, $CDCl_3$) δ 5.15 (s, 4H, OCH_2), 6.73 (s, 1H, CH), 7.05 (d, 4H, *J* = 8.9 Hz, ArH), 7.33-7.45 (m, 10H, ArH), 7.92 (d, 4H, *J* = 8.9 Hz, ArH), 17.08 (s, 1H, OH) ppm. ^{13}C NMR (100 MHz, $CDCl_3$) δ 70.2, 91.6, 114.8, 127.5, 128.2, 128.7, 129.1, 131.4, 136.3, 162.2, 184.6 ppm. FTIR 622, 698, 747, 781, 842, 863, 924, 998, 1085, 1118, 1173, 1222, 1247, 1301, 1377, 1454, 1495, 1598 cm^{-1}. Elemental analysis for $C_{29}H_{24}O_4$: Calcd. C 79.80; H 5.54. Found: C 79.88; H 5.31. Mass M^+ +1: 437.

1-(4-Benzyloxyphenyl)-3-(4-bromophenyl)propane-1,3-dione 132

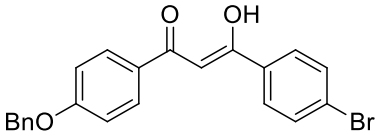

Starting with methyl 4-bromobenzoate (1.0 g, 4.67 mmol) and 4'-benzyloxyacetophenone **126** (1.06 g, 4.67 mmol), the crude material was chromatographed (silica gel, dichloromethane/hexane 1:1) to afford **132** (0.54 g, 28%) as a beige solid. m.p. 150-152 °C. ^{1}H NMR (400 MHz, $CDCl_3$) δ 5.15 (s, 2H, OCH_2), 6.75 (s, 1H, CH), 7.06 (d, 2H, *J* = 8.1 Hz, ArH), 7.33-7.45 (m, 5H, ArH), 7.61 (d, 2H, *J* = 7.8 Hz, ArH), 7.84 (d, 2H, *J* = 7.8 Hz, ArH), 7.97 (d, 2H, *J* = 8.1 Hz, ArH), 16.91 (s, 1H, OH) ppm. ^{13}C NMR (100 MHz, $CDCl_3$) δ 70.2, 92.3, 114.9, 126.9, 127.5, 128.2, 128.3, 128.4, 128.5, 128.7, 129.4, 131.9, 136.2, 162.5, 183.0, 186.2 ppm.

FTIR 629, 696, 739, 780, 820, 843, 916, 1005, 1071, 1112, 1172, 1221, 1253, 1303, 1378, 1452, 1501, 1581, 1601 cm^{-1}. Elemental analysis for $C_{22}H_{17}BrO_3$: Calcd. C 64.56; H 4.19. Found: 64.59, 3.97. Mass M^+ +1: 409.

Boron difluoride 1-(4-benzyloxyphenyl)-3-phenylpropane-1,3-diketonate 133

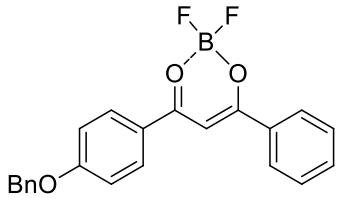

Starting with **128** (600 mg, 1.88 mmol), the crude material was chromatographed (silica gel, dichloromethane/hexane 3:1) to afford **133** (250 mg, 60%) as a yellow solid. m.p. 209-210 °C. ^{1}H NMR (400 MHz, $CDCl_3$) δ 5.19 (s, 2H, OCH_2), 7.08-7.12 (m, 3H, CH and ArH), 7.35-7.45 (m, 5H, ArH), 7.52-7.56 (m, 2H, ArH), 7.64-7.66 (m, 1H, ArH), 8.10-8.16 (m, 4H, ArH) ppm. ^{13}C NMR (100 MHz, $CDCl_3$) δ 70.5, 92.5, 115.5, 124.4, 127.6, 128.5, 128.7, 128.8, 129.1, 131.7, 132.2, 134.7, 135.6, 164.9, 181.7, 182.3 ppm. FTIR 613, 631, 679, 700, 750, 766, 804, 851, 921, 950, 987, 1036, 1069, 1096, 1130, 1181, 1238, 1262, 1309, 1362, 1388, 1426, 1487, 1521, 1603 cm^{-1}. λ_{max} (CH_2Cl_2) 397, 387 nm (log ε 4.79, 4.76). Elemental analysis for $C_{22}H_{17}BF_2O_3$: Calcd. C 69.87; H 4.53. Found: C 69.54; H 4.22. Mass M^+ -19: 359.

Boron difluoride 1-(4-benzyloxyphenyl)-3-(4-methoxyphenyl)propane-1,3-diketonate 134

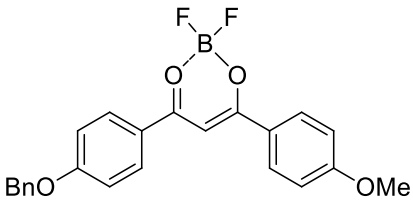

Starting with **129** (500 mg, 1.35 mmol), the crude material was chromatographed (silica gel, dichloromethane/hexane 3:1) to afford **134** (180 mg, 32%) as a greenish-yellow solid. m.p. 211-212 °C. ^{1}H NMR (400 MHz, $CDCl_3$) δ 3.92 (s, 3H, OCH_3), 5.18 (s, 2H, OCH_2), 7.00 (s, 1H, CH), 7.01-7.09 (m, 4H, ArH), 7.39-7.43 (m, 5H, ArH), 8.11-8.13 (m, 2H, ArH), 8.18-8.20 (m, 2H, ArH) ppm. ^{13}C NMR (100 MHz, $CDCl_3$) δ 55.7, 70.5, 91.5, 114.6, 115.4, 124.5, 124.7, 127.6, 128.5, 128.8, 131.23, 131.25, 135.7, 164.4, 165.3, 180.7, 180.9 ppm. FTIR 637, 695, 738,

804, 842, 910, 949, 1029, 1068, 1095, 1178, 1243, 1263, 1306, 1373, 1421, 1496, 1527, 1560, 1605 cm^{-1}. λ_{max} (CH_2Cl_2) 411, 398 nm (log ε 4.79, 4.69). Elemental analysis for $C_{23}H_{19}BF_2O_4$: Calcd. C 67.67; H 4.69. Found: C 67.77; C 4.45. Mass M^+ -19: 389.

Boron difluoride 1-(4-benzyloxyphenyl)-3-(*p*-tolyl)propane-1,3-diketonate 135

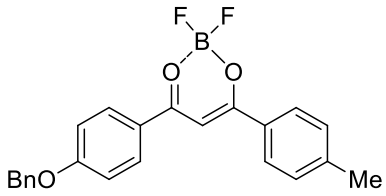

Starting with **130** (350 mg, 1.02 mmol), the crude material was chromatographed (silica gel, dichloromethane) to afford **135** (123 mg, 30%) as a yellow solid. m.p. 213-214 °C. ^{1}H NMR (400 MHz, $CDCl_3$) δ 2.47 (s, 3H, CH_3), 5.19 (s, 2H, OCH_2), 7.06 (s, 1H, CH), 7.09 (d, 2H, *J* = 9.0 Hz, ArH), 7.34 (d, 2H, *J* = 8.2 Hz, ArH), 7.36-7.43 (m, 5H, ArH), 8.03 (d, 2H, *J* = 8.2 Hz, ArH), 8.14 (d, 2H, *J* = 9.0 Hz, ArH) ppm. ^{13}C NMR (100 MHz, $CDCl_3$) δ 21.9, 70.5, 92.1, 115.4, 124.5, 127.5, 128.5, 128.8, 129.5, 129.9, 131.5, 135.6, 164.6, 164.64, 181.5, 181.6 ppm. FTIR 636, 692, 730, 800, 842, 951, 1033, 1069, 1093, 1123, 1180, 1250, 1267, 1318, 1367, 1496, 1527, 1550, 1605 cm^{-1}. λ_{max} (CH_2Cl_2) 402, 390 nm (log ε 4.67, 4.60). Elemental analysis for $C_{23}H_{19}BF_2O_3$: Calcd. C 70.43; H 4.88. Found: C 70.75; H 4.84. Mass M^+ -19: 373.

Boron difluoride 1,3-bis(4-benzyloxyphenyl)propane-1,3-diketonate 136

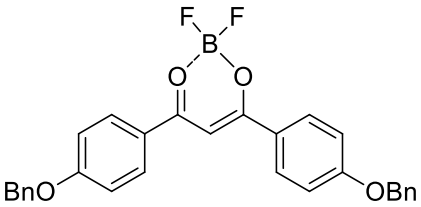

Starting with **131**, the crude material was chromatographed (silica gel, dichloromethane/hexane 3:1) to afford **136** (120 mg, 22%) as a yellow solid. m.p. 225-226 °C. ^{1}H NMR (400 MHz, $CDCl_3$) δ 5.18 (s, 4H, OCH_2), 7.00 (s, 1H, CH), 7.08 (d, 4H, *J* = 9.1 Hz, ArH), 7.40-7.45 (m, 10H, ArH), 8.19 (d, 4H, *J* = 9.1 Hz, ArH) ppm. ^{13}C NMR (100 MHz, $CDCl_3$) δ 70.4, 91.6, 115.4, 124.7, 127.5, 128.5, 128.8, 131.3, 135.7, 164.4, 180.8 ppm. FTIR 619, 693, 738, 805,

843, 908, 949, 1006, 1033, 1068, 1094, 1121, 1176, 1242, 1315, 1374, 1422, 1453, 1498, 1526, 1567, 1605 cm^{-1}. λ_{max} (CH_2Cl_2) 412, 399 nm (log ε 4.75, 4.66). Elemental analysis for $C_{29}H_{23}BF_2O_4$: Calcd. C 71.92; H 4.79. Found: C 71.59; H 4.47. Mass M^+ -19: 465.

Boron difluoride 1-(4-benzyloxyphenyl)-3-(4-bromophenyl)propane-1,3-diketonate 137

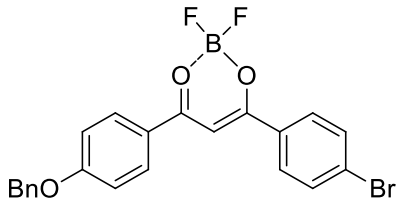

Starting with **132** (410 mg, 1.0 mmol), the crude material was chromatographed (silica gel, dichloromethane/hexane 3:1) to afford **137** (170 mg, 37%) as a yellow solid. m.p. 230-231 °C. ^{1}H NMR (400 MHz, $CDCl_3$) δ 5.20 (s, 2H, OCH_2), 7.05 (s, 1H, CH), 7.11 (d, 2H, *J* = 8.1 Hz, ArH), 7.36-7.43 (m, 5H, ArH), 7.69 (d, 2H, *J* = 7.9 Hz, ArH), 7.97 (d, 2H, *J* = 7.9 Hz, ArH), 8.15 (d, 2H, *J* = 8.1 Hz, ArH) ppm. ^{13}C NMR (100 MHz, $CDCl_3$) δ 70.6, 92.4, 115.6, 121.4, 127.5, 128.5, 128.8, 129.9, 130.2, 131.8, 132.5, 133.8, 135.4, 169.4, 182.2, 182.6 ppm. FTIR 625, 693, 732, 802, 844, 906, 951, 1004, 1033, 1067, 1094, 1119, 1176, 1244, 1268, 1321, 1365, 1407, 1483, 1502, 1523, 1553, 1605 cm^{-1}. λ_{max} (CH_2Cl_2) 404, 393 nm (log ε 4.59, 4.57). Elemental analysis for $C_{22}H_{16}BBrF_2O_3$: Calcd. C 57.81; H 3.53. Found: C 58.15; H 3.83. Mass M^+ -19: 437.

Hydroxy Series

Boron difluoride 1-(4-hydroxyphenyl)-3-phenylpropane-1,3-diketonate 138

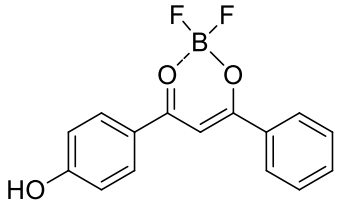

Starting with **133** (50 mg, 0.15 mmol), **138** (24 mg, 63%) was obtained as a bright yellow solid. m.p. 209-211 °C. ^{1}H NMR (400 MHz, DMSO-d_6) δ 6.99 (d, 2H, *J* = 8.1 Hz, ArH), 7.62-7.66

(m, 2H, ArH), 7.76-7.79 (m, 2H, ArH and CH), 8.30-8.33 (m, 4H, ArH) ppm. ^{13}C NMR (100 MHz, DMSO-d_6) δ 93.1, 116.5, 121.6, 128.7, 129.3, 131.8, 132.8, 135.0, 165.7, 179.5, 181.8 ppm. FTIR 686, 709, 774, 809, 844, 945, 1019, 1092, 1111, 1177, 1215, 1244, 1295, 1355, 1437, 1487, 1510, 1543, 1606, 3473 (sharp, OH) cm^{-1}. λ_{max} (CH_2Cl_2) 392, 379 nm (log ε 4.45, 4.43). Elemental analysis for $C_{15}H_{11}BF_2O_3$: Calcd. C 62.54; H 3.85. Found: C 62.82; H 4.10. Mass M^+ -19: 269. The spectroscopic data are in agreement with those reported in the literature.[19]

Boron difluoride 1-(4-hydroxyphenyl)-3-(4-methoxyphenyl)propane-1,3-diketonate 139

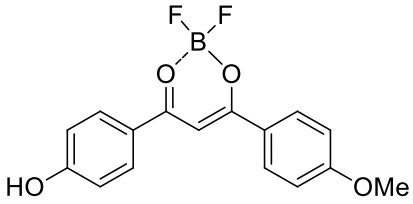

Starting with **134** (60 mg, 0.15 mmol), **139** (40 mg, 85%) was obtained as a bright yellow solid. m.p. 225-227 °C. ^{1}H NMR (400 MHz, DMSO-d_6) δ 3.91 (s, 3H, OCH_3), 6.96 (d, 2H, *J* = 7.9 Hz, ArH), 7.17 (d, 2H, *J* = 8.1 Hz, ArH), 7.65 (s, 1H, CH), 8.25 (d, 2H, *J* = 8.1 Hz, ArH), 8.31 (d, 2H, *J* = 7.9 Hz, ArH) ppm. ^{13}C NMR (100 MHz, DMSO-d_6) δ 55.9, 91.9, 114.8, 116.4, 121.9, 123.9, 131.5, 132.3, 135.3, 165.1, 179.9, 180.2 ppm. FTIR 635, 704, 795, 841, 947, 1023, 1093, 1172, 1239, 1269, 1301, 1368, 160, 1493, 1543, 1601, 3611 cm^{-1}. λ_{max} (CH_2Cl_2) 406, 393 nm (log ε 4.68, 4.56). Elemental analysis for $C_{16}H_{13}BF_2O_4$: Calcd. C 60.42; H 4.12. Found: C 60.19; H 4.34. Mass M^+ -19: 299.

Boron difluoride 1-(4-hydroxyphenyl)-3-(*p*-tolyl)propane-1,3-diketonate 140

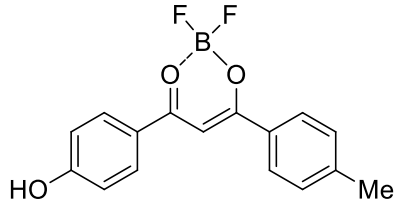

Starting with **135** (50 mg, 0.13 mmol), **140** (28 mg, 74%) was obtained as a bright yellow solid. m.p. 242-244 °C. ^{1}H NMR (400 MHz, DMSO-d_6) δ 2.44 (s, 3H, CH_3), 6.97 (d, 2H, *J* = 8.9 Hz,

ArH), 7.45 (d, 2H, *J* = 8.3 Hz, ArH), 8.22 (s, 1H, CH), 8.25 (d, 2H, *J* = 8.3 Hz, ArH), 8.28 (d, 2H, *J* = 8.9 Hz, ArH) ppm. ^{13}C NMR (100 MHz, DMSO-d_6) δ 21.4, 92.6, 116.4, 121.9, 128.9, 129.0, 129.9, 132.6, 146.2, 165.3, 179.7, 181.3 ppm. FTIR 607, 658, 699, 730, 746, 795, 844, 948, 1029, 1091, 1173, 1244, 1307, 1362, 1492, 1532, 1606, 3544 cm^{-1}. λ_{max} (CH_2Cl_2) 403, 383 nm (log ε 4.60, 4.53). Elemental analysis for $C_{16}H_{13}BF_2O_3$: Calcd. C 63.62; H 4.34. Found: C 55.07; H 3.99. Mass M^+ -19: 283.

Boron difluoride 1,3-bis(4-hydroxyphenyl)propane-1,3-diketonate 141

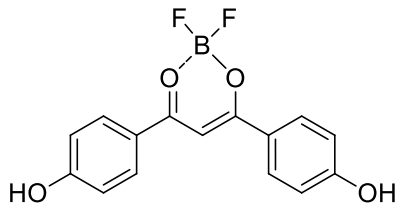

Starting with **136** (55 mg, 0.11 mmol), **141** (25 mg, 74%) was obtained as a bright yellow solid. m.p. 282-284 °C. ^{1}H NMR (400 MHz, DMSO-d_6) δ 6.95 (d, 4H, *J* = 8.8 Hz, ArH), 7.58 (s, 1H, CH), 8.22 (d, 4H, *J* = 8.8 Hz, ArH) ppm. ^{13}C NMR (100 MHz, DMSO-d_6) δ 91.6, 116.2, 122.2, 132.0, 164.6, 179.6 ppm. FTIR 639, 702, 791, 844, 1027, 1092, 1172, 1234, 1273, 1362, 1383, 1492, 1538, 1592, 3596 cm^{-1}. λ_{max} (CH_2Cl_2) 396, 387 nm (log ε 4.59, 4.51). Elemental analysis for $C_{15}H_{11}BF_2O_4.2H_2O$: Calcd. C 52.98; H 4.45. Found: C 52.71; H 4.36. Mass M^+ -19: 286.

1,3-Diphenylpropane-1,3-dione 142

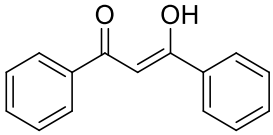

Starting with acetophenone (0.88 g, 7.3 mmol) and methyl benzoate (1.0 g, 7.3 mmol), the crude material was chromatographed (silica gel, dichloromethane/ethyl acetate 95:5) to afford **142** (0.77 g, 47%) as a white solid. m.p. 75-77 °C (lit.[15] 74-76 °C). ^{1}H NMR (400 MHz, $CDCl_3$) δ 6.87 (s, 1H, CH), 7.46-7.59 (m, 6H, ArH), 7.77-8.03 (m, 4H, ArH), 16.89 (br s, 1H, OH) ppm. The spectral data are in agreement with those reported in the literature.[15]

Boron difluoride 1,3-diphenylpropane-1,3-diketone 143

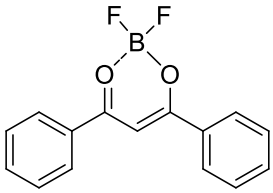

Starting with **142** (540 mg, 1.0 mmol), the crude material was chromatographed (silica gel, dichloromethane) to afford **143** (580 mg, 88%) as a yellow solid. m.p. 194-195 °C (lit.[5] 194-196 °C). ^{1}H NMR (400 MHz, DMSO d_6) δ 7.21 (s, 1H, CH), 7.53-7.59 (m, 4H, ArH), 7.68-7.73 (m, 2H, ArH), 8.14-8.18 (m, 4H, ArH) ppm. λ_{max} (CH_2Cl_2) 364, 382 nm (log ε 4.54, 4.47). The spectral data are in agreement with those reported in the literature.[5]

5.6 References

1. Zawadiak, J.; Mrzyczek, M. *Spectrochim. Acta, Part A* **2010**, *75* (2), 925-929.
2. Cognÿ-Laage, E.; Allemand, J.-F.; Ruel, O.; Baudin, J.-B.; Croquette, V.; Blanchard-Desce, M.; Jullien, L. *Chem. Eur. J.* **2004**, *10*, 1445-1455.
3. Ilge, H. D.; Birckner, E.; Fassler, D.; Kozmenko, M. V.; Kuzmin, M. G.; Hartmann, H. *J. Photochem.* **1986**, *32*, 177-189.
4. Natarajan, A.; Ng, D.; Yang, Z.; Garcia-Garibay, M. A. *Angew. Chem. Int. Ed.* **2007**, *46* (34), 6485-6487.
5. Ono, K.; Yoshikawa, K.; Tsuji, Y.; Yamaguchi, H.; Uozumi, R.; Tomura, M.; Taga, K.; Saito, K. *Tetrahedron* **2007**, *63*, 9354-9358.
6. Mirochnik, A. G.; Gukhman, E. V.; Karasev, V. E.; Zhikhareva, P. A. *Russ. Chem. Bull.* **2000**, *49* (6), 1024-1027.
7. Kumar, G. R.; Thilagar, P. *Dalton Trans.* **2014**, *43* (10), 3871-3879.
8. Mirochnik, A. G.; Fedorenko, E. V.; Gizzatulina, D. K.; Karasev, V. E. *Russ. J. Phys. Chem. A* **2007**, *81* (11), 1880-1883.
9. Mirochnik, A. G.; Bukvetskii, B. V.; Gukhman, E. V.; Zhikhareva, P. A.; Karasev, V. E. *Russ. Chem. Bull.* **2001**, *50* (9), 1612-1615.
10. Fallon, G. D.; Lee, M. A. P.; Langford, S. J.; Nichols, P. J. *Org. Lett.* **2002**, *4* (11), 1895-1898.
11. Crosby, G. A.; Demas, J. N. *J. Phy. Chem.* **1971**, *75* (8), 991-1024.
12. Reichardt, C. *Chem. Rev.* **1994**, *94* (8), 2319-2358.
13. Hubaud, J.; Bombarda, I.; Decome, L.; Wallet, J.; Gaydou, E. M. *J. Photochem. Photobiol., B* **2008**, *92*, 103-109.
14. Davis, B. R.; Hinds, M. G. *Aust. J. Chem.* **1997**, *50* (4), 309-320.

15. Nakaiida, S.; Kato, S.; Niyomura, O.; Ishida, M.; Ando, F.; Koketsu, J. *Phosphorus, Sulfur Silicon Relat. Elem.* **2010**, *185* (5-6), 930-946.

16. Chimenti, F.; Fioravanti, R.; Bolasco, A.; Chimenti, P.; Secci, D.; Rossi, F.; Yáñez, M.; Orallo, F.; Ortuso, F.; Alcaro, S. *J. Med. Chem.* **2009**, *52* (9), 2818-2824.

17. Haslam, E.; Haworth, R. D.; Mills, S. D.; Rogers, H. J.; Armitage, R.; Searle, T. *J. Chem. Soc.* **1961**, (0), 1836-1842.

18. Kuwano, R.; Kusano, H. *Org. Lett.* **2008**, *10* (10), 1979-1982.

19. Kevin, C. J.; Marder, S. R.; Kippelen, B. Polydioxaborines, their monomers and their preparation. WO03084968, **2003**.

Chapter Six

Supramolecular Assembly

6.1 Background

Supramolecular chemistry has been defined as "chemistry beyond the molecule",[1] and supramolecular interactions involve the reversible, non-covalent and spontaneous association of molecules. The self-assembly process has been widely used to construct porphyrin-containing systems that would be difficult to achieve with covalent bonds alone, and this is most frequently driven by co-ordination of suitable ligands to chelated metal ions of porphyrins.[2,3] One of the more common interactions is the binding of pyridines to zinc(II) porphyrins. This interaction is relatively weak, with a binding constant in the range of 10^3-10^4 M^{-1}.[4] An example of such an interaction is shown in Figure 1.11(a). As mentioned in Chapter Five, Section 5.1, two series of boron difluoride 1,3-diaryl-1,3-diketonates were prepared for use in supramolecular studies. The synthesis of the hydroxy-functionalised series (for future studies with tin(IV) porphyrins) is described in Chapter Five, and details on the synthesis of the 4'-pyridyl-functionalised series are given in Chapter Seven, as part of a manuscript for submission to *Tetrahedron*. One of the compounds in the 4'-pyridyl-functionalised series was **144**, shown below, and it was used in the work described in this Chapter in a supramolecular approach for the construction of a porphyrin-chromophore dyad.

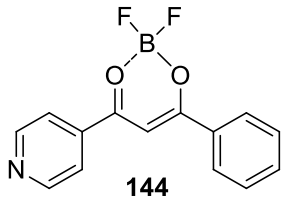

144

6.2 Results and Discussion

Porphyrin **145** was synthesised in an analogous fashion to porphyrin **2** (Scheme 2.4) by refluxing 4-*tert*-butylbenzaldehyde and pyrrole in propanoic acid for 1 h. Crude **145** was used without purification for synthesis of zinc(II) porphyrin **146**, that was obtained in 50% yield after chromatography (Scheme 6.1).

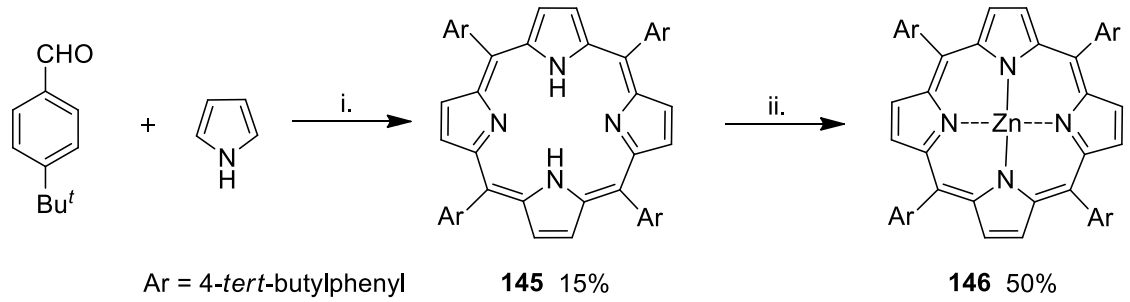

Ar = 4-*tert*-butylphenyl **145** 15% **146** 50%

Scheme 6.1: i. Propanoic acid, reflux; ii. $Zn(OAc)_2$, CH_2Cl_2, reflux.

Porphyrin **146** was chosen for the study due to its increased solubility in organic solvents in comparison to zinc(II) tetraphenylporphyrin, and decreased likelihood of unfavourable steric interactions that may be encountered with the zinc(II) derivative of porphyrin **2**, caused by the bulky 3,5-di-*tert*-butyl groups on the *meso* phenyl rings. **144** was chosen as the ligand for this work as it is a 4'-pyridyl-functionalised boron difluoride 1,3-diketonate that lacks a substitutent on the phenyl ring, and can therefore serve as a reference material for future studies involving functionalised phenyl rings. **144** was also the only ligand used in the present study due to time constraints, but other members of the series (see Chapter Seven) will be examined as part of a future study.

A UV-visible titration experiment (Figure 6.1) was conducted to provide evidence of an interaction between the two species (zinc(II) porphyrin **146** and 4'-pyridyl functionalised boron difluoride 1,3-diketonate **144**) and to obtain an approximate value for the binding constant.

The experiment did not show an isosbestic point, however this is believed to be a result of the large absorbance of **144** at 350 nm, as this has a large effect on the UV spectra at high concentrations. The complex absorbed at 446 nm, which represents a bathochromic shift of 20 nm from the initial Soret band of **146**.

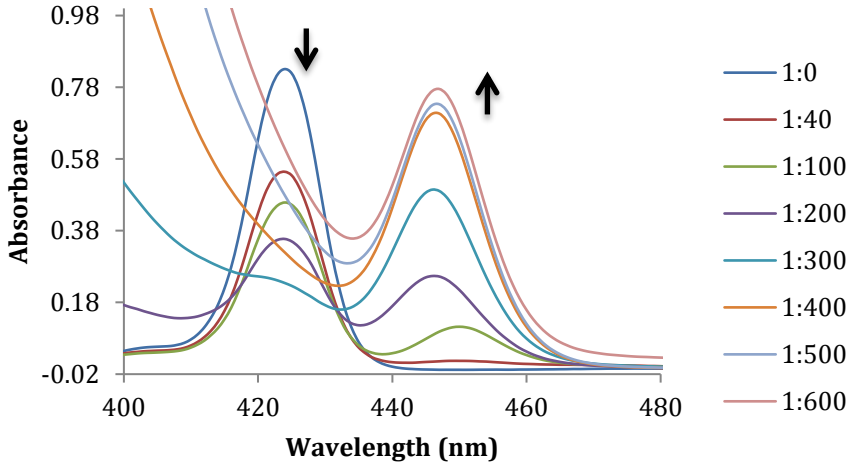

Figure 6.1: Changes in the absorption of **146** in chloroform at the Soret band region and at 446 nm (absorption maximum of the complex) upon increasing concentration of **144** (ratios of **146**:**144** are shown on the right of the Figure).

The binding constant was calculated using Equation 6.7 (page 190) and the data compiled in Table 6.1. A binding constant was calculated for solutions containing a mixture of **146**:**144** in the following ratios; 1:40, 1:100, 1:200 and 1:300, as these points are were less affected by the absorbance value of the free ligand at 446 nm, and then averaged. The binding constant for the complex was calculated to be 4595 M^{-1}. This value is comparable with the value of 5600 M^{-1} obtained by Suslick *et al*.[5] for the binding constant of zinc(II) tetraphenylporphyrin (ZnTPP) and 3-phenylpyridine.

Table 6.1: Data used in the calculation of binding constant

Solutions	$[M]_T(10^{-6})$	$[M] = [M]_T - [ML]$ (10^{-6})	$[L]_T$ (10^{-3})	$[M]_X = A_M/\varepsilon_M$ (10^{-6})	$[ML] = \{[M]_T-[M_T-(A/\varepsilon_M)]\}$ (10^{-6})	Binding Constant K (M^{-1})
1:40	2	1.30	0.08	1.3	0.7	6730
1:100	2	1.11	0.2	1.11	0.89	4009
1:200	2	0.87	0.4	0.87	1.13	3247
1:300	2	0.55	0.6	0.55	1.45	4393
					Avg. K	4595

$[M]_T$ is analytical concentration of host, $[L]_T$ is analytical concentration of ligand, $[M]_X$ is concentration of host at equilibrium, A_M is absorbance of host, ε_M is molar extinction coefficient of host, K is binding constant.

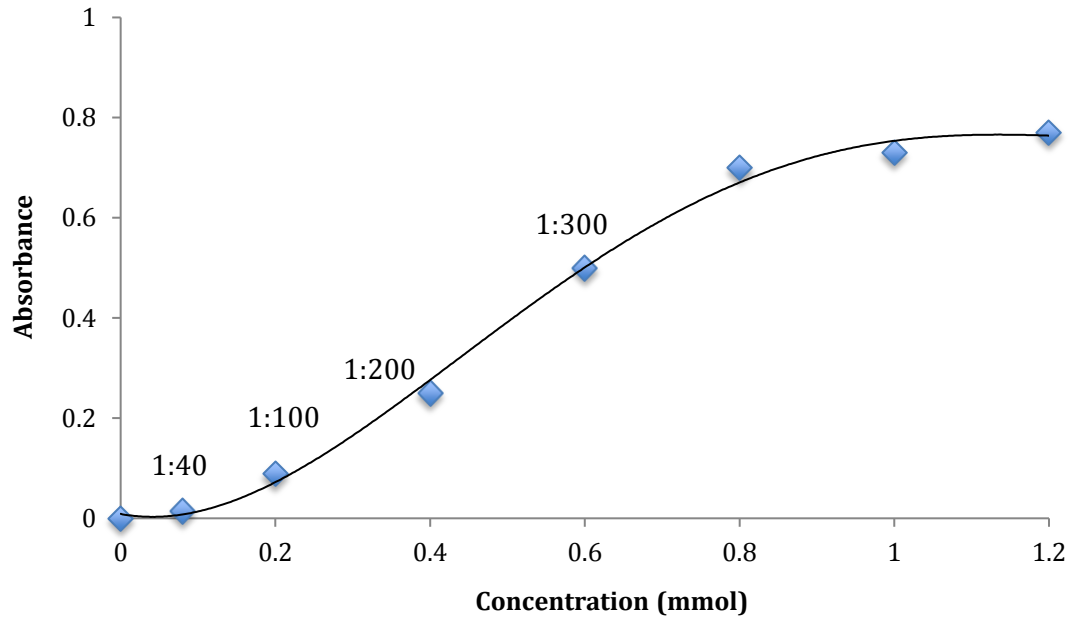

Figure 6.2: A plot of the changing absorbance value at 466 nm as a function of changing ligand **144** concentration. Values shown on the curve refer to the ratio of porphyrin to ligand, **146**:**144**.

6.3 Conclusion

A preliminary calculation of the binding constant established that a complex was formed between the pyridyl ligand **144** and zinc(II) porphyrin **146** with a similar strength of interaction to that measured for other pyridine-based ligands and zinc(II) porphyrins. The binding constant has a large error associated with it (± 2100 given the variation in values in Table 6.1), because

of the increasing contribution of the absorbance from free ligand **144** at the 1:100 and 1:200 ratios. A bathochromic shift of 20 nm was observed compared to 10 nm reported by Suslick and co-workers for the complex form between zinc(II) tetraphenylporphyrin (ZnTPP) and 3-phenylpyridine.[5]

6.4 Experimental

6.4.1 Materials and Methods

UV-visible absorbance spectra of the solutions were recorded on a Varian Cary 1 Bio UV-visible spectrophotometer using a standard 1 cm UV-visible spectroscopy cell at 298 K. The titration experiment was carried out using de-acidified chloroform.

The synthesis of **144** is described in Chapter Seven (where it is numbered as compound **2a** in the manuscript for submission to *Tetrahedron*).

6.4.2 Preparation of Porphyrins for Co-ordination Study

5,10,15,20-Tetrakis(4-*tert*-butylphenyl)porphyrin 145

Ar = 4-*tert*-butylphenyl

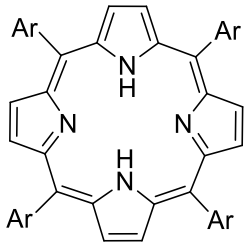

To a stirred mixture of 4-*tert*-butylbenzaldehyde (1.62 g 10.0 mmol) in propanoic acid (125 mL) was added pyrrole (0.67 g, 10.0 mmol). The reaction was heated at reflux for 1 h and the reaction mixture was stirred at room temperature overnight. The reaction mixture was then filtered and washed with ice-cold hexane (20 mL) to afford **145** (0.31 g, 15%) as violet microcrystals that were used without purification. m.p. > 300 °C. ^{1}H NMR (400 MHz, $CDCl_3$) δ -2.73 (br s, 2H, NH), 1.52 (s, 36H, CH_3), 7.76 (d, 8H, *J* = 8.3 Hz, ArH), 8.15 (d, 8H, *J* = 8.3 Hz, ArH), 8.87 (s, 8H, β-pyrrolic H) ppm. The spectroscopic data are in agreement with those reported in the literature.[6]

[5,10,15,20-Tetrakis(4-*tert*-butylphenyl)porphyrinato]zinc(II) 146

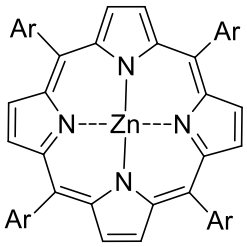

A mixture of 5,10,15,20-tetrakis(4-*tert*-butylphenyl)porphyrin **145** (150 mg, 0.18 mmol) and zinc(II) acetate monohydrate (59 mg, 0.27 mmol) in dichloromethane (25 mL) was heated at reflux for 1 h. On cooling, the organic layer was washed with water (2 x 25 mL), brine (25 mL), dried over sodium sulfate, filtered and evaporated under *vacuo*. The crude product was purified by column chromatography (silica gel, dichloromethane/hexane 1:4) to afford pure **146** (81 mg, 50%) as a purple-red microcrystalline solid. m.p. > 300 °C. ^{1}H NMR (400 MHz, $CDCl_3$) δ 1.52 (s, 36H, CH_3), 7.76 (d, 8H, *J* = 8.1 Hz, ArH), 8.15 (d, 8H, *J* = 8.1 Hz, ArH), 8.97 (s, 8H, β-pyrrolic H) ppm. The spectroscopic data are in agreement with those reported in the literature.[7]

6.4.3 Calculation of Binding Constant

For determination of the binding constant, the batch method was used and a series of solutions were performed. The concentration of host (zinc(II) porphyrin **146**) was 2 μM and the concentration of guest (pyridine ligand **144**) was 80 μM. A series of solutions were made with concentrations of host to guest in the ratio of 1:0, 1:40, 1:100, 1:200, 1:300, 1:400, 1:500 and 1:600. The host concentration was kept constant throughout the experiment.

The spectral data could be explained by assuming 1:1 stoichiometry[4,5,8] for the ligand:host in the formation of the complex. The binding constant can be expressed in equation 6.1.[9]

$$M + L \rightleftharpoons ML$$

$$K = [ML] / [M] [L] \qquad 6.1$$

The concentration of three species can be calculated using absorbance data.

$$[M] = [M]_T - [ML] \qquad 6.2$$

$[L] = [L]_T - [ML]$ 6.3

As $[ML] <<<< [L]_T$

$[L] = [L]_T$ 6.4

$[ML] = A_{ML} / (l \times \varepsilon_{ML})$

Where A_{ML} is the absorbance of complex, l is the path length, ε_{ML} is molar extinction coefficient of the complex, $[M]_T$ is the initial concentration of host and $[L]_T$ is the initial concentration of ligand.

Substituting equation 6.2 and 6.4 in equation 6.1 becomes

$K = [ML] / \{([M]_T - [ML]) [L]_T\}$ 6.5

In this case, ε_{ML} is unknown; hence concentration of complex can be found using following equation.

$[ML] = [M]_T-[M_T-M_X]$ 6.6

$[M]_X$ is concentration of host (zinc(II) porphyrin) at the equilibrium

$[M]x = A / \varepsilon_M$ 6.7

By substituting equation 6.6 and 6.7 in equation 6.5

$K = \{[M]_T-[M_T-(A / \varepsilon_M)]\} / \{([M]_T - [ML]) ([L]_T\}$ 6.8

6.5 References

1. Lehn, J.-M. *Angew. Chem. Int. Ed.* **1988**, *27*, 89-112.
2. Flamigni, L.; Talarico, A. M.; Ventura, B.; Rein, R.; Solladié, N. *Chem. Eur. J.* **2006**, *12* (3), 701-712.
3. Ikeda, C.; Tanaka, Y.; Fujihara, T.; Ishii, Y.; Ushiyama, T.; Yamamoto, K.; Yoshioka, N.; Inoue, H. *Inorg. Chem.* **2001**, *40* (14), 3395-3405.
4. Satake, A.; Kobuke, Y. *Tetrahedron* **2005**, *61* (1), 13-41.
5. Bhyrappa, P.; Vaijayanthimala, G.; Suslick, S. *J. Am. Chem. Soc.* **1999**, *121*, 262-263.

6. Mele, G.; Del Sole, R.; Vasapollo, G.; García-López, E.; Palmisano, L.; Schiavello, M. *J. Catal.* **2003**, *217*, 317-342.

7. Baffreau, J.; Leroy-Lhez, S.; Vân Anh, N.; Williams, R. M.; Hudhomme, P. *Chem. Eur. J.* **2008**, *14* (16), 4974-4992.

8. Kozaki, M.; Ninomiya, Y.; Suzuki, S.; Okada, K. *Tetrahedron Lett.* **2013**, *54*, 3658-3661.

9. Billo, E. *Excel for chemists: A comprehensive guide*. 2nd ed.; John Wiley and Sons, Inc: **2001**; p 349-372.

Chapter Seven

Synthesis and theoretical nonlinear optical properties of pyridyl containing 1,3-diketone boron complexes and their quaternary salts

7.1 Article for Submission to Tetrahedron

The work described in this Chapter is a second aspect to the 4'-pyridyl-functionalised boron difluoride 1,3-diketonate work.

The following article describes the synthesis of three new series of 4'-pyridyl-containing compounds; a series of 4'-pyridyl-1,3-diketones, their corresponding boron difluoride complexes (one of which (compound **2a** in the article, compound **144** in Chapter Six) was used for the studies described in Chapter Six), and the *N*-methyl derivatives of the boron complexes.

The boron difluoride complexes of the 4'-pyridyl-1,3-diketones were initially targeted for self-assembled dyad work (of type described in Chapter Six). However it was felt that the donor-π-linked-acceptor nature of the structures warranted investigation of their potential NLO properties, properties that may be enhanced upon formation of the corresponding *N*-methyl salts. This aspect of the work is the basis of the manuscript.

A statement on contributions to the following manuscript

I, Rajesh K. Raut, performed all synthetic work described in the paper.

As part of my PhD candidature, I worked in the laboratory of Professor N. Sekar, and received training in the use of Gaussian 09 package. During this time I performed 80% of the calculations reported in the paper, working under the supervision of Rahul D. Telore, a PhD candidate in Prof. Sekar's group.

The electrochemical experiments were performed by Thomas Sommerville, a PhD candidate working under the supervision of Dr Danny Wong at Macquarie University.

I wrote a complete draft of the paper, and collected all reference materials referred to in the introduction section. The draft was then modified by my supervisor, Assoc. Prof. Andrew Try, and reviewed by Prof. N. Sekar and Dr Danny Wong.

Rajesh K. Raut

Graphical Abstract

To create your abstract, type over the instructions in the template box below.
Fonts or abstract dimensions should not be changed or altered.

Synthesis and theoretical nonlinear optical properties of pyridyl containing 1,3-diketone boron complexes and their quaternary salts

Leave this area blank for abstract info.

Rajesh K. Raut[a], Rahul D. Telore[b], Thomas A. Sommerville[a], Danny K. Y. Wong[a], Nagaiyan Sekar[b*], and Andrew C. Try[a*]

[a]*Department of Chemistry and Biomolecular Sciences, Macquarie University, NSW 2019, Australia*
[b]*Department of Dyestuff Technology, Institute of Chemical Technology, Mumbai 400 019, India*

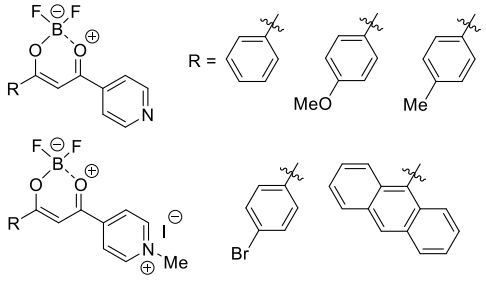

Tetrahedron
journal homepage: www.elsevier.com

Synthesis and theoretical nonlinear optical properties of pyridyl containing 1,3-diketone boron complexes and their quaternary salts

Rajesh K. Raut[a], Rahul D. Telore[b], Thomas A. Sommerville[a], Danny K. Y. Wong[a], Nagaiyan Sekar[b]*, and Andrew C. Try[a]*

[a]*Department of Chemistry and Biomolecular Sciences, Macquarie University, NSW 2019, Australia*
[b]*Department of Dyestuff Technology, Institute of Chemical Technology, Mumbai 400 019, India*

ARTICLE INFO

Article history:
Received
Received in revised form
Accepted
Available online

Keywords:
1,3-diketone
boron complex
nonlinear optics
DFT
hyperpolarizability

ABSTRACT

A series of boron difluoride complexes of 1,3-diketones bearing either pyridyl or *N*-methylpyridinium rings were synthesized and their optical and electrochemical properties were studied. Optimization of the geometry of all compounds was performed and the properties related to potential NLO behavior of the compounds, such as dipole moment and first hyperpolarizability, have been calculated using the B3LYP / LanL2DZ level of Density Functional Theory.

1. Introduction

Boron difluoride 1,3-diketonates are extensively used as fluorophores due to their favourable photo-physical properties[1], such as their intense long UV-visible absorbance and high quantum yields.[2] These properties have resulted in applications in organic electroluminescence devices,[3,4] laser technology[5] and nonlinear optics[6]. The electron deficient -OBF$_2$O- group is reported to aid in delocalization of the electron density across the molecule.[5] The introduction of an electron donating group, such as a methoxy group, creates virtual D-π-A system by lowering the HOMO/LUMO band gap. The photo-physical properties of boron difluoride diketonates are known to be altered by simple modifications, either synthetically or by changing their environment.[4] Mirochnik and coworkers have extensively studied the photo-physical properties of crystalline[7,8] and polymer forms[7] of boron difluoride diketonates with respect to size, solvent and temperature.

There have been a few reports on the nonlinear optical (NLO) properties of metal complexes of β-diketone ligands[9,10] but there is no mention of these properties in relation to the boron complexes. NLO materials are used for optical communication, as amplifiers and sensors.[11,12] Many organic compounds have been reported with improved first hyperpolarizability over ~~inorganic~~ compounds and they are of interest in optical applications due to their larger nonlinear responses, synthetic accessibility and increased resistance to optical damage.[13,14,15] The first hyperpolarizability can be tailored by changing the strength of electron-donor and electron-acceptor groups and varying the conjugation pathway.[13] In the boron difluoride 1,3-diketonates, the -OBF$_2$O- unit behaves like an electron acceptor that creates electron affinity in the molecule, resulting in a change in the dipole moment in comparison with the free ligand.[2]

In the present work, the features of pyridinium salts (that have been reported as materials for nonlinear optics due to their transparency in the visible spectrum[16]) and boron difluoride complexes of 1,3-diketone ligands have been combined. The synthesis, characterization, photo-physical and electrochemical studies of (4-pyridyl)-1,3-diketone boron complexes and their quaternary pyridinium salts are reported. The geometries of the structures were optimized using DFT and theoretical calculations of their NLO properties were performed.

2. Results and Discussion

2.1. Synthesis

The synthetic route to the *N*-methyl pyridinium boron complexes involves three steps, as shown in Scheme 1. 1,3-Diketones **1a-1e** were synthesized by condensation of methyl 4-isonicotinate and

* Corresponding author. Tel.: +91-22-3361-2707; fax: +91-22-3361-1020; e-mail: nethi.sekar@gmail.com (Nagaiyan Sekar)

* Corresponding author. Tel.: +612-9850-8291; fax: +612-9850-8313; e-mail: andrew.try@mq.edu.au

substituted acetyl functionalized arenes (acetophenone (a), 4'-methoxyacetophenone (b), 4'-methylacetophenone (c), 4'-bromoacetophenone (d) and 9'-acetylanthracene (e)) in dimethoxyethane, using sodium hydride (60% in oil) as a base. The boron complexes **2a-2e** were obtained by refluxing compounds **1a-1e** with boron trifluoride diethyletherate in dichloromethane for 2 h. In the third step, the *N*-methyl pyridinium boron complexes **3a-3e** were obtained by refluxing boron complexes **2a-2e** with methyl iodide for 3-4 days. All new compounds were characterized by ^{1}H and ^{13}C NMR, FTIR, mass spectrometry and elemental analysis. In ^{1}H NMR spectra, the synthesis of the diketones was confirmed by the presence of the characteristic peaks of the vinylic proton at δ = 6.66-6.88 ppm and enolic proton at δ = 16.31-16.64 ppm, whilst in the boron complexes the enolic proton was absent.

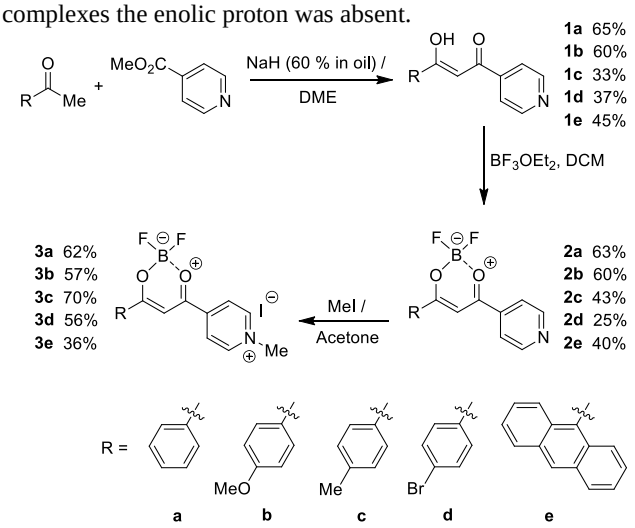

Scheme 1. Synthesis of 1,3-diketones, their boron complexes and their *N*-methyl pyridinium salts.

2.2. Photo-physical Properties

The important parameters associated with the UV-visible absorption and fluorescence emission spectra of compounds **2a-2e** and **3a-3e** in *N*,*N*-dimethylformamide (DMF) are summarized in Table 1. The quantum yield of both series of compounds was recorded against quinine sulfate in 0.1 M H_2SO_4.

The pyridine boron complexes **2a-2d** absorb in the range of 310-410 nm (Figure 1), with **2e** absorbing across a wider region. Compared to **2a**, **2b** and **2c** (containing electron-donating groups) show a bathochromic shift of 9 nm and 25 nm, respectively. The *N*-methyl pyridinium boron complexes **3a-3e** absorb much more weakly (Figure 2). The absorption maxima of **3b** exhibits a bathochromic shift of 23 nm in comparison with **2b**, consistent with an enhanced dipole moment of **3d**.

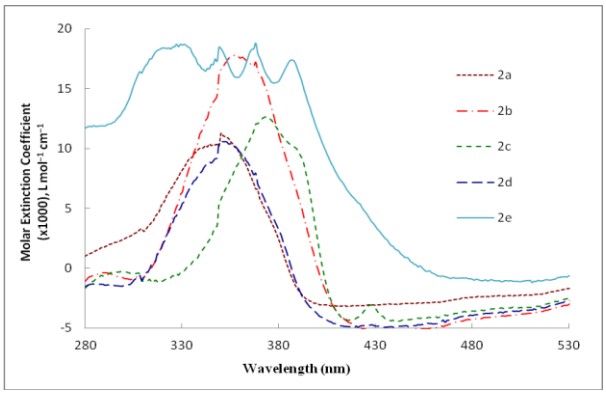

Figure 1. UV-visible spectra of pyridine boron complexes **2a-2e**.

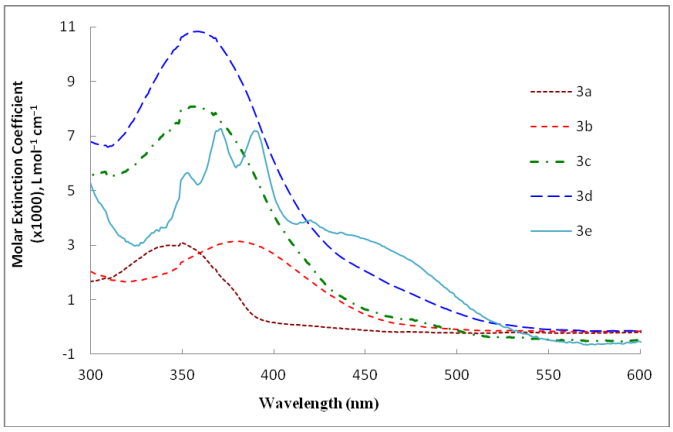

Figure 2. UV-visible spectra of *N*-methyl pyridinium boron complexes **3a-3e**.

Fluorescence emission spectra for **2a-2e** were recorded in DMF (Figure 3). The fluorescence peak was recorded at a constant wavelength for each anthracene compound **2e** and **3e**, irrespective of the excitation wavelength (three were used; 386, 368 or 349 nm for **2e**: 389, 371or 352 nm for **3e**). The Stokes shift of **2a-2e** was observed in the range of 37-78 nm and 48-112 nm for **3a-3e**. The relative quantum yield was measured using quinine sulfate (ϕ=0.55) as a reference standard in DMF.

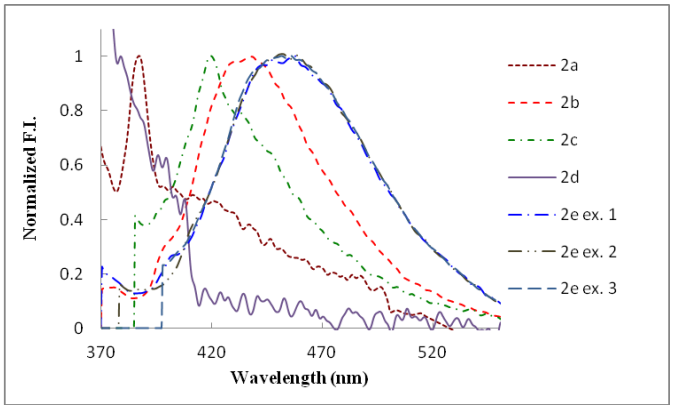

Figure 3. Normalized fluorescence spectra of pyridine boron complexes **2a-2e**.

All compounds were excited at λ_{abs} (see Table 1) and quinine sulfate at was excited at 349 nm. All of the pyridine boron complexes **2a-2e** exhibit poor quantum yields, and the *N*-methyl pyridinium boron complexes **3a-3e** show quantum yields an order of magnitude less and no significant trend was observed (fluorescence emission spectra are not shown); the quantum yield was observed in the range of 0.0031-0.0058. The relative quantum yields of both series of compounds are given in Table 1.

2.3. Cyclic Voltammetry

Cyclic voltammetry (in anhydrous DMF) was performed on both series of boron complexes to examine redox potentials (Table 2). Both series showed quasi-reversible peaks. All compounds show only reduction potential versus Fc / Fc^{+}, and the oxidation potential was non-existent up to +1.5 V. The *N*-methyl pyridinium series shows lower reduction potentials (-1.00 to -1.12 V) than the pyridine series (-1.12 to -1.45 V), reflecting the increased electron affinity as a result of methylation.

Table 1. Absorption maxima wavelength (λ_{abs}, nm); Log_{10} of molar extinction coefficient (Log ε_{max}); fluorescence maxima wavelength (λ_{em}, nm); Stokes shift ($\Delta\lambda$, nm); relative quantum yield (ϕ) to quinine sulfate of **2a-2e** and **3a-3e** in DMF

	λ_{abs}	Log ε_{max}	λ_{em}	$\Delta\lambda$	ϕ		λ_{abs}	Log ε_{max}	λ_{em}	$\Delta\lambda$	ϕ
2a	349	4.05	386	37	0.045	**3a**	349	3.38	456	107	0.0053
2b	358	4.25	436	78	0.016	**3b**	381	3.80	476	95	0.0031
2c	374	4.28	418	44	0.011	**3c**	368	3.70	471	103	0.0054
2d	350	4.03	387	37	0.036	**3d**	358	3.68	470	112	0.0058
2e	386	4.24	452	66	0.015	**3e**	389	3.87	437	48	0.0053
	368	4.27	452	84			371	3.86	437	66	
	349	4.27	452	103			352	3.75	437	85	

Table 2. Reduction potentials of boron complexes **2a-2e** and **3a-3e**

	E_{onset} vs Ferrocence (V)		E_{onset} vs Ferrocence (V)
2a	-1.37	**3a**	-1.00
2b	-1.12	**3b**	-1.03
2c	-1.19	**3c**	-1.00
2d	-1.45	**3d**	-1.07
2e	-1.22	**3e**	-1.12

0.1 M *n*-Bu_4NClO_4 in DMF, Ag/AgCl electrode, scan rate 100 mVs^{-1}

2.4. Computational Studies

The ground state geometry of compounds was optimized using the B3LYP functional with the LanL2DZ basis set. The choice of functional and basis set is well justified as the method has been used for similar compounds.[4] All compounds except **2e** and **3e** were found to have a planar geometry, as expected. The two fluorine atoms attached to the tetrahedral boron atom are out of plane in both series. As examples of the planar structures, the optimized ground state structure of compound **2b** is shown in

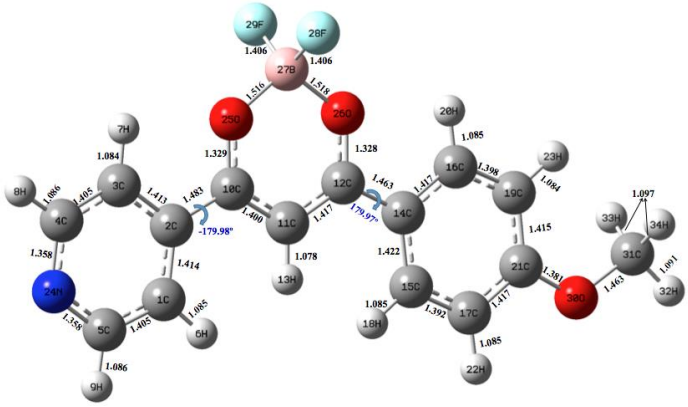

Figure 4. Optimized geometry parameters (bond length and dihedral angles shown) of compound **2b** in the ground state.

The dihedral angles between the pyridine and the boron-containing ring (25O-10C-2C-1C) and benzene and the boron-containing ring (26O-12C-14C-15C) are almost 0° in **2b**. A similar trend was observed for both series except for compounds **2e** and **3e** containing the anthracene moiety.

The optimized ground state structure of compound **2e** is shown in Figure 5. The dihedral angle between anthracene and the boron-containing ring in **2e** (16O-12C-20C-22C) is 49.03° and the corresponding angle in **3e** is 42.08°. The dihedral angle between pyridine and the boron-containing ring (15O-10C-2C-1C) is 2.90° in **2e**, while in **3e** it is 0.17°.

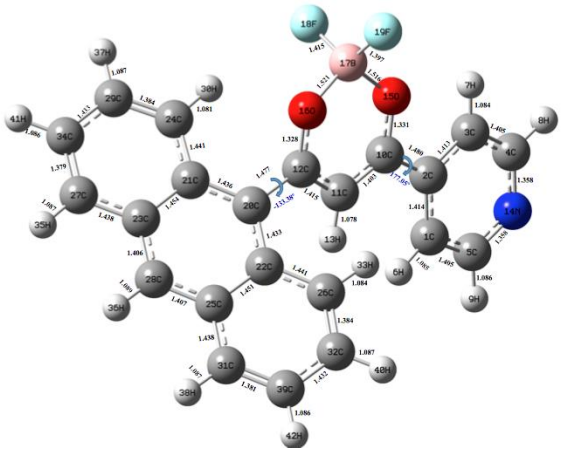

Figure 5. Optimized geometry parameters (bond length and dihedral angles shown) of compound **2e** in the ground state.

The frontier molecular orbitals (FMO) were studied to understand charge transfer and charge delocalization processes within the molecule. The highest occupied molecular orbitals (HOMO) and lowest unoccupied molecular orbitals (LUMO) in the ground state were obtained from geometry optimization of the structures and shown in Figure 6. In both series, the HOMO shows delocalization on benzene / anthracene and boron-containing units, while the LUMO shows delocalization over the entire molecule.

The calculated HOMO, LUMO and band gap values for the compounds are provided in Table 3. The band gap values of the pyridine series are in the range of 2.49-3.78 eV. All values follow the trend that as the strength of the electron-donating group increases, the HOMO-LUMO band gap decreases, with the exception of **2e** (with the out-of-plane anthracene moiety), which has the lowest band gap of 2.49 eV. The HOMO-LUMO band gap of **2b**, with a strong electron-donating group, shows the lowest value (excluding **2e**) of 3.49 eV. The *N*-methyl pyridinium series shows comparatively lower HOMO-LUMO band gap values ranging 1.49-2.78 eV. A similar trend across

this series was observed, again with exception of the out-of-plane anthracene-containing compound **3e**, which has the lowest HOMO-LUMO band gap of 1.49 eV.

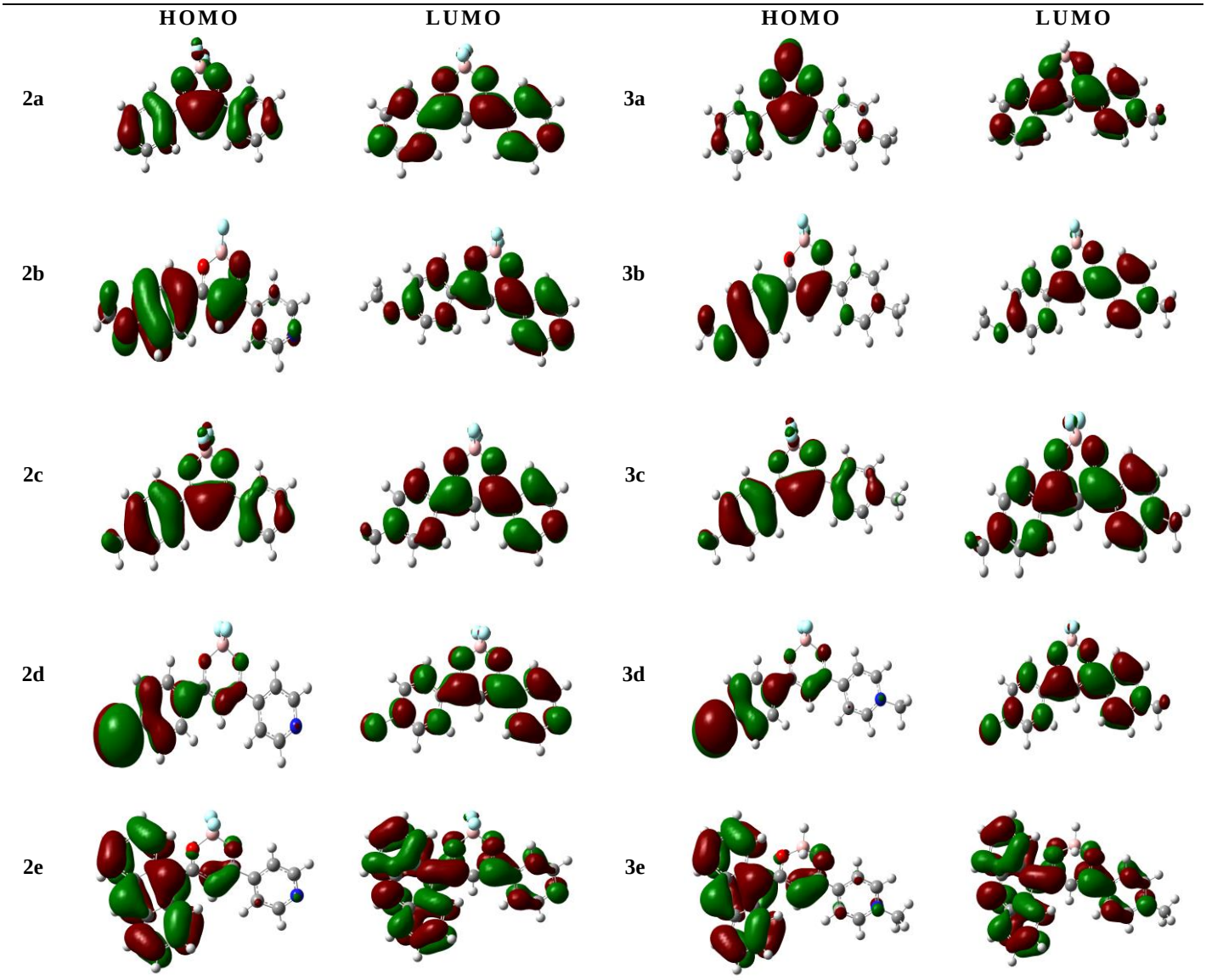

Figure 6. Frontier molecular orbitals of **2a-2e** and **3a-3e** in the ground state.

Table 3. Calculated HOMO and LUMO values and the HOMO-LUMO gap (in eV) for the ground state

	Ground State		HOMO-LUMO gap		Ground State		HOMO-LUMO gap
	HOMO	LUMO			HOMO	LUMO	
2a	-7.48	-3.70	3.78	**3a**	-7.97	-5.19	2.78
2b	-7.00	-3.51	3.49	**3b**	-9.33	-7.11	2.22
2c	-7.36	-3.60	3.76	**3c**	-9.84	-7.24	2.60
2d	-7.52	-3.85	3.67	**3d**	-9.74	-7.40	2.34
2e	-6.13	-3.64	2.49	**3e**	-8.20	-6.71	1.49

Hyperpolarizability (β_o) in a molecule is the measure of nonlinear optical activity. The extent of hyperpolarizability is associated with Intramolecular Charge Transfer (ICT) in the molecule. Generally, large hyperpolarizability is observed in molecules with an extended π-conjugation system and through the placement of electron-donor and electron-acceptor groups at opposite ends of the molecule. Hyperpolarizability (β) values were calculated using density functional theory (DFT) with B3LYP/ LanL2DZ based on finite-field approach. The first hyperpolarizability (β_o) is defined below.[11]

Table 4. First hyperpolarizability and its components for **2a-2e** and **3a-3e** in a.u. and e.s.u.

β-tensors (a.u.)	**2a**	**2b**	**2c**	**2d**	**2e**	**3a**	**3b**	**3c**	**3d**	**3e**
β_{xxx}	-1110.67	5502.37	2935.81	-5264.32	-7976.19	10595.16	26737.69	15898.16	26009.72	47797.51
β_{xxy}	1462.30	1966.88	1654.27	1590.42	-2145.49	1319.62	1231.53	1626.44	754.08	-1959.47
β_{xyy}	-64.43	-269.08	-174.04	470.82	-246.07	-485.52	-193.95	350.85	279.94	-1334.08
β_{yyy}	-188.88	-181.57	-194.53	-47.15	241.55	-109.75	-342.68	-299.26	-323.47	-151.07
β_{xxz}	0.73	-0.53	-0.15	-0.12	618.57	94.82	-45.85	-19.24	-26.25	-1564.34
β_{xyz}	-0.078	0.01	0.01	-0.004	-125.29	40.03	0.31	3.98	3.18	-219.70
β_{yyz}	0.169	-0.16	-0.05	-0.035	5.56	5.83	-17.26	-23.94	-22.61	-67.34
β_{xzz}	15.32	-32.43	-26.91	-21.96	117.98	-10.63	18.35	-10.56	48.51	-436.52
β_{yzz}	-44.48	-32.56	-39.69	-33.39	35.83	-13.57	-48.93	-54.73	-42.73	5.24
β_{zzz}	0.0584	-0.075	-0.02	-0.01	-29.53	-10.58	-12.35	-2.03	-2.46	-62.269
β_o (a.u.)	1689.789	5488.27	3081.56	5046.63	8338.03	10170.02	26575.47	16288.29	26341.07	46106.16
β_o(e.s.u.) x 10^{-30}	14.60	47.41	26.62	43.6	72.03	87.86	229.59	140.72	227.57	398.32

$$\beta_o = (\beta_x^2 + \beta_y^2 + \beta_z^2)^{1/2}$$

$$\beta_x = \beta_{xxx} + \beta_{xyy} + \beta_{xzz}$$

$$\beta_y = \beta_{yyy} + \beta_{xxy} + \beta_{yzz}$$

$$\beta_z = \beta_{zzz} + \beta_{xxz} + \beta_{yyz}$$

The first hyperpolarizability (β_o) of compounds is listed in Table 4 and was compared with urea (0.38 x 10^{-30} e.s.u.).[17] The hyperpolarizability values of the pyridine series of boron complexes **2a-2e** ranges from 14.60-72.03 x 10^{-30} e.s.u. The *N*-methyl pyridinium series of boron complexes **3a-3e** shows higher β_o values in the range of 87.86-398.32 x 10^{-30} e.s.u. Compounds **2b** and **3b** show β_o values 125 and 605 times higher than urea, respectively. A similar trend to that for the HOMO-LUMO gap was observed with hyperpolarizabilities (β); the stronger the electron-donor group, the lower the HOMO-LUMO band gap, suggesting electron transfer from the electron donating group to the electron acceptor group, and hence the higher β_o value. Within their series, compounds **2e** and **3e** show the strongest β_o values of 72.03 x 10^{-30} e.s.u. and 398.32 x 10^{-30} e.s.u. that are 190 and 1048 times higher than urea, respectively.

3. Conclusion

Novel *N*-methyl pyridinium boron complexes, having potential NLO applications, were synthesized and characterized. In terms of fluorescence properties, both series of boron complexes exhibited Stokes shift values ranging from 37nm to 103nm, but poor fluorescence intensity and quantum yields. Electrochemical studies were carried out to record redox potentials. The ground state geometry of compounds was optimized using the B3LYP functional with the LanL2DZ basis set. All compounds except **2e** and **3e** were found to have a planar geometry. The two fluorine atoms attached to the boron atom are out of plane in both series. Calculated HOMO-LUMO band gap values follow the trend that as the strength of the electron-donating group increases, the HOMO-LUMO band gap decreases. The calculated hyperpolarizability values of the *N*-methyl pyridinium series of boron complexes **3a-3e** were found to be significantly enhanced in comparison to the pyridine boron complexes **2a-2e**.

4. Experimental Section

4.1. Materials and Equipment

Solvents and reagents were purified using standard techniques. All commercial solvents were either routinely distilled prior to use or purchased in high-purity form (HPLC quality). Hexane refers to the fraction of b.p. 60-80 °C. Where solvent mixtures were used, the portions are given by volume. Column chromatography was routinely carried out using the gravity feed column techniques on Merck silica gel type 9385 (230-400 mesh) with the stated solvent systems. All reactions were monitored by using Thin Layer Chromatography (TLC) on 0.25 mm E-Merck silica gel 60 F254 pre-coated plates (0.2 mm). Melting points were recorded on Stuart Scientific SM10 and are uncorrected. ^{1}H (400 MHz) and ^{13}C (100 MHz) NMR spectra were recorded at 25 °C on a Bruker DPX400 spectrometer using $CDCl_3$ (7.26 ppm for ^{1}H and 77 ppm for ^{13}C) and DMSO d_6 (2.49 ppm for ^{1}H and 39.5 ppm for ^{13}C) as solvent and also as internal standards. Signals were recorded in terms of chemical shifts, multiplicity, relative integral values, and coupling constants (in Hz), in that order. The following abbreviations for multiplicity are used: s, singlet; d, doublet; t, triplet; m, multiplet; dd, doublet of doublets; br, broad; q, quartet; qn, quintet. IR spectra were recorded on a Nicolet iS10 FT-IR spectrometer at 298 K unless otherwise stated. The following abbreviations for peak characteristics are used; s, strong; m, medium; w, weak; br, broad. UV-vis absorbances were recorded on a Varian Cary 1 Bio UV-visible spectrophotometer using a UV-vis spectroscopy cell. Fluorescence emission was recorded on a Perkin Elmer Luminescence spectrometer LS50B using a fluorescence

spectroscopy cell. Cyclic voltammetry and square wave voltammetry were performed using an E-corder 201 potentiostat (eDAQ Pty Ltd, Australia). Electrochemical impedance spectroscopy (EIS) and square wave voltammetry were conducted using an Autolab PGStat12 (MEP Instruments Pty Ltd, NSW, Australia). A three-electrode cell consisting of a 3-mm diameter glassy carbon disc-working electrode, platinum coil auxiliary electrode and a Ag|AgCl reference electrode (Bioanalytical System Inc., Indiana USA) was used. Tetrabutylammonium perchlorate (0.1 M) used as supporting electrolyte. Prior to measurements and modification, glassy carbon electrodes were sequentially polished in slurries of 1.0, 0.3 and 0.05 μm alumina powder (Leco Australia, Pty. Ltd., Sydney, Australia), before they were rinsed and ultrasonicated in a Cole-Parmer CP130 Ultrasonic processor (Extech equipment Pty. Ltd., Victoria, Australia) containing deionised water. Solutions were purged in nitrogen for 1 h. The relative quantum yield (Φ) was calculated by using quinine sulfate as reference.[18] Quinine sulfate (Φ_{ST} = 0.54, $\lambda_{excitation}$ 350 nm) was dissolved in 0.1 M H_2SO_4 (refractive index: 1.33)[19] and all the compounds were dissolved in DMF (refractive index: 1.43)[19]. The relative quantum yield was calculated according to the following equation:

$$\Phi_X = \Phi_{ST}\left(\frac{m_X}{m_{ST}}\right)\left(\frac{\eta_X^2}{\eta_{ST}^2}\right)$$

Where Φ is the fluorescence quantum yield, *m* is the slope of the plot of integrated fluorescence intensity versus absorbance, and η is the refractive index of the solvent. The subscript ST and X refer to the reference and sample compounds, respectively. Excitation and emission slit widths were set at 5.0 nm when recording their fluorescence spectra.

4.2. Computational Methods

All computations were performed using the Gaussian 09 Package.[20] Optimization and hyperpolarizability of molecules in the gas phase were calculated using Density Functional Theory (DFT). Becke3-Lee-Yang-Paar (B3LYP) functional with LanL2DZ basis set was used for the calculations.

*4.3. Synthesis of Diketones **(1a-1e)***

General Procedure. To a mixture of sodium hydride (583 mg, 60% in oil, 14.6 mmol) in dimethoxyethane (30 mL), methyl isonicotinate (1.0 g, 1.0 mL, d = 1.001 g/mL, 7.3 mmol) and the acetophenone (7.3 mmol) were added. The reaction mixture was heated to reflux overnight and monitored by TLC (dichloromethane). The reaction mixture was poured over acetic acid (9 N, 40 mL). The aqueous layer was extracted in diethyl ether (3 x 50 mL). The combined organic layers were washed with brine (50 mL), dried over anhydrous sodium sulfate, filtered and evaporated to dryness under vacuum. The crude product was purified using the conditions detailed below.

3-Phenyl-1-(pyridin-4-yl)propane-1,3-dione **1a**. Starting with acetophenone (0.88 g, 0.85 mL, d = 10.3 g/mL, 7.3 mmol), the crude material was chromatographed (silica gel, dichloromethane/ethyl acetate 95:5) to afford **1a** (1.07 g, 65%) as a white solid: m.p. 82-84 °C (lit.[21] 84-85 °C). ^{1}H NMR (400 MHz, $CDCl_3$) δ 6.88 (s, 1H, CH), 7.49-7.53(m, 3H, ArH), 7.78-7.79 (m, 2H, ArH), 7.99-8.01 (m, 2H, ArH), 8.79-8.80 (m, 2H, ArH), 16.51 (br s, 1H, OH) ppm. The spectral data are in agreement with that reported in the literature.[22]

3-(4-Methoxyphenyl)-1-(pyridin-4-yl)propane-1,3-dione **1b**. Starting with 4-methoxyacetophenone (1.09 g, 7.3 mmol), the crude material was chromatographed (silica gel, dichloromethane/ethyl acetate 95:5) to afford **1b** (1.12 g, 60%) as an off-white solid: m.p. 132-34 °C (lit.[23] 132-133 °C). ^{1}H NMR (400 MHz, $CDCl_3$) δ 3.89 (s, 3H, OCH_3), 6.82 (s, 1H, CH), 6.97-7.01 (m, 2H, ArH), 7.76-7.78 (m, 2H, ArH), 7.97-8.01 (m, 2H, ArH), 8.77-8.79 (m, 2H, ArH), 16.64 (br, 1H, OH) ppm. The spectral data are in agreement with that reported in the literature.[23]

1-(Pyridin-4-yl)-3-(4-tolyl)propane-1,3-dione **1c**. Starting with 4-methylacetophenone (0.98 g, 7.3 mmol), the crude material was chromatographed (silica gel, ethyl acetate/hexane 3:1) to afford **1c** (0.58 g, 33%) as a beige solid: m.p. 118-120 °C (lit.[24] 118-120 °C). ^{1}H NMR (400 MHz, $CDCl_3$) δ 2.44 (s, 3H, CH_3), 6.86 (s, 1H, CH), 7.30-7.32 (m, 2H, ArH), 7.76-7.78 (m, 2H, ArH), 7.89-7.92 (m, 2H, ArH), 8.78-8.79 (m, 2H, ArH), 16.57 (br, 1H, OH) ppm. The spectral data are in agreement with that reported in the literature.[24]

3-(4-Bromophenyl)-1-(pyridin-4-yl)propane-1,3-dione **1d**. Starting with 4-bromoacetophenone (1.45 g, 7.3 mmol), the crude material was chromatographed (silica gel, ethyl acetate/hexane 3:1) to afford **1d** (0.82 g, 37%) as a beige solid: m.p. 162-164 °C. ^{1}H NMR (400 MHz, $CDCl_3$) δ 6.83 (s, 1H, CH), 7.65 (d, 2H, *J* 8.5 Hz, ArH), 7.77 (d, 2H, *J* 6.0 Hz, ArH), 7.86 (d, 2H, *J* 8.5 Hz, ArH), 7.80 (d, 2H, *J* 5.7 Hz, ArH), 16.43 (s, 1H, OH) ppm. ^{13}C NMR (100 MHz, $CDCl_3$) δ 93.8, 120.4, 128.2, 128.9, 132.2, 134.1, 142.1, 150.8, 181.7, 187.1 ppm. IR (cm^{-1}) 652, 683, 704, 735, 763, 772, 808, 830, 938, 974, 998, 1008, 1022, 1035, 1062, 1211. 1236, 1269, 1425, 1453, 1499, 1563, 1593, 1641. Anal Calcd for $C_{14}H_{10}BrNO_2$: C, 55.29; H, 3.31; N, 4.61. Found: C, 54.73; H, 3.19; N, 4.96.

3-(Anthracen-9-yl)-1-(pyridin-4-yl)propane-1,3-dione **1e**. Starting with 9-acetylanthracene (1.61 g, 7.3 mmol), the crude material was chromatographed (silica gel, ethyl acetate/hexane 3:1) to afford **1e** (1.06 g, 45%) as a beige solid: m.p. 178-180 °C. ^{1}H NMR (400 MHz, $CDCl_3$) δ 6.66 (s, 1H, CH), 7.48-7.54 (m, 4H, ArH), 7.73-7.75 (m, 4H, ArH), 8.03 (m, 4H, ArH), 8.56 (s, 1H, ArH) 8.75-8.77 (m, 2H, ArH), 16.31 (s, 1H, OH) ppm. ^{13}C NMR (100 MHz, $CDCl_3$) δ 102.2, 120.5, 125.0, 125.6, 127.0, 128.3, 128.7, 129.6, 131.1, 131.5, 141.7, 150.9, 180.5, 193.7 ppm. IR (cm^{-1}) 678, 730, 791, 839, 895, 931, 956, 984, 1063, 1093, 1143, 1166, 1183, 1226, 1261, 1289, 1317, 1353, 1407, 1444, 1484, 1520, 1581. Anal Calcd for $C_{22}H_{15}NO_2$: C, 81.21; H, 4.65; N, 4.30. Found: C, 80.62; H, 4.66; N 4.48.

*4.4. Synthesis of Boron Complexes **(2a-2e)***

General Procedure. The 1,3-diketone **1a-1e** (1.0 mmol) and boron trifluoride diethyletherate (114 mg, 0.09 mL, d = 1.27 g/mL, 1.2 mmol) in dichloromethane (5 mL) were heated to reflux for 2 h. On cooling, the reaction mixture was filtered and washed with hexane (20 mL). The crude product was purified using the conditions detailed below.

Boron difluoride 3-phenyl-1-(pyridin-4-yl)propane-1,3-diketonate **2a**. Starting with **1a** (225 mg, 1.0 mmol), the crude material was chromatographed (silica gel, dichloromethane/ethyl acetate/hexane 3:1) to afford **2a** (172 mg, 63%) as a yellow solid: m.p. 178-180 °C. ^{1}H NMR (400 MHz, DMSO d_6) δ 7.46 (s, 1H, CH), 7.57-7.69 (m, 3H, ArH), 8.04-8.05 (m, 2H, ArH), 8.19-8.21 (m, 2H, ArH) ppm. ^{13}C NMR (100 MHz, DMSO d_6) δ 96.0, 122.5, 128.0, 129.0, 134.0, 134.5, 145.5, 146.7, 177.5, 189.3 ppm. IR (cm^{-1}) 662, 692, 704, 743, 788, 842, 899, 941, 993, 1006, 1047, 1069, 1180, 1227, 1266, 1485, 1538, 1586, 1607. UV λ_{max} (DMF) 349 nm (log ε 4.05).Anal Calcd for $C_{14}H_{10}BF_2NO_2$: C, 61.62; H, 3.69; N, 5.13. Found: C, 61.62; H, 3.64; N, 5.36.

Boron difluoride 3-(4-methoxyphenyl)-1-(pyridin-4-yl)propane-1,3-diketonate **2b**. Starting with **1b** (255 mg, 1.0 mmol), the crude material was chromatographed (silica gel, ethyl acetate/hexane 3:1) to afford **2b** (182 mg, 60%) as a yellow solid: m.p. 134-136 °C. ^{1}H NMR (400 MHz, DMSO d_6) δ 3.87 (s, 3H, OCH_3), 7.11 (d, 2H, *J* 9.0 Hz, ArH), 7.40 (s, 1H, CH), 8.02 (d, 2H, *J* 6.2 Hz, ArH), 8.20 (d, 2H, *J* 9.0 Hz, ArH), 8.79 (d, 2H, *J* 6.2 Hz, ArH) ppm. ^{13}C NMR (100 MHz, DMSO d_6) δ 55.7, 94.0, 114.3, 120.4, 127.1, 130.3, 141.3, 150.6, 163.8, 179.0, 188.3 ppm. IR (cm^{-1}): 687, 786, 840, 1022, 1175, 1239, 1310, 1504, 1541. UV λ_{max} (DMF) 358 nm (log ε 4.25). Anal Calcd for $C_{15}H_{12}BF_2NO_3$: C, 59.45; H, 3.99; N, 4.62. Found: C, 59.81; H, 3.84; N, 4.76.

Boron difluoride 1-(pyridin-4-yl)-3-(4-tolyl)propane-1,3-diketonate **2c**. Starting with **1c** (239 mg, 1.0 mmol), the crude material was chromatographed (silica gel, ethyl acetate/hexane 3:1) to afford **2c** (123 mg, 43%) as a yellow solid: m.p. 275-277 °C. ^{1}H NMR (400 MHz, DMSO d_6) δ 2.42 (s, 3H, CH_3), 7.41 (d, 2H, *J* 8.1 Hz, ArH), 7.53 (s, 1H, CH), 8.13 (d, 2H, *J* 8.1 Hz, ArH), 8.28 (d, 2H, *J* 6.0 Hz, ArH), 8.92 (d, 2H, *J* 6.0 Hz, ArH) ppm. ^{13}C NMR (100 MHz, DMSO d_6) δ 21.2, 94.3, 120.6, 127.9, 129.5, 131.9, 141.4, 144.3, 150.5, 180.2, 188.2 ppm. IR (cm^{-1}) 664, 690, 739, 794, 862, 1009, 1048, 1120, 1178, 1241, 1281, 1408, 1474, 1513, 1560, 1597. UV λ_{max} (DMF) 374 nm (log ε 4.28). Anal Calcd for $C_{15}H_{12}BF_2NO_2$: C, 62.76; H, 4.21; N, 4.88. Found: C, 62.53; H, 4.19; N, 4.80.

Boron difluoride 3-(4-bromophenyl)-1-(pyridin-4-yl)propane-1,3-diketonate **2d**. Starting with **1d** (304 mg, 1.0 mmol), the crude material was chromatographed (silica gel, ethyl acetate/hexane 3:1) to afford **2d** (88 mg, 25%) as a beige solid: m.p. 163-165 °C. ^{1}H NMR (400 MHz, DMSO d_6) δ 7.45 (s, 1H, CH), 7.45 (d, 2H, *J* 8.5 Hz, ArH), 8.03 (d, 2H, *J* 6.0 Hz, ArH), 8.13 (d, 2H, *J* 8.5 Hz, ArH), 8.80 (d, 2H, *J* 6.0 Hz, ArH) ppm. ^{13}C NMR (100 MHz, DMSO d_6) δ 95.2, 121.2, 128.4, 130.5, 132.7, 134.4, 141.9, 151.5, 182.2, 187.9 ppm. IR (cm^{-1}) 664, 693, 739, 774, 841, 1007, 1053, 1073, 1180, 1222, 1293, 1412, 1496, 1522, 1585. UV λ_{max} (DMF) 350 nm (log ε 4.03). Anal Calcd for $C_{14}H_9BBrF_2NO_2$: C, 47.78; H, 2.58; N, 3.98. Found: C, 47.69; H, 2.42; N, 4.11.

Boron difluoride 3-(anthracen-9-yl)-1-(pyridin-4-yl)propane-1,3-diketonate **2e**. Starting with **1e** (325 mg, 1.0 mmol), the crude material was chromatographed (silica gel, ethyl acetate/hexane 3:1) to afford **2e** (149 mg, 40%) as a yellow-orange solid: m.p. 173-175 °C. ^{1}H NMR (400 MHz, DMSO d_6) δ 7.10 (s, 1H, CH), 7.57-7.62 (m, 4H, ArH), 7.96-7.98 (m, 2H, ArH), 8.06-8.09 (m, 2H, ArH), 8.17-8.21 (m, 2H, ArH), 8.76-8.78 (m, 2H, ArH), 8.81 (s, 1H, ArH) ppm. ^{13}C NMR (100 MHz, DMSO d_6) δ 102.5, 120.8, 124.8, 125.8, 125.9, 127.4, 127.6, 128.79, 128.82, 129.4, 130.7, 150.8, 181.1, 192.3 ppm. IR (cm^{-1}) 678, 731, 760, 788, 840, 895, 957, 985, 1064, 1166, 1184, 1242, 1290, 1408, 1504, 1591. UV λ_{max} (DMF) 386, 368, 349 nm (log ε 4.24, 4.27, 4.27). Anal Calcd for $C_{22}H_{14}BF_2NO_2$: C, 70.81; H, 3.78; N, 3.75. Found: C, 70.84; H, 3.60; N, 3.75.

*4.5. Synthesis of N-methylpyridine Quaternary Salts **(3a-3e)***

General Procedure. Methyl iodide (106 mg, 0.05 mL, d = 2.28 g/mL, 0.75 mmol) was added to the boron complex **2a-2e** (0.15 mmol) in chloroform (10 mL) solution. The reaction mixture was heated to reflux for 4 days. On cooling, the reaction mixture was filtered and the residue of methylated salt was washed with dichloromethane (20 mL).

Boron difluoride *N*-methyl-3-phenyl-1-(pyridinium-4-yl)propane-1,3-diketonate iodide **3a**. Starting with **2a** (40 mg, 0.15 mmol), **3a** (38 mg, 62%) was obtained as a yellow solid: m.p. 238-240 °C. ^{1}H NMR (400 MHz, DMSO d_6) δ 4.40 (s, 3H, CH_3), 7.61-7.75 (m, 4H, ArH; CH), 8.25 (d, 2H, *J* 7.4 Hz, ArH), 8.73 (d, 2H, *J* 5.4 Hz, ArH), 9.19 (d, 2H, *J* 5.3 Hz, ArH) ppm. ^{13}C NMR (100 MHz DMSO d_6) 48.5, 97.8, 121.1, 125.0, 128.3, 129.5, 134.9, 147.1, 151.2, 174.4, 190.9. IR (cm^{-1}) 647, 661, 682, 703, 733, 774, 816, 844, 933, 1017, 1046, 1152, 1238, 1282, 1448, 1516, 1560, 1595. UV λ_{max} (DMF) 349 nm (log ε 3.38). Anal Calcd for $C_{15}H_{13}BF_2INO_2$: C, 43.41; H, 3.16; N, 3.38. Found: C, 43.08; H, 3.44; N, 3.08.

Boron difluoride *N*-methyl-3-(4-methoxyphenyl)-1-(pyridinium-4-yl)propane-1,3-diketonate iodide **3b**. Starting with **2b** (45 mg, 0.15 mmol), **3b** (38 mg, 57%) was obtained as a beige solid: m.p. 222-224 °C. ^{1}H NMR (400 MHz, DMSO d_6) δ 3.89 (s, 3H, OCH_3), 4.39 (s, 3H, CH_3), 7.16 (d, 2H, *J* 9.1 Hz, ArH) 7.67 (s, 1H, CH), 8.25 (d, 2H, *J* 9.1 Hz, ArH), 8.70 (d, 2H, *J* 6.9 Hz, ArH), 9.16 (d, 2H, *J* 6.9 Hz, ArH) ppm. ^{13}C NMR (100 MHz, DMSO d_6) δ 48.2, 56.1, 97.5, 115.1, 124.9, 127.8, 131.6, 147.2, 148.9, 165.3, 173.2, 191.1 ppm. IR (cm^{-1}) 663, 695, 742, 795, 827, 850, 870, 1026, 1051, 1123, 1164, 1185, 1241, 1259, 1294, 1394, 1408, 1449, 1512, 1560, 1588. UV λ_{max} (DMF) 381 nm (log ε 3.80). Anal Calcd for $C_{16}H_{15}BF_2INO_3$: C, 43.18; H, 3.40; N, 3.15. Found: C, 43.56; H, 3.73; N, 3.14.

Boron difluoride *N*-methyl-1-(pyridinium-4-yl)-3-(4-tolyl)propane-1,3-diketonate iodide **3c**. Starting with **2c** (43 mg, 0.15 mmol), **3c** (45 mg, 70%) was obtained as a yellow solid: m.p. 250-252 °C. ^{1}H NMR (400 MHz, DMSO d_6) δ 2.43 (s, 3H, CH_3), 4.40 (s, 3H, CH_3), 7.44 (d, 2H, *J* 8.1 Hz, ArH) 7.69 (s, 1H, CH), 8.16 (d, 2H, *J* 8.1 Hz, ArH), 8.71 (d, 2H, *J* 6.8 Hz, ArH), 9.18 (d, 2H, *J* 6.8 Hz, ArH) ppm. ^{13}C NMR (100 MHz, DMSO d_6) δ 21.3, 48.0, 97.1, 124.4, 128.6, 129.7, 131.9, 145.3, 146.5, 148.0, 173.4, 190.4 ppm. IR (cm^{-1}) 679, 710, 775, 809, 865, 957, 997, 1050, 1105, 1161, 1245, 1282, 1309, 1356, 1398, 1492, 1513, 1537, 1561, 1592. UV λ_{max} (DMF) 368 nm (log ε 3.70). Anal Calcd for $C_{16}H_{15}BF_2INO_2$: C, 44.79; H, 3.52; N, 3.26. Found: C, 45.13; H, 3.69; N, 3.19.

Boron difluoride *N*-methyl-3-(4-bromophenyl)-1-(pyridinium-4-yl)propane-1,3-diketonate iodide **3d**. Starting with **2d** (53 mg, 0.15 mmol), **3d** (42 mg, 56%) was obtained as a yellow solid: m.p. 260-262 °C. ^{1}H NMR (400 MHz, DMSO d_6) δ 4.40 (s, 3H, CH_3), 7.71 (s, 1H, CH), 7.86 (d, 2H, *J* 8.4 Hz, ArH), 8.18 (d, 2H, *J* 8.4 Hz, ArH), 8.72 (d, 2H, *J* 6.5 Hz, ArH), 9.19 (d, 2H, *J* 6.5 Hz, ArH) ppm. ^{13}C NMR (100 MHz, DMSO d_6) δ 48.1, 97.3, 124.5, 128.6, 130.1, 132.2, 133.6, 146.6, 147.7, 174.0, 189.3 ppm. IR (cm^{-1}) 666, 683, 739, 766, 798, 843, 854, 1004, 854, 1048, 1068, 1113, 1153, 1178, 1193, 1240, 1394, 1470, 1513, 1561. UV λ_{max} (DMF) 358 nm (log ε 3.68). Anal Calcd for $C_{15}H_{12}BBrF_2INO_2$: C, 36.48; H, 2.45; N, 2.84. Found: C, 36.65; H, 2.33; N, 2.53.

Boron difluoride *N*-methyl-3-(anthracen-9-yl)-1-(pyridinium-4-yl)propane-1,3-diketonate iodide **3e**. Starting with **2e** (56 mg, 0.15 mmol), **3e** (28 mg, 36%) was obtained as a red solid: m.p. 263-265 °C. ^{1}H NMR (400 MHz, DMSO d_6) δ 4.36 (s, 3H, CH_3), 7.24-7.27 (br s, 1H, CH), 7.59-7.62 (m, 4H, ArH), 8.05-8.07 (m, 2H, ArH), 8.19-8.21 (m, 2H, ArH), 8.57-8.68 (m, 2H, ArH), 8.81 (s, 1H, ArH), 9.08-9.09 (m, 2H, ArH) ppm. ^{13}C NMR (100 MHz, DMSO d_6) δ 48.0, 104.6, 122.3, 124.7, 124.8, 125.9, 127.5, 128.8, 129.7, 130.66, 130.68, 146.5, 206.7 ppm. IR (cm^{-1}) 654, 664, 717, 726, 737, 748, 794, 817, 830, 917, 1086, 1141, 1171, 1179, 1193, 1258, 1278, 1447, 1486, 1515, 1553, 1602. UV λ_{max} (DMF) 389, 371, 352 nm (log ε 3.87, 3.86, 3.75). Anal Calcd for $C_{23}H_{17}BF_2INO_2$: C, 53.63; H, 3.33; N, 2.72. Found: C, 53.73; H, 3.52; N, 2.59.

Acknowledgement

This work has been supported by iMQRES to Rajesh Raut scholarship (form Macquarie University) and an APA award to Thomas Sommerville (from the Australian Government). Rahul Telore is grateful to UGC-CAS for providing a fellowship under SAP.

References

1. E. Cognÿ-Laage, J.-F. Allemand, O. Ruel, J.-B. Baudin, V. Croquette, M. Blanchard-Desce and L. Jullien, *Chem. Eur. J.*, 2004, **10**, 1445-1455.
2. H. D. Ilge, E. Birckner, D. Fassler, M. V. Kozmenko, M. G. Kuzmin and H. Hartmann, *J. Photochem.* , 1986, **32**, 177-189.
3. A. Natarajan, D. Ng, Z. Yang and M. A. Garcia-Garibay, *Angew. Chem. Int. Ed.*, 2007, **46**, 6485-6487.
4. K. Ono, K. Yoshikawa, Y. Tsuji, H. Yamaguchi, R. Uozumi, M. Tomura, K. Taga and K. Saito, *Tetrahedron*, 2007, **63**, 9354-9358.
5. A. G. Mirochnik, E. V. Gukhman, V. E. Karasev and P. A. Zhikhareva, *Russ. Chem. Bull.*, 2000, **49**, 1024-1027.
6. G. R. Kumar and P. Thilagar, *Dalton Trans.*, 2014, **43**, 3871-3879.
7. A. G. Mirochnik, E. V. Fedorenko, D. K. Gizzatulina and V. E. Karasev, *Russ. J. Phys. Chem. A*, 2007, **81**, 1880-1883.
8. A. G. Mirochnik, B. V. Bukvetskii, E. V. Gukhman, P. A. Zhikhareva and V. E. Karasev, *Russ. Chem. Bull.*, 2001, **50**, 1612-1615.
9. A. Valore, A. Colombo, C. Dragonetti, S. Righetto, D. Roberto, R. Ugo, F. De Angelis and S. Fantacci, *Chem. Commun.*, 2010, **46**, 2414-2416.
10. P. Espinet, J. Etxebarría, C. L. Folcia, J. Ortega, M. B. Ros and J. L. Serrano, *Adv. Mater.*, 1996, **8**, 745-748.
11. C. Ravikumar, I. H. Joe and V. S. Jayakumar, *Chem. Phys. Lett.*, 2008, **460**, 552-558.
12. T. J. J. Muller and U. H. F. Bunz, *Functional organic materials*, Wiley-VCH, 2007.
13. E. Chauchard, C. Combellas, E. Hendrickx, G. Mathey, C. Suba, A. Persoons and A. Thiebault, *Chem. Phys. Lett.*, 1995, **238**, 47-53.
14. C. K. Lakshmana Perumal, A. Arulchakkaravarthi, P. Santhanaraghavan and P. Ramaswami, *J. Cryst. Growth*, 2002, **240**, 212-217.
15. D. S. Chemla and J. Zyss, *Non-linear optical properties of organic molecules and crystals*, Academic Press, London, 1987.
16. P. Boy, C. Combellas, G. Mathey, S. Palacin, A. Persoons, A. Thiébault and T. Verbiest, *Adv. Mater.*, 1994, **6**, 580-583.
17. M. Snehalatha, C. Ravikumar, J. I. Hubert, N. Sekar and V. S. Jayakumar, *Spectrochim. Acta, Part A*, 2009, **72**, 654-662.
18. G. A. Crosby and J. N. Demas, *J. Phy. Chem.*, 1971, **75**, 991-1024.
19. C. Reichardt, *Chem. Rev.*, 1994, **94**, 2319-2358.
20. M. J. Frisch, G. W. Trucks, H. B. Schlegel, G. E. Scuseria, M. A. Robb and J. R. Cheeseman, *Journal*, 2010.
21. R. Levine and J. K. Sneed, *J. Am. Chem. Soc.*, 1951, **73**, 5614-5616.
22. L. F. Lindoy, M. Dudek, J. K. Clegg, C. R. K. Glasson, N. Kelly, K. Gloe, K. Gloe, A. Kelling, H. Buschmann, K. A. Jolliffe and G. V. Meehan, *Cryst. Growth Des.*, 2011, **11**, 1697-1704.
23. G. Dorota, *Tetrahedron: Asymmetry*, 2005, **16**, 1377-1383.
24. S. Z. Zhan, M. Li, X. P. Zhou, J. H. Wang, J. R. Yang and D. Li, *Chem. Commun.*, 2011, **47**, 12441-12443.

Chapter Eight

Overview of the Project Outcomes and Future Directions

8.1 Overview of the Project Outcomes

The work described in this Thesis was predominately performed in the area of organic synthesis. Specifically, it reports on the syntheses of families of porphyrin-chromophore conjugates, linked *via* covalent bonds, employing the three different porphyrin frameworks depicted in Figure 1.21. The first framework was one that has been widely reported in the literature and involved the attachment of the auxiliary chromophores to a *meso*-phenyl ring. This approach required the initial synthesis of porphyrins with one *meso*-phenyl ring substituted with either a nitro or a methyl ester group at the *ortho*-, *meta*-, or *para*-positions. These compounds were successfully prepared, using mixed-aldehyde reactions, essentially following literature procedures.[1,2,3] The nitro groups were then reduced to amino groups, and the esters were converted to formyl groups, after initially being reduced to alcohols that were then selectively oxidised to the aldehydes. All of this chemistry is summarised in Schemes 2.2 and 2.3.

The second and third porphyrin frameworks have been less studied in the literature, and incorporate π-extended porphyrin macrocycles. The key precursor to both frameworks was the porphyrin dione **21**, first reported by Crossley (Scheme 2.4).[4] Condensation reactions with the appropriately functionalised benzaldehydes and ammonium acetate, or with 1,2-diaminobenzenes, afforded the desired phenyl-substituted imidazoloporphyrins or quinoxalinoporphyrins (Schemes 2.5-2.8), respectively. Further manipulations of the nitro and ester functionalities, in an analogous manner to the chemistry performed on the substituted *meso*-phenyl porphyrins, afforded the desired amino- and formyl-functionalised compounds. However, the *ortho*-methyl ester-functionalised phenyl-substituted imidazoloporphyrin **71** could not be reduced to the desired alcohol, and therefore one of the targeted formyl porphyrins was not obtained.

All of the above reactions were required to access the necessary starting materials for this project (and represents the synthesis of 41 porphyrins, 16 of which are new compounds), for use in the syntheses of the new conjugates described in this Thesis.

The three chromophores that were targeted for conjugation to the functionalised porphyrin building blocks were boranils (two were examined, Chapter Three, Schemes 3.1-3.3), α-cyanostilbenes (three were examined, Chapter Four, Schemes 4.1-4.3) and boron difluoride 1,3-diketonates, whose syntheses proved unsuccessful in this work. None of these chromophores have been previously studied as part of a porphyrin-conjugate dyad.

Chapter Three outlined the details of the syntheses of the porphyrin-boranil conjugates, in a three step process from amino-functionalised porphyrin building blocks; formation of the anils, followed by boron chelation and finally metallation of the porphyrins with zinc(II) acetate. Chapter Four detailed the use of the corresponding formyl-functionalised building blocks to make porphyrin α-cyanostilbene conjugates and their zinc(II) adducts.

^{1}H NMR analysis of the *ortho*-substituted *meso*-phenyl conjugates provides evidence of orientation of the auxiliary chromophores over the porphyrin macrocycle, based on the observed upfield chemical shifts of protons on the auxiliary chromophores. Unfortunately, the corresponding series of compounds (where the auxiliary chromophores were moved from the *para*- to *meta*- to *ortho*- positions) with the imidazoloporphyrins was not complete. In the case of the boranil conjugates, anils could not be prepared from **31** (Scheme 3.2), and in the case of the α-cyanostilbene conjugates, the necessary formyl building block **40** could not be accessed (Scheme 2.6). This is thought to be the result of interactions between the imidazole NH and the amino and ester groups, respectively.

In both Chapters Three and Four some preliminary photo-physical characterisation work was reported, consisting of simple UV-visible absorption and fluorescence emission spectroscopy, together with calculations of the quantum yield for several of the conjugate systems. The aim of

this aspect of the work was to determine if there were any trends in terms of porphyrin-chromophore interactions. Such an interaction may result in an enhancement or reduction of the intensity of an absorption or emission peak or in the quantum yield of a compound(s) in comparison with other members of the family under consideration. Perhaps the one figure that shows some clear trend is Figure 4.5. The figure shows the normalised fluorescence emission spectra for the zinc(II) *meso*-phenyl porphyrin α-cyanostilbene conjugates. The nitro compounds fluoresce the weakest, and within the unsubstituted and 4-bromo α-cyanostilbene series, there are decreasing fluorescence intensities as the α-cyanostilbene is moved from the *para*-, to *meta*-, to *ortho*-positions.

A number of attempts at converting various methyl ester-functionalised porphyrins into porphyrin-1,3-diketone conjugates resulted in isolation of the carboxylic acid-functionalised porphyrins as hydrolysis products. In the cases where THF was used as the solvent, it was obtained freshly distilled from a blue solution (from the presence of the sodium benzophenone ketyl radical), indicating that it was in anhydrous form. The same solvent, used under identical reaction conditions, was used successfully to make other 1,3-diketones. Dimethoxyethane (DME) was also used unsuccessfully in the porphyrin reactions, but was successfully used as the solvent in the synthesis of nine 1,3-diketones described in Chapter Five, and another five compounds described in Chapter Seven.

The methoxy-functionalised 1,3-diketones and their boron difluoride complexes described in Chapter Five were prepared as model reactions, prior to the unsuccessful reactions involving porphyrins. They also served as reference compounds for the characterisation of the benzyoxyl series (the UV-visible absorption and fluorescence emission properties for corresponding members of the series were almost identical). The benzyloxy series were prepared as precursors to the hydroxy-functionalised boron difluoride 1,3-diketonates that will be used in supramolecular studies (see Section 8.2).

Chapter Six described an experiment that showed a pyridyl-functionalised boron difluoride 1,3-diketonate forms a supramolecular complex with a zinc(II) porphyrin, and an approximate binding constant of 4600 ± 2100 M^{-1} was calculated.

Chapter Seven represents a different aspect of the research, as it was recognised that the boron difluoride complexes of pyridyl appended 1,3-diketones, initially conceived as ligands for supramolecular studies with zinc(II) porphyrins, are set-up as donor-conjugated linker-acceptor systems, typical of organic nonlinear optical compounds. The same set-up is present in any non-symmetric 1,3-diketone, bearing an electron-withdrawing group on one side and an electron-donating substituent on the other, but these systems have never been studied in this context. It was also apparent that the polarised nature of the molecules should be enhanced by methylation of the pyridine nitrogen. The NLO properties of the compounds are yet to be evaluated experimentally, but computational studies are consistent with the expected properties.

8.2 Future Directions

Whilst several series of porphyrin-chromophore conjugates were prepared, it is apparent that for future energy transfer studies the absorption properties of the auxiliary chromophores need to be tuned so that their absorption maxima are shifted away from the Soret band. This will allow selective excitation of their major absorption band so that any potential electron / energy transfer processes may be observed. This can be most easily achieved by extending the conjugation of the auxiliary chromophores, which will result in a bathochromic (red)-shift in their spectra. Whilst this is not a trivial task, it can be done, and the additional steps required can be incorporated into the approaches taken in this Thesis. A similar approach can be taken, potentially more easily, with chromophores as ligands in self-assembly processes with suitable metalloporphyrins.

The self-assembly process of tin(IV) porphyrins and hydroxyl-functionalised boron difluoride 1,3-diketonates (suitably functionalised to allow for selective excitation) should also be examined.

Other chromophores / electron accepting units could also be studied with the porphyrin frameworks prepared in this work. Given the previous reported studies of porphyrin-fullerene conjugates shown in Figure 1.14, a similar approach could be taken to constructing new dyads with formyl porphyrins **38** and **39** (Scheme 2.6), and **45** (Scheme 2.8).

Another area for future work is the synthesis of some new porphyrin dimers from building blocks described in Chapter Two, whereby the formyl porphyrins are used as "benzaldehydes" and reacted with porphyrin dione **21** using the chemistry described in Scheme 2.6. This work is currently being conducted by another PhD candidate in the Try research group.

8.3 References

1. Imahori, H.; Hagiwara, K.; Aoki, M.; Akiyama, T.; Taniguchi, S.; Okada, T.; Shirakawa, M.; Sakata, Y. *J. Am. Chem. Soc.* **1996**, *118* (47), 11771-11782.
2. Salom-Roig, X. J.; Chambron, J.-C.; Goze, C.; Heitz, V.; Sauvage, J.-P. *Eur. J. Org. Chem.* **2002**, *2002* (19), 3276-3280.
3. Tkachenko, N. V.; Lemmetyinen, H.; Sonoda, J.; Ohkubo, K.; Sato, T.; Imahori, H.; Fukuzumi, S. *J. Phys. Chem. A* **2003**, *107* (42), 8834-8844.
4. Crossley, M. J.; Burn, P. L. *J. Chem. Soc., Chem. Commun.* **1987**, 39-40.

Appendix

A1 Building Blocks

With the exception of the porphyrins used in Chapter Five (that had 4-*tert*-butyl rings at the *meso*-positions), all of the porphyrin compounds prepared in this work were substituted at the *meso* positions with the 3,5-di-*tert*-butylphenyl ring, which is omitted in the following diagrams for clarity. The numbering system employed for the various free base porphyrin skeletons discussed throughout this Thesis is illustrated below, together with the nomenclature used in the experimental section. The metal chelates of these compounds are named by adding the suffix "ato" to the word porphyrin, enclosing the name of the free base system in brackets and then listing the nature of the metal ion present. This system of nomenclature is followed only in the experimental section as its use in other areas of the text becomes too cumbersome. In the discussion section of this Thesis, therefore, compounds are named simply by describing the number and nature of the substituents present.

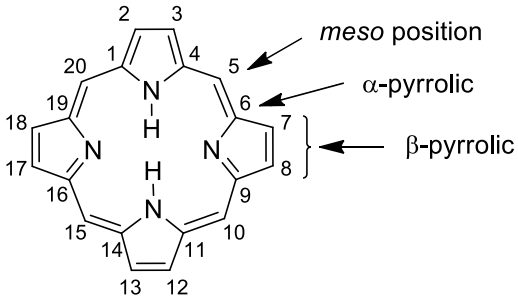

Figure A1: Numbering system for the simple unsubstituted porphyrin ring: 5,10,15,20-tetrakis(3,5-di-*tert*-butylphenyl)porphyrin.

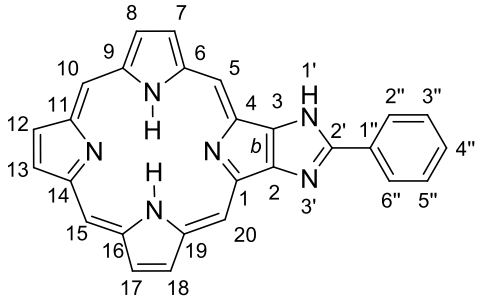

Figure A2: Numbering system for the imidazolo-porphyrins: 5,10,15,20-tetrakis(3,5-di-*tert*-butylphenyl)porphyrin[2,3-*b*]imidazole.

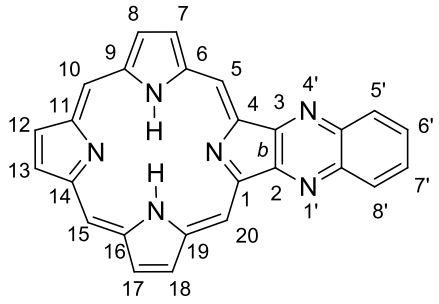

Figure A3: Numbering system for the quinoxaline-porphyrins: 5,10,15,20-tetrakis(3,5-di-*tert*-butylphenyl)porphyrin[2,3-*b*]quinoxaline.

A2 Porphyrin-Boranil Conjugates

The porphyrin-anil conjugates were named as imines, as the "ylidene" derivative of the corresponding amine. The corresponding boranil was then named simply as the "boron difluoride chelate" of the anil.

In the case of the *meso*-substituted systems, numbers were not primed in the names as in the simple 5,10,15,20-tetrakis(3,5-di-*tert*-butylphenyl)porphyrin, the 3- and 5- labels on the phenyl ring are not written as 3'- or 5'. They are numbered in Figure A4 to highlight the different numbering systems associated with each ring, which are contained within different levels of parentheses in the name.

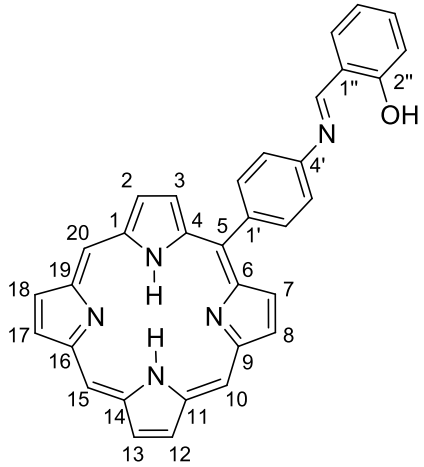

Figure A4: Numbering system for the *meso*-porphyrin anil conjugates: *eg.* 5-([(2-hydroxyphenyl)methylidene]-4-aminophenyl)-10,15,20-tris(3,5-di-*tert*-butylphenyl) porphyrin.

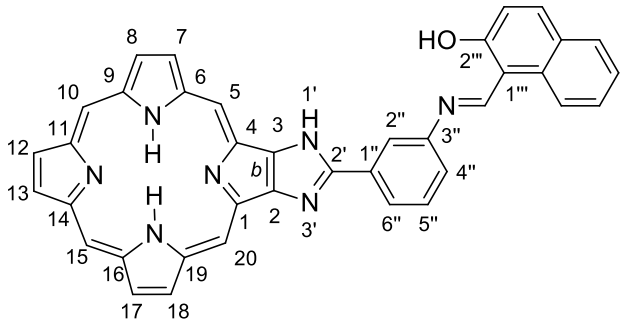

Figure A5: Numbering system for the imidazolo-porphyrin anil conjugates: *eg.* (5,10,15,20-tetrakis(3,5-di-*tert*-butylphenyl)porphyrin[2,3-*b*]-1'*H*-imidazol-2'-yl)-([(2'''-hydroxy-naphthyl)methylidene]-3''-aminophenyl.

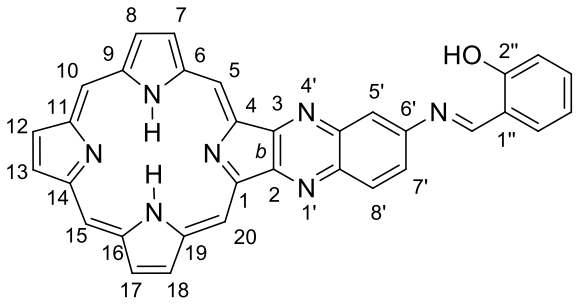

Figure A6: Numbering system for the quinoxalino-porphyrin anil conjugates: *eg.* (5,10,15,20-tetrakis(3,5-di-*tert*-butylphenyl)porphyrin[2,3-*b*]-[(2''-hydroxyphenyl)-methylidene]-6'-aminoquinoxaline.

A3 Porphyrin-α-Cyanostilbene Conjugates

The porphyrin-α-cyanostilbene conjugates were named as substituted cyanoethanes.

As for the porphyrin-anil conjugates, in the case of the *meso*-substituted systems, numbers were not primed in the names as in the simple 5,10,15,20-tetrakis(3,5-di-*tert*-butylphenyl)porphyrin, the 3- and 5- labels on the phenyl ring are not written as 3'- or 5'. They are numbered in Figure A7 to highlight the different numbering systems associated with each ring, which are contained within different levels of parentheses in the name.

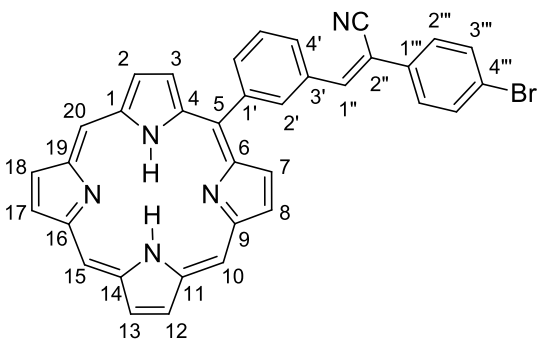

Figure A7: Numbering system for the *meso*-porphyrin-α-cyanostilbene conjugates: *eg.* 5-(phenyl-3-[(*Z*)-2-cyano-2-(4'-bromophenyl)ethenyl])-10,15,20-tris(3,5-di-*tert*-butylphenyl)-porphyrin.

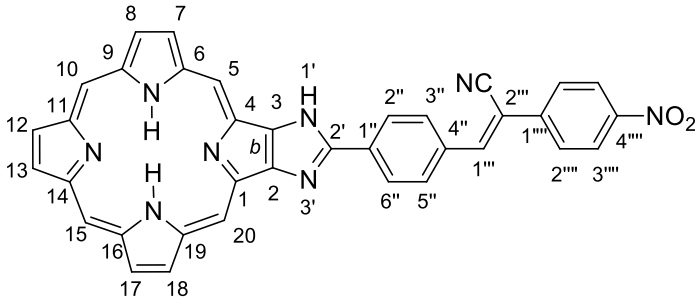

Figure A8: Numbering system for the imidazolo-porphyrin-α-cyanostilbene conjugates: *eg.* 5,10,15,20-tetrakis(3,5-di-*tert*-butylphenyl)porphyrin[2,3-*b*]imidazole-2'-phenyl-4''-[(*Z*)-2'''-cyano-2'''-(4''''-nitrophenyl)ethenyl].

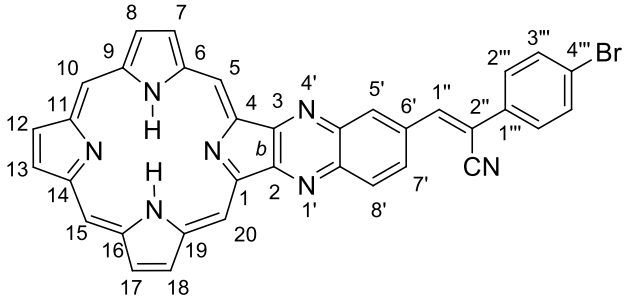

Figure A9: Numbering system for the quinoxalino-porphyrin-α-cyanostilbene conjugates: *eg.* 5,10,15,20-tetrakis(3,5-di-*tert*-butylphenyl)porphyrin[2,3-*b*]-6'((*Z*)-2''-cyano-2''-(4'''-bromophenyl)ethenyl)quinoxaline.

A4 1,3-Diketones

The 1,3-diketones were named as substituted propane-1,3-diones. The numbers were not primed in the names as the numbers and names associated with individual ring systems were enclosed in parentheses. The structure is numbered in Figure A10 to highlight the different numbering systems associated with each ring.

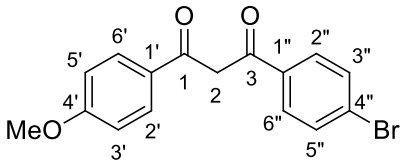

Figure A10: Numbering system used for the 1,3-diketones in Chapter Five: *eg.* 1-(4-bromophenyl)-3-(4-methoxyphenyl)propane-1,3-dione.

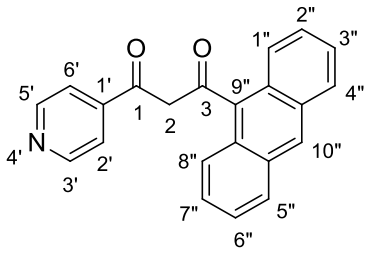

Figure A11: Numbering system used for the 1,3-diketones in Chapter Seven. *eg.* 3-(anthracen-9-yl)-1-(pyridin-4-yl)propane-1,3-dione.

A5 Boron Complexes of 1,3-Diketones

The boron difluoride complexes of the 1,3-diketones were named by placing the words "boron difluoride" in front of the name for the 1,3-diketone, and changing the word "dione" to "diketonate".

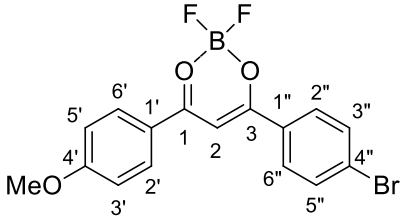

Figure A12: Numbering system used for the 1,3-diketones in Chapter Five: *eg.* boron difluoride 1-(4-bromophenyl)-3-(4-methoxyphenyl)propane-1,3-diketonate.